SCHOOL OF CHEMISTRY

CARDIFF UNIVERSITY

Novel monomers for polymers of intrinsic microporosity (PIMs)

Thesis submitted for the degree of Doctor of Philosophy by:

Mariolino Carta

Supervisor: Neil B. McKeown **2008**

ProQuest LLC
789 East Eisenhower Parkway
P.O. Box 1346
Ann Arbor, MI 48106-1346

Declaration

This work has not previously been accepted in substance for any degree and is not concurrently submitted in candidature for any degree.

Signed..... 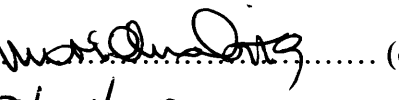 (candidate)

Date....19/01/09....

STATEMENT 1

This thesis is being submitted in partial fulfilment of the requirements for the degree of Doctor of Philosophy.

Signed..... 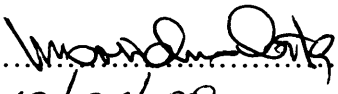 (candidate)

Date..19/01/09....

STATEMENT 2

This thesis is the result of my own independent work/investigation, except where otherwise stated. Other sources are acknowledged by explicit references.

Signed..... 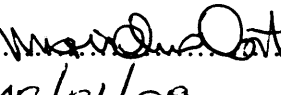 (candidate)

Date....19/01/09....

STATEMENT 3

I hereby give consent for my thesis, if accepted, to be available for photocopying and for interlibrary loan, and for the title and summary to be made available to outside organisations.

Signed..... 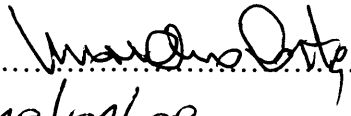 (candidate)

Date..19/01/09....

To my grandma who would have been very proud

Acknowledgments

First of all I would like to thank my supervisor Neil McKeown for the constant help and support (and good ideas!) during my PhD work. I would like also to thank Dr. Peter Budd for managing my crystals in Manchester University and to all people in Manchester X-ray Crystallography Facility for solving the structures, always rapidly and professionally. Particular gratitude goes to Dr Kadhum Msayib for its help and suggestions in lab from the very first start of my PhD experience.

Many thanks to all friends that made life in Cardiff really enjoyable, in particular Manu, Vane, Caterina, Debs, Eugene, Dave, Jean, Adrien (Frenchie), Paula, Massimo, Antonio R., Anabel, Txell, Niek, Veronica, Vincenzo, Eli, Nick, Damien, Richard (Baz), Rhys, Jono, Alex, all people that enjoyed playing (friendly) basketball in Talybont, hoping that I remembered all of them.

Big thanks as well to the other expats with whom I shared the same experience, Gianluca, Alessandra, Antonio F., Simona and Sergio (to have even been my best man).

To my family for being always very close even if they're far away in a beautiful place called Sardinia!

...and to Mrs Grazia Bezzu for the simple fact to exist, "I can't even begin to thank you"...

Abstract

The research described in this thesis is directed towards the synthesis of novel monomers for preparing Polymers of Intrinsic Microporosity (PIMs). Each new monomer contains two catechol units fused via a spiro-centre, which adds a necessary *site of contortion*, and all are compatible with an efficient polymerisation reaction with 2,3,5,6-tetrafluoroterephthalonitrile. It was anticipated that the resulting PIMs would possess enhanced properties (e.g. microporosity, solubility gas permeability etc.) due to the polar and polarisable substituents that these novel monomers contribute to the polymer structure.

This first part of this work describes the synthesis of two families of monomers. The first is based on the spiro-bisindane structural unit in which the spiro centre is shared by two fused five-membered rings, similar to the commercially available 4,4',5,5'-tetrahydroxy-3,3,3',3'-tetramethyl-1,1'-spirobisindane, which was found to provide highly microporous polymers in previous work. Various groups (e.g. ketone, phenyl, fluorene) were introduced in place of the four methyl substituents. The second family of monomers is based upon 1,1'-spiro-bis(1,2,4,5-tetrahydro-6,7-dihydroxynaphthalene) in which the spiro-centre fuses two six-membered rings. Similar substituents were introduced in order to make a direct comparison of properties to those of the polymers derived from the spirobisindane family. Additionally, the concept of adding "sacrificial" thioketal groups to the 4,4',5,5'-tetrahydroxy-3,3'-keto-1,1'-spirobisindane monomer was investigated, with the aim of temporarily increasing the solubility and processability of the poorly soluble ketone-containing PIM.

The last part of the work is concerned with the results of the polymerisation reactions of these novel monomers with 2,3,5,6-tetrafluoroterephthalonitrile, followed by the characterization of the resulting polymers. In particular, the important physical properties of the polymers were assessed such as solubility, molecular mass (by Gel Permeation Chromatography - GPC), microporosity (using nitrogen adsorption), and thermal stability (by Thermo-Gravimetric Analysis - TGA).

Abbreviations

APCI	Atmospheric pressure chemical ionisation
Å	Angstrom
aq	aqueous
Ar	Unspecified aryl substituent
BET	Brunauer, Emmett, and Teller
br	Broad
calc.	Calculated
CAN	Cerium(IV) Ammonium Nitrate
COF	Covalent-Organic-Frameworks
DCM	Dichloromethane
DMAc	N,N-Dimethylacetamide
DMF	*N*,*N*–Dimethylformamide
DMSO	Dimethyl sulphoxide
DSC	Differential scanning calorimetry
EA	Ethyl acetate
EI	Electron Impact
equiv. or eq.	Equivalent
ES	Electrospray
Et	Ethyl
Et_2O	Diethylether
EtOH	Ethanol
g	Grams
GPC	Gel Permeation Chromatography
h	Hour/s
HATN	Hexachloro-hexaAzaTriNaphthylene
HRMS	High Resolution Mass Spectrometry
Hz	Hertz
IR	Infra Red
IUPAC	International Union of Pure and Applied Chemistry
J	Coupling constant (in Hz)
lit.	Literature
LRMS	Low Resolution Mass Spectrometry
m	Multiplet
Me	Methyl
MeCN	Acetonitrile
MeOH	Methanol
min	Minute(s)
mmol	Millimole(s)

M*n*	Number-average molecular weight
MOF	Metal Organic Framework
mp	Melting point
M*w*	Mass-average molecular weight
nm	nano meters
NMP	*N*-methyl pyrrolidone
NMR	Nuclear Magnetic Resonance
Ph	Phenyl
PIM	Polymers of Intrinsic Microporosity
PPA	PolyPhosphoric Acid
q	quartet
r.t.	room temperature
s	singlet
t	triplet
***t*-Bu**	tert butyl
TFA	TrifluoroAcetic acid
TGA	Thermo-Gravimetric Analysis
THF	Tetrahydrofuran
TLC	Thin Layer Chromatography
TMS	Trimethylsilyl
vs.	versus

List of recurrent molecules

Short name	*Structure*	*N°*
PIM-1	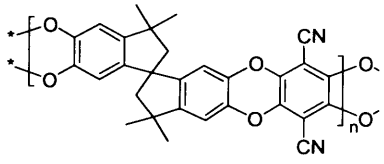	**PIM-1**
4,4',5,5'-tetrahydroxy-3,3,3',3'-tetramethyl-1,1'-spirobisindane	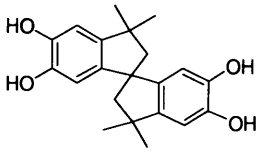	**A1 = 22**
2,3,5,6-tetrafluoroterephthalonitrile		**28**
Diethyl ester spiroindane precursor	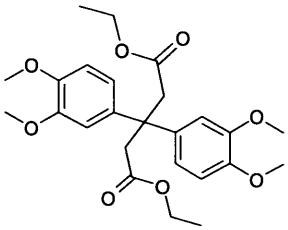	**43**
Spiro-ketone	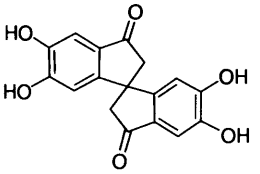	**44**
3,3'-diphenyl-1,1'-spirobisindene	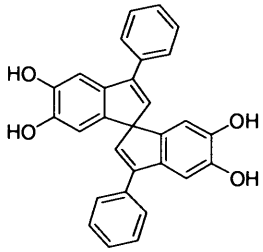	**46**
"Lactone"	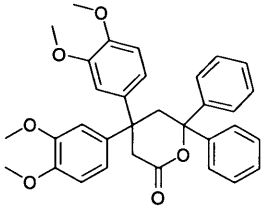	**48**

Tetraphenyl spiroindane 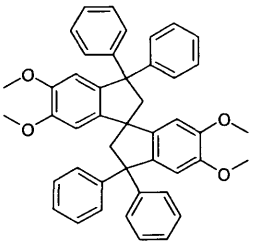 **47**

Di-Phenyl-ketone spirobisindane 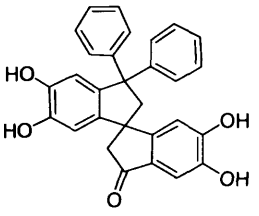 **54**

Bis Fluorene 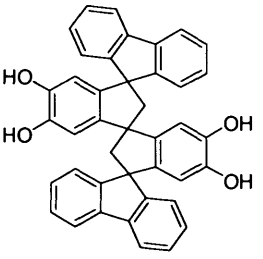 **57**

Fluorene-ketone 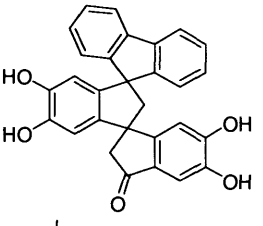 **59**

tert-Butyl Fluorene 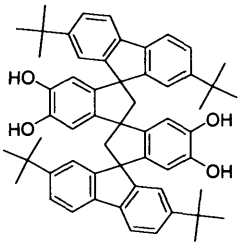 **64**

tert-Butyl Fluorene-ketone 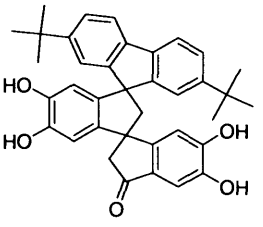 **65**

1,3-dithiolane 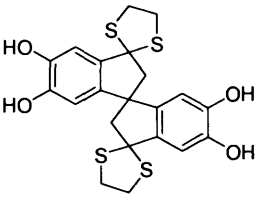 **69**

1,3-dithiane 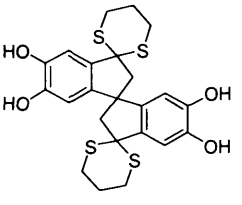 **70**

Spiro-indane	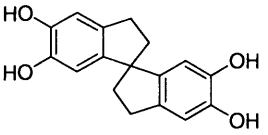	**72**
Diethyl ester "spiro-bisnaphthalene" precursor	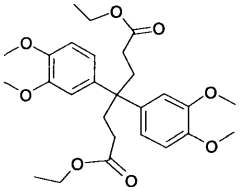	**73**
"Spiro-bisnaphthalene" ketone	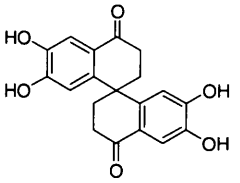	**76**
Phenyl "spiro-bisnaphthalene"	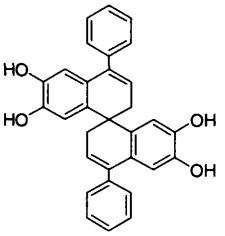	**78**
Tetra-phenyl "spiro-bisnaphthalene"	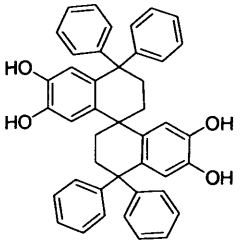	**81**
Fluorene-containing "spiro-bisnaphthalene"	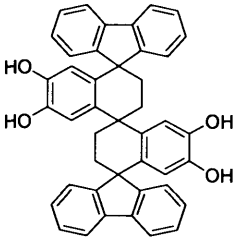	**84**
Fluorene-ketone "spiro-bisnaphthalene"	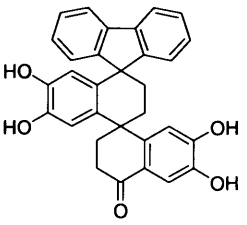	**85**
Tetra-methyl "spiro-bisnaphthalene"	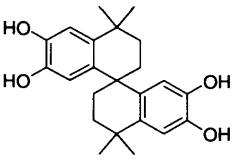	**88**

Table of contents

Chapter 1

1.1 Microporous materials

A pore, which can be widely defined as a limited space or spatial confinement, is one of the most ancient concepts. The understanding, design, and manipulation of pores have significantly advanced science and technology, and are playing increasingly important roles in new technologies[1].

Of particular interest is the fact that porous materials have higher surface areas than non-porous materials. According to the International Union of Pure and Applied Chemistry (IUPAC), pores can be assigned to one of three classes[2]: channels and pores with diameters less than 2 nm are commonly known as micropores, and these generally represent the largest portion of the material's surface area, whereas, pores with diameters between 2 and 50 nm are known as mesopores and pores with diameters greater than 50 nm are defined as macropores.

In the past decades, the study of microporous materials has become of increasing importance in chemistry, leading to the diversification and further improvement of this class of solids for established and new applications. There are, in fact, many areas of current academic and industrial activity where the use of high surface area materials may have significant impact, mainly for energy storage and separations technologies, including nanostructured materials for highly selective adsorption/separation processes[3,4,5], for instance H_2O, H_2S, or CO_2 removal from natural gas, high capacity gas storage of H_2 and CH_4[6] for fuel storage applications and high selectivity/high permeability gas separations such as O_2 enrichment[7] and H_2 separation and recovery.

1.2 Surface area measurement

Gas sorption (both adsorption and desorption) at the clean surface of dry solid powders is the most established method for determining the surface area of microporous

materials as well as the pore size distribution. Due to the weak interactions involved between gas molecules and the surface, adsorption is a reversible phenomenon. Gas physisorption is non-selective, so it starts filling the surface step by step (or layer by layer) depending on the available solid surface and the relative pressure. Filling the first layer enables the measurement of the surface area of the material, because the amount of gas adsorbed when the mono-layer is saturated is proportional to the entire surface area of the sample. In a gas sorption experiment, the material is first heated and degassed by vacuum force or inert gas purging to remove adsorbed molecules. Then controlled doses of an inert gas, such as nitrogen are introduced and the gas is adsorbed, or alternatively, withdrawn and desorbed. The sample material is placed in a vacuum chamber at a constant and very low temperature, usually at the temperature of liquid nitrogen (77K), and subjected to a range of pressures, to generate adsorption and desorption isotherms. For a conventional volumetric analysis, the gas sorption by the material (adsorbent) is determined by the pressure variations on introduction of a known quantity of gas (adsorbate). Knowing the area occupied by one adsorbate molecule, σ (for example, $\sigma = 16.2$ Å^2 for nitrogen), and using an adsorption model, the total surface area of the material can be determined. The most widely used model is the BET (Brunauer, Emmett, and Teller)[8] equation for multilayer adsorption:

$$\frac{P}{n(P-P_0)} = \frac{1}{cn_m} + \frac{c-1}{cn_m}\frac{P}{P_0}$$

In which, P, P_0, c, n, n_m are the adsorption pressure, the saturation vapour pressure, a constant, the amount adsorbed (moles per gram of adsorbent) at the relative pressure P/P_0, and the monolayer capacity (moles of molecules needed to make a monolayer coverage on the surface of one gram of adsorbent), respectively. Through the slope and intercept of a plot of $P/[n(P_0-P)]$ against (P/P_0), n_m can be resolved. The specific surface area, S, can then be derived:

$$S = N_A n_m \sigma$$

In Eq. 2, N_A is Avogadro's number. The specific surface area that can be determined by gas sorption ranges from 0.01 to over 5000 m^2/g. In addition, the determination of pore size and pore size distribution of porous materials can be made from the

adsorption/desorption isotherm using an assessment model, based on the shape and structure of the pores. The range of pore sizes that can be measured using gas sorption is from a few Ångstroms up to about half a micron. The complete adsorption/desorption analysis is called an adsorption isotherm. The IUPAC classification of adsorption isotherms[2] is illustrated in Fig 1.1 associated with microporous (type I), nonporous or macroporous (types II, III, and VI) or mesoporous (types IV and V) materials.

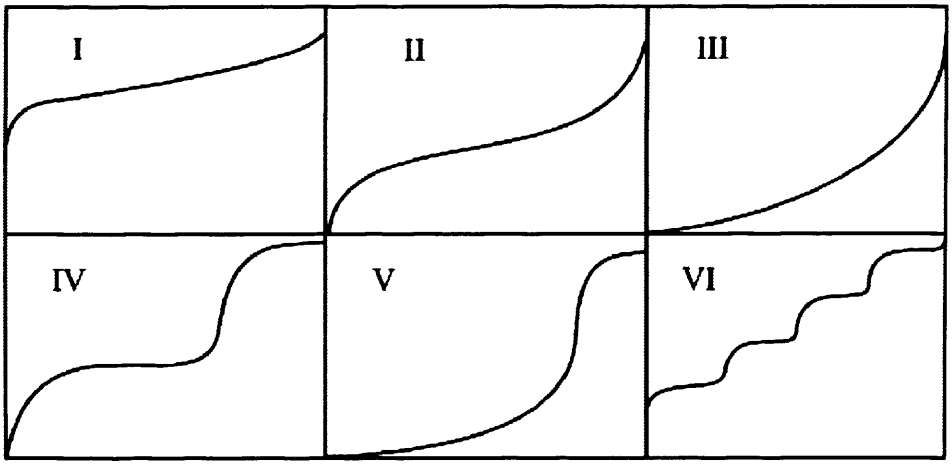

Fig 1.1 Type I is microporous. Type II, III, VI is a material without pores. Type IV, V is mesoporous.

The differences between types II and III isotherms and between types IV and V isotherms arise from the relative strengths of the fluid-solid and fluid-fluid attractive interactions: types II and IV are associated with stronger fluid-solid interactions and types III and V are associated with weaker fluid-solid interactions. The hysteresis loops usually exhibited by types IV and V isotherms are associated with capillary condensation in the mesopores. The type VI isotherm represents adsorption on nonporous or macroporous solids where stepwise multilayer adsorption occurs. Adsorption by mesopores is dominated by capillary condensation, whereas filling of micropores (type I) is controlled by stronger interactions between the adsorbate molecules and pore walls[6]. It is noteworthy that this nomenclature addresses pore width but not pore shape, and pore shape and hystersis can be important in some circumstances, such as when dealing with shape selective molecular sieve behaviour.

Studying microporous materials we are, of course, interested in isotherms type I in which at low pressures there can be a great quantity of nitrogen adsorbed for an almost

imperceptible increase of P/P_0 ratio. This is the part of the curve which signifies the microporosity of the material (Fig 1.2).

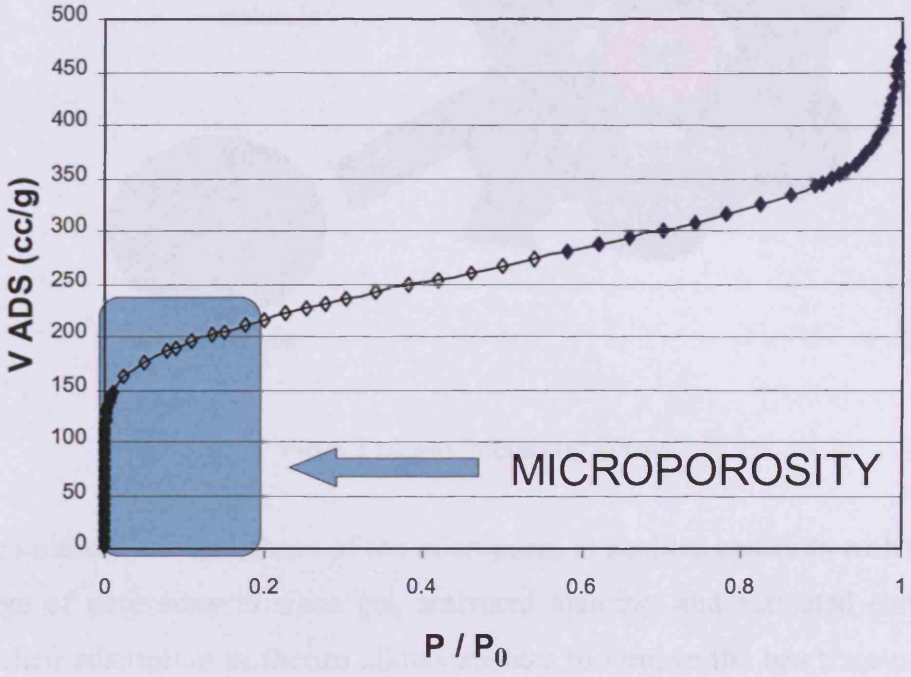

Fig 1.2 Nitrogen adsorption isotherm for a microporous material

1.3 Zeolites

Zeolites were discovered in 1755 by Swedish mineralogist Axel Fredrick Cronstedt. They have been used for years in a variety of applications including water softening[9], water purification[10], arsenic control[11], detergents[12], construction, enriching poor soils, and converting crude oil into gasoline and other fuels[13,14,15].

A zeolite is a crystalline, hydrated aluminosilicate of alkali and alkaline earth cations having an infinite, open, three-dimensional structure with a surface area per gram of material that can range from 400 to 700 m^2/g. It is further able to lose and gain water reversibly and to exchange extra-framework cations, both without change of crystal structure. The large structural cavities and the entry channels leading into them contain water molecules, which form hydration spheres around exchangeable cations. On removal of water by heating at 350-400 °C, small molecules can pass through entry channels, but larger molecules are excluded creating the so called "molecular sieve" property of crystalline zeolites (Fig 1.3).

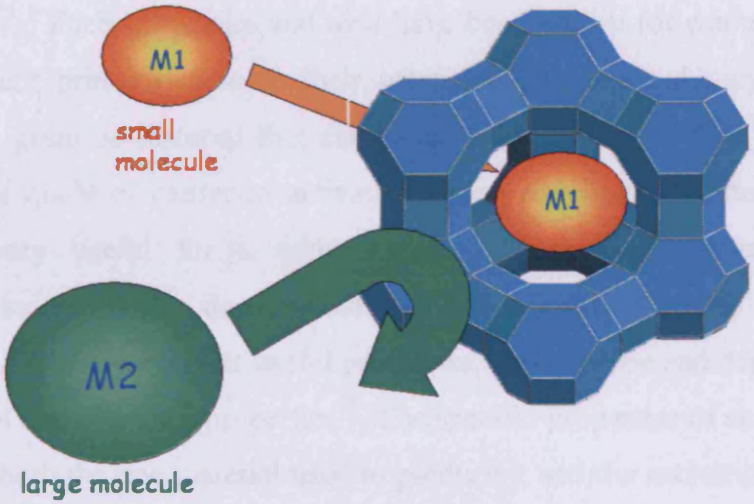

Fig 1.3 zeolite "molecular sieves"

The uniform size and shape of the micropores in zeolites contrasts with the relatively wide range of pore sizes in silica gel, activated alumina, and activated carbon, and the shape of their adsorption isotherms allows zeolites to remove the last trace of a particular gas from a system (e.g., H_2O from refrigerator[16]). Furthermore, zeolites adsorb small polar molecules with high selectivity. Thus, polar CO_2[17] is adsorbed preferentially by certain zeolites, allowing impure methane[18] or natural gas[19] streams to be upgraded.

Two principal uses of these synthetic "molecular sieves" are the purification of gaseous hydrocarbons and the preparation of catalysts for petroleum refining. In general, natural zeolites do not compete with their synthetic counterparts in adsorption or catalytic applications because of their inherent lower adsorption capacities and, to some extent, to the presence of traces of Fe and other catalyst "poisons"[20,21]. Most natural materials have smaller pore openings than the synthetics. Despite the low cost of the natural materials (a few pence per kilogramme), the economics of hardware construction, activation, and regeneration favour the more expensive synthetics.

1.4 Activated carbon

In his appropriately-titled book, "Activated Carbon", Bansal[22] offers a most concise definition of activated carbon: "a wide range of amorphous carbon-based materials prepared to exhibit a high degree of porosity and an extended interparticulate surface area". Activated carbons are remarkable, highly adsorbent materials with a large number of

applications[23,24,25]. Their properties and uses have been known for centuries. They are an effective absorbent primarily due to their extensive porosity and very large available surface area per gram of material that can range from 400 to 2500 m^2/g as previously reported[26]. These qualities confer to activated carbon excellent adsorbent characteristics that make it very useful for a wide variety of processes, including filtration[27], purification[28], deodorization[29], decolourization[30] and separation[22]. The activation of the carbon provides it with many of its useful properties, and the type and degree of activation affect its physical and chemical properties[31]. The specific properties of an activated carbon are the result of both the raw material used to produce it and the activation process, which boosts its adsorbent qualities. A variety of raw materials, including wood and coal, are used in activated carbon manufacture, making it plentiful, relatively inexpensive, and versatile. In the most popular granular form, activated carbon is used as a filter medium through which contaminated water or air is passed. The structural properties of activated carbon are very important to its effectiveness as an adsorbent, though activated carbon's structure is not fully understood and is difficult to explain with text. In general, activated carbon is sometimes described as having a "crumpled" layered surface, in which flat sheets are broken and curved back upon themselves. This unique structure creates activated carbon's very large surface area. It can be more properly visualized with the attached images (Fig 1.4).

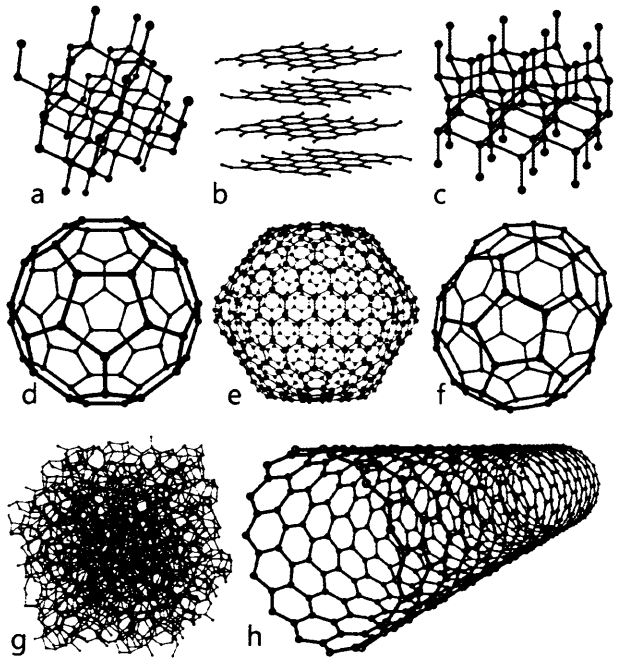

Fig 1.4 The allotropes of carbon. (a) diamond, (b) graphite, (c) lonsdaleite (d) fullerene C60 (e) fullerene C540 (f) fullerene C70; (g) amorphous activated carbon; (h) carbon nanotube.

However during the carbonisation of coals and wood, cross-linking occurs, which leads to extended graphitisation. The resulting network polymer, composed of randomly arranged graphene sheets, is intrinsically microporous[32]. Given the method of preparation, it is unsurprising that most activated carbons possess a wide distribution of pore sizes ranging from microporous to mesoporous (20–50 nm) to macroporous (> 50 nm). Furthermore, the surface of activated carbons is chemically ill-defined with a large variety of oxygen- and nitrogen- containing functional groups present, in addition to the polycyclic aromatic units that form the graphene sheets[33,34]. The heterogeneous structure and chemical nature of the exposed surface area explains the ability of activated carbons to adsorb a wide range of organic compounds and metal ions, but limits their potential for chemo-selective processes.

1.5 Organic microporous materials

1.5.1 Preparation of Hypercrosslinked Polymers

Recently, Germain[35] and Cooper[36], independently reported the use of porous polymers based mostly on simple styrenic monomers for hydrogen storage. These materials are typically produced in a porous form via the suspension polymerization of a monomer mixture containing a high percentage of the crosslinker and a porogenic solvent. Davankov had previously developed this synthetic methodology based on the crosslinking of swollen chloromethylated polystyrene via Friedel-Crafts alkylation[37,38] that leads to polymers with very high surface areas.

Germain *et al.* [35] prepared polymers from two precursors using the detailed procedure reported by Ahn *et al.*[39]. The first precursor, poly (vinylbenzyl chloride) **3** crosslinked with 2.5% divinylbenzene, was prepared via suspension polymerization of a mixture consisting of divinylbenzene **1**, vinylbenzyl chloride **2**, and 2,2'-azobisisobutyronitrile. The post-crosslinking reaction was carried out using the polymeric precursor and the Friedel-Crafts catalyst, added to the slurry cooled in an ice bath. After allowing the catalyst to homogeneously disperse in the mixture, and the mixture to come to room temperature, the crosslinking reaction was allowed to proceed at 80 °C for 24 h obtaining the polymer **4** (Scheme 1.1).

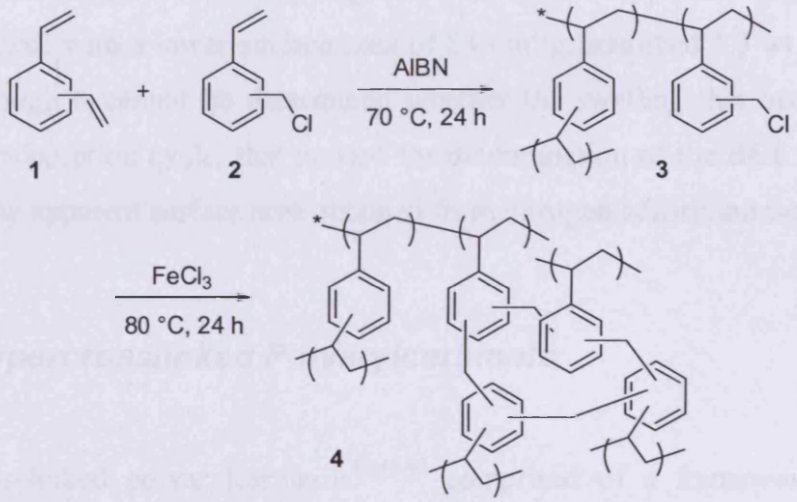

Scheme 1.1. Hypercrosslinked Polystyrene synthesis.

Adsorption/desorption experiments, were carried out to evaluate their ability to adsorb hydrogen and nitrogen, using as comparison a large number of commercial porous resins prepared by both direct copolymerization and post-crosslinking, obtaining very good results ranging from 600 to almost 2000 m^2/g of surface area and with a maximum loading of H_2 evaluated as 2.2% at 0.12 MPa, 77 K (Fig 1.5).

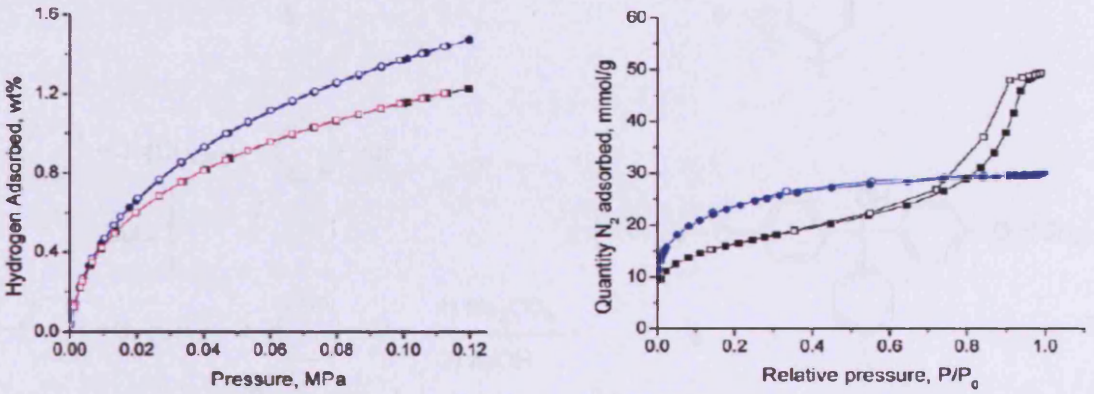

Fig 1.5 Hydrogen adsorption (A) prepared from gel (blue) and macroporous (pink) poly(chloromethylstyrene*co*-divinylbenzene) and nitrogen adsorption (B) gel (blue) and macroporous (black).

Differences were noted in the capability of the polymers to adsorb H_2 and nitrogen in relation to the surface area, for instance a commercial resin with a BET surface area of

1060 m^2/g adsorbed only 0.8 wt % hydrogen at 0.12 MPa, 77 K, while a hypercrosslinked polystyrene-based, with a lower surface area of 840 m^2/g, adsorbed 1.3 wt % at the same pressure. Although it cannot be determined whether the swelling that occurs during the portion of the adsorption cycle, that is used for determination of the BET surface area, it might distort the apparent surface area obtained from nitrogen adsorption isotherms[38].

1.5.2 *Hypercrosslinked Polyarylcarbinols*

Hypercrosslinked polyarylcarbinols[40,41,42] comprised of a framework of rigid-rod connecting units held together by tri-functional tie points, give rise to a number of unusual properties, such as microporosity and extreme swellability. Scheme 1.2 shows the synthesis of these hypercrosslinked polymers. Due to the nature of the cross-linking process, a structural framework possessing a large internal void volume is formed. This results in surface areas as high as 1000 m^2/g. These materials are good candidates as catalyst supports and adsorbents.

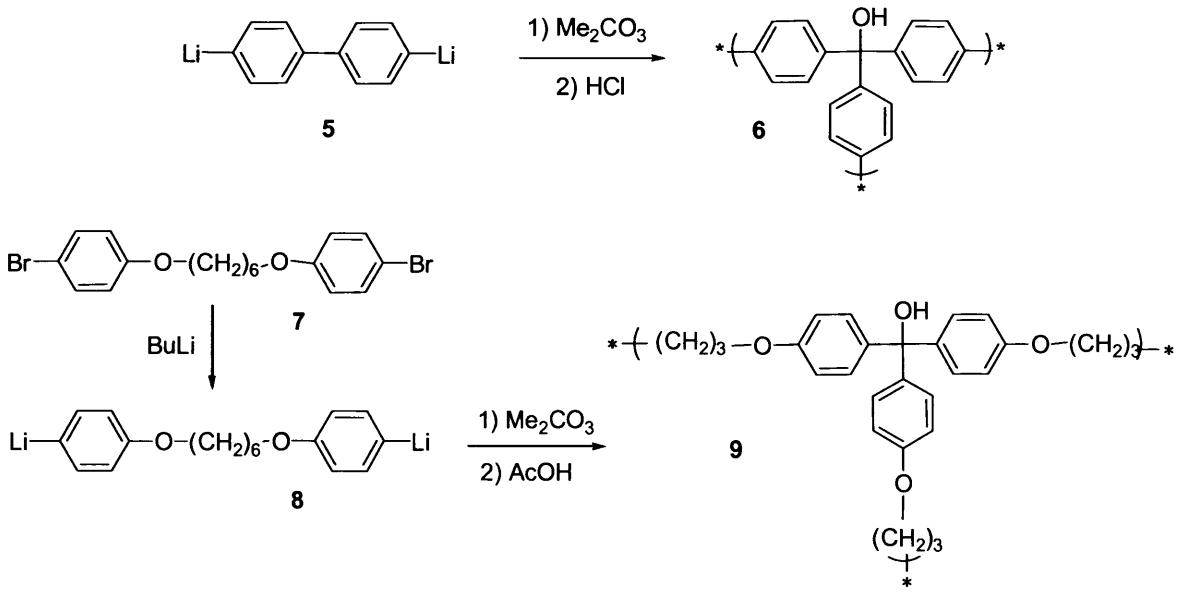

Scheme 1.2. Polyarylcarbinols polymers synthesis.

These hypercrosslinked polymers, swell 200-300% in most organic solvents. This behaviour is poorly understood and, since they neither dissolve nor melt, very little information is available to explain their pore structure and morphology. One explanation, involves the formation of highly crosslinked particles having a high microporosity during

the early polymerization stages which give rise to the observed high surface area. The swelling can be explained based on the assumption that the solvent filled micropores which are formed during polymerization contract when the polymer is dried and the solvent removed (Fig 1.6). Since the network structure is rigid, the pores cannot collapse completely, imposing a very high stress on the dry network. To release this stress, the polymers swells, even in thermodynamically poor solvents, in order to regain the conformation that they had during the cross-linking reaction.

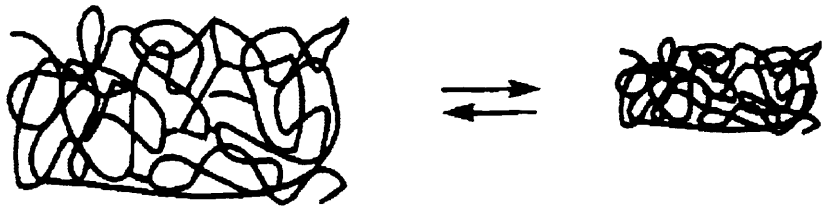

Solvent filled **solvent free**

Fig 1.6. Swelling behaviour of polymer with a homogeneous morphology

1.5.3 Poly (dialkoxyzirconium) microporous powder

The work of Sawaki's group[43] concerned the creation of catalytically active porous metal-organic solids, which can be characterized on the basis of the criteria applied to conventional zeolites.

The treatment of anthracenebisresorcinol **10** (a tetraphenol) with $Zr(OtBu)_4$ in THF, resulted in polycondensation to give an O-Zr-O network and afforded a poly(dialkoxyzirconium phenoxide), $\mathbf{10}^{4-}$ * 2 $[Zr(OtBu)_2]$ (Zr host), as insoluble, amorphous, microporous powder with a particle size of ~ 0.7 μm, a pore size of ~ 0.7 nm, and a specific surface area of ~ 200 m^2/g. Their method, based on the Zr(IV) material obtained from $Zr(OtBu)_4$ **10**, reported a well-behaved porosity and remarkable catalytic performance of the material, which encouraged the construction of other environmentally friendly metal-organic catalysts for organic transformations.

The sol-gel reaction[44] of tetrol **10** and $Zr(OtBu)_4$ in THF solution results in precipitation of grey-brown fine particles with concomitant liberation of tBuOH (eq 1).

$$\mathbf{10} + 2[Zr(O^tBu)_4] \longrightarrow \mathbf{10}^{4-} * [Zr(O^tBu)_2] + 4^tBuOH \quad \text{(eq 1)}$$

The resulting network proved insoluble in all common aprotic and protic organic solvents and could not be recrystallized as a consequence.

$$\mathbf{10}^{4-} * [Zr(O^tBu)_2] + 8H^+ \longrightarrow \mathbf{10} + 2Zr^{4+} + 4^tBuOH \quad \text{(eq 2)}$$

However, when treated with 1 N HCl or HNO_3, it decomposed into its components (eq 2). The actual network may be random, as suggested by the amorphous nature of the material.

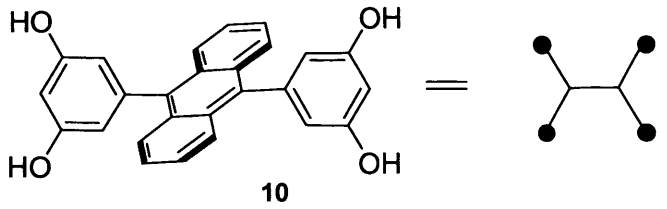

10

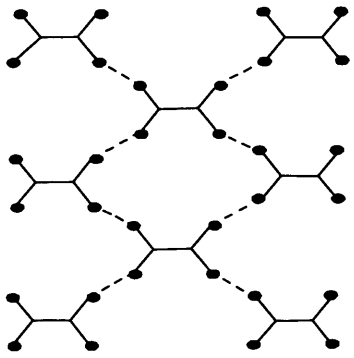

11

Scheme 1.3. Poly(dialkoxyzirconium) synthesis.

This simple method allowed the immobilization of soluble metal complexes in a known cavity-forming hydrogen-bonded network via polycondensation with a scheme like $O{\cdot}H\cdots O\text{-}H + MXn \rightarrow O^{\cdot}\cdots [MXn\text{-}2]^{2+}\cdots O^{-} + 2HX$ ($X = RO^{-}$, etc)[45] (Scheme 1.3). In the large cavities left have been incorporated two guest molecules via host-guest hydrogen-bonding. The crystal structures of the resulting adduct have been determined[46] (Fig 1.7).

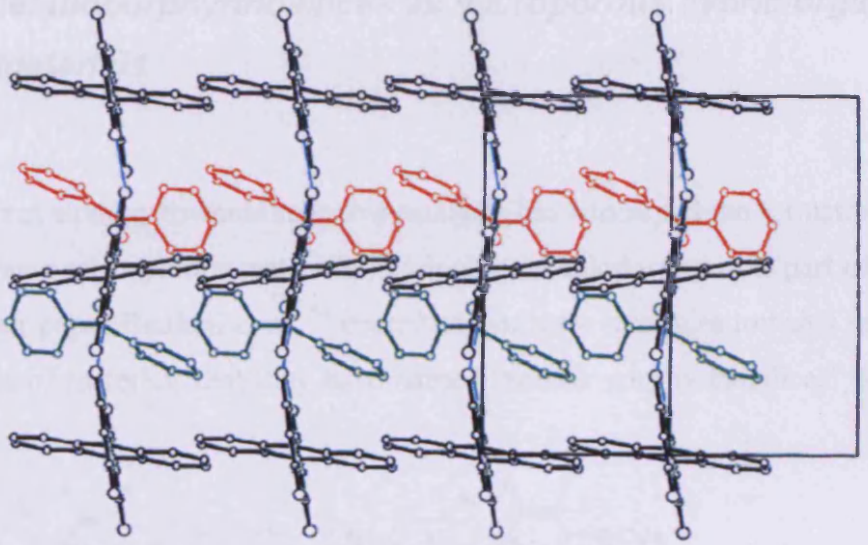

Fig 1.7. Arrangement of adjacent guest-binding supramolecular cavities in the crystal

The N_2 adsorption on the Zr host at 77 K showed a typical type I isotherm[2] with a BET surface area of 200 m^2/g, but also exhibits characteristics of multilayer formation at higher guest pressures, and it must, therefore, be porous. The adsorption isotherms for organic guests are similar to that for N_2. The BET plots[43] give Vm = 6.9, 14, and 15 ml/g for hexane, benzene, and ethyl acetate, respectively, at 298 K.

This Zr material was successfully used as heterogeneous catalyst for the Diels-Alder reaction between acrolein and 1,3-cyclohexadiene[47].

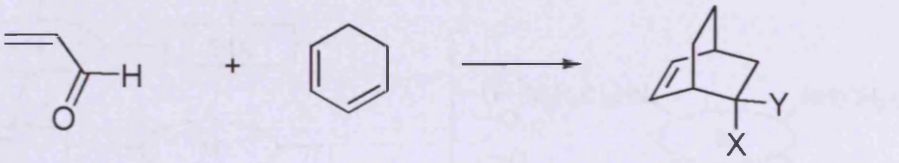

12 **13** **14**

endo : X = CHO Y = H
exo : X = H Y = CHO

Scheme 1.4. Catalysis with poly (dialkoxyzirconium)

The reaction (Scheme 1.4) was complete in 3 h when a mixture of dienophile and diene was stirred at 25 °C with a 3 mol % of the Zr host (**10**$^{4-}$ * 2[$Zr(OtBu)_2$]). The solid catalyst recovered weighed 98% of the original catalyst.

1.5.4 Metalloporphyrinosilicas as microporous hybrid organic-inorganic materials

A different strategy towards selective catalysis has concerned the formation of hybrid organic-inorganic microporous materials in which a metalloporphyrin is part of the matrix [48,49,50]. In their paper Battioni *et al.* [51] described synthetic strategies towards the synthesis of a new class of materials that they have named "metalloporphyrinosilicas" for catalytic applications.

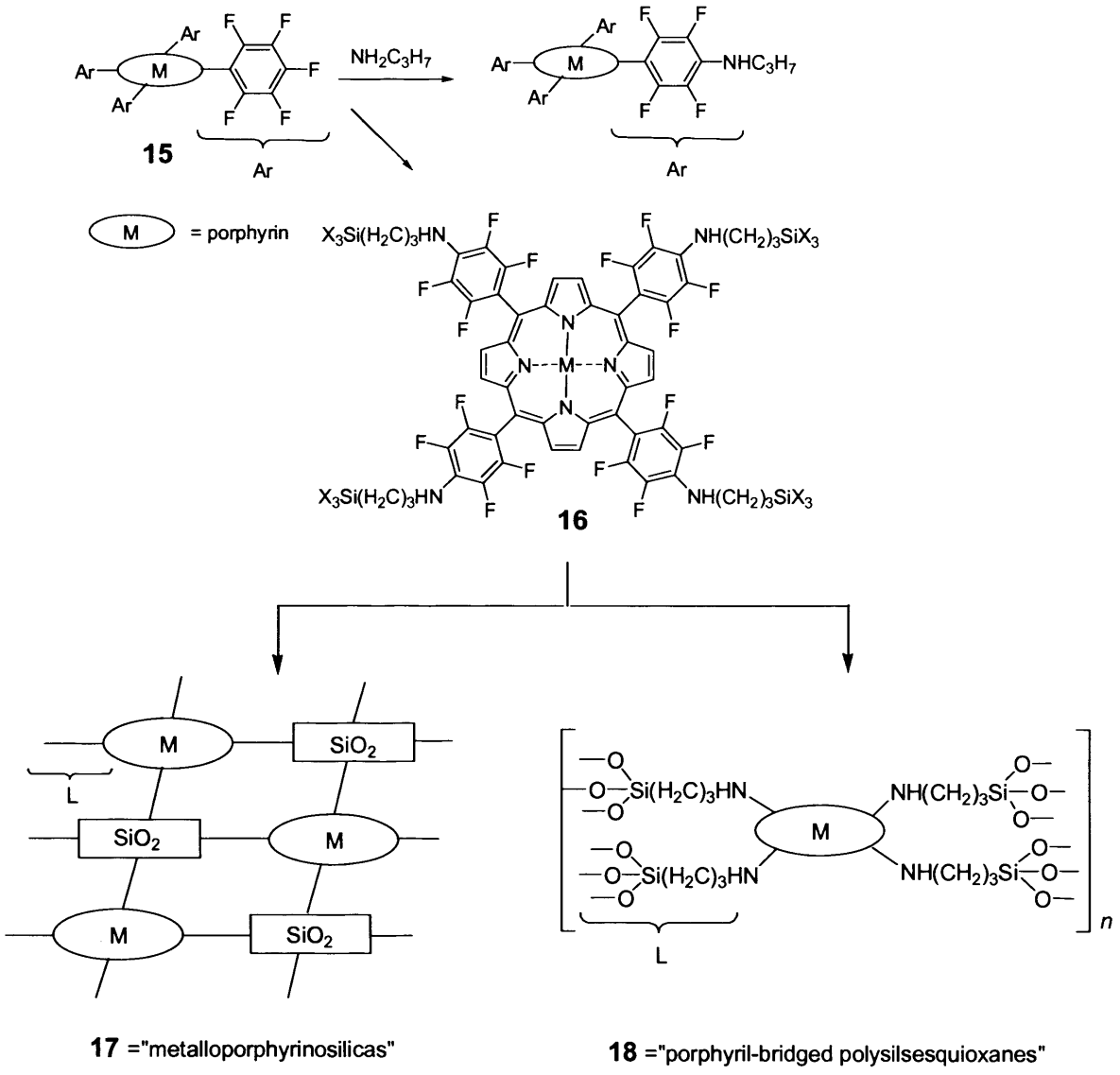

Scheme 1.5. Different hybrid organic-inorganic materials based on metalloporphyrinosilicas

The porphyrin precursors of bridged porphyryl-polysilsesquioxanes and porphyrinosilicas were synthesized as outlined in Scheme 1.5. These materials are

prepared by polycondensation, or co-condensation with tetra-alkoxysilanes, via a sol-gel process, of iron porphyrino-trifluorosilane monomers, creating insoluble polymers, which were shown to catalyse hydrocarbon oxidation by PhIO and ButOOH.

Porphyrinosilane monomer **16** was prepared by reaction of meso-tetrakis-pentafluorophenylporphyrin **15** with excess 3-aminopropyltriethoxysilane[52,53] (APTES). "Iron porphyrinosilicas" **17** were prepared according to the well known sol-gel procedure,[54,55] by hydrolysis and co-condensation of **16** with Si(OEt), in EtOH in presence of water and concentrated HCl as catalysts. Bridged porphyrylpolysilsesquioxanes **18** were prepared by hydrolysis and polycondensation of **16** in a biphasic DCM-H_2O. Porphyrin loadings were obtained by measuring the amount of iron and fluorine in the resulting materials. For porphyrylpolysilsesquioxanes **18** the porphyrin content was high and reached 84% (m/m). Porphyrin loading in "porphyrinosilicas" **17** varied between 0.5 and 50%. It is noteworthy that homopolymers **18** exhibited lower specific surface areas (30-105 m^2/g) than copolymers **17** (> 690 m^2/g). All the iron porphyrinosilicas are reported to catalyse the epoxidation of cyclooctene in high yields[51] (> 90%) as well as the hydroxylation of cyclohexane and heptane with PhIO with yields of *ca.* 50%.

1.5.5 Metal organic frameworks (MOFs)

Compared to conventional microporous inorganic materials such as zeolites, the metal organic frameworks are attractive because of the possibility of the control of the architecture and functionalization of the pores. Usually, the inability of open coordination frameworks to support permanent porosity and to avoid collapsing in the absence of guest molecules, such as solvents, has represented a problem for their utilization[56,57]. However a breakthrough was reported[6], in the late 1990s of coordination networks, termed metal-organic-frameworks (e.g. MOF-5), which remains crystalline, as evidenced by X-ray single-crystal analyses and stable when fully desolvated and on heating up to 300 °C. The synthesis of this class of material was achieved by borrowing ideas from metal carboxylate cluster chemistry, where an organic dicarboxylate linker is used in a reaction that gives supertetrahedron clusters when capped with monocarboxylates.

It was found found that diffusion of triethylamine into a solution of zinc(II) nitrate and benzene-1,4-dicarboxylic acid (H_2BDC) **19** in DMF/chlorobenzene resulted in the deprotonation of H_2BDC and its reaction with Zn^{2+} ions (Scheme 1.6). A small amount of

hydrogen peroxide was added to the reaction mixture in order to facilitate the formation of O^{2-} expected at the centre of the secondary building unit.

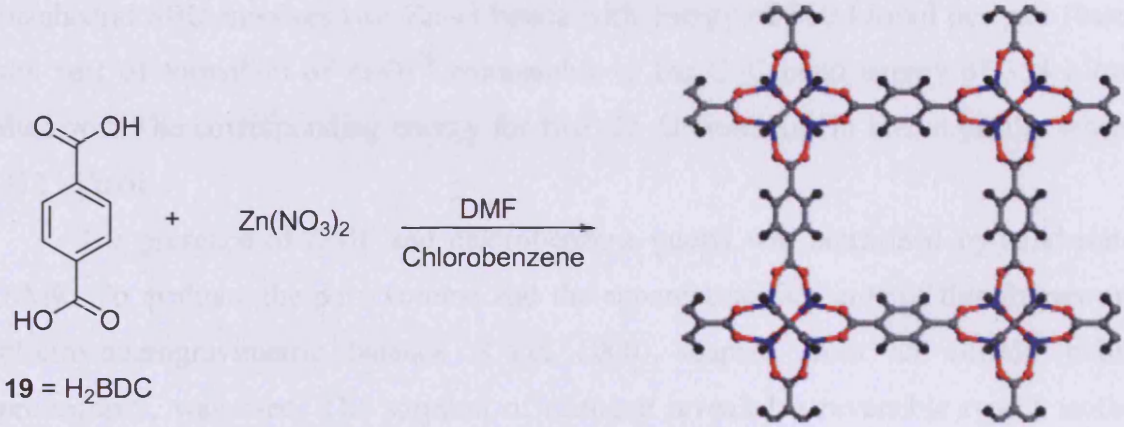

19 = H_2BDC

Scheme 1.6. MOF-5 formation

The rigid character of the added linker allows the articulation of the clusters into a three-dimensional framework resulting in a structure with higher apparent surface area and pore volume than most porous crystalline zeolites creating a material with potentially high gas-storage applications.

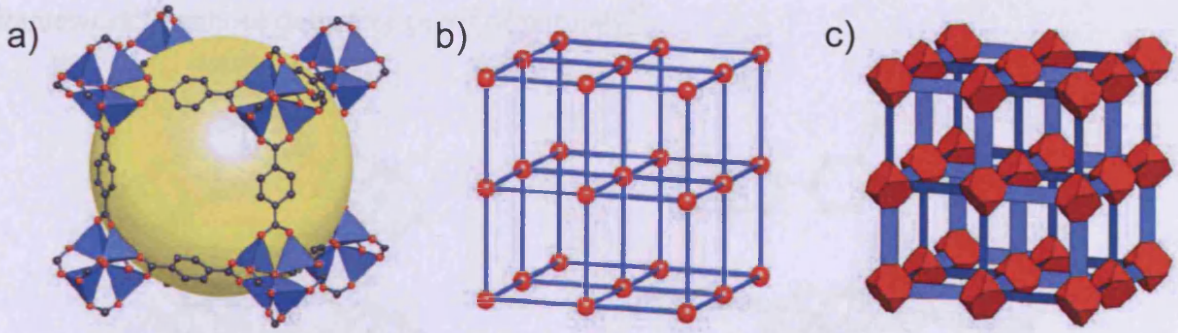

Fig 1.8. Structure models for MOF-5

The exceptional stability of MOF-5 can be understood by comparing its basic network, composed of single atom vertices (Fig. 1.8 b), with the actual structure of MOF-5, which has cationic clusters at those vertices (Fig. 1.8 a). The basic network has no resistance to shear if the links are considered to be universal joints. However, in the actual MOF-5 structure, the cationic clusters have a truncated tetrahedral envelope (Fig. 1.8 c), and the rigidly planar O_2C-C_6H_4-CO_2 linkers have a planar envelope. Furthermore, in contrast to frameworks of the metal bipyridine type, which are known to collapse upon

removal of guests, MOFs constructed with oxide SBUs are far more robust, owing to the presence of multiple strong metal–oxygen bonds. For example, in MOF-5 each link to an octahedral SBU involves two Zn–O bonds with energy of 360 kJ/mol per pair (based on the heat of formation of ZnO)[58] comparable to the C–C bond energy of 358 kJ/mol in diamond. The corresponding energy for two Cu–O bonds (as in linked paddle wheels) is 372 kJ/mol.

The presence of DMF and chlorobenzene guests was confirmed by solid-state ^{13}C NMR. To evaluate the pore volume and the apparent surface area of this framework, an electro-microgravimetric balance (Cahn 1000) adapted from an already published procedure[59], was used. The sorption of nitrogen revealed a reversible type I isotherm[2]. Similar to those of most zeolites, the isotherms are reversible and show no hysteresis upon desorption of gases from the pores. The apparent surface area was estimated at 2900m^2/g.

The diversity and directionality of the rigid aromatic carboxylic acids and the inorganic SBUs, provided a means for the logical synthesis of a wide variety of frameworks (Fig 1.9). An important aspect of this approach is that the large sizes of SBUs inevitably lead to spaces within these structures where solvent and/or counter-ion guests reside. In many cases[60], such solids are interchangeably referred to as "porous" and "open-framework", without definitive proof of porosity[61].

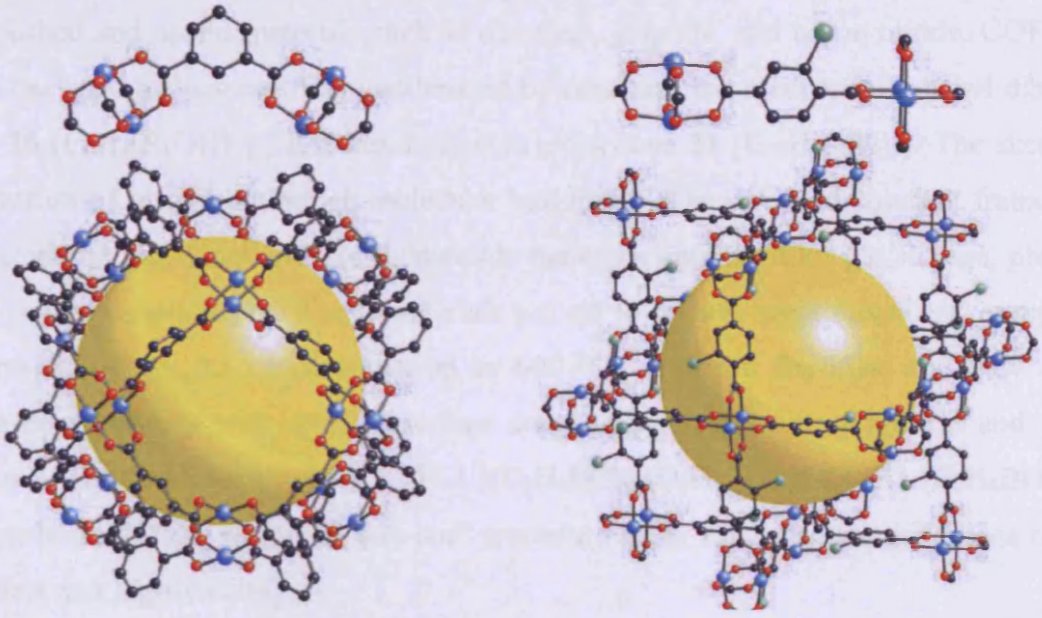

Fig 1.9. MOFs with various SBUs

Many MOFs are exceptionally porous with pore diameters and volumes which far exceed those of the most porous zeolites[62,63,64].

1.5.6 Covalent-Organic-Frameworks (COFs).

The preparation of crystalline extended organic structures in which the building blocks are linked by strong covalent bonds was, until recently, a poorly developed area of research. It was widely believed that the required microscopic reversibility of the crystallization of linked organic molecules into such solids is difficult if not impossible to achieve.

Recently, Yaghi and co-workers initiated a program aimed at challenging this notion by constructing porous, crystalline, covalent organic frameworks[65] (COFs) solely from light elements (H, B, C, N, and O) that are known to form strong covalent bonds in well-established and useful materials such as diamond, graphite, and boron nitride. COFs have been designed and successfully synthesized by condensation reactions of phenyl diboronic acid **20** ($C_6H_4[B(OH)_2]_2$) and hexahydroxytriphenylene **21** [$C_{18}H_6(OH)_6$]. The successful realization of materials through molecular building blocks provided covalent frameworks that could be functionalized into lightweight materials optimized for gas storage, photonic, and catalytic applications. These materials proved to possess rigid structures, exceptional thermal stabilities (to temperatures up to 600 °C), and low densities, and they exhibit permanent porosity with specific surface areas surpassing those of zeolites and porous silicates. The first two members, COF-1 [$(C_3H_2BO)_6 \cdot (C_9H_{12})$] and COF-5 ($C_9H_4BO_2$), can be synthesized using a simple "one-pot" procedure under mild reaction conditions that are efficient and high-yielding.

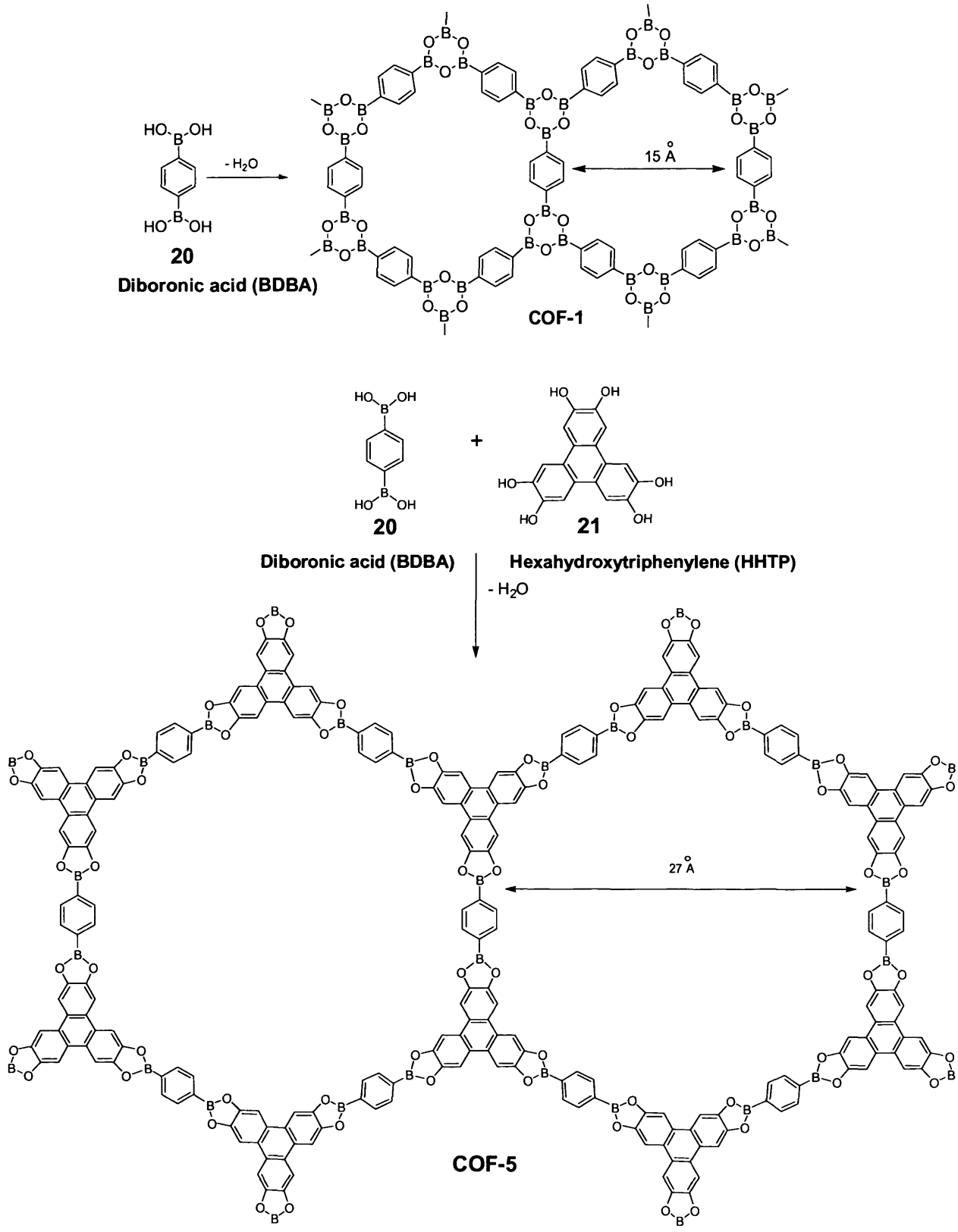

Scheme 1.7. COF-1 and COF-5 synthesis

The synthesis of COF-1 is based on the molecular dehydration reaction, in which the 1,4-benzenediboronic acid **20** (BDBA) was heated and a layered hexagonal framework was

formed upon the dehydration as shown in (Scheme 1.7). Typically, such molecular structures of cyclotrimerized boronic acids are held in planar conformations[66]. The mesoporous COF-5, was prepared from an analogous dehydration reaction between phenylboronic acid **20** and 2,3,6,7,10,11-hexahydroxytriphenylene **21** (HHTP)[67]. The sparing solubility of BDBA in the solvent system controls the diffusion of the building blocks into solution and facilitates the nucleation of a crystalline material. Powder X-ray diffraction (PXRD) analysis of both products confirmed the crystallinity of the COFs.

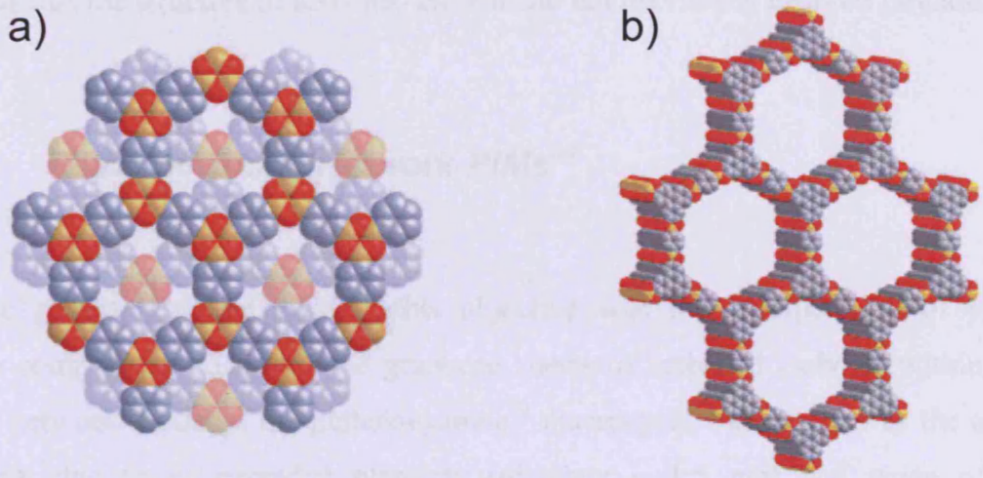

Fig 1.10. Structural representation of a) COF-1 and b) COF-5, based on modelling

The architectural stability and porosity of COF-1 and COF-5 were confirmed by measuring the N_2 gas adsorption of the guest-free material. The isotherm for COF-1 at 77 K allowed an apparent surface area of 711 m^2/g to be calculated[68]. The isotherm is fully reversible and reproducible, a feature of stable materials whose structures exhibit permanent porosity. The N_2 adsorption isotherm of COF-5, measured under the same conditions as COF-1, showed a reversible type-IV isotherm[2] characteristic of mesoporous materials, with a remarkably high BET surface area of 1590 m^2/g. (Fig. 1.10).

1.6 Polymers of intrinsic microporosity (PIMs)

A few years ago a research programme was initiated with the objective of preparing synthetic polymers with microporous structures similar to that of activated carbon, but with a range of well-defined surface chemistries. Considering its enormous commercial importance and the limited scope for systematic chemical or structural modification, it is surprising that the structure of activated carbon had not previously inspired imitation.

1.6.1 Phthalocyanine Network-PIMs[69]

The general strategy towards this objective was the incorporation of extended aromatic components, to mimic the graphene sheets of activated carbons, within a rigid polymer network. Initially, the phthalocyanine[70] macrocycle was selected as the aromatic component due to its extended planarity (diameter ~ 1.5 nm) and range of useful properties.

Previously prepared phthalocyanine network polymers[71] showed a strong tendency of the macrocycles to aggregate into columnar stacks, due to strong noncovalent interactions (primarily π– π interactions), resulting in nonporous solids[72]. Therefore, it was essential to use a highly rigid and nonlinear linking group between the phthalocyanine subunits that would ensure their space-inefficient packing, thus preventing structural relaxation and consequent loss of microporosity. Perfectly suited to fulfil these requirements is a linking group derived from the commercially available 5,5',6,6'-tetrahydroxy-3,3,3',3'-tetramethyl-1,1'-spirobisindane (monomer **22**, Scheme 1.8). The spiro-centre (the single tetrahedral carbon atom shared by two rings) of **22** provides the nonlinear shape, and the fused-ring structure the required rigidity. Phthalocyanine network polymers are generally prepared from a bis (phthalonitrile) precursor through a cyclotetramerisation reaction that is usually facilitated by a metal-ion template. Such a reaction using the bis (phthalonitrile) **24**, prepared from the dioxane-forming reaction between monomer **22** and 4,5-dichlorophthalonitrile **23**, gives network polymers as free-flowing, highly coloured powders.

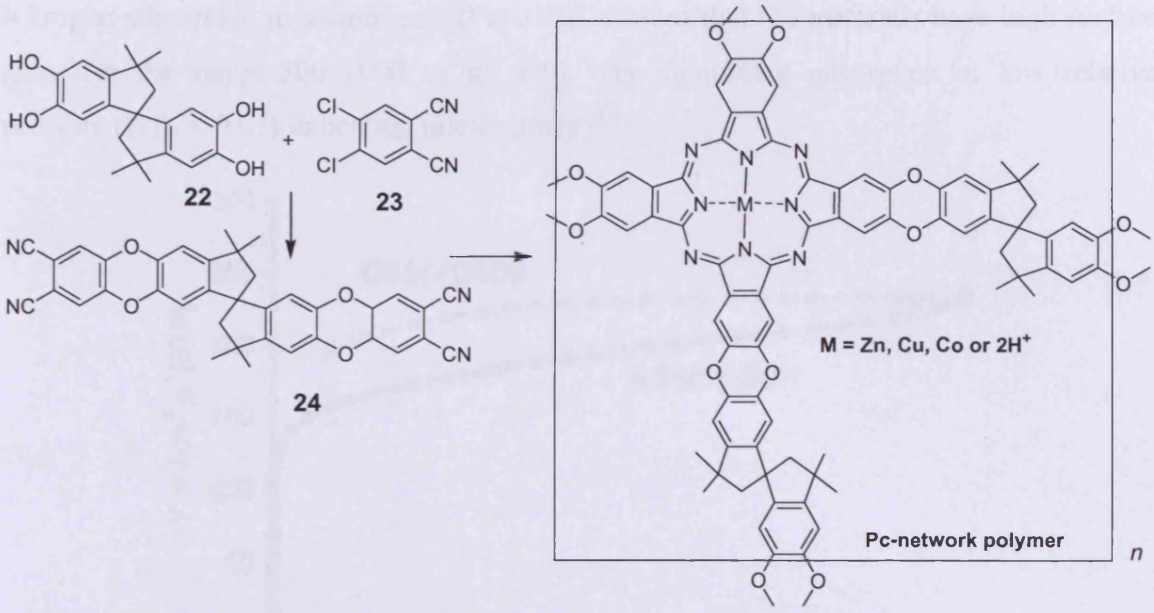

Scheme 1.8. Phthalocyanine network polymer formation.

Spectroscopic (ESR, UV/visible absorption) and SAXS (Small Angle X-ray Scattering) analyses of the network polymers confirm that the spiro-cyclic crosslinks prevent a close packing of the phthalocyanine components, giving an amorphous microporous structure as depicted by the model shown in Fig 1.11.

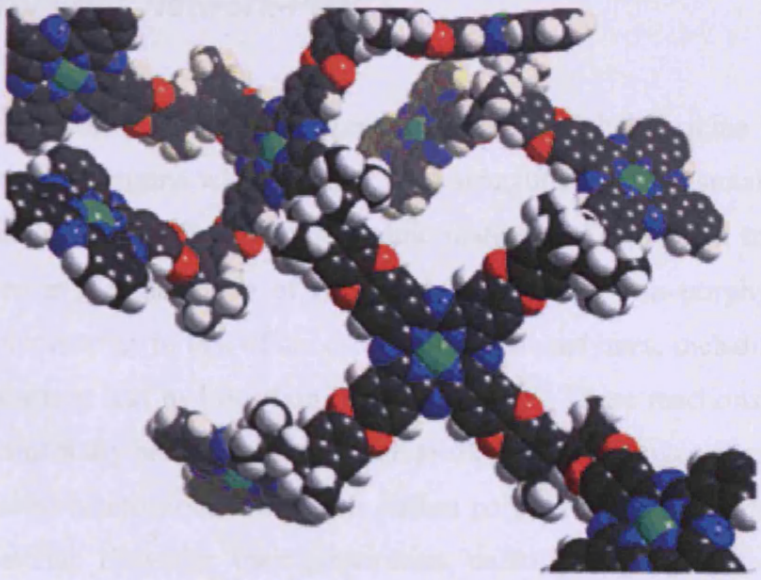

Fig 1.11 molecular model of a phthalocyanine network polymer.

Nitrogen adsorption measurements (Fig 1.12) showed that the materials have high surface areas (in the range 500–1000 m^2/g) with very significant adsorption at low relative pressure ($P/P_0 < 0.01$) indicating microporosity[69].

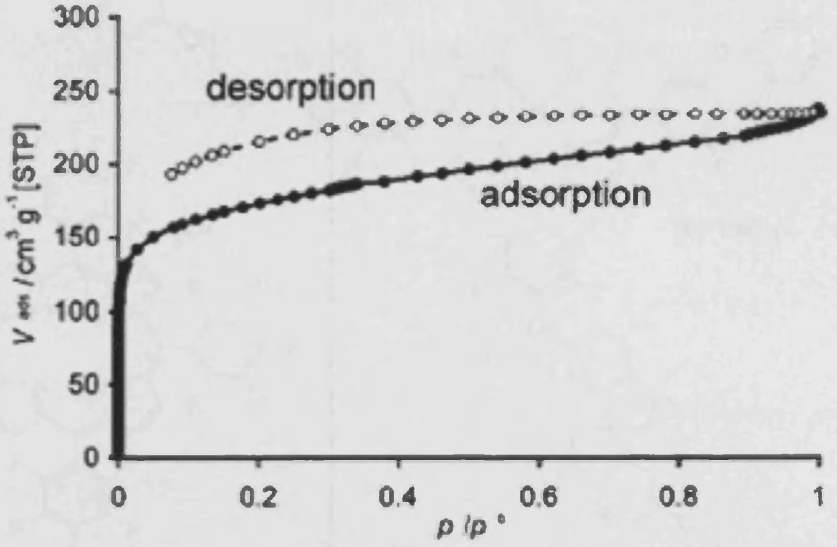

Fig 1.12. Nitrogen adsorption/desorption of a microporous phthalocyanine network polymer

1.6.2 *Porphyrins Network-PIMs*[73]

Following on from the successful preparation of the phthalocyanine Network-PIMs, it was of interest to determine whether other rigid structures are also suitable components for use in the assembly of microporous organic materials. The related metal-containing porphyrins are an important family of catalysts, for example, iron–porphyrin derivatives can display similar activity to that of the cytochromeP450 enzymes, including the catalysis of alkene epoxidations and hydrocarbon hydroxylations[74]. These reactions were achieved by using environmentally benign oxidants, such as oxygen or hydrogen peroxide. Thus, the possibility of useful heterogeneous catalysis makes porphyrins desirable components of a microporous material. However, their preparation, unlike phthalocyanine formation, is a low-yielding reaction that is unsuitable for polymer network assembly. Instead, rigid spiro-cyclic linking groups were introduced directly between preformed porphyrin subunits by means of the efficient dioxane-forming reaction between the meso-tetrakis(pentafluorophenyl)porphyrin (monomer **25**, Scheme 1.9) and the monomer **22**.

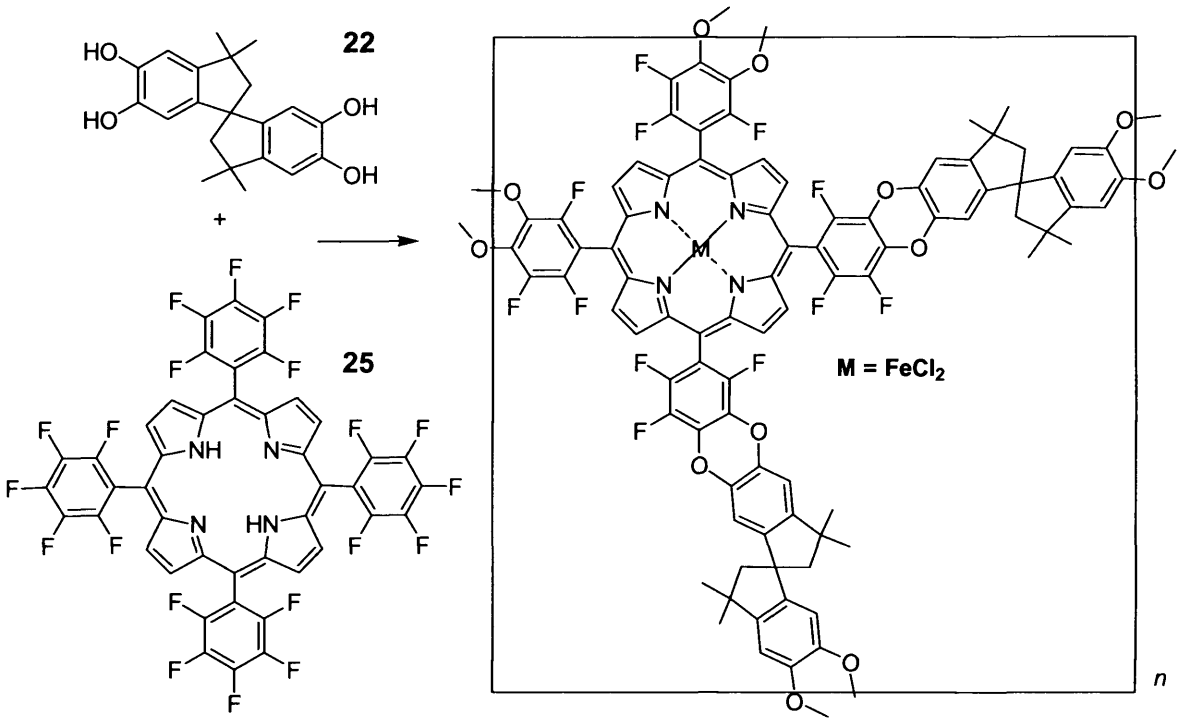

Scheme 1.9. Porphyrin network polymer formation

Although in this case the linking group is not wholly composed of fused rings, there is significant steric restriction to rotation about the single carbon–carbon bond at the meso-positions of the porphyrins to prevent structural relaxation, as demonstrated by the attainment of Network-PIMs of high surface areas (900–1100 m^2/g)[73].

1.6.3 HATN network-PIM[75]

This network-PIM was formed from the reaction between the spiro-cyclic monomer **22** and hexachlorohexaazatrinaphthylene [76] **26** (Scheme 1.10).

The important precursor, hexachlorohexaazatrinaphthylene **26**, was readily prepared in good yield from the condensation reaction between hexaketonecyclohexane and 4,5-dichlorophenylene-1,2-diamine[77,78].

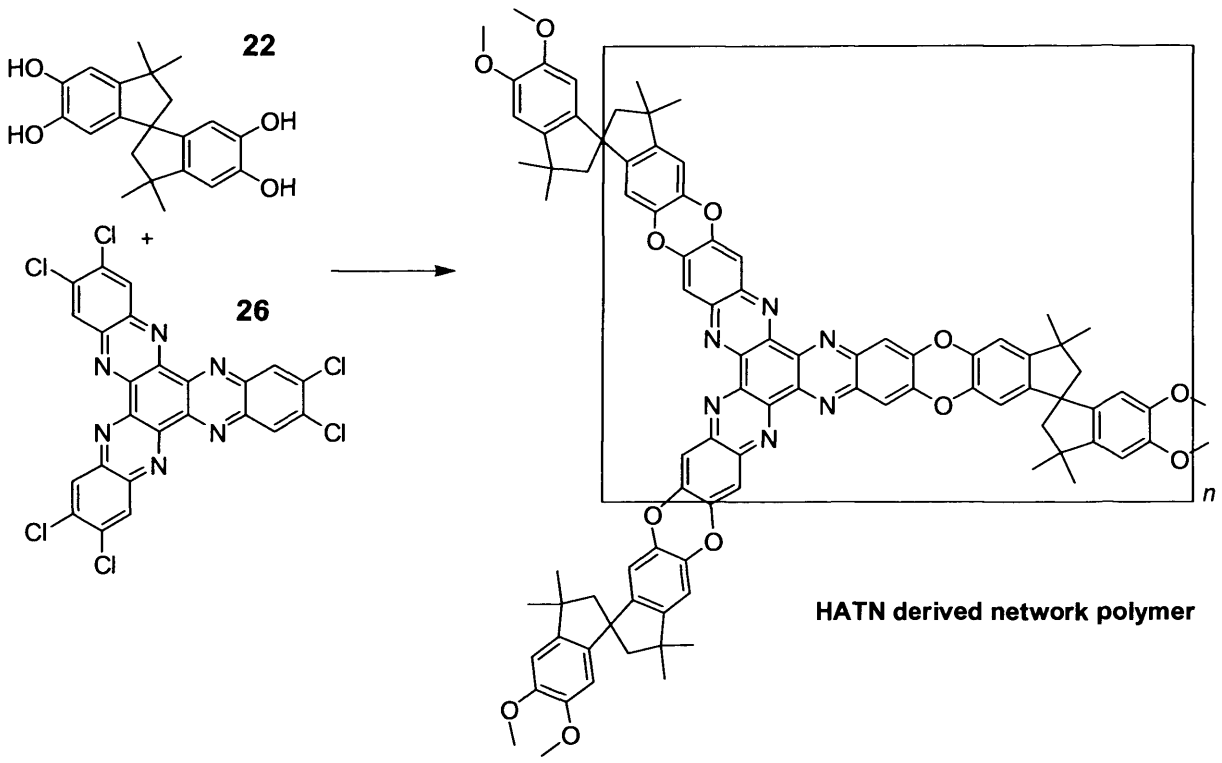

Scheme 1.10. HATN network polymer derived formation

Nitrogen adsorption measurements give BET values for the surface area of this polymer in the range 750–850 m^2/g. The shape of the adsorption isotherms and their marked hysteresis are similar to those obtained from the porphyrin and phthalocyanine networks and are consistent with a wide distribution of pore size, spanning the microporous range. In addition, the HATN-network-PIM has in-built ligands for metal complexation and the Pd(II) loaded material is proving an excellent heterogeneous catalyst for Suzuki aryl–aryl coupling reactions[79].

1.6.4 CTC network-PIM

In the context of gas adsorption, PIMs may offer an attractive combination of properties including low intrinsic density (they are composed of only light elements C, H, N, O a real advantage over MOFs materials), chemical homogeneity (an advantage over carbons), thermal and chemical stability, and synthetic reproducibility. Of particular interest is the potential to tailor the micropore structure by choice of monomer precursors, for example, by the use of monomers that contain pre-formed cavities to provide sites of an appropriately small size for hydrogen adsorption[75].

To investigate this possibility, the bowl-shaped receptor monomer, cyclotricatechylene[80] (CTC) **27** was incorporated within a network-PIM by using the usual benzodioxane-forming reaction between CTC and tetrafluoroterephthalonitrile **28**. (Scheme 1.11)

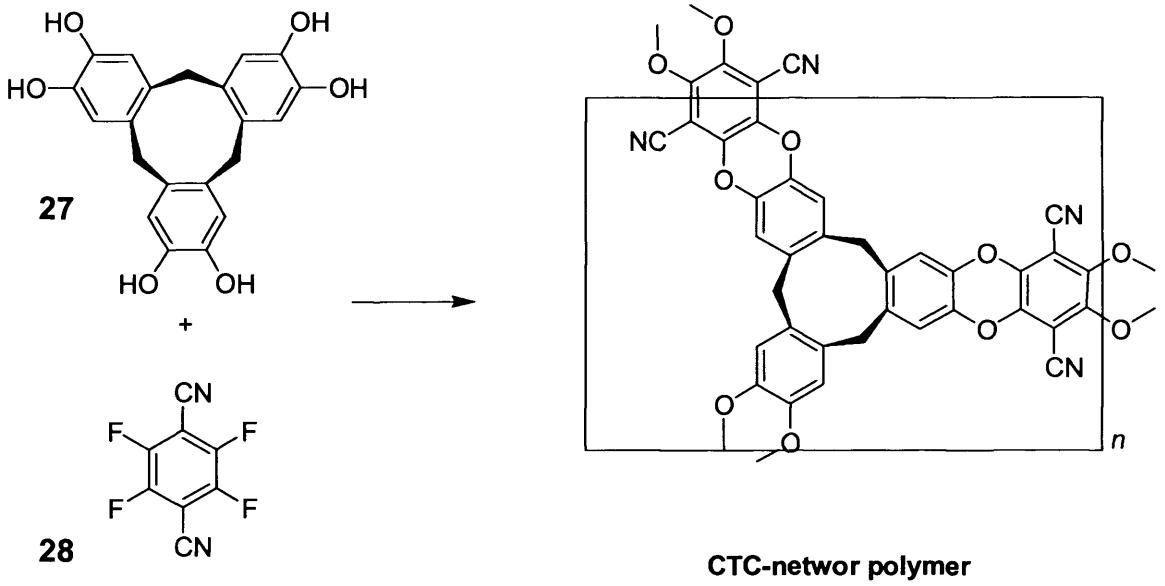

Scheme 1.11. CTC network polymer formation

The gas-adsorption properties of the resulting material, designated CTC-network-PIM were compared to those of HATN-network-PIM. Complementary sorption isotherms for each of the PIMs were obtained for ultra pure, dry H_2 at 77 K by using both gravimetric analysis (Hiden IGA-1), over the pressure range 0 to 20 bar, and volumetric analysis (Micromeritics ASAP 2020), over the range 0 to 1 bar, the obtained results are listed in Table 1.1.

PIM	BET Area (m^2/g)	% mass H_2 (1 bar, 77K)	% mass H_2 (10 bar, 77 K)	H_2 per fused ring
HATN	820	1.37	1.56	0.43
CTC	830	1.43	1.70	0.56

Table 1.1. Gas adsorption data for PIMs

The BET surface area of each PIM is in the region of 800 m^2/g as measured by nitrogen adsorption at 77 K. Analysis of the low-pressure nitrogen adsorption data by the Horvath–Kawazoe method indicates that in each case the pore size distribution is strongly biased towards pores in the range 0.6 – 0.7 nm (Fig 1.13).

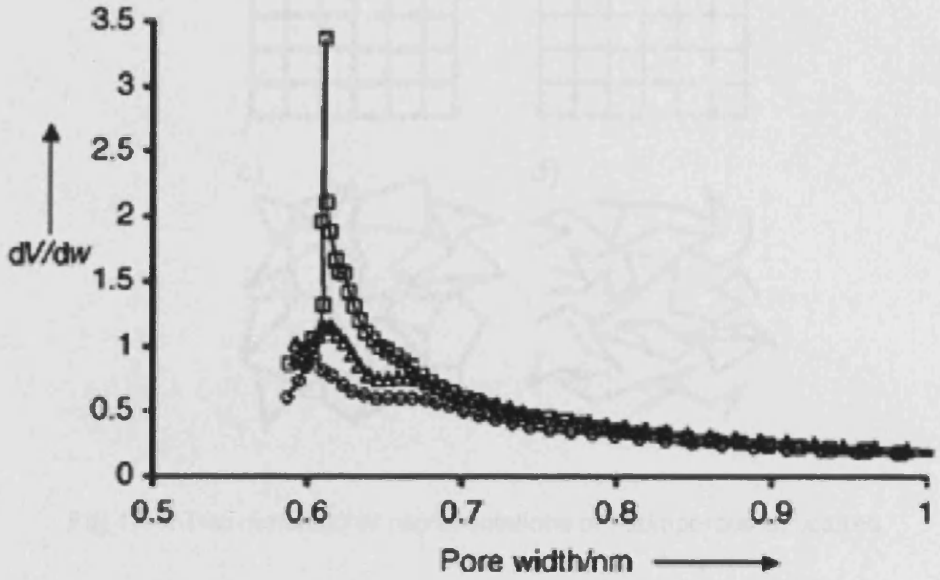

Fig 1.13. Apparent micropore size distribution

The particularly marked concentration of micropores of 0.6 nm diameter for the CTC-network-PIM appears related to the internal dimensions of the bowl-shaped CTC subunit and suggests that pore size distribution within PIMs can be tuned by the choice of monomer precursor.

1.7 Soluble-PIMs[81]

All conventional microporous materials are network polymers held together by robust covalent bonds (*e.g.* zeolites Fig 1.14a). Network-PIMs showed an amorphous structure similar to activated carbon (Fig 1.14 c). Crystalline zeolite analogues are effectively networks with strong noncovalent cross-links composed of metal–ligand or multiple hydrogen bonds (*e.g.* MOFs[60] Fig 1.14 b). Some of these display swelling in the

presence of an adsorbate. The relatively weak intermolecular interactions within such a material could be reversibly disrupted by solvent to allow solution processing, a clear advantage over other microporous materials.

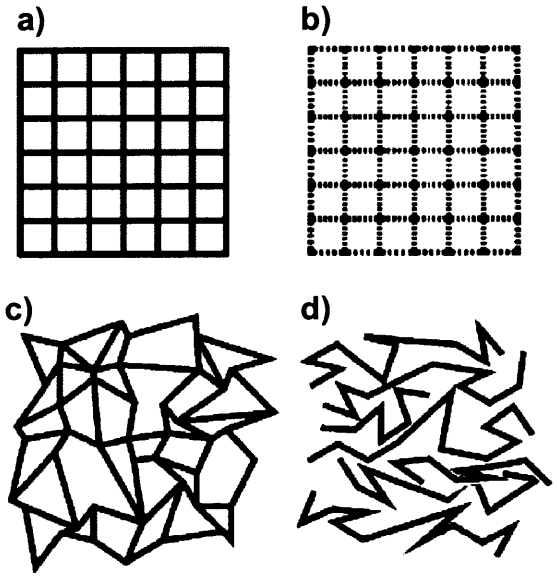

Fig 1.14. Two dimensional representations of microporous structures.

Generally, polymers pack space efficiently because the macromolecules can bend and twist to maximise intermolecular interactions. However, it has long been recognised that some polymers can possess large amounts of void space, which is usually referred to as free volume. In this context, are shown non-network polymers (Fig 1.14 d) from various combinations of the bifunctional monomers (Scheme 1.12; f_{av} = average functionality = 2) that proved successful in forming Network-PIMs. The reaction between the aromatic tetrol monomers **22, 29, 30** with the appropriate fluorine-containing compounds **28, 31, 32** gave soluble PIMs **1–6** (Scheme 1.12 and Table 1.2). With the exception of the readily prepared 1,2,4,5-tetrahydroxybenzene[82] (**30**), the monomers are all commercially available.

The combination of the fact that one of the two precursor monomers contains a "site of contortion" (*e.g.* **22**), with the planarity of the dibenzodioxane ring formed during the polymerization, induces microporosity in this family of non-network polymers simply because their highly rigid and contorted molecular structures cannot fill space efficiently. In particular, the lack of rotational freedom along the polymer backbone ensures that the macromolecules cannot rearrange their conformation to collapse the open structure of the material, resulting in solids that possess high surface areas (500–780 m^2/g).

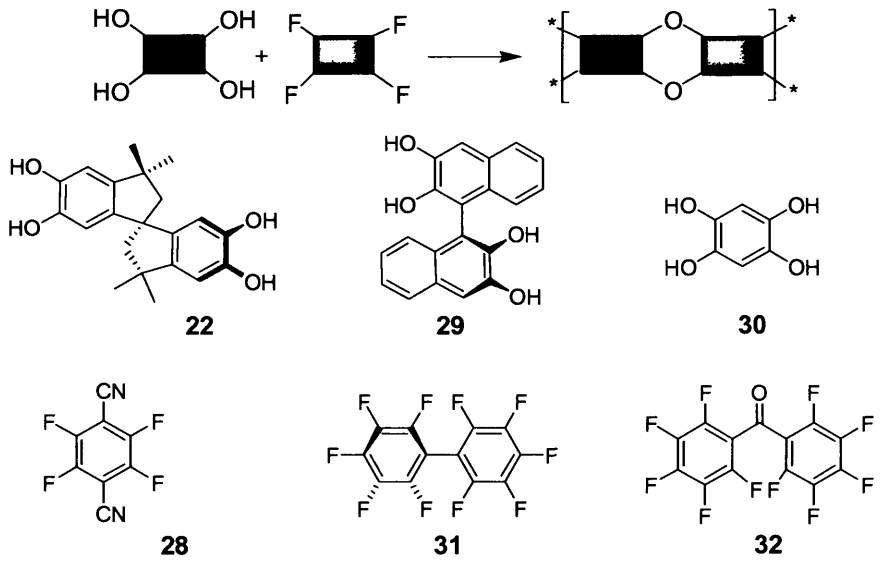

Scheme 1.12. Different monomers

In addition, unlike conventional microporous materials, they are soluble and can be processed readily using solvent-based techniques. With the exception of PIM-**6**, which is soluble only in acidic solvents (*e.g.* TFA), the polymers are freely soluble in polar aprotic solvents (*e.g.* THF, DMAc) and this allows their average molecular mass to be estimated by gel permeation chromatography (GPC) relative to polystyrene standards (Table 1.2).

The two polymers derived from the reaction of **30** and **28** or **30** and **32** are likely to be linear (dibenzodioxane is planar[83]) and thus able to pack efficiently. Indeed, these polymers proved to be highly insoluble, non-porous materials (BET surface area < 20 m^2/g).

PIM	Monomer A	Monomer B	$M_w/10^3$ g/mol	M_w/M_n	Surface area m^2/g
1	22	28	270	2.8	780
2	22	31	36	4.3	600
3	22	32	171	3.1	560
4	29	28	5	1.9	440
5	29	31	15	1.7	540
6	30	31	Insoluble	Insoluble	430

Table 1.2. Molecular mass measured by GPC vs. polystyrene as standard and BET surface area, from nitrogen adsorption for **PIMs 1-6**

Thermal analysis of each of the polymers shows no glass transition or melting point below the temperature of thermal decomposition. Surface area determination demonstrates that **PIMs 1–6** are microporous with high surface areas. Micropore analysis (Horvath–Kawazoe method)[84] indicates a significant proportion of micropores with dimensions in the range 0.4–0.8 nm. There is also evidence of some mesoporosity. The marked hysteresis at low pressures may be attributed to pore network effects (for example, mesopores accessible only through micropores).

1.7.1 PIMs derived from Bis (phenazyl) Monomers [85]

A large number of bis (catechol) monomers have been used for PIM synthesis[81] but there are no readily available tetra-halide monomers that contain spiro-centres to provide a suitable site of contortion. This was remedied by the simple synthesis of suitably reactive tetrachloride monomers based on phenazine units prepared directly from suitable bis (catechol) monomers such as **22** and 2,3,6,7-tetrahydroxy-9,10-dimethyl-9,10-ethanoanthracene **35**. This is achieved by oxidation of the bis-catechol with nitric acid[86], or more efficiently with CAN[87], to produce the bisquinones **33** and **36** that, on reaction with 1,2-diamino-4,5-dichlorobenzene, provide the monomers **34** and **37** (Scheme 1.13).

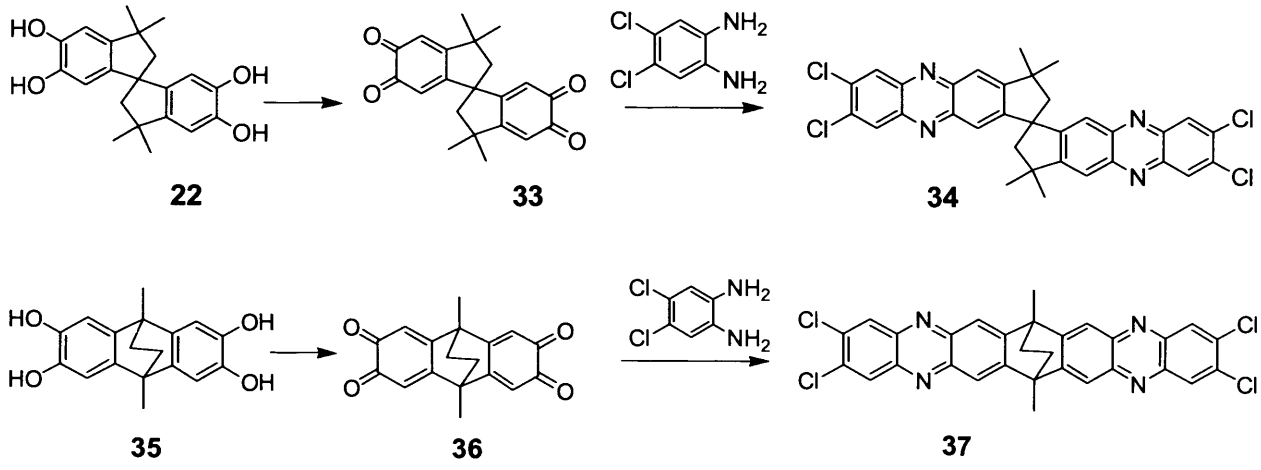

Scheme 1.13. Preparation of halogenated monomers

PIMs-**7-10** were prepared by the reactions between monomers **22** and **34**, **35** and **34**, **22** and **37**, and **35** and **37**, respectively (Scheme 1.14). PIMs-**7-9** are soluble in a range of organic solvents (especially $CHCl_3$), but PIM-**10** is soluble only in *m*-cresol and concentrated H_2SO_4.

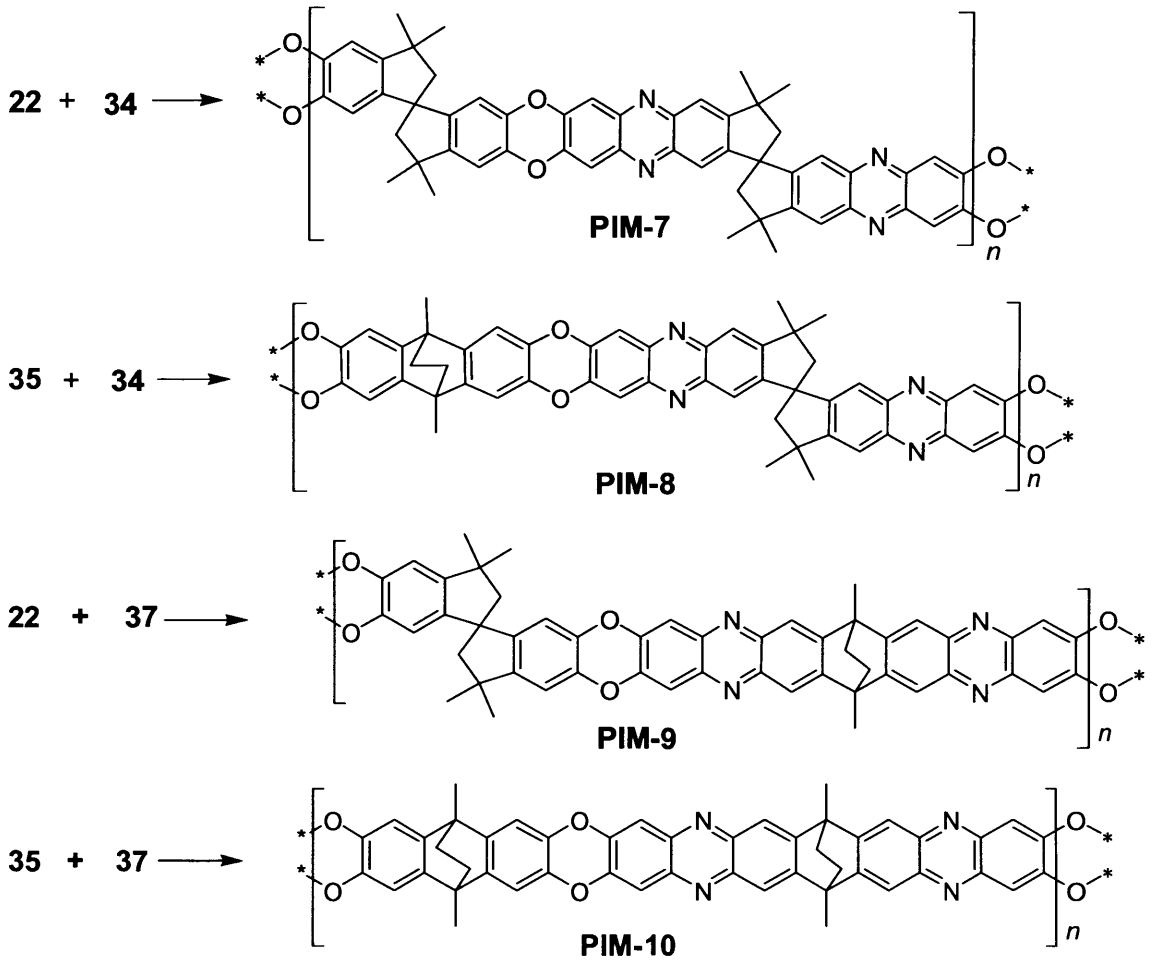

Scheme 1.14. Preparation of **PIMs 7-10**

GPC confirmed that the polymers possess reasonably high average molecular mass. For example, purified PIM-7 prepared under optimized reaction conditions has apparent average molecular masses of Mn = 26000 and Mw = 51000 g/mol relative to polystyrene standards. ^{1}H NMR spectra of PIMs-**7-9** are consistent with their anticipated structures.

Nitrogen adsorption isotherms measured at 77 K confirms that PIMs-**7-10** are microporous (Table 1.3) as shown by the significant adsorption at low pressure ($P/P_0 <$ 0.1). BET analysis of the isotherms provides an apparent surface area for each polymer of more than 650 m^2/g.

	PIM-7	**PIM-8**	**PIM-9**	**PIM-10**
Surface area (m^2/g)	680	677	661	713
Pore volume (cm^3/g)	0.56	0.48	0.47	0.44

Table 1.3. surface areas of PIM **7-10** from nitrogen adsorption isotherms

1.8 Aims of the project

The excellent properties shown by certain PIMs as hydrogen storage materials and as components for gas separation membranes seem to be related to their strong interactions with gas molecules. Therefore, we were interested in preparing novel PIMs that will have even stronger intermolecular interactions (i.e. van der Waals forces) due to a greater concentration of aromatic and polar components. Also, by selecting appropriate monomers, it is possible to introduce specific molecular recognition or catalytic sites, thus facilitating chemo-selective adsorption and the design of efficient heterogeneous catalysts. Therefore new synthetic approaches to preparing suitable monomers for PIMs are required.

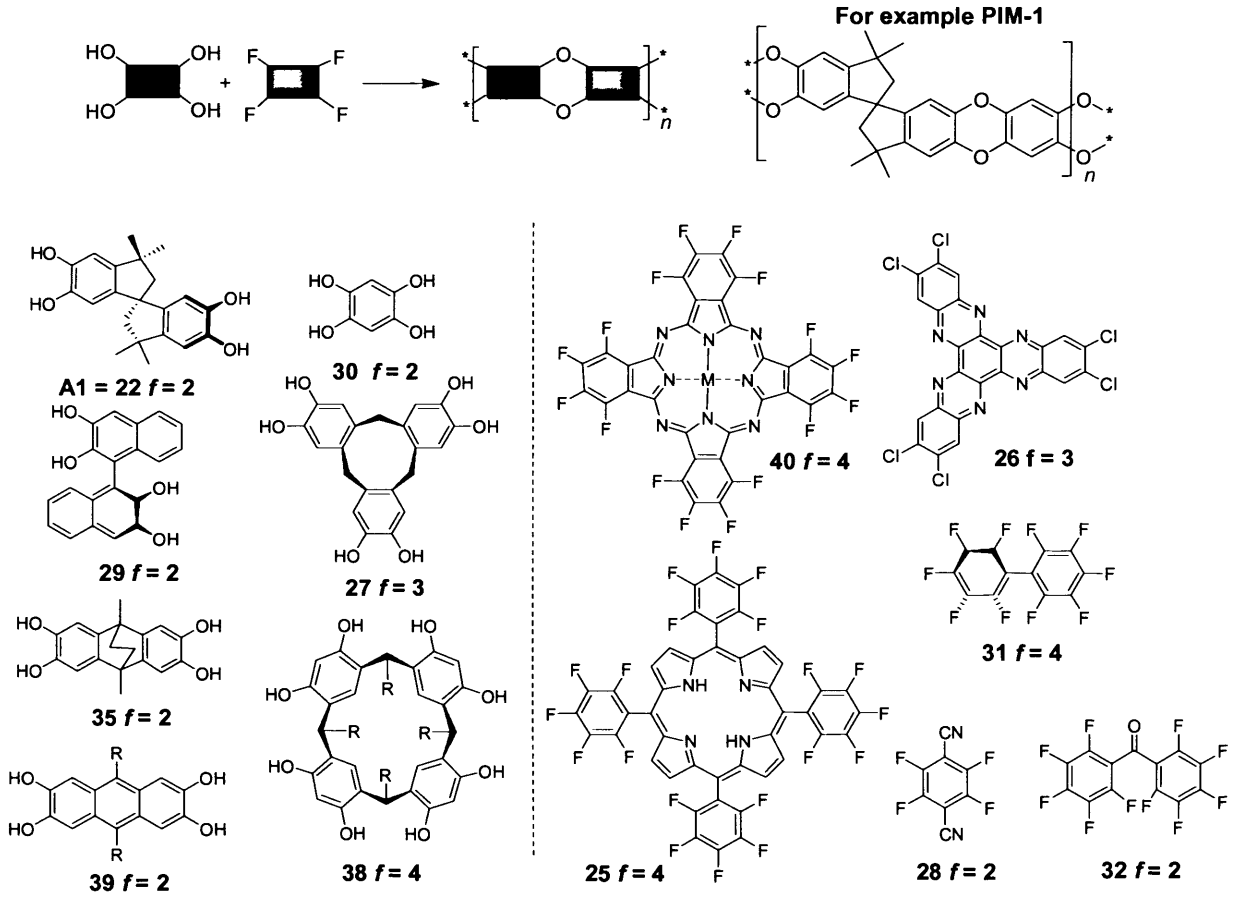

Scheme 1.15. Choice of monomers for PIMs.

As noted, PIMs are prepared via a dioxane-forming polymerisation reaction (a double aromatic nucleophilic substitution) using a combination of appropriate hydroxylated aromatic monomers and fluorinated (or chlorinated) aromatic monomers. For

microporosity, at least one of the monomers must contain a *site of contortion*, which may be a spiro-centre (*e.g.* **22**), a single covalent bond around which rotation is hindered (e.g. **25**, **29** and **31**) or a rigid, non-planar skeleton (e.g. **27, 35** and **38**). To obtain an insoluble network polymer, the average functionality (f_{av}) of the monomer combination should be greater than two ($f_{av} > 2$) whereas to prepare a soluble PIM should be used a combination of monomers both of which having $f = 2$. The aim of the research described in this thesis has been mostly focused on the synthesis of new bis-catechol monomers with a structure similar to **22** (i.e. a spirobisindane structure) compatible with efficient polymerisation with monomer **28**, in order to generate new ladder polymers soluble in common organic solvents but with enhanced gas adsorption properties due to greater contribution from polar and polarisable substituents. From this perspective, a simple analysis of the molecular structure of PIM-**1** suggests that the, apparently, least useful components in structure of PIM-**1** (Scheme 1.16) are the four methyl groups per repeat unit, which contribute neither polarity nor polarisability. Therefore, our objective was to prepare novel spirobisindane-based biscatechol monomers in which the methyl groups are replaced with a range of relevant polar and polarisable substituents.

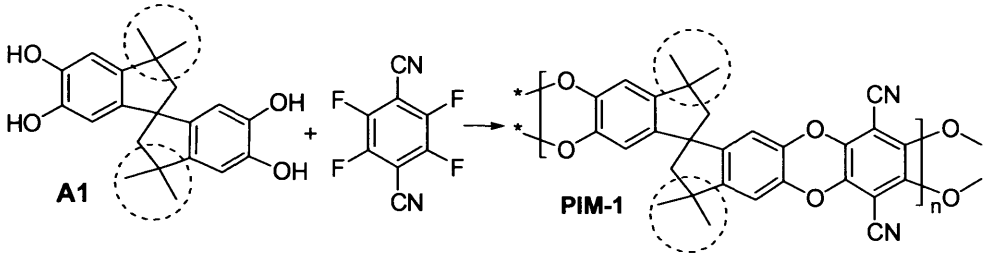

Scheme 1.16. PIM-1 synthesis and the proposed sites for modification.

Looking at the well-established preparation of the monomer **22** (5,5',6,6'-tetrahydroxy-3,3,3',3'-tetramethyl-1,1'-spiro-bisindane), by simple acid-mediated condensation of acetone and catechol[88], it appeared difficult to make simple modifications to this chemistry that would lead to desired target monomers. For that reason, we decided initially to attempt the synthesis of spirobisindane monomers containing, for example, ketone groups that are potential sites for further substitution. Similarly, it was desired to determine the effect on the polymer microporosity of changing the size of the spiro-fused rings. The development of synthetic routes for the introduction of sacrificial groups which may leave additional space (i.e. microporosity) behind once removed was also a key objective of the research programme.

Chapter 2

2.1 Novel spirobisindane monomers

The starting point for the synthetic investigations was the known 5,5',6,6'-tetramethoxy-spiro(bisindane)-3,3'-dione **41** (Fig 2.1) which could be used as a precursor for introducing aromatic substituents at the 3,3' positions of the spirobisindane unit.

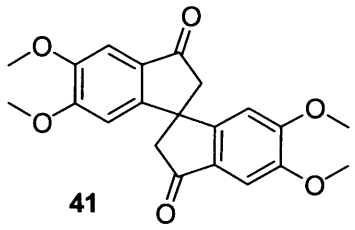

Scheme 2.1. Spiro-ketone (5,5',6,6'-tetramethoxy-spiro(bisindane)-3,3'-dione) **41**

2.1.1 Previous synthesis of the spiro-ketone monomer 41

The spiro-monomer **41** was previously reported by Baker and Williams[89] who used a four-step synthesis (Scheme 2.2) including a reduction and oxidation step with an overall modest yield (12%). The use of the oxidant chromium trioxide is also an unattractive feature of this route.

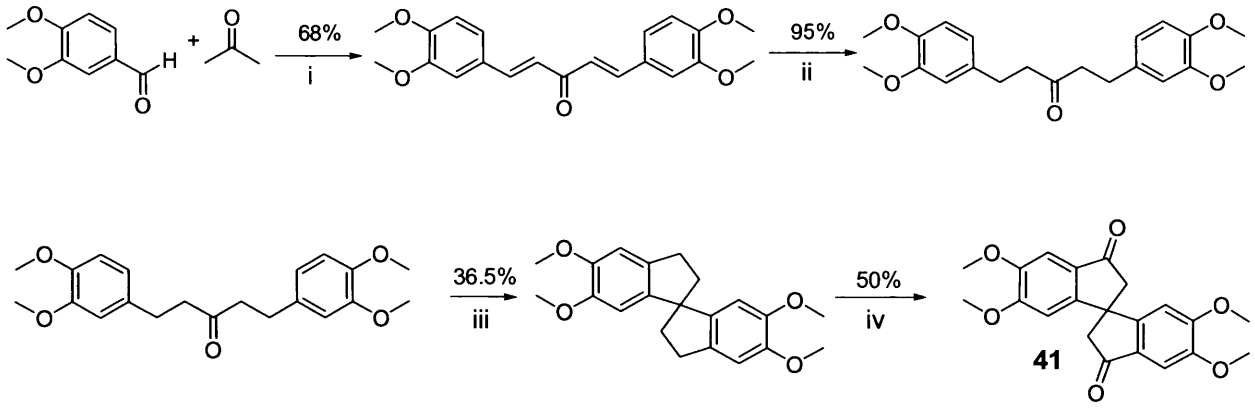

Scheme 2.2 Reported Synthesis of precursor **41**. *Reagent and conditions*: i. NaOH, ii. H_2 Pd/C, iii. $POCl_3$, iv. CrO_3

2.1.2 A novel approach to the synthesis of the spiro-ketone monomer 41

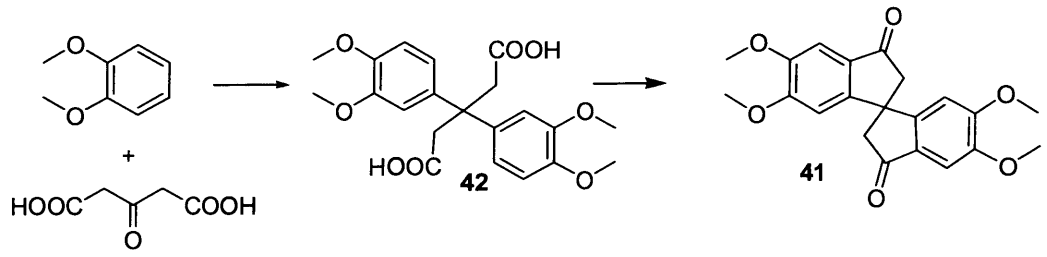

Scheme 2.3. Proposed new synthesis of the spiro-ketone monomer **41**

It was clear that large amounts of the precursor **41** were going to be required and therefore a more direct and efficient synthesis was devised (Scheme 2.3). It was planned to use the new intermediate 3,3-bis(3,4-dimethoxyphenyl) pentanedioic acid **42** and prepare **41** via a double intramolecular Friedel-Craft acylation. Initially the diacid **42** was to be prepared using a method similar to that reported by Korgaonkar *et a.l*[90] using veratrole and acetone dicarboxylic acid with sulfuric acid as solvent (Scheme 2.4).

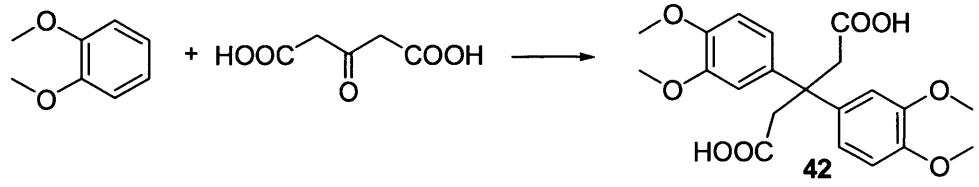

Scheme 2.4. Synthesis of dicarboxylic acid **42**. *Reagent and conditions*: H_2SO_4, RT

This reaction gave different results depending upon the kind and the amount of acid used, the temperature of the reaction and, most importantly, the number of equivalents of veratrole. In fact, the stated starting conditions, using 2.5 equivalents of veratrole, always proved inadequate for the formation of the required product, so the amount of veratrole was increased following a systematic investigation. The acids used were sulfuric acid (concentrated and 60% aqueous) and polyphosphoric acid (PPA). The best result, as shown in Table 2.1, was achieved using 1.5 ml (per equivalent of veratrole) of concentrated sulfuric acid at room temperature. Higher temperatures and larger amounts of acid seemed to give more side products and decomposition of the starting materials, whereas the use of a lesser amount of acid reduced the yield.

Veratrole (eq)	Acid used	T (°C)	Yield of 42
2.5	$H_2SO_{4\ conc}$	RT	no product
5	$H_2SO_{4\ conc}$	RT	10%
8	**$H_2SO_{4\ conc}$**	**RT**	**30%**
2.5	$H_2SO_{4\ conc}$	60 °C	no product
8	$H_2SO_{4\ conc}$	60 °C	poor yield
2.5	Diluted H_2SO_4	RT	no product
8	Diluted H_2SO_4	RT	no product
8	Diluted H_2SO_4	60 °C	no product
8	PPA	50 °C	no product
8	PPA	80 °C	poor yield

Table 2.1. Reaction with veratrole and dicarboxylic acid

These results were much less satisfactory than we expected, thus we decided to study an alternative but related procedure involving the substitution of the acetone dicarboxylic acid, with diethyl 1,3-acetone dicarboxylate (Scheme 2.5), to give initially 3,3-bis(3,4-dimethoxyphenyl) pentanedioate and the reaction was investigated by the same systematic procedures as used previously.

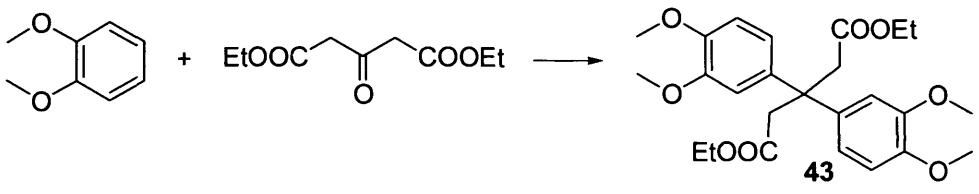

Scheme 2.5. Synthesis of ester **43**. *Reagent and conditions*: H_2SO_4, RT

The use of the diethyl ester gave better results, with an optimised yield of 59% (Table 2.2). Furthermore, being an ester rather than a diacid, the purification proved much easier. In fact, the final product was isolated either by flash chromatography or, preferentially, simply by removal by vacuum distillation of the excess veratrole followed by recrystallisation from methanol.

Veratrole (eq)	Acid used	T (°C)	Yield of 43
2.5	$H_2SO_{4\ conc}$	RT	no product
5	$H_2SO_{4\ conc}$	RT	30%
8	**$H_2SO_{4\ conc}$**	**RT**	**59%**
2.5	$H_2SO_{4\ conc}$	60 °C	no product
8	$H_2SO_{4\ conc}$	60 °C	40%
2.5	Dilute H_2SO_4	RT	no product
8	Dilute H_2SO_4	RT	poor yield
8	Dilute H_2SO_4	60 °C	no product
8	PPA	50 °C	poor yield
8	PPA	80 °C	32%

Table 2.2. Reaction with veratrole and diethyl ester.

The subsequent hydrolysis of the ester **43** to give diacid **42** was achieved in a mixture of 40% aqueous NaOH and MeOH at 40 °C, leading us to 3,3-bis(3,4-dimethoxyphenyl) pentanedioic acid **42** in near quantitative yield (Scheme 2.6).

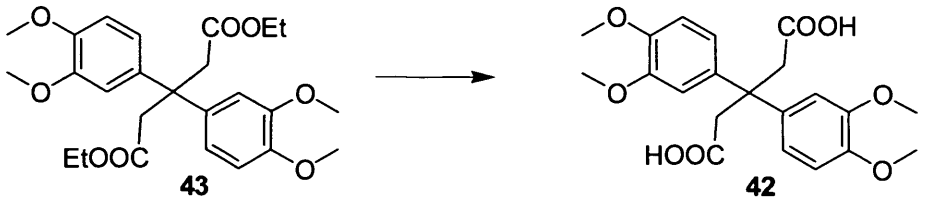

Scheme 2.6. Ester hydrolysis. *Reagent and conditions*: NaOH/MeOH, 40 °C

The reaction of cyclodehydration of the dicarboxylic acid **1** to give the desired diketone **41** was achieved in polyphosphoric acid, following existing procedures.[91,92,93,94] The reaction time and temperature were crucial factors and after a few attempts we found that the best conditions were 80 °C for 3 h. Polyphosphoric acid appeared to be a good solvent for oxygen-containing organic compounds. At room temperature it is a very viscous liquid but at 50-60 °C it becomes sufficiently mobile that no difficulty is encountered in stirring the reaction mixture. The substance does not react violently with water, so even warm reaction mixtures may be decomposed without inconvenience by

addition to water or ice, which was the method used to precipitate **41** to give a 60% yield (Scheme 2.7). An alternative to the often problematic use of polyphosphoric acid, especially due to its high viscosity, is Eaton's reagent[95], a commercially available 10 wt % solution of phosphorous pentoxide in methanesulfonic acid[96], now widely used as dehydrating agent especially for cyclizations[97,98]. In our case, as well as making the reaction easier to handle, its use brought an improvement of the yield up to 84% and an easier purification of the product. The same reaction was also attempted in concentrated sulfuric acid at 60 °C but, as predicted by the literature[92], gave a lower yield (30%). The only significant problem represented by Eaton's reagent is its expense compared to PPA and sulfuric acid, although it is easy and cheaper to prepare on a laboratory scale. The overall yield of the entire process of making diketone **41** is an excellent 47%.

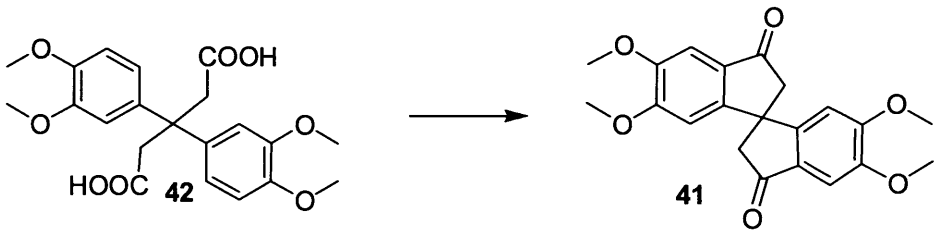

Scheme 2.7. Synthesis of spiro-ketone **41**. *Reagent and conditions*: Eaton's reagent, RT

To complete the synthesis of the first monomer **44**, the demethylation of the spiro-ketone **41**, was performed. Based on previous literature work[99,100], the reaction was carried out with boron tribromide (BBr_3) as demethylating agent in inert atmosphere and was attempted in two different ways: the first one using a 1 M solution of BBr_3 in dichloromethane, the second utilizing neat BBr_3. Even though we found the 1 M solution easier to handle, with the pure BBr_3 the reaction proved to be faster and provided a near quantitative yield (Scheme 2.8).

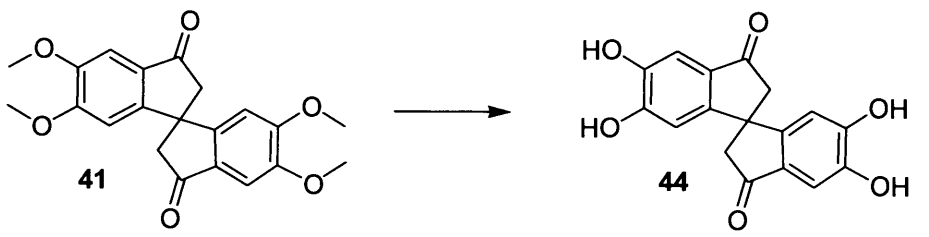

Scheme 2.8. Spiro-ketone demethylation. *Reagent and conditions*: BBr_3, DCM

2.1.3 Synthesis of 3,3'-diphenyl-1,1'-spirobisindene monomer 45

One of the most important reactions of the ketone group involves the use of Grignard reagents and this provided a direct route to the addition of aromatic substituents onto the spirobisindane unit (Scheme 2.9). A solution of the diketone **41** in THF was reacted with freshly prepared phenyl magnesium bromide. Despite the high reactivity of this Grignard reagent, we obtained the best result by leaving the solution at room temperature for 24 h, this is principally due to the poor solubility of the monomer in solvents commonly used to carry out this class of reaction (THF, Et_2O, toluene). The resulting tertiary alcohol proved difficult to isolate, it was preferred to treat the crude product with aqueous sulfuric acid to accomplish the dehydration of the molecule and thus to form the spirobisindene unit in good yield (74%).

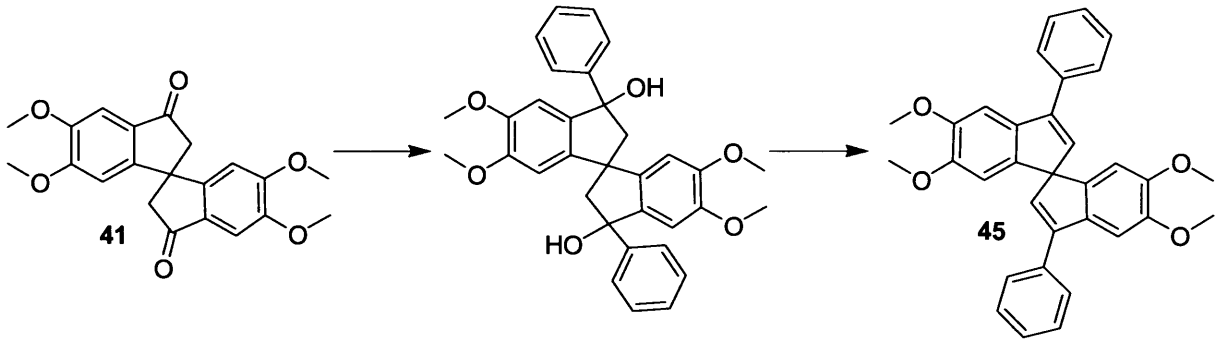

Scheme 2.9. Spirobisindene 45 synthesis. *Reagent and conditions*: i PhMgBr, ii $20\%_{aq}$ H_2SO_4

To accomplish the synthesis of the new monomer, we performed the demethylation of the spiro-indene with boron tribromide. The reaction did not present any problems and we obtained the bis-catechol **46** in good yield (Scheme 2.10).

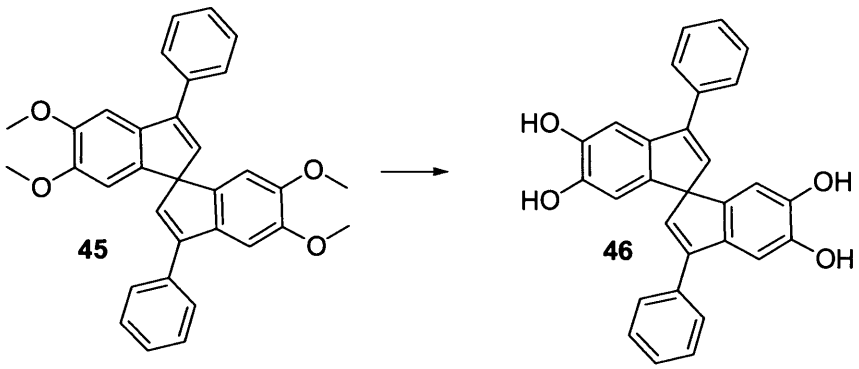

Scheme 2.10. Spiro indene **46** synthesis. *Reagent and conditions*: BBr_3, DCM

2.1.4 Attempted synthesis of the tetraphenylspirobisindane monomer 47

An obvious target monomer was the spirobisindane, 5,6,5',6'-tetrahydroxy-3,3,3',3'-tetraphenyl-1,1'-spirobisindane **47**, which is analogous to **A1** but with four phenyl rings instead of four methyl groups at the 3,3' positions. Our first approach towards this molecule started from the previously isolated ester **43** and, using an excess of phenyl magnesium bromide, we tried to perform a double addition on each ester group, aiming to obtain the tetraphenyl-substituted product, which could undergo an intramolecular cyclization (Scheme 2.11).

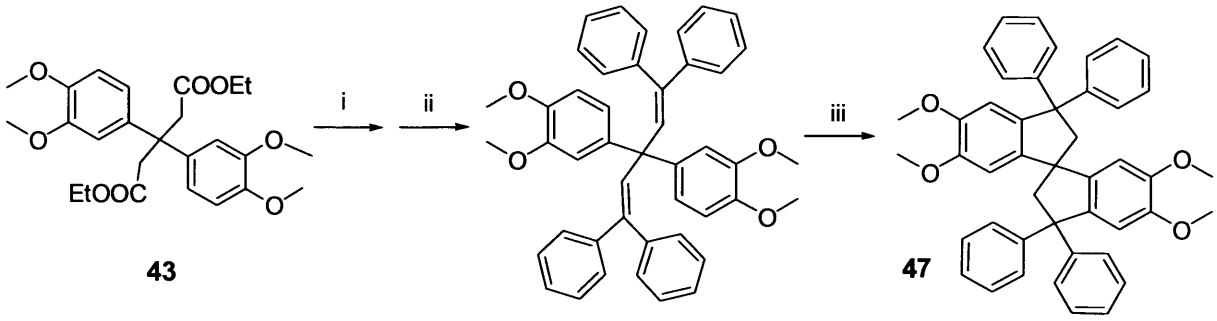

Scheme 2.11. Proposed synthesis of **47**. *Reagent and conditions*. i PhMgBr, ii 20%$_{aq}$ H_2SO_4, iii PPA

Unfortunately, this reaction plan proved much more complicated than anticipated (Scheme 2.12) and gave some unexpected products. The first problem emerged with the reaction of the phenyl magnesium bromide on the ester **43**, which surprisingly yielded the six-member lactone **48** (Scheme 2.13), instead of the desired product.

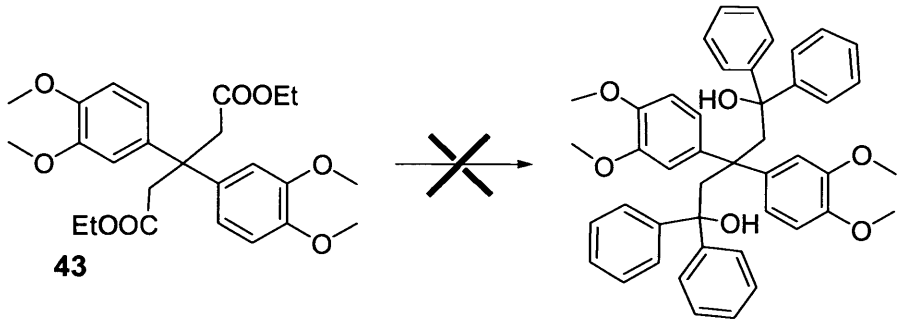

Scheme 2.12. *Reagent and conditions*. PhMgBr, THF

The efficient synthesis of the lactone **48** can be ascribed to the relatively rapid intramolecular cyclisation and the remarkable stability of the lactone towards further Grignard addition. Further addition of Grignard reagent to the isolated lactone proved futile even under forcing conditions (e.g. large excess of Grignard and refluxing THF). Although rare, there are precedents for stable lactone formation from the addition of Grignard reagent to diesters in the literature.[101,102]

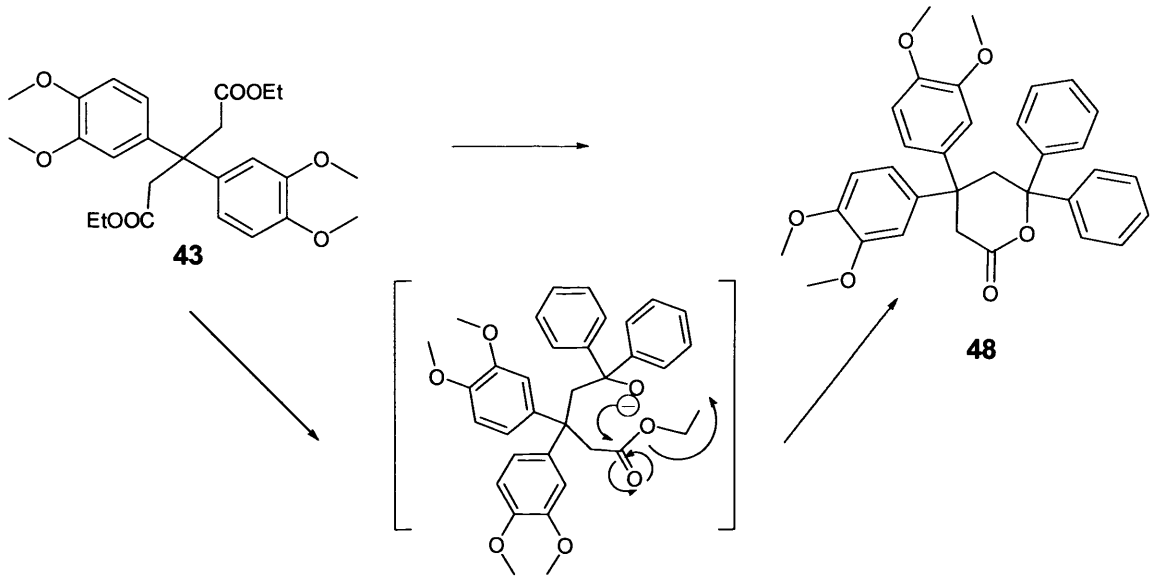

Scheme 2.13. Proposed mechanistic path for the formation of the lactone **48**.

Moving toward the possible synthesis of the tetra-phenyl monomer, an acid mediated transesterification of the lactone with methanol was attempted (Scheme 2.14). As hoped, this transesterification was accompanied by an efficient intramolecular cyclisation to provide one of the indane subunits to give **49**. A similar result was obtained using ethanol as solvent.

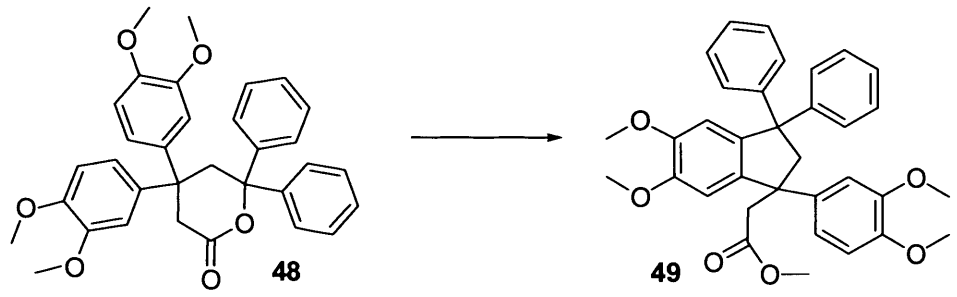

Scheme 2.14. *Reagent and conditions.* H_2SO_4, MeOH

The ester **49** reacted with further phenyl magnesium bromide to give, without any particular problems of isolation and purification, the tertiary alcohol **50** as shown in Scheme 2.15.

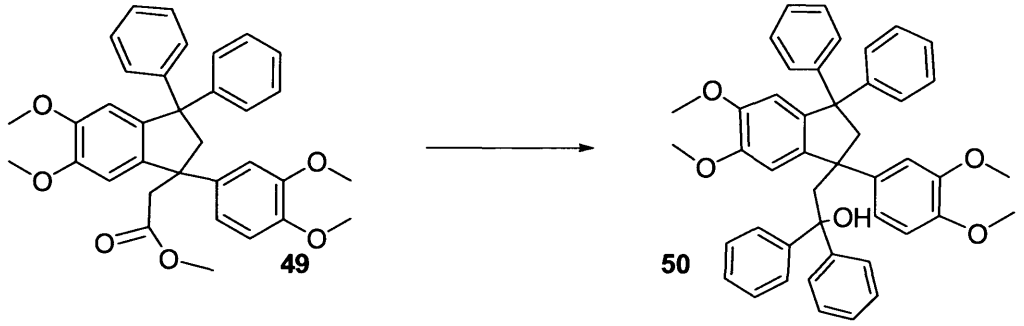

Scheme 2.15. *Reagent and conditions.* PhMgBr, THF

The reaction to give the desired tetraphenyl-spirobisindane monomer **47**, *via* the apparently straightforward acid mediated, ring-closure of the alcohol, gave unpredicted and unwanted products in very high yield (90%) via fragmentation of the molecule (Scheme 2.16). Despite all attempts, conducted with a very wide range of acids and conditions, as shown in Table 2.3, and following similar procedures found in the literature,[103,104,105] fragmentation prevented isolation of the desired molecule **47**.

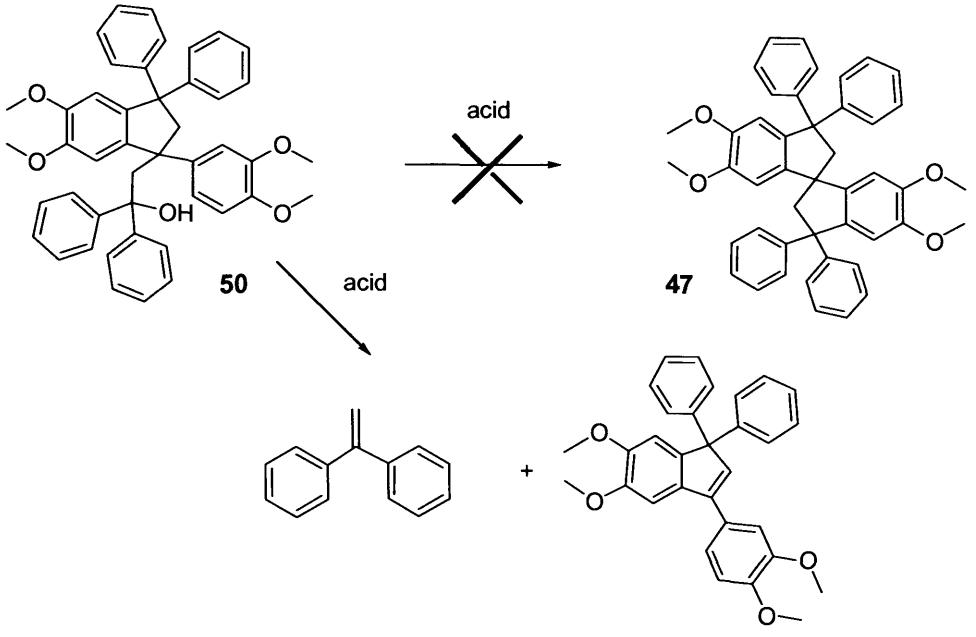

Scheme 2.16. Fragmentation reaction

The mechanism occurs via initial formation of a carbocation stabilised by two unsubstituted phenyl rings, whereas fragmentation provides a carbocation whose stability is enhanced by two electron-rich 3,4-dimethoxyphenyl substituents (Scheme 2.17).

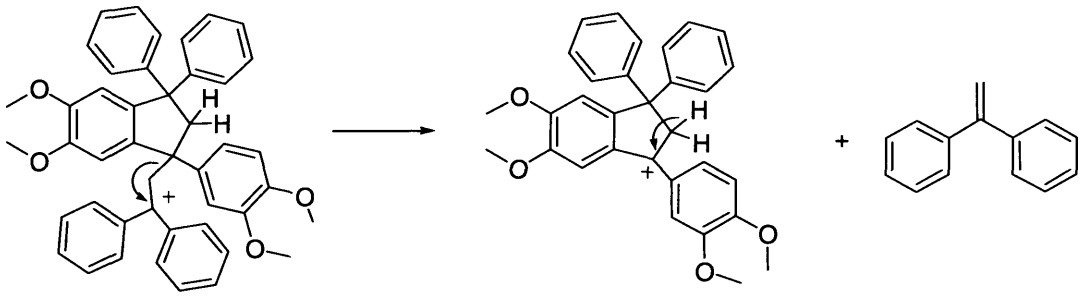

Scheme 2.17. Proposed mechanism for the fragmentation reaction

Acid used	Condition
H_2SO_4 conc	RT and 0 °C
H_2SO_4 60%	RT and 0 °C
$POCl_3$	RT
CH_3COCl + acetic anhydride[106]	RT
Eaton's reagent	RT and 0 °C
BF_3•Et_2O	RT
TFA[107,108]	RT
BBr_3	RT
ZnBr[109]	RT

Table 2.3. Acid and Lewis acids used for the attempted ring closure of **47**.

Further attempts at synthesising the desired tetra-phenyl monomer started from the previously synthesised phenyl indene **45** by using a direct addition of benzene under reflux (Scheme 2.18) with an equivalent amount of trifluoromethanesulfonic acid[110]. It did not lead us to the desired product, probably because of steric hindrance surrounding the spiro centre. Similar reactions using the isolated precursor tertiary alcohol with acid and benzene did not provide the desired monomer but, only, to the phenyl indene **45**.

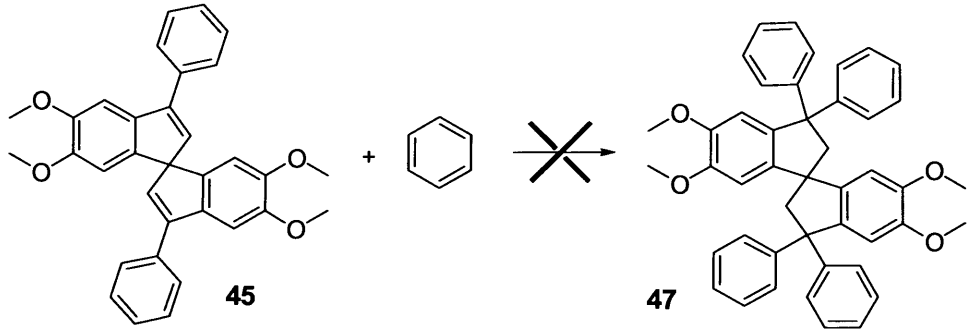

Scheme 2.18. Attempted benzene substitution

Due to the poor results obtained with the benzene, we decided to try the same type of reaction but using a more activated substrate such as aniline, with the aim of subsequent removal of the amino groups *via* conversion to the diazonium salt (Scheme 2.19).

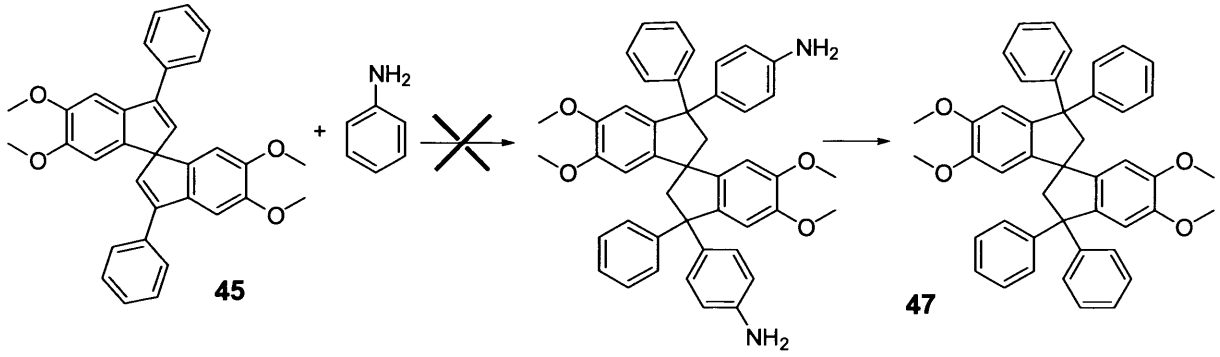

Scheme 2.19. Attempted aniline addition to the phenyl indene

Unfortunately, even aniline did not show the desired reactivity presumably as a consequence of steric hindrance. Additional efforts to substitute the aniline have been tried starting from the bis-ketone **41**, by using similar conditions that brought us to the double aromatic substitution of the veratrole to form the ester **43.** Despite this type of reaction being well-established in the literature[111,112], the tetra-aniline product was never obtained, once again perhaps due to the inaccessibility of the ketone and as a result of the poor solubility of the diketone **41** in the reaction solvent. The only compounds isolated from the reaction mixture were the starting material **41** and the diimine **51** shown in Scheme 2.20, in poor yield.

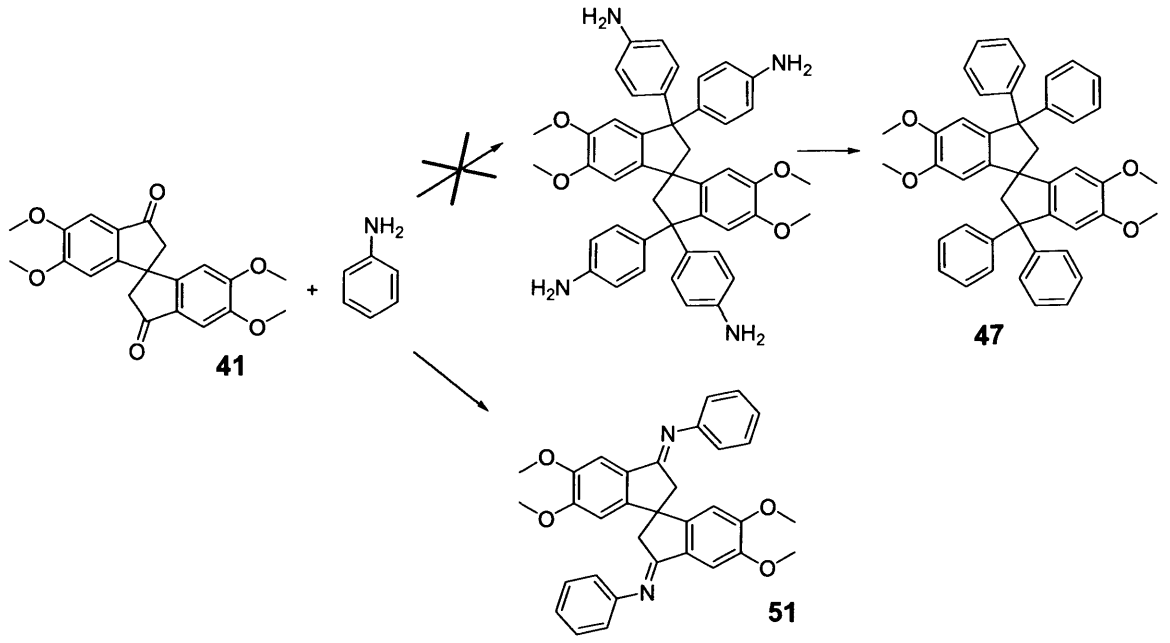

Scheme 2.20. Attempted addition of aniline on the ketone **41**

Another approach to the tetraphenyl monomer **47** from ketone **41**, was an addition of aryl groups using the classical Friedel-Crafts reaction of the tetrachloro compound **52** prepared from the diketone **41**, prepared by the use of phosphorous pentachloride.

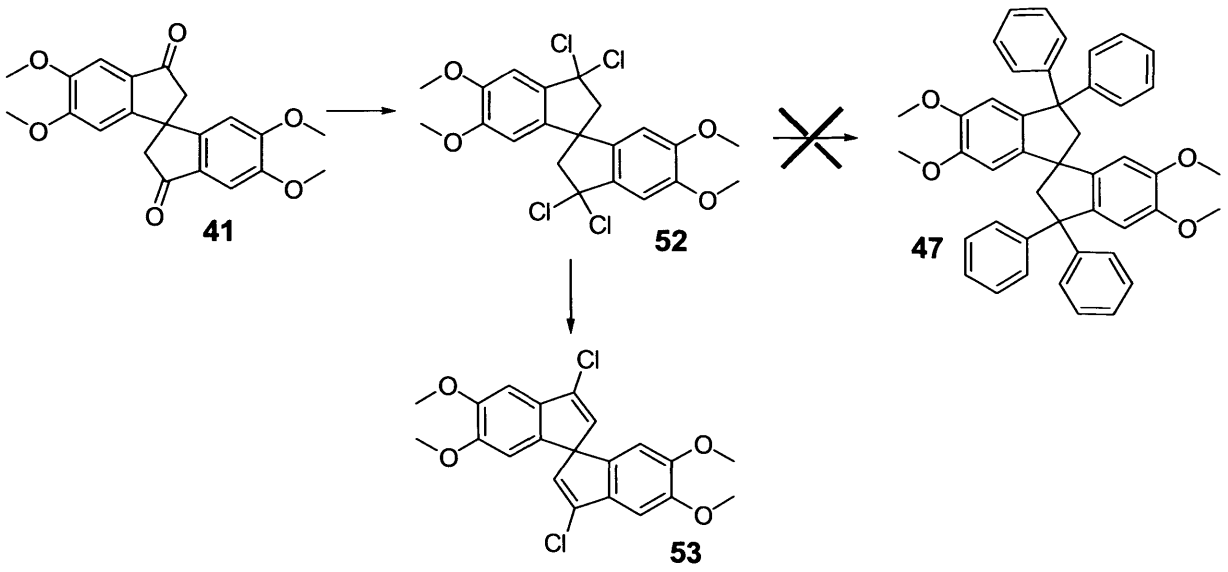

Scheme 2.21. Reaction with phosphorous pentachloride

With strict control of the reaction conditions, especially regarding the temperature, we succeeded in carrying out the formation of this particular intermediate **52**, in analogy with reactions reported in the literature[113,114]. Unfortunately, it proved to be too unstable to

be handled easily, leading rapidily to the elimination of hydrogen chloride[115] and to the formation of the unsaturated compound **53** as shown in Scheme 2.21. Even the repeated attempts to perform the Friedel-Crafts reaction on the crude tetrachloro **52** at low temperature never yielded any traces of the desired tetraphenyl spirobisindane **47**.

2.1.5 Di-Phenyl-ketone spirobisindane monomer 54

Since the six-membered lactone **48** was a potential precursor to a monomer for the formation of a PIM, its demethylation was attempted to provide a new bis-catechol. Surprisingly, during the reaction with the BBr_3, a ring-opening of the lactone and successive double ring closure was mediated by the strongly Lewis acid conditions to provide a useful monomer with two phenyl groups on one side of the spirobisindane and a ketone on the other (Scheme 2.22).

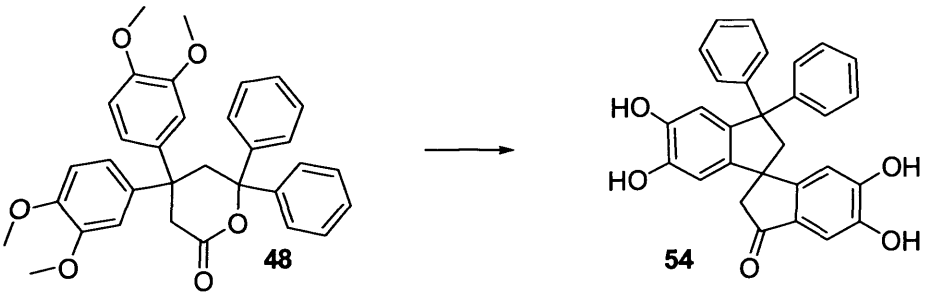

Scheme 2.22. Synthesis of **54**. *Reagent and conditions.* BBr_3, DCM

Even though, again, we were surprised at the result of the reaction, in this case a useful hybrid monomer containing structural components of the desired tetraphenyl monomer **47** and the diketone monomer **41** was obtained. In addition, because of the ketone group, there was scope for further functionalization.

2.1.6 Fluorene-containing monomer 57

Due to the unforeseen complications on the path to the synthesis of the tetra-phenyl spirobisindane monomer, we turned our attention to a new kind of monomer containing fluorene subunits as the rigid bulky substituents, *via* the addition of 2-biphenyl magnesium

bromide to the previously synthesized diketone **41**. The formation of this Grignard reagent, starting from the commercial 2-bromobiphenyl, proved to be rather difficult to achieve, confirming the reports by other research groups[116,117]. It proved easy to decompose, even in dilute solution, and furthermore light sensitive, requiring the use of strictly dry and dark condition. Despite the relatively low yield of the addition reaction with diketone **41** (Scheme 2.23), probably as a result of the limited accessibility of the ketone groups for such a large reagent, added to the poor solubility of the bis-ketone in THF, we succeeded in obtaining the desired product, as usual avoiding the difficult isolation of the tertiary alcohol by the immediate dehydration of the crude product to gave the spirobisindene **55**.

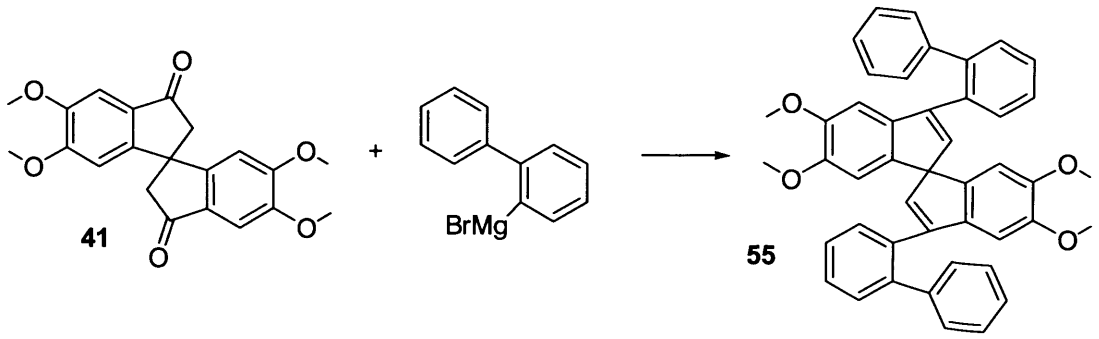

Scheme 2.23. Synthesis of precursor **55**. *Reagent and conditions.* i.THF, reflux. ii, HCl 10%, MeOH

The intramolecular cyclization of **55** (Scheme 2.24) proceeded smoothly providing the desired precursor to the bis-fluorene based monomer **56**. This synthetic pathway allowed the preparation of a compound with three spiro-centres. It was anticipated that this highly rigid system would ultimately enhance the microporosity of the resulting PIM by frustrating packing of the macromolecules in the solid state. In addition, the presence of the bulky fluorene groups was expected to enhance the solubility of the polymer in most common organic solvents.

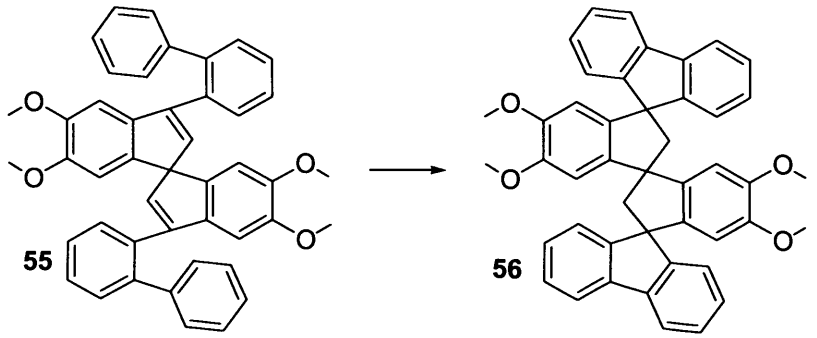

Scheme 2.24. Preparation of precursor **56**. *Reagents and conditions.* Eaton's reagent, RT.

The demethylation of the fluorene-containing precursor to give monomer **57** proved straightforward. In fact, after the usual reaction with boron tribromide, we recovered a very high yield in a reasonably short time (Scheme 2.25, 90% within 0.5 h).

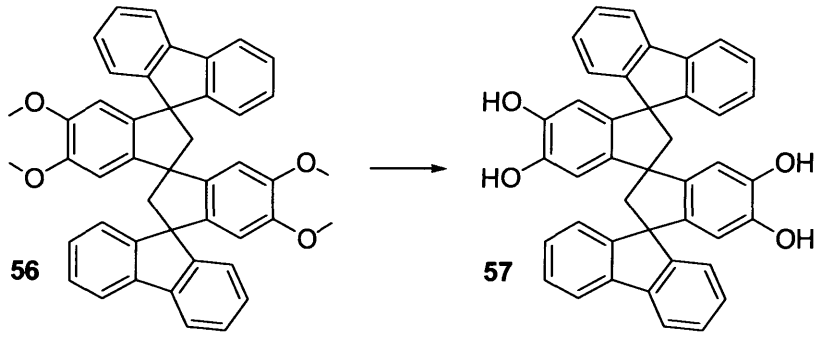

Scheme 2.25. Synthesis of monomer **57**. *Reagents and conditions.* BBr_3, DCM.

2.1.7 Fluorene-ketone monomer 59

Encouraged by the successful synthesis of the fluorene monomer we decided to carry out a full investigation of its preparation, in the attempt to improve its yield. In one of these efforts, purifying the monomer by flash chromatography instead of the already successful recrystallization from methanol, we noticed by TLC the presence of a second spot below the bisfluorene compound **56**, which was found to be the mono-substituted fluorene **58** (Scheme 2.26). This result, not only gives a partial explanation for the poor yield in the bis-fluorene, but moreover provides us with the potential for preparing a new monomer containing a single fluorene and a ketone group, which could be used for further functionalization. Furthermore, compound **58** was reacted with additional biphenyl magnesium bromide in the attempt to convert it to the bis-fluorene precursor **56**, although once again addition was incomplete, presumably due to the combination of steric inaccessibility of the ketone in **58** and bulk of the Grignard reagent. Indeed, we never succeeded in improving the yield of **56** over 40%, despite trying different conditions and

the use of organolithium chemistry, such as the exchange of Li/Br as suggested by Krasovskiy *et al.*[118] or replacing the 2-biphenyl magnesium bromide with the 2-biphenyl lithium as reported by Kimura *et al.*[119]

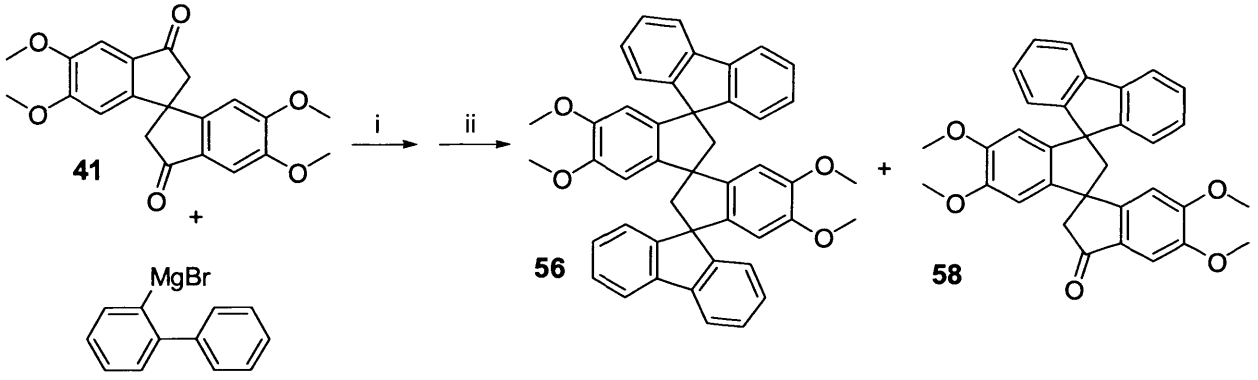

Scheme 2.26. Synthesis of monomers **56** and **58**. *Reagents and conditions.* i THF, reflux, ii Eaton's reagent

The reaction with boron tribromide produced the bis-catechol of the fluorene-ketone monomer **58** easily and in good yield (90% within 3 h, Scheme 2.27).

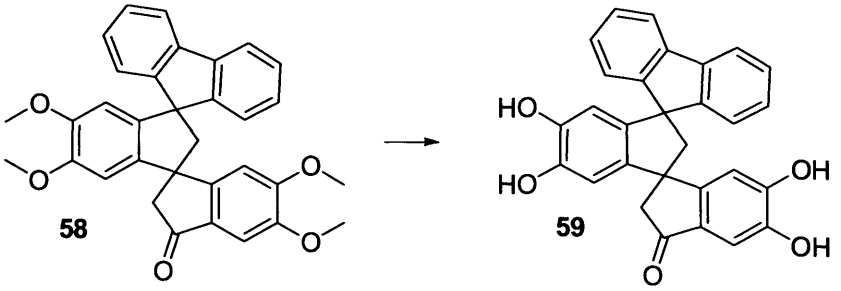

Scheme 2.27. Synthesis of monomer **59**. *Reagents and conditions.* BBr_3, DCM.

2.1.8 *tert*-Butyl fluorene-containing monomers 64 and 65

In an attempt to improve the features of the fluorene monomer and, especially, in order to further enhance the solubility of the final polymer, we thought to introduce substituents onto the bisfluorene spirobisindane monomers. Initially, the addition of *tert*-

butyl groups was attempted as it was anticipated that such bulky rigid groups should maintain a high surface area in the solid state and increase the solubility of the polymer in organic solvents. Starting from the commercial 4,4'-di-*tert*-butyl biphenyl, we proceeded with bromination in the 2-position (Scheme 2.28), using a standard procedure already described in literature[120]. Problems with stability of the Grignard reagent prepared from this compound did not allow us to store it but forced us to use it freshly prepared.

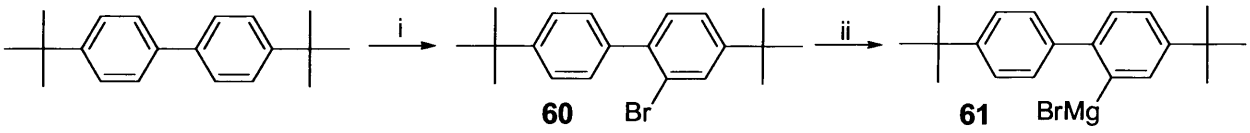

Scheme 2.28. *Reagent and conditions.* i Br_2, CCl_4, ii Mg, THF.

The reaction between this new Grignard reagent and the diketone **41** was successful (Scheme 2.29), affording the desired di-*tert*-butylfluorene-based precursors **62** and **63**. However, the complex mixture of products was best separated following the cyclization step with Eaton's reagent, performed on the crude product of the reaction, followed by flash chromatography.

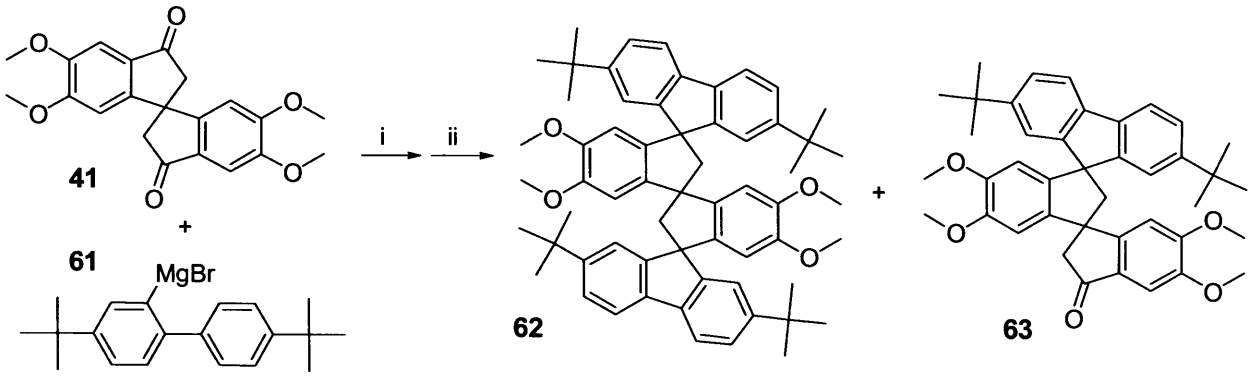

Scheme 2.29. Synthesis of monomer **62** and **63**. *Reagent and conditions.* i THF, reflux, ii Eaton's reagent

Demethylation to give the two bis-catechols **64** and **65**, proceeded with the usual high yield (Scheme 2.30, 89% for **64** and 88% for **65**).

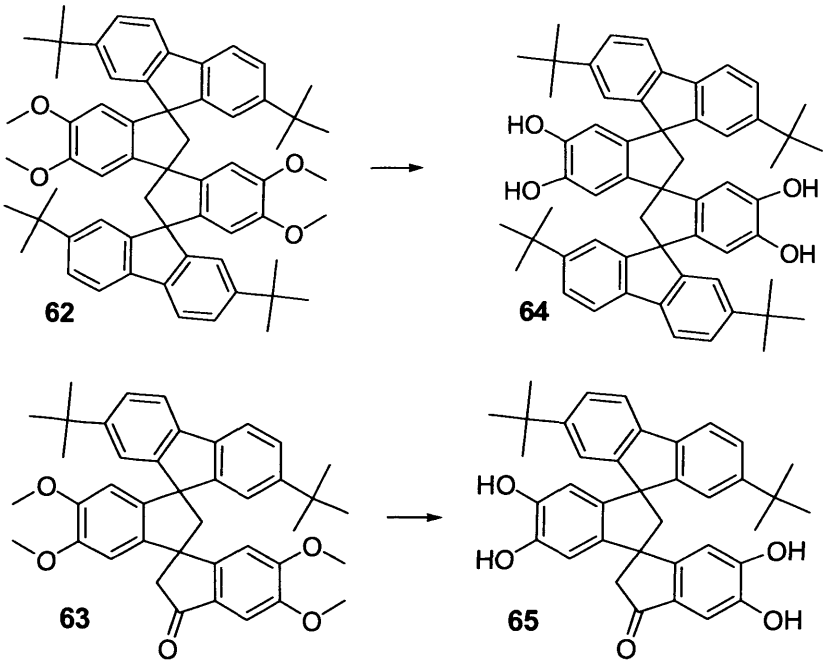

Scheme 2.30. Synthesis of monomers **64** and **65**. *Reagents and conditions*. BBr_3, DCM.

2.2 Thioketal protected spirobisindane monomers

Exploring the different possibilities for functionalization of the bis-ketone **41**, we considered the protection of the ketone with a "sacrificial" group, in order to undertake the polymerization with the protected monomer and eventually to cleave the protecting group, to reform the ketone. The aim of this was to determine the differences in the physical properties between the polymer synthesized without the sacrificial group and the one synthesized with it and eventually deprotected. In particular, we were interesting to determine whether the removal of a bulky sacrificial group could introduce further microporosity

The first attempt toward this type of synthesis was the attempted protection of the diketone **41** with ethylene glycol to form a ketal, using well known literature procedures[121,122,123]. Surprisingly, the reaction never succeeded in producing the protected bis-ketal (Scheme 2.31), despite employing a range of different reaction conditions. For example, use of montmorillonite clay, as suggested in previously reported work which successfully gave ketal-containing monomer precursors to aromatic polyetherketones[124,125].

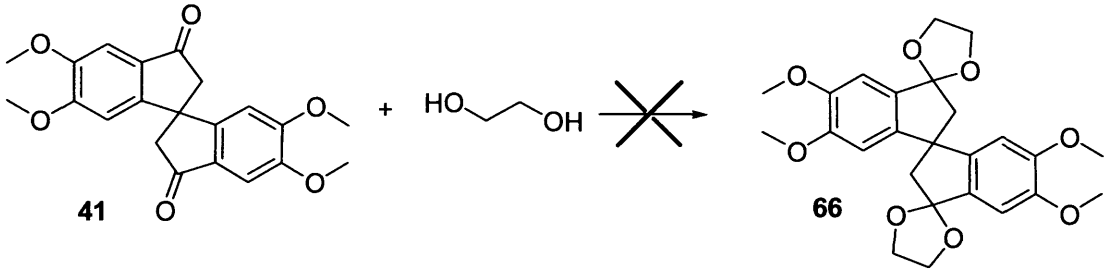

Scheme 2.31. Attempted preparation of ketal protected monomer **66**. *Reagents and conditions.* Ethylene glycol, toluene, *p*-toluensulfonic acid, reflux.

2.2.1 Tetra-methoxy thioketal monomers 69 and 70

Due to the failure of ketal functionalisation, the use of dithiols instead of glycols, was investigated because of the enhanced nucleophilicity of the sulphur, compared to the oxygen. Following existing procedures[126] using 1,2-ethanedithiol in strong acid media (trifluoroacetic acid plus $BF_3 \cdot Et_2O$ in DCM), we achieved the protection of the bis-ketone **41** in very high yield (88%, Scheme 2.32).

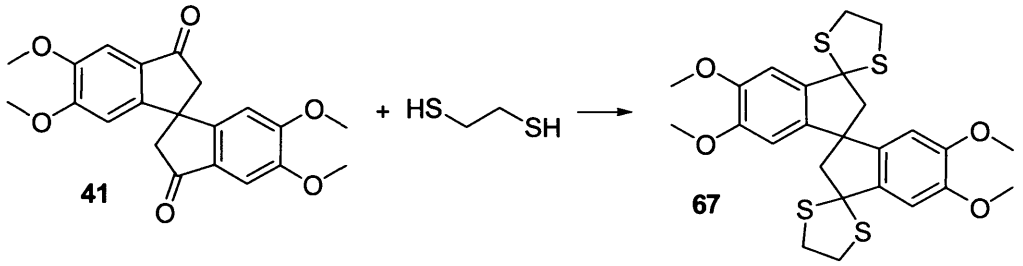

Scheme 2.32. Synthesis of bis thioketal **67**. *Reagents and conditions.* 1,2-Ethanedithiol, DCM.

The confirmation of the remarkably efficiency of dithioacetalisation was shown by the reaction of 1,3-propanedithiol on diketone **41**, using same conditions as above, obtaining the protected compound **68** in even better yield (90%, Scheme 2.33).

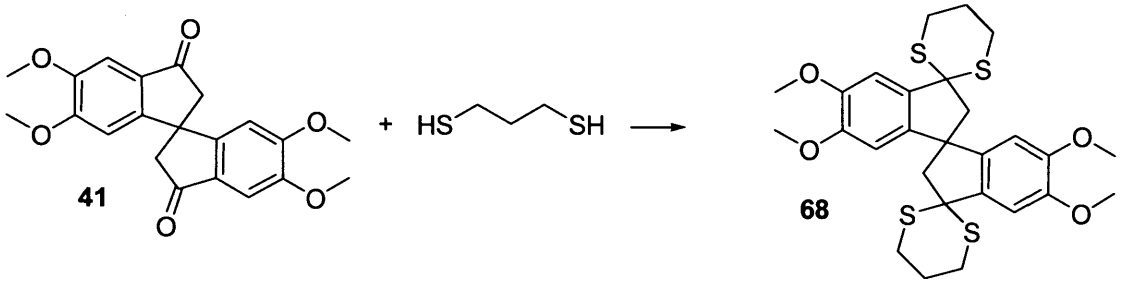

Scheme 2.33. Synthesis of bis thioketal **68**. *Reagents and conditions.* 1,3-Propanedithiol, DCM.

Planning the demethylation of the thio-ketal-containing precursors **67** and **68** to obtain the bis-catechol we expected some problems, due to the risk of the simultaneous cleavage of the thioketals groups. As we feared, the usual demethylation with BBr_3 did not work for **67** and **68** but not because of the cleavage of the ketal group (Scheme 2.34). Instead, a few minutes after the addition of the BBr_3 a solid precipitate was formed. Surprisingly, by NMR spectroscopy we found that the thioketal protecting group was still present and the methoxy groups had almost disappeared, but the interpretation of the spectra was very difficult due to the formation of a mixture of different products. In trying to find an explanation in the literature[127], we found that the cause of the failure of the reaction could be attributed to the formation of the sulfonium salt of the thioketal during the addition of boron tribromide. In fact, a typical reaction that occurs in thio-compounds in the presence of methyl halides is the transfer of the methyl group onto the sulphur to form the stable and insoluble salt.[128] Our opinion is that the demethylation releases methyl bromide [99], which reacts with the thioketal forming the salt, and causing the precipitation from solution.

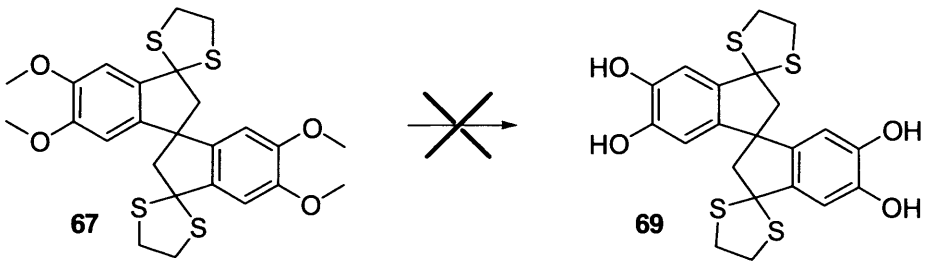

Scheme 2.34. Attempted demethylation of **67**. *Reagents and conditions*. DCM, BBr_3

At this point we decided to attempt the protection with the dithiols directly onto the monomer **44**, a reaction that we did not try at first due to worries about possible side-reactions of the more reactive bis-catechol in the strong acidic media. The reaction worked well using the same conditions as were previously employed for the tetra-methoxy **67**, despite the total insolubility of **44** in DCM, a fact that forced us to leave the reaction for three days at room temperature to allow the dithiol to react under heterogeneous conditions. We recovered the pure product **69** and **70,** in 45% yield for the 1,3-dithiolane **69** and 37% for the 1,3-dithiane **70,** after flash chromatography (Scheme 2.35).

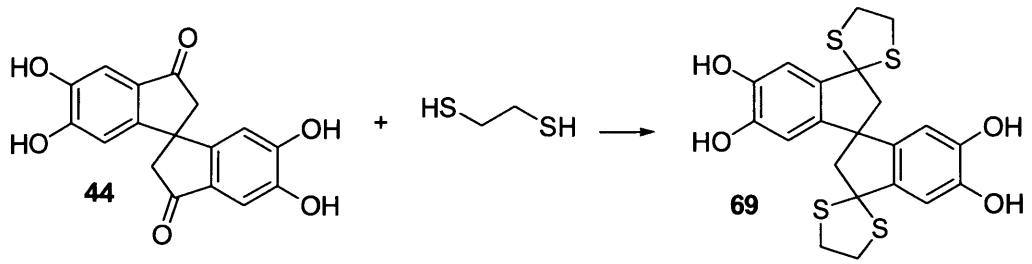

Scheme 2.35. Synthesis of monomer **69**. *Reagents and conditions*. 1,2-Ethanedithiol, THF.

After purification by chromatography column, the solubility of the new bis-catechol monomers **69** and **70** in THF was noted, so we decided to try the same ketal-forming reaction but replacing the DCM with THF. Despite the initial poor solubility of bis-ketone **41** in THF, the reaction became homogeneous after three days. The reaction was complete after a further two days as monitored by the disappearance of the starting material by TLC. This small change in the synthesis brought excellent yields of 89% for the 1,3-dithiolane **69** (Scheme 2.36) and 87% for the 1,3-dithiane **70** (Scheme 2.36) and, moreover, the purification could be achieved by a simple recrystallisation.

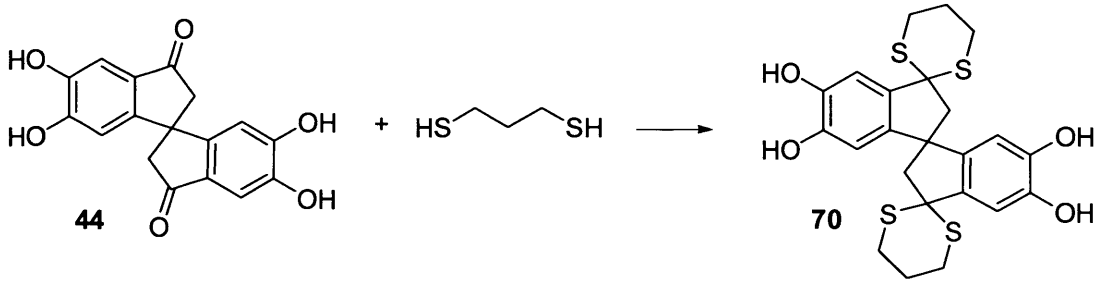

Scheme 2.36. Synthesis of monomer **70**. *Reagents and conditions*. 1,3-Propanedithiol, THF.

2.2.2 *Synthesis of the Spiro-indane monomer 72*

Another reaction that we tried with the dithiol protected precursors, was the cleavage of the thioketal **68** with Raney Nickel, a well known procedure in organic synthesis[129,130], to obtain the unsubstituted spiro-indane, already obtained by Baker[89] using a different route. The reaction worked very well despite the poor solubility of the thio-monomer **68** in ethanol, affording the final product in excellent yield and purity (86%, Scheme 2.37). The

subsequent demethylation of the precursor **71** provided the bis-catechol **72** without difficulty.

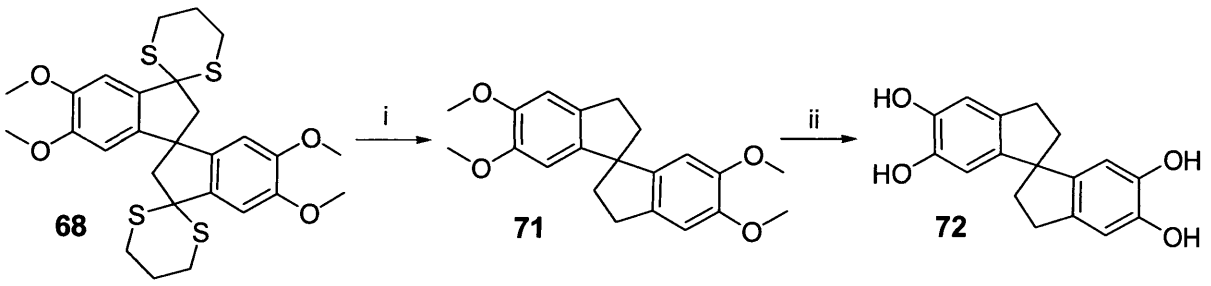

Scheme 2.37. *Reagents and conditions.* i Raney Nickel, ethanol, ii BBr_3

2.3 "Spiro-bisnaphthalene" based monomers

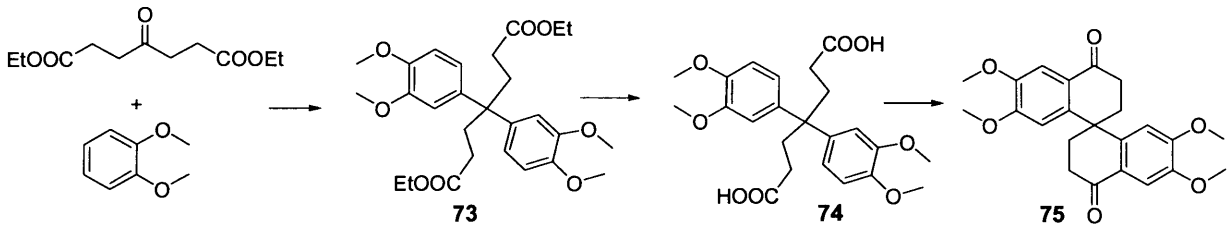

Scheme 2.38 Proposed synthesis of the new "spiro-bisnaphthalene" monomer **75**

The inspiration for the design of a new family of monomers for PIMs with an expanded fused ring system came from the difficulties in obtaining the tetraphenyl-substituted monomer **47,** due to the unforeseen fragmentation reaction shown in Scheme 2.16. In analogy with the synthesis of monomer **41** the first step was the reaction of veratrole with 4-diethyloxopimelate to provide the precursor ester **73** (Scheme 2.39).

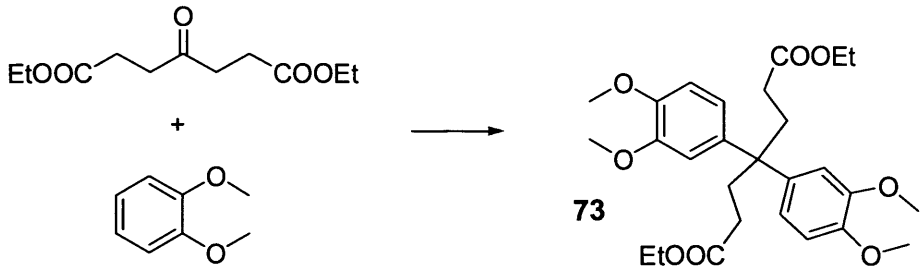

Scheme 2.39 Synthesis of the di-Ester **73**. *Reagents and conditions:* Eaton's reagent, RT

This reaction, though looking very similar to one used formerly (Scheme 2.5), gave us several problems, most likely as a result of the reduced reactivity of the new starting material, and often led us to mixtures of different products with only traces of the desired diester. The reaction was investigated systematically. Initially, looking for a better dehydrating agent that might assist the formation of the carbocation, the initial choice was polyphosphoric acid but, in this case, despite the numerous attempts and conditions ranging from room temperature to 80 °C, only the two starting materials were recovered. Reasonable results were eventually achieved by using Eaton's reagent[131] at room temperature, a reagent that combines the excellent dehydrating properties of phosphorous pentoxide with the strong acidity of methanesulfonic acid. It was noticed that the product formed only when the ester was added to the Eaton's reagent, at room temperature, and the

large excess of veratrole was poured into the solution after one hour (even in this instance the best results have been obtained with 8 equivalent of veratrole). The adjustments of these conditions allowed us to carry out the synthesis of the precursor **73**, although with modest yield and with extended reaction times (32%, within 7 days). The many attempts to obtain better results with different acid or conditions failed. By monitoring the reaction carefully, we observed the partial hydrolysis of the ester, most likely because of the combination of the very strong acid–media with the slowness of the reaction. Hence, the isolation of the ester was avoided and its complete hydrolysis with aqueous NaOH (Scheme 2.40), to obtain the acid **74**, was performed. In addition to the improvement of the entire synthesis, this last step also allowed us to easily remove the excess of veratrole by keeping the salt of the dicarboxylic acid **74** in water, removing the organic residues with a diethyl ether extraction and precipitation of the diacid via addition of aqueous acid. In this way we also avoided a difficult flash chromatography for the precursor.

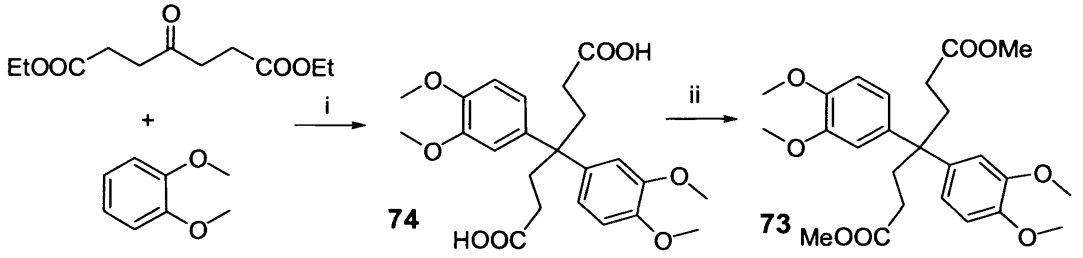

Scheme 2.40. Synthesis *of* **73** and **74.** *Reagent conditions.* i (1) Eaton's reagent, veratrole (2) $NaOH_{aq}$, ii H_2SO_4, MeOH

The esterification of the di-carboxylic acid **74**, carried out with methanol (or ethanol) in dilute sulfuric acid, to reach the initially desired ester precursor **73** in very high yield (95 % within 2h).

2.3.1 "Spiro-bisnaphthalene" ketone monomer 75

Cyclisation of the diacid **74** to provide the diketone **75** was achieved by following the same conditions used for the related five membered ring based bis-ketone **41**. With polyphosphoric acid at 80 ° C we succeeded in obtaining the desired product in reasonably

good yield (68%), although not as good as that obtained for **41**. In this case, the replacement of the PPA with Eaton's reagent did not show the same improvement in yield, so we decided to keep the initial conditions because PPA was much cheaper (Scheme 2.41).

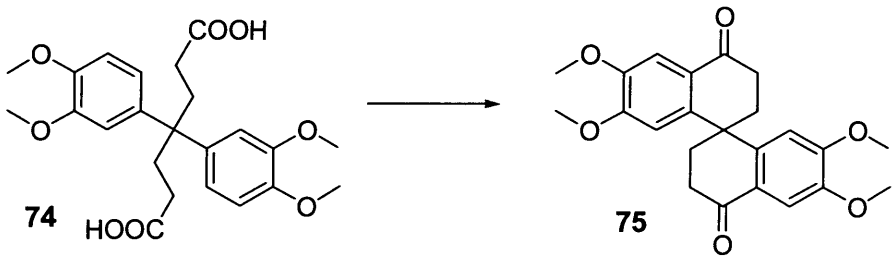

Scheme 2.41. Synthesis of **75**. *Reagent and conditions.* PPA. 80° C

The demethylation of the bis-ketone **75** was carried out as usual using BBr_3 in DCM (Scheme 2.42). The isolation of the bis-catechol **76**, proved to be somewhat problematic, since the product easily decomposed, showing a high sensitivity to moisture and oxygen never noticed in the related five-membered ring bis-ketone **44**.

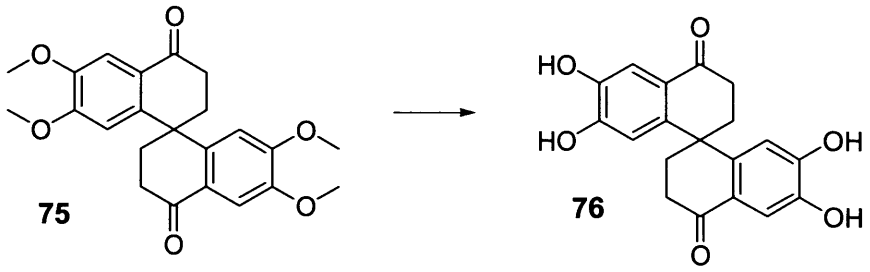

Scheme 2.42. Synthesis of **76.** *Reagent and conditions.* BBr_3, DCM.

We succeeded in the isolation of **76** by performing the work-up under strictly inert atmosphere, quenching the reaction with degassed water and collecting the solid with a nitrogen-inlet equipped sinter funnel. Despite this, the desired product was obtained in good yield (73%). As a consequence of its sensitivity, **76** has to be stored under inert and dry conditions.

2.3.2 *Phenyl "spiro-bisnaphthalene" monomer 78*

To fully compare the properties of the polymers derived from the spirobisindane and "spiro-bisnaphthalene" families, we prepared the analogous di-phenyl monomer **77** to **45** by the phenyl magnesium bromide addition to the bis-ketone **75**, obtaining the desired product **77** without complications, in a similar yield as **45** (78%, Scheme 2.43).

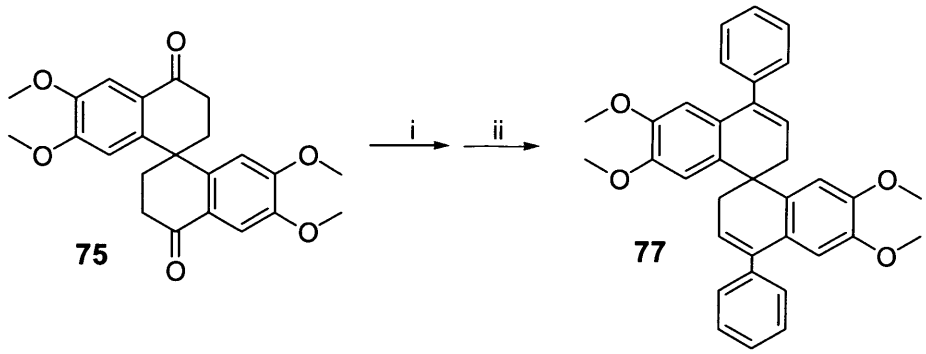

Scheme 2.43. Synthesis of spiro-indene **77**. *Reagent and conditions*: i PhMgBr, THF ii $20\%_{aq}$ H_2SO_4

The subsequent demethylation of the precursor **77** was carried out, without any problems, using boron tribromide, providing the bis-catechol monomer **78** in excellent yield (88%, Scheme 2.44).

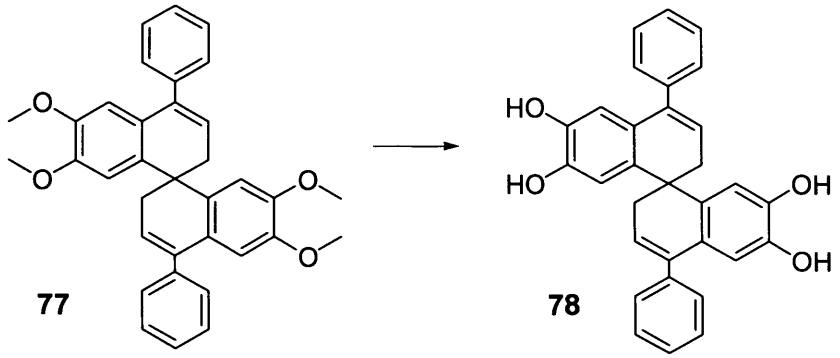

Scheme 2.44. Synthesis of monomer **78**. *Reagent and conditions* BBr_3, DCM.

2.3.3 *Tetra-phenyl "spiro-bisnaphthalene" monomer 81*

In order to synthesise the tetra-phenyl monomer **80** of the "spiro-bisnaphthalene" system, the analogue of **47** which proved so difficult to obtain in the spirobisindane

system, we decided to use the first strategy (see scheme 2.11) that failed for that synthesis, i.e. the attack of the phenyl Grignard reagent on the ester groups of the precursor **73**, followed by a double intramolecular Friedel-Craft alkylation (Scheme 2.45).

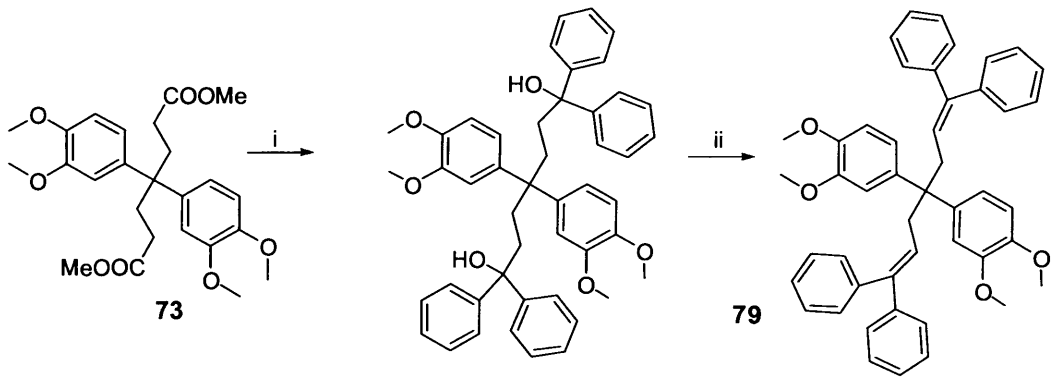

Scheme 2.45. Synthesis of precursor **79**. *Reagents and conditions*, i PhMgBr, THF, ii HCl 10% (EtOH).

In this case, the reaction of the phenyl-magnesium bromide on the methyl-ester proceeded as anticipated. In contrast with the same reaction previously attempted in the failed synthesis of the spirobisindane precursor, lactone formation is disfavoured due to the well-established unfavourability of eight-membered rings. Due to the instability of the diphenylcarbinol groups towards elimination, a simple dehydration with aqueous hydrochloric acid was carried out prior to isolation of the unsaturated product **79** in good yield (75%).

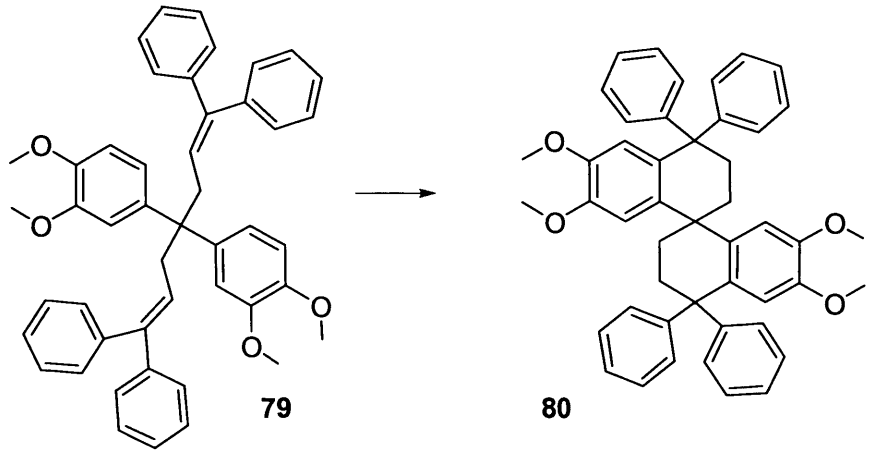

Scheme 2.46. Synthesis of **80**. *Reagents and conditions*, Eaton's reagent, RT.

The attempted cyclization with polyphosphoric acid showed decomposition of the

starting material leading to a complex product mixture, probably due to the high temperature required for its use. The same reaction mediated by Eaton's reagent proved more efficient, faster and easier to purify than the one performed with polyphosphoric acid, demonstrating this reagent's utility for intramolecular cyclization, as strongly supported by literature precedent[132,133,134]. The tetra-phenyl precursor **80** was obtained in 73% yield (Scheme 2.46).

The demethylation of the new monomer, with boron tribromide, followed by recrystallization with hexane/dichloromethane, allowed us to reach the bis-catechol monomer **81** in good yield (73%, Scheme 2.47).

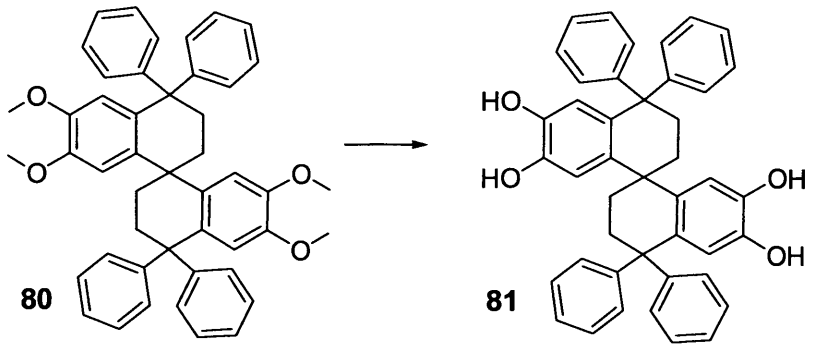

80 **81**

Scheme 2.47. Synthesis of monomer **81**. *Reagents and conditions*, BBr_3, DCM

2.3.4 *Fluorene-containing "spiro-bisnaphthalene" monomers 84 and 85*

As for the fluorene-containing spirobisindane-based system we wished to increase both the rigidity, bulk and the solubility of the final polymer, therefore we attempted the synthesis of the fluorene-containing "spiro-bisnaphthalene" monomer **82** using the same strategy that successfully led to monomer **56** (Scheme 2.23). Thus, a freshly prepared solution of 2-biphenyl magnesium bromide was added to **75** (Scheme 2.48).

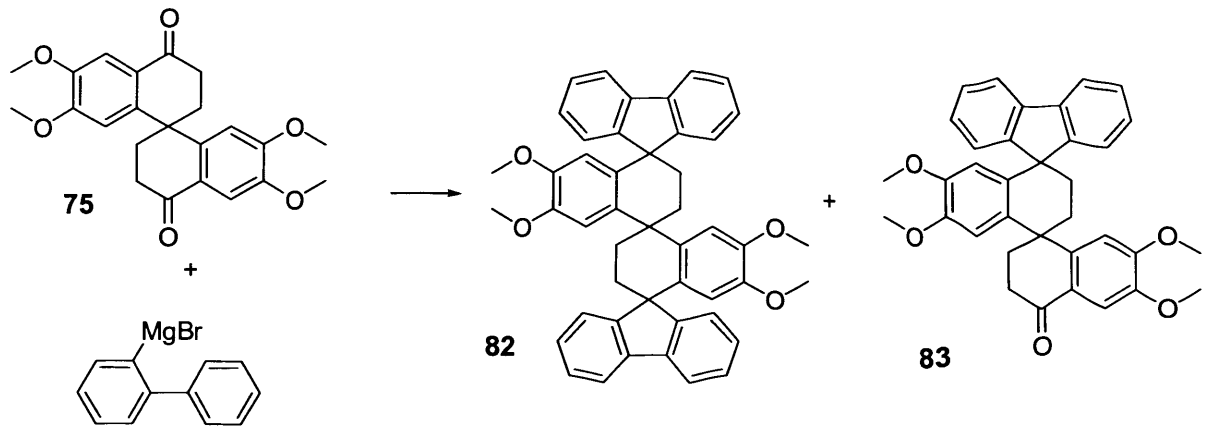

Scheme 2.48. Synthesis of monomers **82** and **83**. *Reagents and conditions*. i THF, reflux, ii Eaton's reagent

Surprisingly, considering the greater accessibility for the attack of the Grignard reagent the superior solubility of **75** in the reaction solvent, this synthesis led us to a lower yield than the equivalent spirobisindane compound **56**. The yield was an underwhelming 19% for the bis-fluorene **82** and 50% in the mono-substituted **83**. The isolation of these two precursors was best achieved by performing the cyclization with Eaton's reagent directly on the crude product and then proceeding with separation by flash chromatography.

The demethylation of **82** was easily achieved and with the usual excellent yield (Scheme 2.49, 90%, within 1 hour).

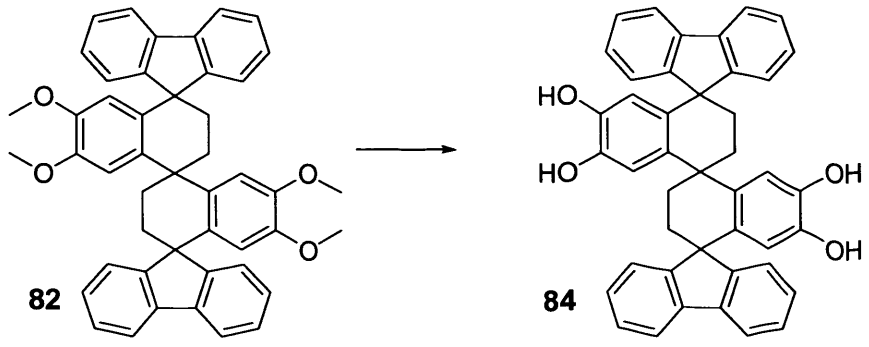

Scheme 2.49. Synthesis of monomer **84**. *Reagents and conditions*, BBr_3, DCM

The demethylation of "spiro-bisnaphthalene" fluorene-ketone monomer to reach the bis-catechol **85**, once more, proved as easy as the one for the related five membered ring

monomer, allowing us to isolate the desired product with the, usual, excellent yield (Scheme 2.50, 85%, within 2 hours).

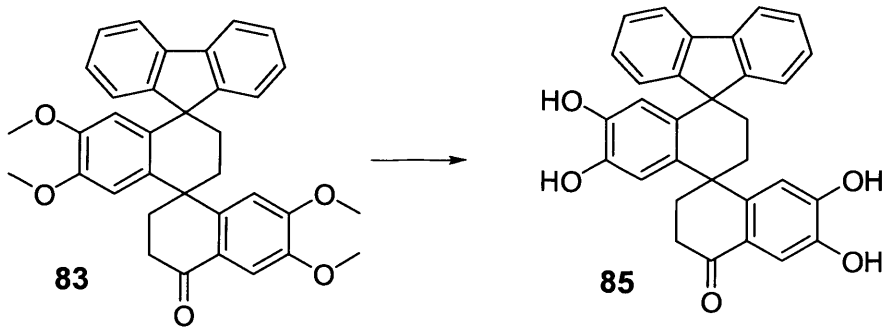

Scheme 2.50. Synthesis of monomer **85** *Reagents and conditions*, BBr_3, DCM

2.3.5 Tetra-methyl "spiro-bisnaphthalene" monomer 88

One of the most direct comparisons between the spirobisindane and "spiro-bisnaphthalene" families of monomer, would be facilitated by the synthesis of the tetra-methyl monomer **88** which is an analogue of monomer **A1**. In order to prepare this important monomer we applied the same methodology as had succeeded in the synthesis of the tetraphenyl monomer **80**.

The addition of a methyl Grignard reagent to **73** worked very well, allowing us to obtain the bis alcohol in high yield (91% within only one hour at room temperature, Scheme 2.51). In addition, it proved very easy to isolate, presumably because of the absence of aromatic rings which encouraged elimination to such a degree that we had previously been forced to proceed with the complete dehydration of the product.

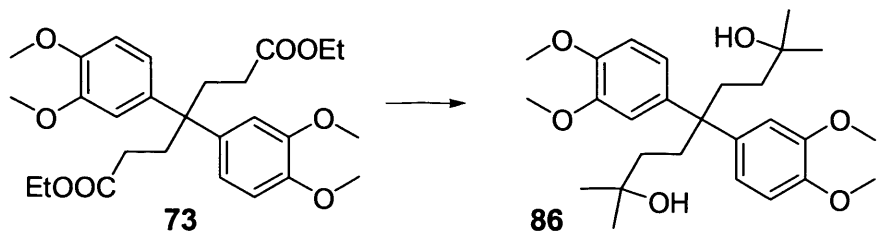

Scheme 2.51. *Reagents and conditions.* CH_3MgBr, THF

The Friedel-Craft cyclization of the precursor proved much more complicated than we predicted (Scheme 2.52). Initially, we thought to perform this intramolecular cyclization with dilute acids.

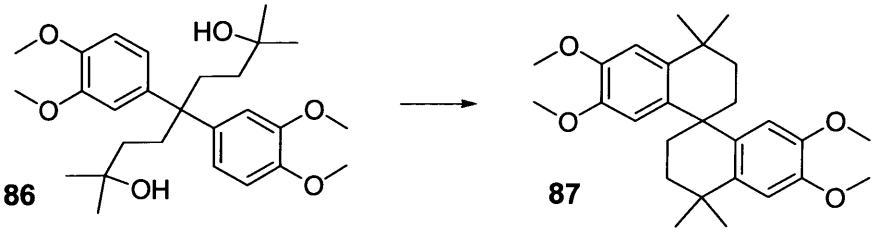

Scheme 2.52. Synthesis of **87**. *Reagents and conditions.* CH_3SO_3H, RT

After the first few attempts with dilute HCl and H_2SO_4 in which we recovered only the starting material, we moved to more concentrated acids but isolated only the dehydrated compound (in the case of the HCl), and found decomposition of the product (for H_2SO_4), never succeeding in the synthesis of the desired molecule **87**. We decided, at this point, to attempt the cyclization with the help of Lewis acids. Initially we thought about the use of BBr_3, which we had previously shown to be effective in this type of reaction (Scheme 2.22), but in this instance we observed, by NMR spectroscopy, a complicated mixture of demethylated product and only modest evidence of cyclization, along with other by-products. Supported by reported work for similar molecules[135], we attempted the use of BF_3•Et_2O but recovered a mixture of starting material and dehydrated product. We then tried a very common reagent for this class of cyclization, tin tetrachloride [136,137,138]. Unfortunately, even this reagent proved unsuccessful. Finally, we accomplished the isolation of the cyclized monomer by the use of Eaton's reagent at 50 °C, but with very poor yield, whereas the best result was eventually obtained by use of methanesulfonic acid, firstly at room temperature and then 50 °C. All the subsequent attempts to improve the yield of this reaction proved unsuccessful (Table 2.4).

Acid used	Conditions	Yield
HCl dilute (20% in MeOH)	RT, 50 °C	0%, 0%
HCl_{conc}	RT	0%
H_2SO_4 dilute (20% MeOH)	RT, 50 °C	0%
$H_2SO_{4\,conc}$	RT	0%
BBr_3	RT	0%
$BF_3{\bullet}Et_2O$	RT	0%
$SnCl_4$	RT	0%
CH_3SO_3H	RT, 50 °C	15%, 20%
Eaton's reagent	RT, 50 °C	0%, 10%

Table 2.4. Yields for the attempted synthesis of **87**

The demethylation of **87** did not cause any problems, allowing us to obtain the bis-catechol **88** in the usual high yield (94% within 1 hour, Scheme 2.53).

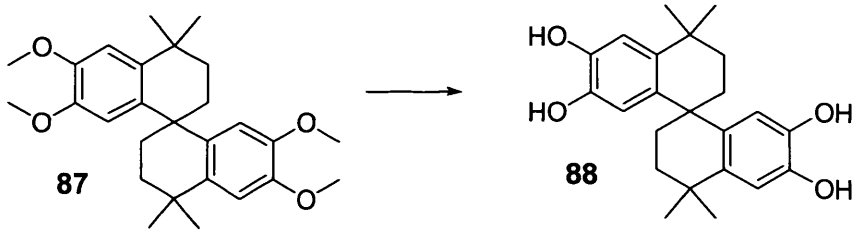

Scheme 2.53. *Reagents and conditions*, BBr_3, DCM

2.4 Analysis of crystal structures formed by monomers

During this synthesis project, we succeeded in growing single crystals for several monomer products. The technique used for the crystallization was the slow diffusion of a non-solvent into a solution of the purified monomer. This is normally carried out by placing a small amount of solution in a small vial, then placing this vial inside a larger vial that contains a small volume of a solvent in which the sample is insoluble. The outer vial is then sealed. Vapours from the solvent of the outer vial then diffuse into the solution in the inner vial, promoting the slow growth of crystals.

It was of interest to attempt to correlate the basic properties of the polymers (e.g. ease of formation, solubility, microporosity) to the molecular structure of the monomers and their precursors obtained from X-ray diffraction analysis, and in particular the angles between the planes formed by the two aromatic rings (i.e. catechol units).

2.4.1 Spiro-ketone bisindane monomer crystal structure

The first single crystals that we grew were the tetramethoxy-bisketone **41**, through slow diffusion of *n*-hexane into a solution in DCM.

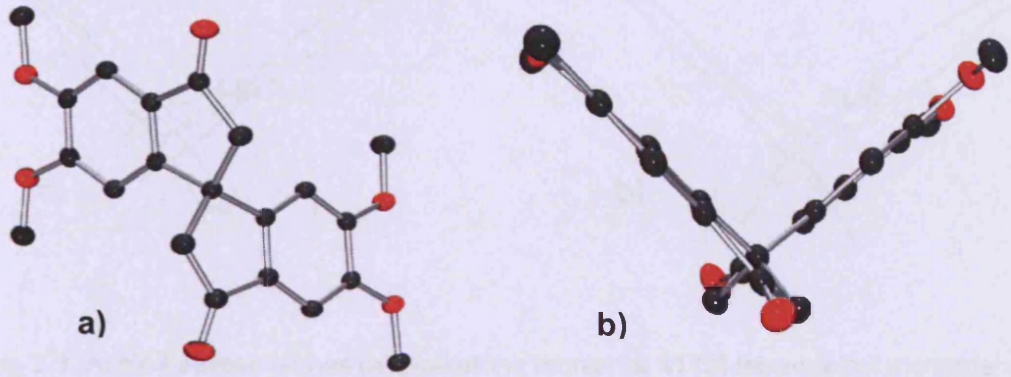

Fig 2.1. Solid state structure of the bis-ketone monomer **41** (a) Facial view. (b) Side view

The solid state structure, obtained by X-ray crystallographic analysis, is shown in Fig. 2.1, in which the non planarity of the molecule due to the spiro-centre is readily observed (Fig 2.1 b).

It is important to base any comparison of monomer structure with that of the tetra-methyl bis-catechol used to make PIM-1 and for which a crystal structure has been published[139]. It is possible to notice the similarity in the structure of these two spiro-compounds (Fig 2.2 b).

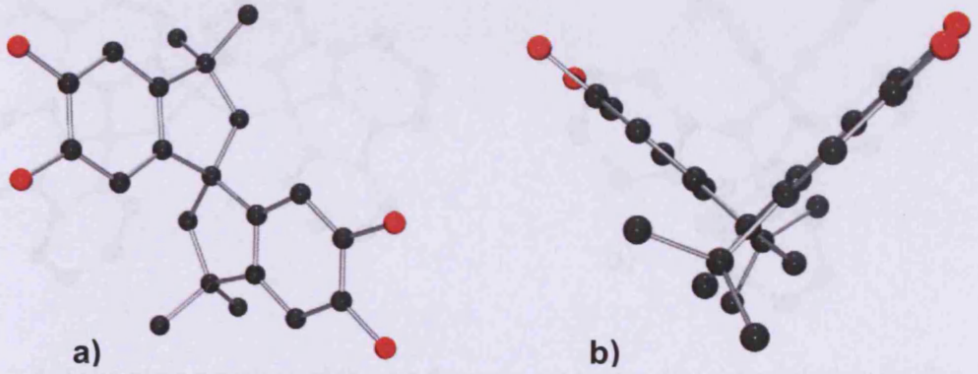

Fig 2.2. Solid state structure of the tetra-methyl catechol **A1** (a) Facial view. (b) Side view

A more quantitative comparison between the two compounds using the software programme Mercury (version 1_4_2) allows the angle between the two planes formed by the aromatic rings to be calculated as 84.8° for the bis-ketone monomer **41** (Fig 2.3 a) and 84.7° for the tetra-methyl bis-catechol **A1** (Fig 2.3 b).

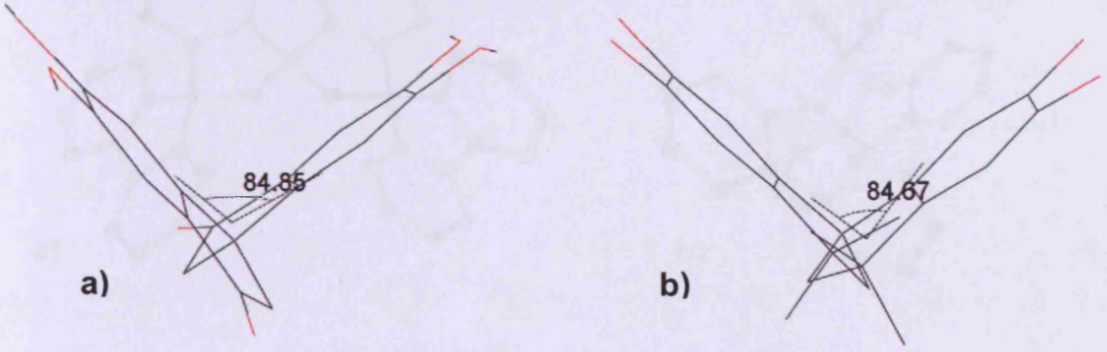

Fig 2.3. Angle between planes (a) bis-ketone monomer **41** (b) tetra-methyl monomer **A1**

2.4.2 *Fluorene-containing monomers*

The slow diffusion of *n*-hexane into an ethyl acetate solution gave high quality crystals of the fluorene-containing compounds **56** and **58**. Fig 2.4 shows the solid state structure from X-ray analysis, which illustrates the contorted shape of the molecule due to

its three spiro-centres (Fig 2.4 b). The crystal is a clathrate as it contains a molecule of ethyl acetate per unit cell, which has been omitted from the figure for clarity.

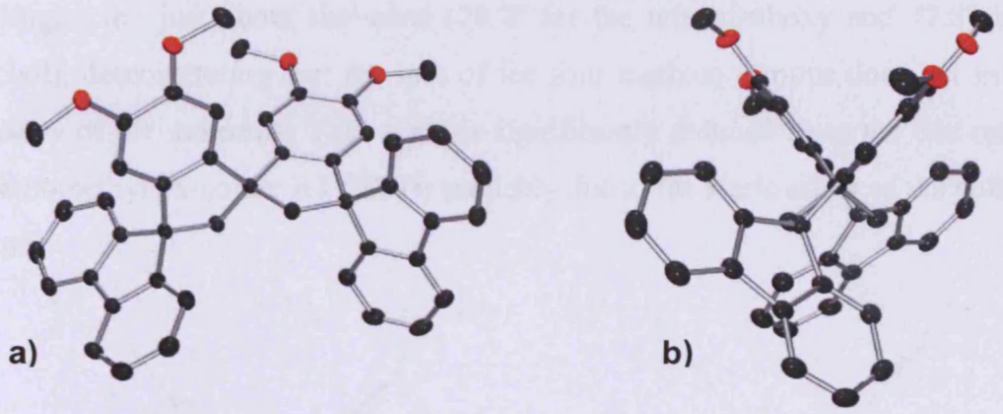

Fig 2.4. Solid state structure of the bis-fluorene monomer **56** (a) Facial view (b) Side view

To make comparison between with the tetra-methoxy monomer, single crystals were grown also for the bisfluorene catechol **57** (DCM into ethyl acetate solution) as showed in Fig 2.5.

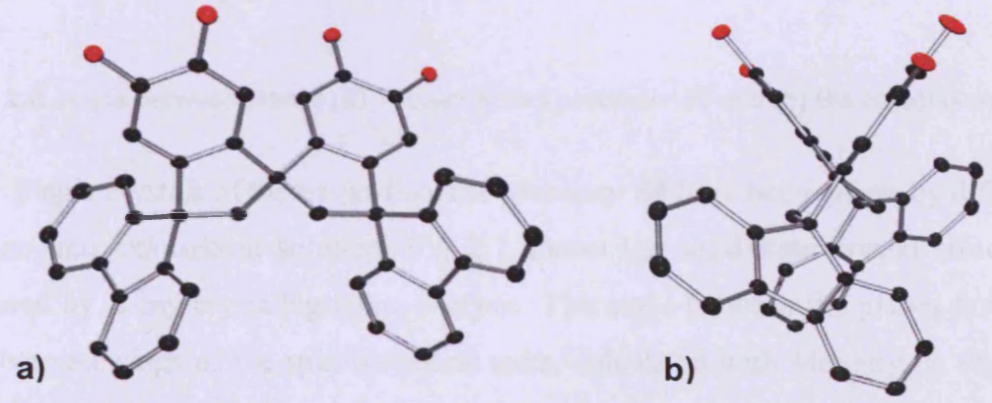

Fig 2.5. Solid state structure of the bis-catechol fluorene monomer **57**.
(a) Facial view. (b) Side view.

The crystal growth of the bis-catechol **57** proved much more difficult than the one for its precursor **56,** probably because of the well-established ability of bis-catechols to include solvent molecules in the crystal[139]. The data collected, in fact, showed one molecule of ethyl acetate per unit cell, as for **56**, but in addition, there was some disordered solvent, assumed to be water. This result was confirmed by TGA analysis on the bis-catechol **57** powder, which showed loss of solvent (3%, by mass) around 100 °C.

Fig 2.6 shows the comparison of the angle between the planes formed by the two benzene rings of the spirobisindane units in the tetra-methoxy (Fig 2.6 a) and the bis-catechol (Fig 2.6 b) compounds **56** and **57**, calculated with Mercury version 1_4_2. The two angles are just about the same (78.7° for the tetra-methoxy and 77.8° for the bis-catechol), demonstrating that the loss of the four methoxy groups does not influence the geometry of the molecule. This angle is significantly reduced from the one measured for the tetra-methyl monomer **A1** (84.7°) probably due to the steric effect of the bulky fluorene groups.

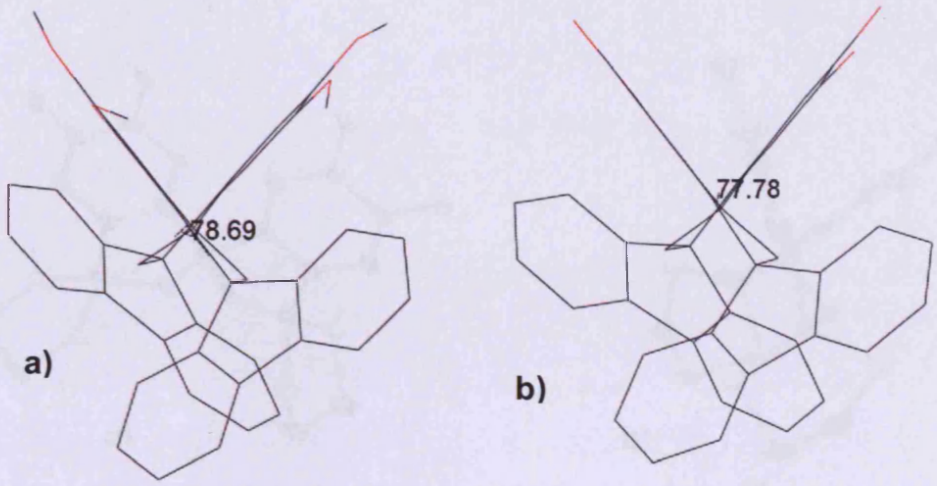

Fig 2.6. Angle between planes (a) Tetra-methoxy precursor **56** and (b) Bis catechol monomer **57**

Single crystals of the mono-fluorene precursor **58** have been grown by diffusion of *n*-hexane into chloroform solution. Fig 2.7 shows the solid-state crystal structure of **58** obtained by X-ray crystallographic analysis. The angle between the planes formed by the two benzene rings of the spirobisindane units, calculated with Mercury, is 88.3°, slightly higher than that one found in the tetra methyl monomer **A1** (84.7 °), but remarkably bigger than in the bis-fluorene monomer **56** (78.7°).

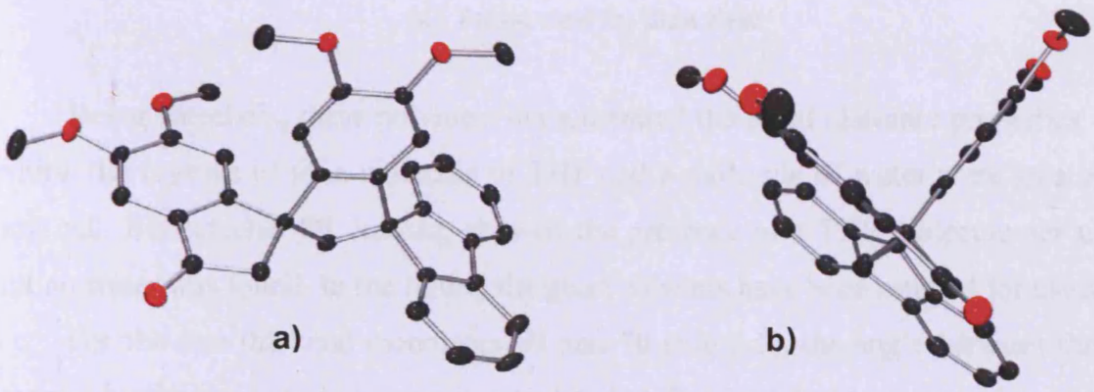

Fig 2.7. Solid state structure of the fluorene-ketone precursor **58**. (a) Facial view. (b) Side view

2.4.3 Thioketal-containing monomers

Both single crystals of the two thioketal-containing monomers **69** and **70** were grown by slow diffusion of chloroform into a THF solution. The structures determined by single crystal X-ray analysis are shown in Fig 2.8.

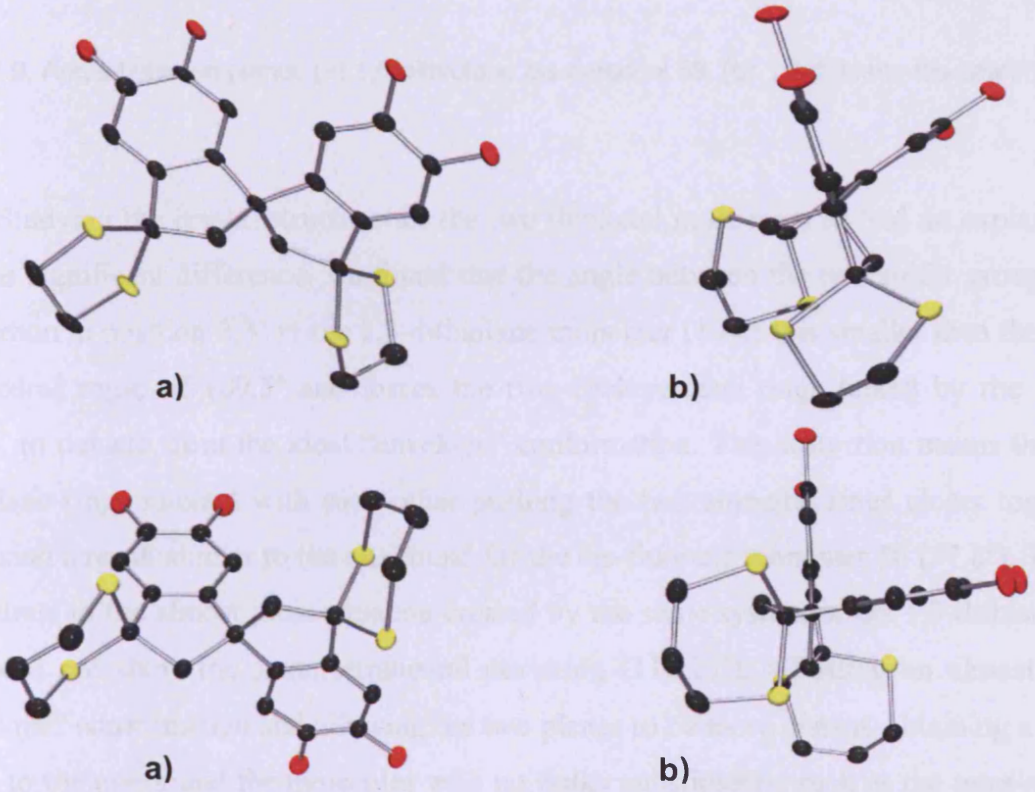

Fig 2.8. Solid-state structure of 1,3-dithiolane **69** and 1,3-dithiane bis-catechol **70** .
(a) Facial view (b) Side view

Being catechols, these polymers demonstrated the usual clathrate properties. In fact, whitin the crystals of **69** a molecule of THF and a molecule of water were located in the unit cell. Bis-catechol **70**, instead, showed the presence of a THF molecule per unit cell, but no water was found. In the figure, the guest solvents have been omitted for clarity.

For the two thioketal monomers **69** and **70** (Fig 2.9), the angle between the planes formed by the two catechol group is calculated at 73.4° and 83.4° respectively.

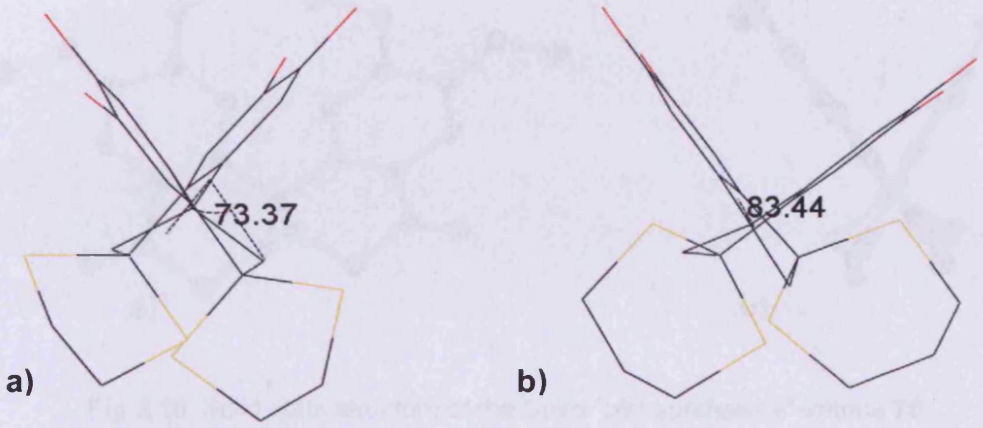

Fig 2.9. Angle between planes (a) 1,3-dithiolane bis-catechol **69**. (b) 1,3-dithiane bis-catechol **70**

Studying the crystal structure for the two thioketal monomers to find an explanation for this significant difference, we found that the angle between the two sulfur groups and the carbon in position 3,3' in the 1,3-dithiolane monomer (107.5°) is smaller than the ideal tetrahedral angle of 109.5° and forces the two cyclopentane rings linked by the spiro-centre, to deviate from the ideal "envelope" conformation. This distortion means that the dithiolane rings interact with each other pushing the two aromatic rings closer together, producing a result similar to the one found for the bis-fluorene monomer **56** (77.8°). This is in contrast to the almost ideal situation created by the same system in the 1,3-dithiane **70**, that does not show the same tetrahedral deviation (110.17°), affording an almost ideal "envelope" conformation and allowing the two planes to be more distant, obtaining a result closer to the one found for molecules with no bulky substituents, such as the tetra-methyl and the bis-ketone bis-catechol (84.8° and 84.6°).

2.4.4 "Spiro-bisnaphthalene"ketone monomer crystal structure

The successful achievement of the crystal growth of some "spiro-bisnaphthalene" monomers, allowed us to make a nice comparison between the two different families. The first crystals structure of this class of monomer was the spiro-ketone "spiro-bisnaphthalene" monomer **75**, obtained by slow diffusion of petroleum ether into a chloroform solution (Fig 2.10).

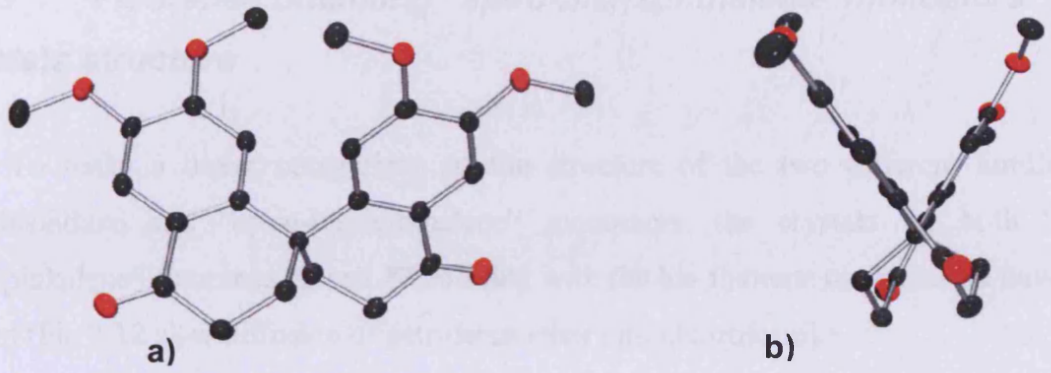

Fig 2.10. Solid-state structure of the Spiro-"bisnaphthalene"-ketone **75**.
(a) Facial view. (b) Side view

The structure appears very different from the one measured for the related bis-ketone **41**. In effect, though keeping the usual contorted profile caused by the spiro-centre, it is possible to observe that the shape of this "spiro-bisnaphthalene" monomer (Fig 2.11 a) looks much more twisted, probably as a consequence of the superior flexibility of the whole molecule due to the six membered rings.

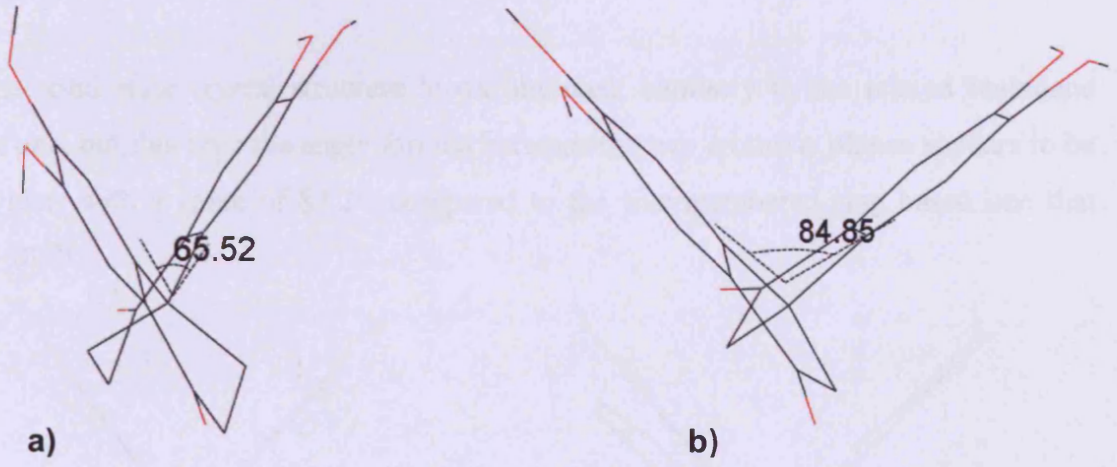

Fig 2.11. Angle between planes (a) Spiro-"bisnaphthalene"-ketone **75** (b) Bis-ketone monomer **41**

The angle between the planes formed by the two aromatic rings of the "spiro-bisnaphthalene" unit (65.5°) was much more acute than the respective angle calculated for the ketone spirobisindane **41** (84.8°, Fig 2.11 b). This result is unusual in the context of the equivalent angle measured for the other "spiro-bisnaphthalene" compounds below.

2.4.5 Fluorene-containing "spiro-bisnaphthalene" monomers crystals structure

To make a direct comparison of the structure of the two different families of, spirobisindane and "spiro-bisnaphthalene" monomers, the crystals for both "spiro-bisnaphthalene" fluorenes **82** and **83**, starting with the bis-fluorene monomer **82** have been grown (Fig 2.12 slow diffusion of petroleum ether into chloroform).

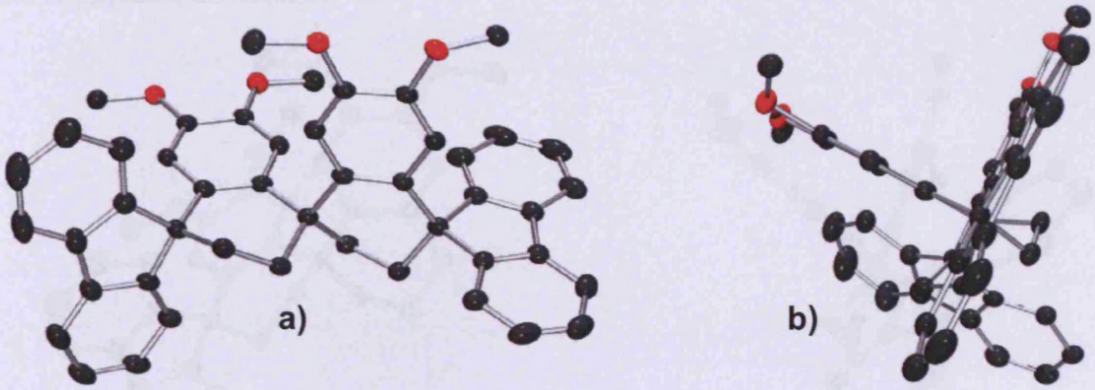

Fig 2.12. Solid state structure of the monomer **82**. (a) Facial view. (b) Side view

The solid state crystal structure looks hindered, similarly to the related bisindane fluorene one, but this time the angle formed between the two aromatic planes appears to be much wider, with a value of 87.2°, compared to the five-membered ring based one that showed 78.7°.

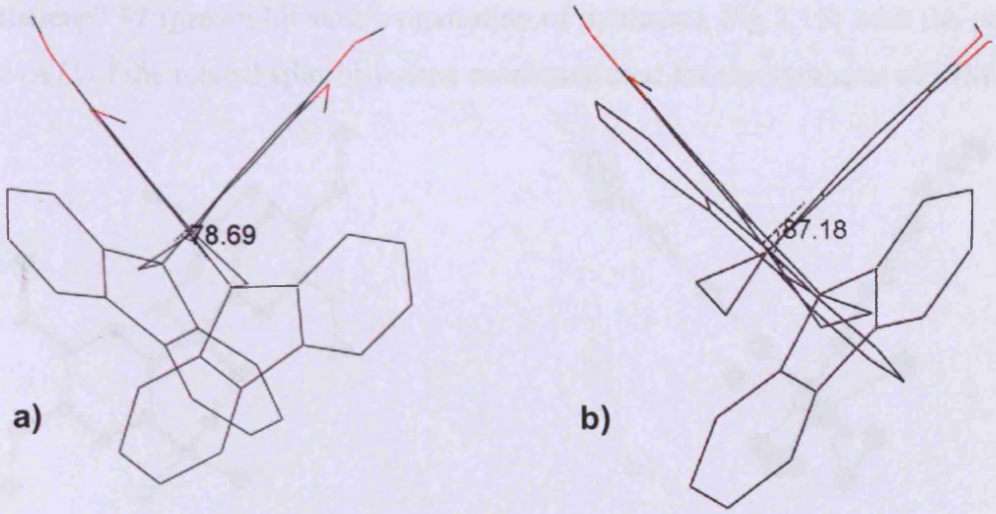

Fig 2.13. Angle between planes (a) Spiro-indane fluorene **56** (b) "Spiro-bisnaphthalene"-fluorene **82**

We attribute this pronounced difference to the greater flexibility of the six-membered rings which allows the spiro centre to be close to ideal tetrahedral geometry (Fig 2.13 b).

After the measurement of the structure of the mono-substituted fluorene crystals **83** (petroleum ether in chloroform, Fig 2.14), it was noticed that that the angle between the aromatic planes (87.40°) for this fluorene-ketone monomer, was very close to the one formed by the related bis-fluorene one (87.18°), showing no substituents-effect for this set of molecule, a result that is in contrast with the spirobisindane equivalent, in which there was a significant difference.

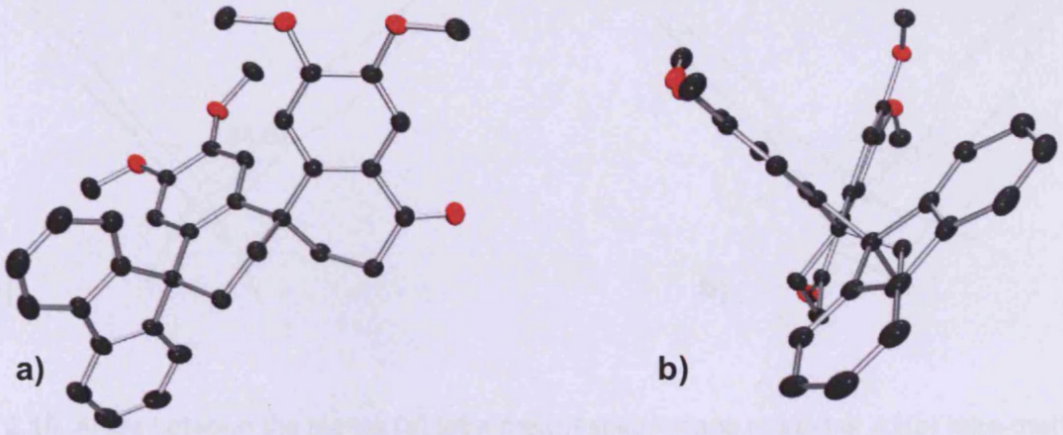

Fig 2.14. Solid state structure of the monomer **83** (a) Facial view. (b) Side view

2.4.6 *Tetra-methyl "spiro-bisnaphthalene" crystal structure*

The last comparison was with the crystal structure of the tetra-methyl "spiro-bisnaphthalene" 87 (grown by slow evaporation of methanol, Fig 2.15) with the published structure (**A1**) of the related spirobisindane monomer used for the synthesis of PIM-1.

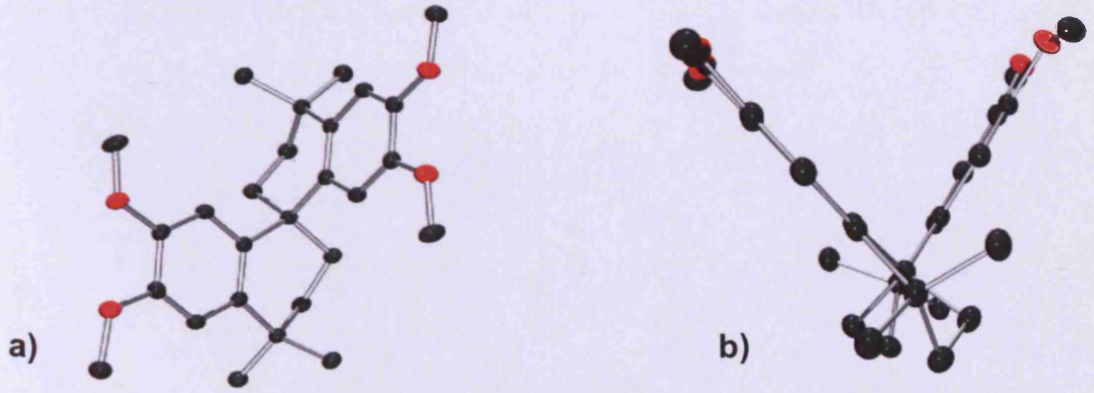

Fig 2.15. Solid-state structure of the "spiro-bisnaphthalene"-tetra-methyl **87**
(a) Facial view. (b) Side view

The angle formed between the planes of the veratrole ring (72.0°) is, once again, very different from the one observed for the related bis-catechol of the tetra-methyl spiro-indane monomer **A1** (84.7°, Fig 2.16). The structure of the tetra-methyl "spiro-bisnaphthalene" should represent the most ideal situation for this class of molecule, since nearly all the theoretical tetrahedral angles are respected so it is difficult to understand this relatively small angle.

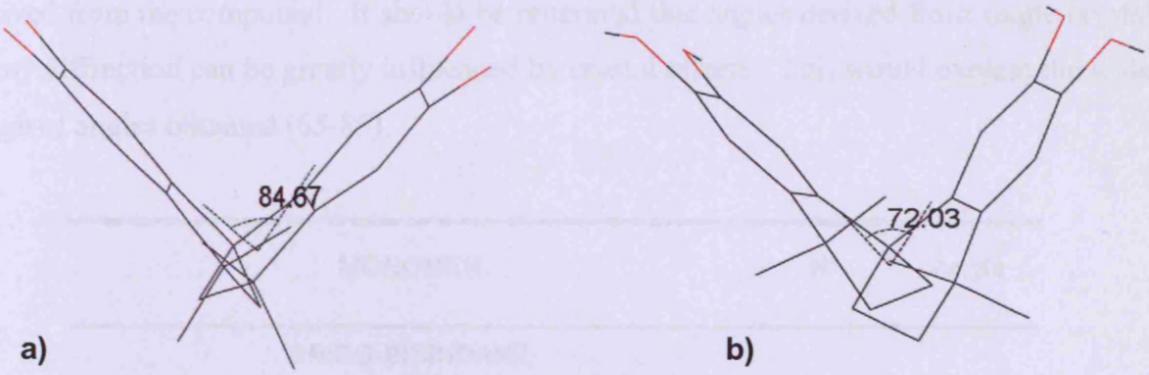

Fig 2.16. Angle between the planes (a) tetra-methyl spiro-indane monomer **A1**(b) tetra-methyl "spiro-bisnaphthalene" monomer **87**

2.5 Summary of crystals angles

Table 2.6 summarizes the angles formed between the aromatic planes for all structures obtained in this work. There seemed no particular pattern in the size of this angle and no correlation could be made between this parameter and the properties of the polymer derived from the compound. It should be reiterated that angles derived from single crystal X-ray diffraction can be greatly influenced by crystal effects. This would explain the wide range of angles obtained (65-85).

MONOMER	N°	Angle
SPIRO-BISINDANE		
Tetra-methyl spiro-indane (PIM-1)	**A1**	84.67°
Bis-ketone spiro-indane	**41**	84.85°
Bis-Fluorene spiro-catechol	**57**	77.78°
Bis-Fluorene spiro-indane	**56**	78.69°
Fluorene-Ketone spiro-indane	**58**	88.25°
"THIOKETALS"		
1,3- dithiolane spiro-catechol	**69**	73.37°
1,3- dithiane spiro-catechol	**70**	83.44°
"SPIRO-BISNAPHTHALENE"		
Tetra-methyl "spiro-bisnaphthalene"	**87**	72.03°
Bis-ketone "spiro-bisnaphthalene"	**75**	65.52°
Bis-Fluorene "spiro-bisnaphthalene"	**82**	87.18°
Fluorene-Ketone "spiro-bisnaphthalene"	**83**	87.40°

Table 2.6. Angles between planes for spiro-monomers

Tables 2.7 and 2.8, report the main parameters of the unit cells for all of the crystals measured during this project.

MONOMER	N°	Space group	Crystal System	Cell parameters	Z
SPIRO-BISINDANE					
Spiro-ketone	**41**	*P 21/c*	Monoclinic	a 9.8000(5) b 17.8710(9) c 10.4100(5) *β* 106.6280(10)	4
Fluorene	**56**	*P 21/n*	Monoclinic	a 13.5670(9) b 12.7930(8) c 22.1960(14) *β* 96.6630(10)	4
Fluorene catechol	**57**	*P 21/c*	Monoclinic	a 17.8884(9) b 8.6504(4) c 22.3939(11) *β* 94.0540(10)	4
Fluorene-Ketone	**58**	*P 21/c*	Monoclinic	a 9.7460(13) b 30.291(4) c 8.6740(12) *β* 97.111(3)	4
"THIOKETALS"					
1,3-dithiolane	**69**	*P -1*	orthorhombic	a 10.082(2) b 11.237(2) c 11.836(2) *α* 99.445(5) *β* 96.390(5) γ 103.035(4)	2
1,3-dithiane	**70**	*P 21/c*	Monoclinic	a 16.6331(8) b 12.4250(6) c 13.8082(7) *β* 107.2460(10)	4

Table 2.7. Cell parameters for spiro-bisindane crystals

MONOMER	N°	Space group	Crystal System	Cell parameters	Z
		"SPIRO-BISNAPHTHALENE"			
Spiro-ketone "spiro-bisnaphthalene"	**75**	*P 21/n*	Monoclinic	a 12.6940(9) b 7.7267(6) c 19.9754(15) β 97.2200(10)	4
Fluorene "spiro-bisnaphthalene"	**82**	*P c*	Monoclinic	a 15.594 b 12.564 c 18.339 β 90.2240(10)	4
Fluorene-Ketone "spiro-bisnaphthalene"	**83**	*P 21/c*	Monoclinic	a 16.8137(14) b 10.5577(9) c 31.344(3) β 103.6180(10)	8
Tetra-methyl "spiro-bisnaphthalene"	**87**	*P 2/c*	Monoclinic	a 8.1659(19) b 7.5298(18) c 19.130(5) β 97.935(4)	2

Table 2.8. Cell parameters for"spiro-bisnaphthalene" crystals

Chapter 3

3.1 Novel spirobisindane polymers

3.1.1 General procedure for polymerisation and purification.

Following the synthesis of the monomers, we proceeded systematically with their reaction with 2,3,5,6-tetrafluoroterephthalonitrile, to create new polymers to be tested as microporous materials.

The general procedure use for the polymerisations is based upon the optimized synthesis of PIM-1[81]. Since such step-growth polymerisations shows exceptional sensitivity to stoichiometry and impurities, rigorous reaction conditions are required. These include anhydrous DMF as solvent, inert nitrogen atmosphere and, importantly, careful measurement of the mass of the two monomers to 3 decimal places to ensure equimolar amounts, in order not to restrict the mass of the resulting polymer. As for previous preparations of PIMs, the two starting materials are added to the DMF, the mixture is heated to 65-70 °C and, only when they are completely dissolved, is the K_2CO_3 base added to start the reaction. The formation of a bright yellow suspension is usually noticed after 15-30 minutes during which oligomeric material is formed. Then the mixture is kept under stirring at constant speed for 72-96 hours, to obtain higher mass polymers. The purification of the solid, after quenching the reaction with water, depends on the solubility of the product in organic solvents. If it is completely soluble in low boiling organic solvents (usually THF or $CHCl_3$), then purification consisted of reprecipitation by dropping the solution into a mixture of acetone/methanol. This helps to remove oligomers from the crude product. This purification procedure is typically repeated at least two times.

When the resulting polymer was completely insoluble, the crude material was washed with THF, refluxed, filtered and washed repeatedly with mixtures of acetone/methanol 1:1. Some polymer products proved soluble only in high boiling solvents such as quinoline, DMAc or NMP but re-precipitation was avoided due to the difficulties encountered in the complete removal of the high boiling solvent. Therefore, these materials were purified simply by washing as for the insoluble polymers.

3.1.2 *Polymer from spiro-ketone 89*

The spiro-ketone **44** reacted with 2,3,5,6-tetrafluoroterephthalonitrile (Scheme 3.1) in high yield (80%) as shown in Scheme 3.1.

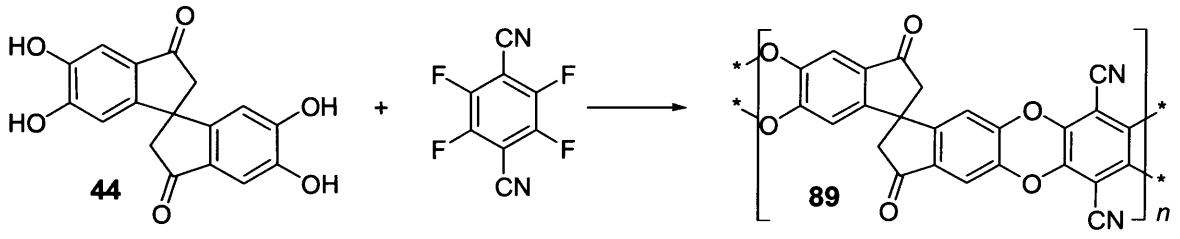

Scheme 3.1. Spiro-ketone polymer synthesis **89**. *Reagents and conditions*, K_2CO_3, DMF, 70 °C.

Unfortunately, the new polymer did not show solubility in any solvent other than conc. H_2SO_4, a result that confirms that the product was not a network polymer as networks polymers are insoluble in all solvents. Insolubility precluded characterisation by solution NMR and by GPC, which is the standard method used for the determination of a polymer's molecular weight. Probably, the reduced solubility of this polymer can be explained by its enhanced cohesive intermolecular interactions due to the polarity of the ketone groups.

The nitrogen adsorption isotherm (Fig 3.1) of the amorphous solid showed the typical curve[2] of type I, yielding a surface area value of 501 m^2/g with a very significant adsorption at $P/P_0 < 0.01$, that indicates the microporosity of the material, though with a result rather lower than obtained[81] for PIM-1, which was 780 m^2/g.

This lower surface area is, perhaps, due to the inferior bulkiness of the monomer. The methyl groups bond to the quaternary carbons in the monomer **A1** (PIM-1) are, possibly, able to generate a larger amount of voids in the material when packing in the solid state, whereas the ketone groups in this new PIM, may allow more efficient packing, with consequent loss of microporosity. The greater polymer cohesive interaction energy, caused by the more polar ketone group, may also lead to a denser packing.

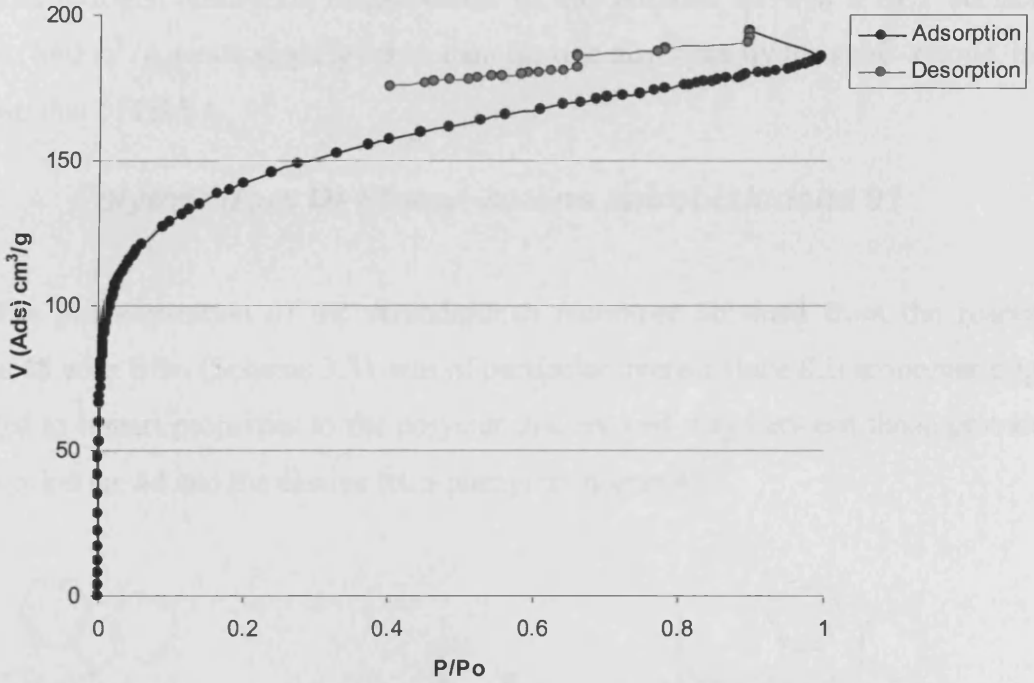

Fig 3.1. Nitrogen adsorption/desorption of the spiro-ketone polymer **89**

3.1.3 *Polymer from 3,3'-Diphenyl-1,1'-spirobisindene 90*

The polymerization of the spirobisindene monomer **46** provided a material that showed only scarce solubility in THF and $CHCl_3$, preventing the verification of the structure by NMR. However, compared to the polymer derived from the bis-ketone monomer **44** it proved more soluble in NMP and DMAc and completely soluble in quinoline. Once again, this hindered measurement of molecular weight by GPC but demonstrated that the replacement of the ketone groups with less polar components improved solubility.

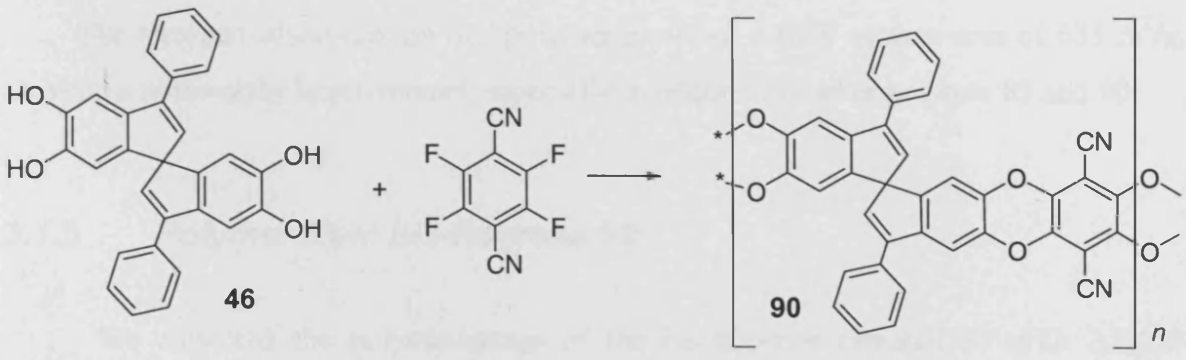

Scheme 3.2. Spirobisindene polymer **90**

The nitrogen adsorption measurement of this polymer showed a BET surface area value of 560 m^2 /g, result slightly better than the one displayed by the spiro-ketone, but still less than that of PIM-1.

3.1.4 Polymer from Di-Phenyl-ketone spirobisindane 91

The polymerization of the serendipitous monomer obtained from the reaction of lactone **48** with BBr_3 (Scheme 3.3), was of particular interest since this monomer might be expected to impart properties to the polymer that are mid-way between those provided by the spiro-ketone **44** and the elusive tetra-phenyl monomer **47**.

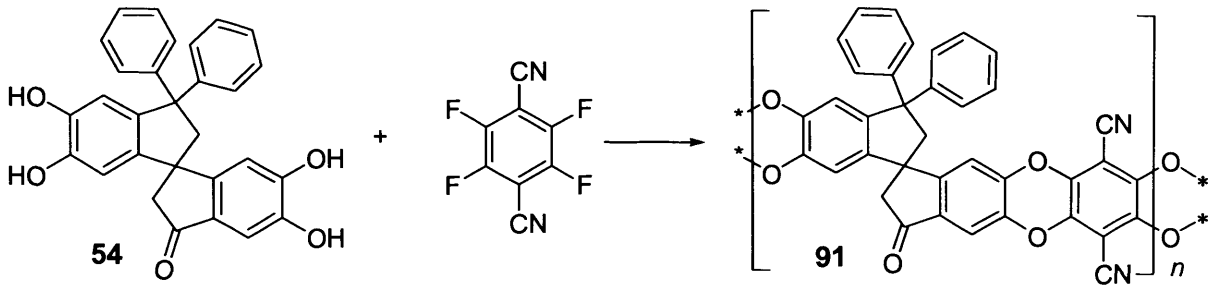

Scheme 3.3. Di-phenyl-ketone polymer.

This polymer showed good solubility in selected organic solvents including moderate solubility in both THF and $CHCl_3$, which allowed the acquisition of a solution NMR spectrum in which the peaks were substantially broadened. Due to its enhanced solubility, this polymer was the first for which GPC analysis could be obtained. The measurement yielded a M*n* value of 19000 and a M*w* = 26000, a result that indicates a relatively high molecular mass.Unfortunately, this polymer, did not result in good film-formation due to brittleness.

The nitrogen adsorption on this polymer provided a BET surface area of 685 m^2/g, showing a noteworthy improvement, especially in relation to earlier polymer **89** and **90**.

3.1.5 Polymer from bis-fluorene 92

We expected the polymerization of the bis-fluorene catechol **57** with 2,3,5,6-tetrafluoroterephthalonitrile, to provide an interesting material, due to the bulk and rigidity of the fluorene groups (Scheme 3.4).

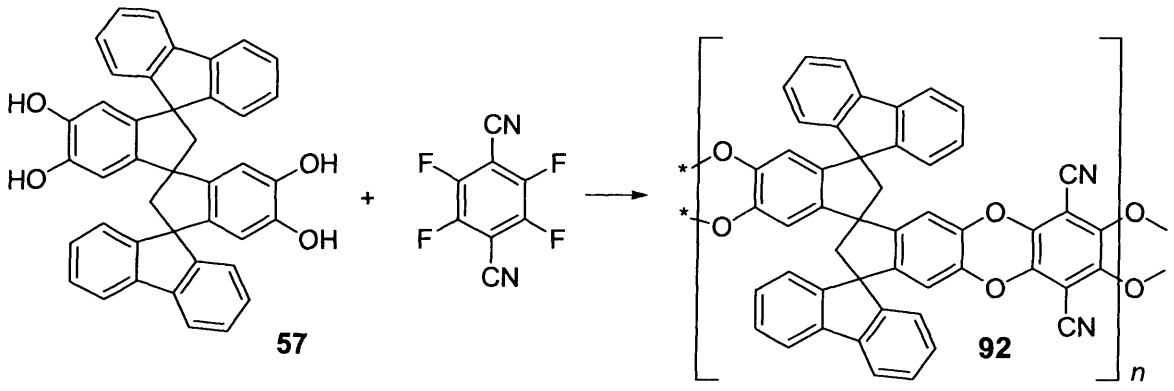

Scheme 3.4. Bis- fluorene polymer **92**.

As we hoped, the polymer turned out to be the first one of this series to be completely soluble in $CHCl_3$, a feature that allowed us to record a relatively well-defined NMR spectrum (Figure 3.2).

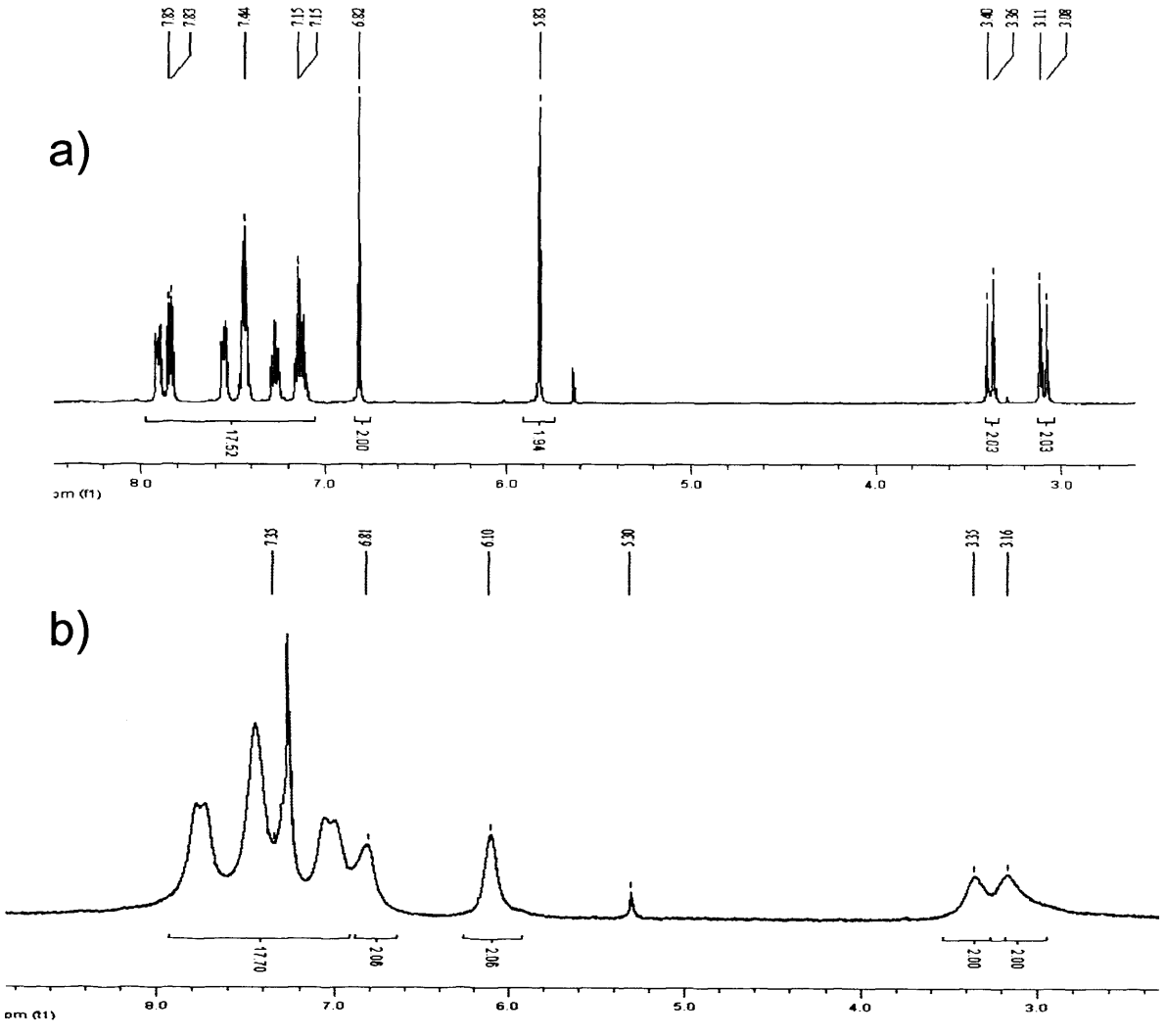

Fig 3.2. NMR spectrum of a) bis-fluorene bis catechol 57. b) bis fluorene polymer

From Fig 3.2 it is possible to observe that the chemical shifts and integration of the peaks are approximately the same as obtained for the monomer (Fig 3.2 a), but the loss of definition due to peak broadening is obvious (Fig 3.2 b) and can be attributed to the rigidity and lack of conformational freedom within the polymer.

GPC analysis on this polymer (Fig 3.3) gave figures of M_n = 16000 and M_w = 75000 showing a respectable molecular mass for this material, although, even in this instance, the polymer formed only a fragile membrane, preventing the evaluation of its gas permeability properties.

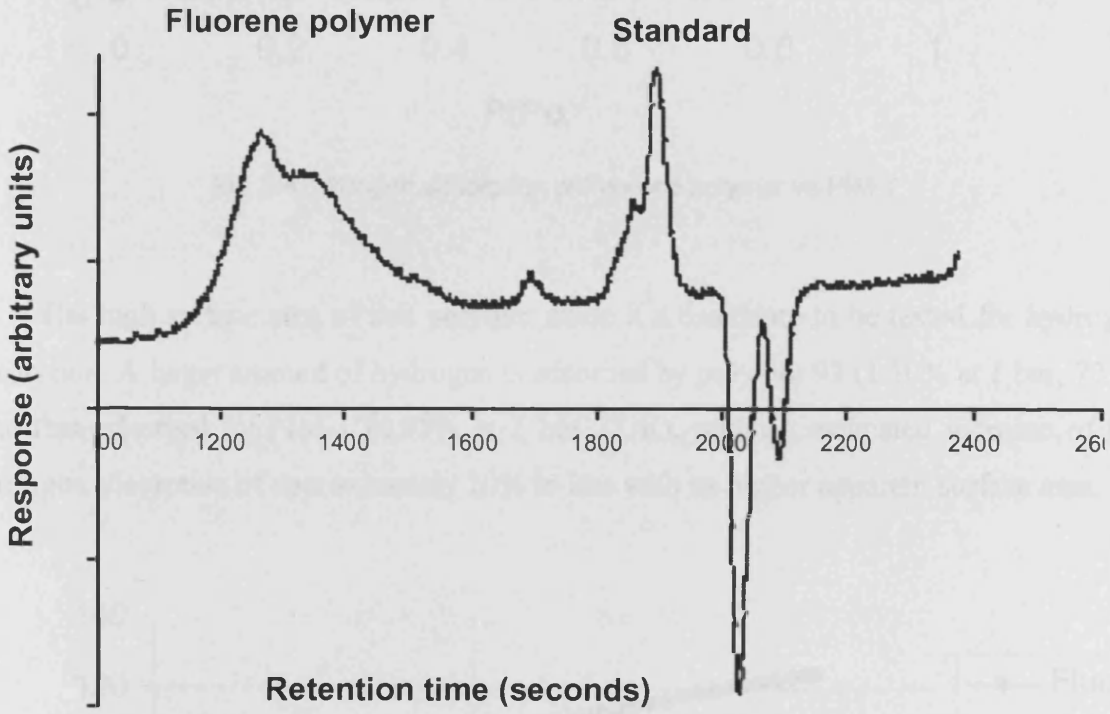

Fig 3.3. GPC analysis of the fluorene polymer relative to polystyrene standard

The most remarkable result for this polymer was obtained from nitrogen adsorption analysis from which a BET surface area of 895 m^2/g was calculated, an excellent result for this class of soluble PIMs and beating the previous best demonstrated by PIM-1 (Fig 3.4, desorption curves have been removed for clarity).

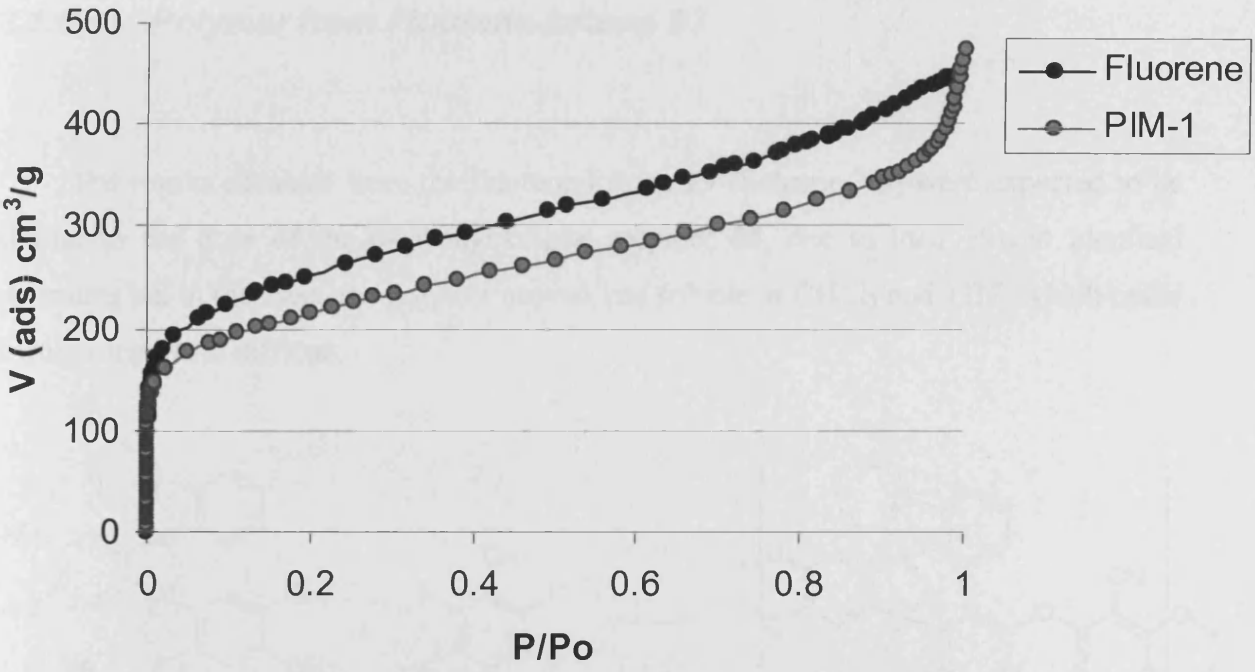

Fig 3.4. Nitrogen adsorption of fluorene polymer vs PIM-1

The high surface area of this polymer made it a candidate to be tested for hydrogen adsorption. A larger amount of hydrogen is adsorbed by polymer **92** (1.10% at 1 bar, 77 K) than that adsorbed by PIM-1 (0.95% at 1 bar 77 K), with an estimated increase of the hydrogen adsorption of approximately 10% in line with its higher apparent surface area.

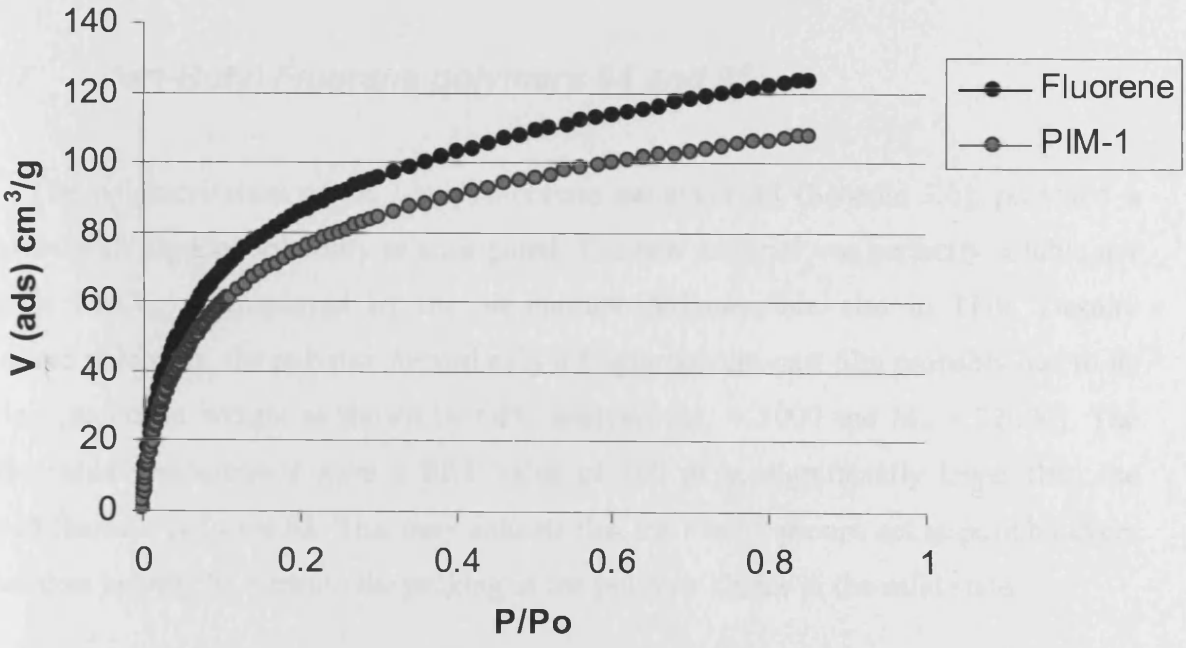

Fig 3.5. Hydrogen adsorption of fluorene polymer vs PIM-1

3.1.6 Polymer from Fluorene-ketone 93

The results obtained from the fluorene-ketone **59** (Scheme 3.5) were expected to be similar to the ones of the di-phenyl-ketone polymer **54**, due to their almost identical structures but in this case, the polymer proved less soluble in $CHCl_3$ and THF, which made a true comparison difficult.

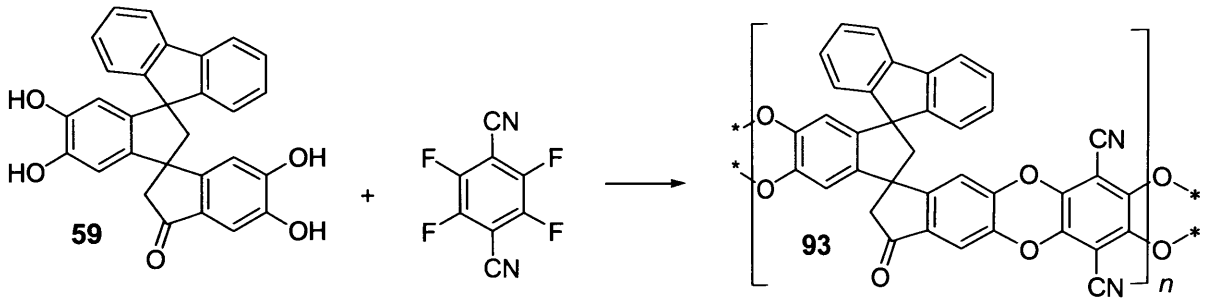

Scheme 3.5. Synthesis of fluorene-ketone polymer **93**

On the other hand, the nitrogen adsorption measurement for this polymer, provided a BET surface area of 658 m^2/g which is similar to that of the diphenyl-ketone polymer **91**.

3.1.7 tert-Butyl Fluorene polymers 94 and 95

The polymerization of the *t*-butyl fluorene monomer **64** (Scheme 3.6), provided a polymer with superior solubility as anticipated. The new material was perfectly soluble not only in $CHCl_3$, as displayed by the bis-fluorene polymer, but also in THF. Despite enhanced solubility, the polymer formed only a fragile solvent-cast film probably due to its modest molecular weight as shown by GPC analysis (M_n = 7000 and M_w = 22000). The surface area measurement gave a BET value of 760 m^2/g, significantly lower than the related fluorene polymer **92**. This may indicate that the *t*-butyl groups act as pore blockers rather than helping to frustrate the packing of the polymer chains in the solid state.

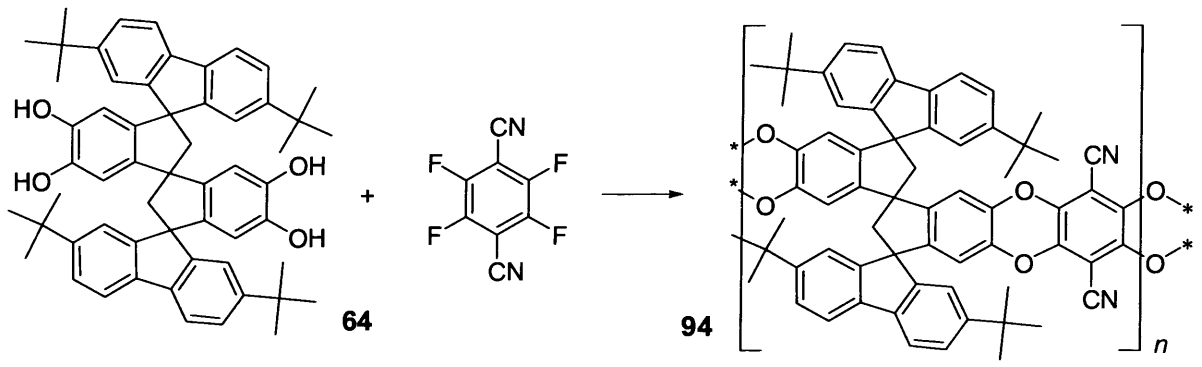

Scheme 3.6. Synthesis of the *t*-Butyl bis-fluorene polymer **94**

The polymer derived from the *t*-butyl fluorene–ketone **65** (Scheme 3.7) showed similar behaviour to its related mono-fluorene polymer **93**, although noticeably less soluble in THF. The calculated BET surface area (580 m^2/g) proved consistent with the values obtained from the related polymers, and showing the cumulative effects of the ketone and *t*-butyl groups in reducing microporosity.

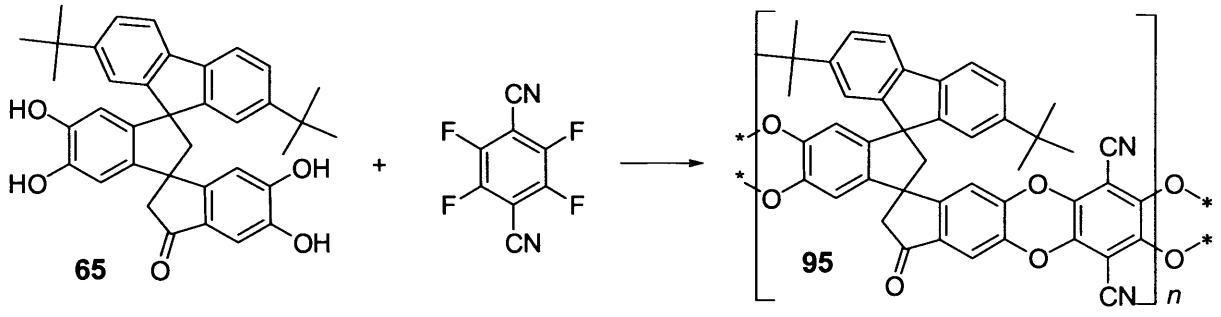

Scheme 3.7. Synthesis of *t*-Butyl-fluorene-ketone polymer **95**

3.2 "Spiro-bisnaphthalene"based polymers

The polymerizations of the "spiro-bisnaphthalene" monomers were achieved by the same procedure. This new set of polymers was considered with interest since the expansion of the spiro-fused rings was expected to enhance solubility of the resulting polymers.

3.2.1 "Spiro-bisnaphthalene"ketone polymer 96

The polymerisation of the bis-ketone **76** (Scheme 3.8) caused some concern because of the instability of the monomer towards moisture and air, which forced meticulous attention regarding the maintenance of the inert atmosphere, especially during the addition of the starting materials.

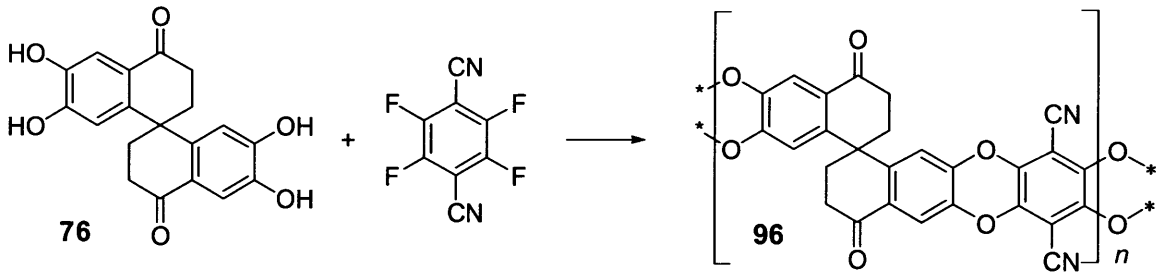

Scheme 3.8. Synthesis of "spiro-bisnaphthalene"ketone **96**

This polymer proved insoluble in all solvents including conc. sulfuric acid, perhaps due to cross-linking. This structural feature may help the microporosity as shown by the unexpectedly high BET surface area of 713 m^2/g. It was expected that the increased flexibility of the spiro-unit would tend to reduced microporosity.

3.2.2 Phenyl-"spiro-bisnaphthalene" polymer 97

The surface area result obtained for this polymer proved to be the least satisfactory of all of the polymers studied giving a value of only 203 m^2/g, although the shape of the isotherm the typical was typical for a PIM, with relatively high adsorption at $P/P_0 < 0.01$

and with a marked hysteresis. This result perhaps confirms the prediction that the spiro-bisnaphthalene structure is less compatible with the development of microporosity than the spirobisindane structure. This polymer proved completely insoluble in all organic solvents with the exception of quinoline, which is similar to the behaviour of the related spiro-bisindene **90**. In view of this fact, we decide to attempt the purification of the polymer by re-precipitation from quinoline solution into MeOH/Acetone. This procedure allowed us to improve the, initially, lower surface area result (100 m^2/g) but also required a prolonged Soxhlet-washing of the solid with hot MeOH, to purge the high boiling solvent.

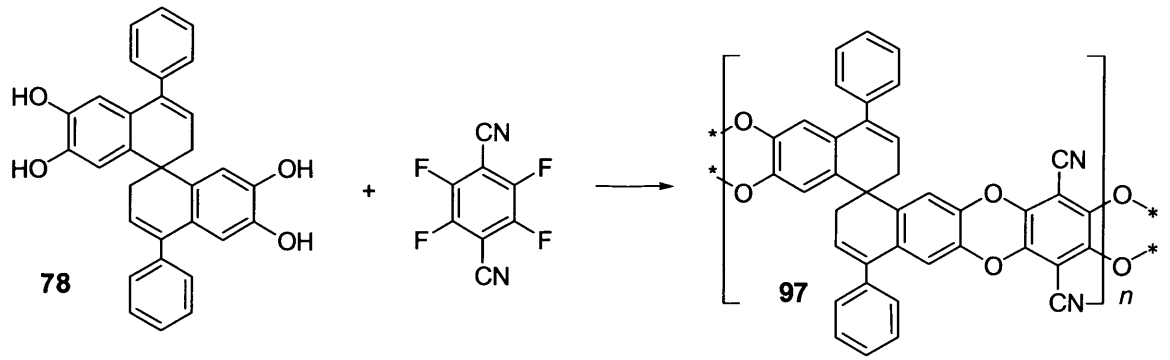

Scheme 3.9. Phenyl-"spiro-bisnaphthalene" polymer **97**

3.2.3 *Tetra-phenyl "spiro-bisnaphthalene" polymer 98*

Much interest was aroused by this polymer in order to ascertain the effect of the four phenyl components in the same monomeric unit, especially in order to predict the properties of the infuriatingly unobtainable spiro-bisindane tetra-phenyl polymer.

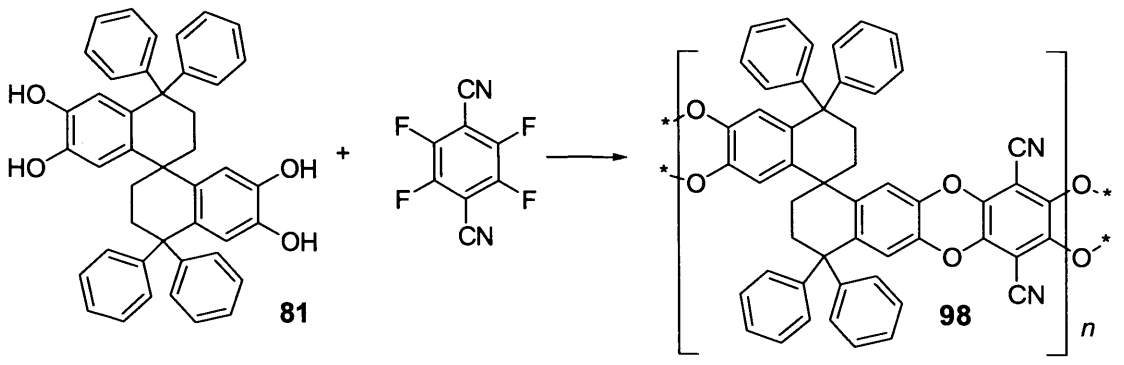

Scheme 3.10. Tetra-phenyl-spiro-"bisnaphthalene" polymer **98**

The solubility of this new material proved complete in THF and moderate in $CHCl_3$, leading us to the first fully processable polymer of this series of "spiro-bisnaphthalene" based polymers. The GPC analysis indicated an excellent molecular weight, with M_n = 18000 and M_w = 93000. However, this high molar mass did not help the formation of a good solvent-cast film, which proved, once more, brittle. It is of interest that samples of PIM-1 of similar molecular mass do form robust solvent cast films. The isotherm nitrogen adsorption provided a BET surface area of 395 m^2/g, slightly lower than we expected, which is possible to connect with the enhanced flexibility of the monomer. Nevertheless, it can be deduced that the four phenyl groups per repeat unit do not enhance either the microporosity or the film-forming characteristics of the PIM as compared to the four methyl groups per repeat unit of PIM-1.

3.2.4 *Fluorene-containing "spiro-bisnaphthalene" polymers 99 and 100*

Following the contradictory results shown by the previous polymers, we hoped, with the synthesis of the fluorene-containing "spiro-bisnaphthalene" polymer, to find a more reliable comparison between these two different families of PIMs (Scheme 3.11) to confirm that the spirobisindane unit is better suited for the attainment of intrinsic microporosity.

The solubility of polymer **99** proved excellent, being completely soluble both in THF and $CHCl_3$. Unfortunately, GPC analysis showed a relatively low molecular weight with M_n = 5000 and M_w = 26000; a result that is in contrast with the high mass obtained for the similar tetra-phenyl polymer **98**.

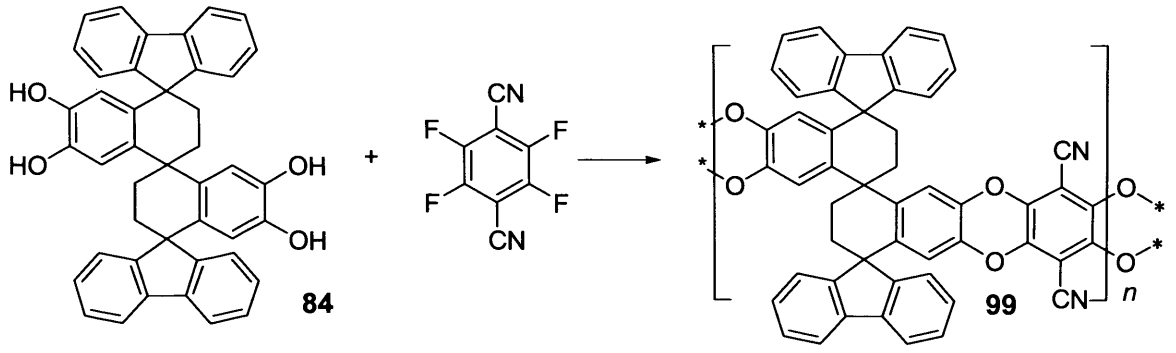

Scheme 3.11. Synthesis of bis-fluorene "spiro-bisnaphthalene" **99**

The value of the BET surface area was found to be 590 m^2/g, which is significantly lower than that demonstrated for the fluorine-based spiro-bisindane polymer, confirming the relatively inferior contribution of the "spiro-bisnaphthalene"unit to intrinsic microporosity as compared to the spiro-bisindane unit probably due to its greater flexibility.

The properties of the fluorene-ketone "spiro-bisnaphthalene" polymer **100** (Scheme 3.12) also confirmed this conclusion by demonstrating a BET surface area of only 300 m^2/g. In addition, it demonstrated comparable solubility to the other fluorene-ketone based polymer **93**.

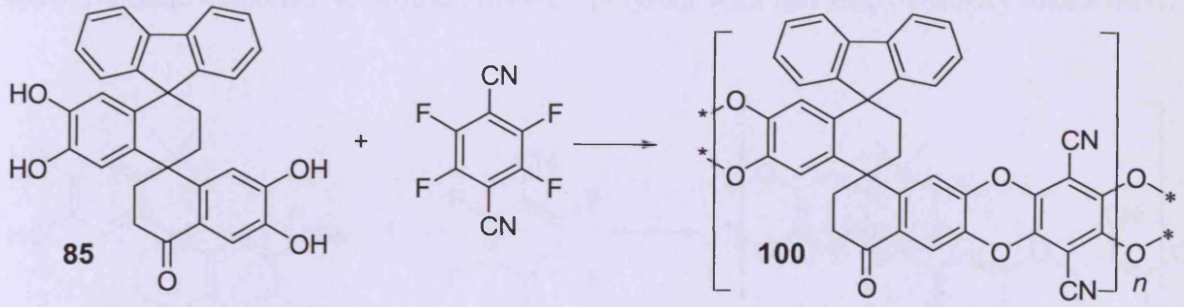

Scheme 3.12. Synthesis of the fluorene-ketone spiro-"bisnaphthalene" polymer **100**

Comparing the two, spiro-indane and "spiro-bisnaphthalene", fluorene-containing polymers, we noticed consistency in the ratio between their surface area values (Fig 3.6).

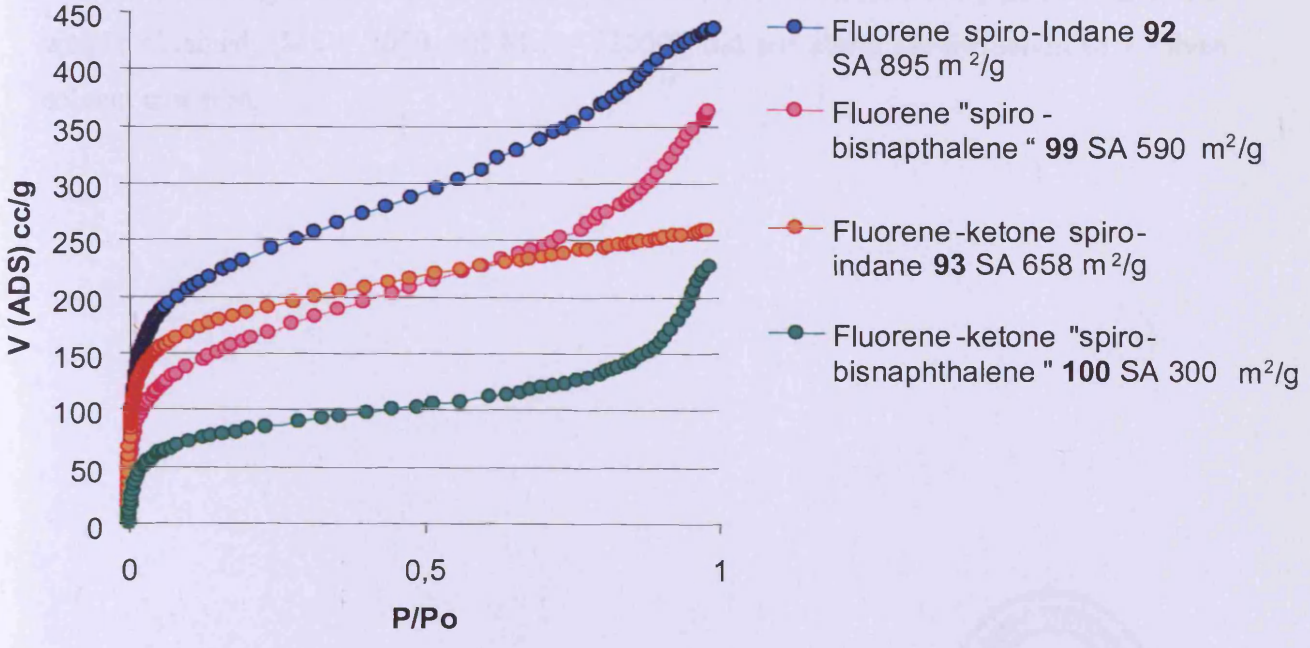

Fig 3.6. Comparison of the nitrogen adsorption isotherms for the fluorene-containing polymers.

3.2.5 *Tetra-methyl "spiro-bisnaphthalene" polymer 101*

As the last term of reference between the spirobisindane and "spiro-bisnaphthalene" families of spiro-based polymers, we proceeded with the reaction of 2,3,5,6-tetrafluoroterephthalonitrile and the tetra-methyl "spiro-bisnaphthalene" catechol **88** to obtain the polymer corresponding directly to PIM-1 for this expanded-ring family (Scheme 3.13). The BET surface area was found to be 432 m^2/g. Although this value is significantly less than that of PIM-1, it is higher than that obtained for the tetra-phenyl polymer **98** (395 m^2/g), a result that backs the conclusion that the unavailable tetraphenyl spirobisindane monomer **47** would provide a polymer with less microporosity than PIM-1.

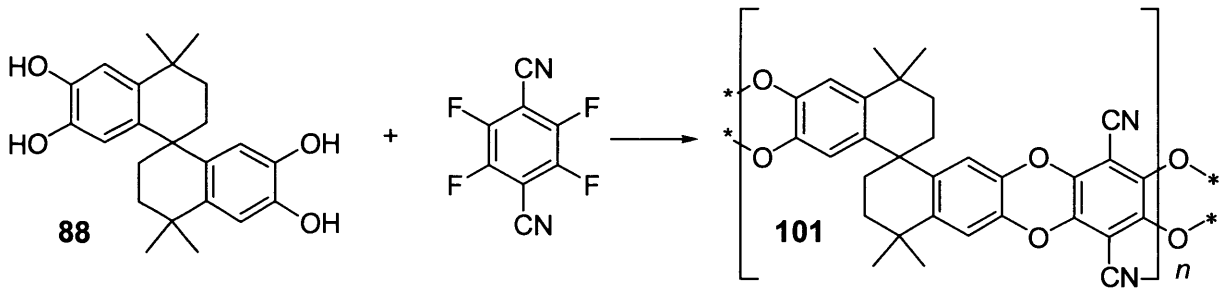

Scheme 3.13. Synthesis of tetra-methyl "spiro-bisnaphthalene" polymer **101**

In addition, the excellent solubility of this new material confirmed its similarities with PIM-1, being entirely soluble both in THF and in $CHCl_3$. However, the low molecular weight obtained, (M*n* = 7000 and M*w* = 22000), did not allow the formation of a robust solvent cast film.

3.3 Thioketal protected spirobisindane polymers

3.3.1 Thioketal-based polymers 102 and 103

The use of thioketal protecting groups was anticipated to improve the solvent processability of the spiro-ketone polymer by masking temporarily the polar groups and at the same time, to check for any variation in the physical properties of the material after the cleavage of the protecting groups, due to possible differences in the step-growth polymerization. This idea of using soluble precursor polymers is a common one in polymer science and thioketals have been used previously to sulubilize existing polymers.[126]

The reaction of both thioketal-protected monomers **69** and **70** with 2,3,5,6-tetrafluoroterephthalonitrile, was carried out with the usual procedure (Scheme 3.14), but immediate differences with previous reactions were noted. After a few minutes a very large amount of precipitate formed in the reaction and, after approximately one hour, the solution became so viscous that stirring became very difficult and further addition of DMF was required.

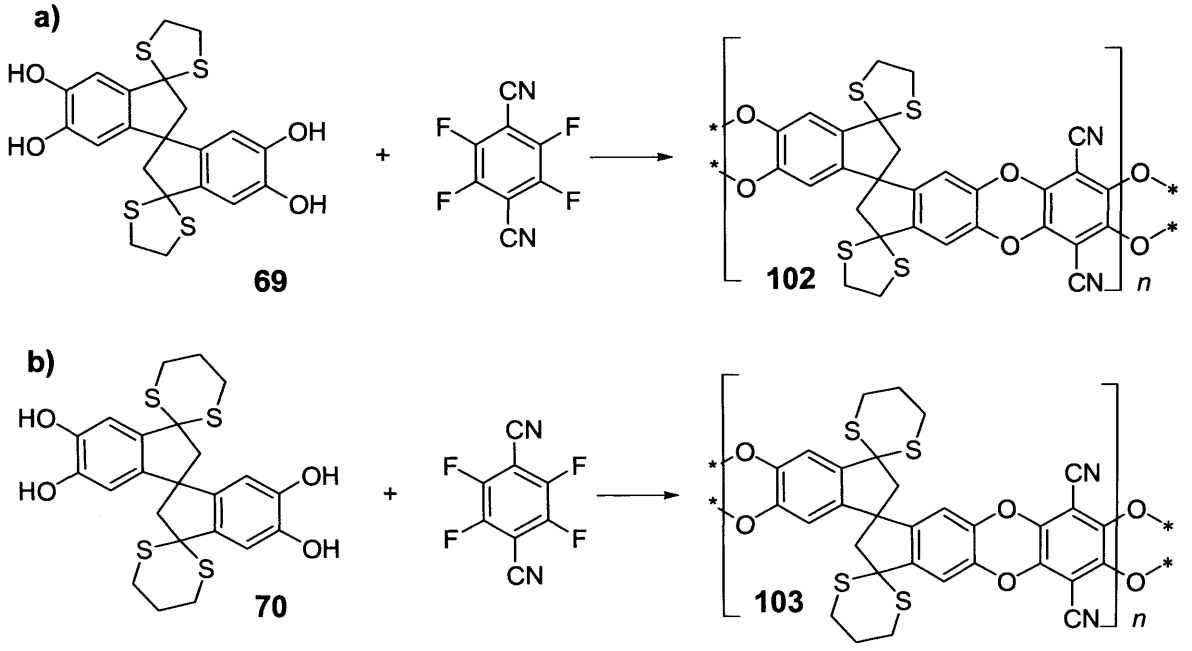

Scheme 3.14. Thioketal protected polymers. a) 1,3 dithiolane **102** b) 1,3 dithiane **103**

After the initial work up we noticed, with disappointment, that the material was only slightly more soluble that the spiro-ketone monomer. The solubility test, in fact, showed a complete solubility in NMP (with only a partial dissolution in THF) for the 1,3-dithiolane polymer **102** (Scheme 3.14 a), and a complete solubility in quinoline for the 1,3-dithiane polymer **103** (Scheme 3.14 b), even in this case only slightly soluble in THF.

The enhanced solubility of these polymers in high boiling solvent, however, led us to attempt purification by re-precipitation, but the removal of the traces of these high-boiling solvents proved really arduous. After washing of the solid with hot methanol, the measurement of the surface area of these sulfur-containing polymers, gave an unsatisfactory 205 m^2/g for the 1,3-dithiolane and an even worse (82 m^2/g) for the 1,3-dithiane, both of them far lower than the spiro-ketone which afforded 501 m^2/g. It is possible that the bulky thioketals are filling the pores of the material.

3.3.2 *Attempted deprotection*

After the rather unsatisfactory results obtained from the thioketal-containing polymers, both regarding their solubility and especially concerning their surface areas, we attempted their cleavage to allow the restoration of the ketone group in the spiro-centre part of the polymer, to allow comparison of the properties of the resulting polymers with those of polymer **89**, previously synthesized directly from the spiro-ketone bis-catechol (Scheme 3.15).

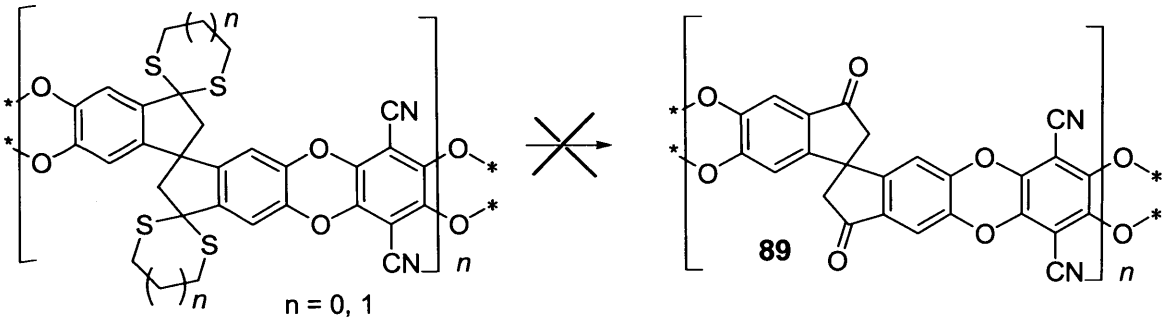

Scheme 3.15. Thioketal polymer deprotection

Different methods to perform this reaction are reported in the literature, but just a few are suitable to polymers so some were excluded a priori. As reported in previous work on thioketal-containing polymers from Colquhoun *et al.*[126] we discarded the methods using hydrogen peroxide[140] and 3-chloroperbenzoic acid (*m*CPBA)[141], trusting that if the same reaction did not work with their polymers, it would not work with ours. Instead, the deprotection reaction that proved successful for poly(aryl ether ketone), involving treatment with both 2-iodo-2-methylpropane and dimethylsulfoxide[142], was attempted. However, in our hands this reaction succeeded in only a partial deprotection of the thioketals, as monitored by TGA analysis and further confirmed by the measurement of the BET surface area, which did not give similar results to those previously obtained for the spiro-indane bis-ketone polymer. In addition, the elemental analysis on the resulting powder, demonstrated the presence of a relevant large amount of sulfur in the material, calculated as 60% of its starting weight a result that was consistent with the TGA measurements. Further attempts at deprotection of the rest of the polymer, using this procedure, proved unsuccessful.

In the literature are present some other promising methods[127,143] including some that could be useful in our case, including some which can be performed in the absence of solvent[144] that will be investigated in the near future.

3.3.3 Spiro-indane polymer 104

Another polymer derived from the work on the thioketal-protected monomers, was the unsubstituted spiro-indane **72**, obtained from the complete cleavage of the thioketal groups from the monomers with Raney Nickel (see part **2.1.10**). This peculiar polymer did not demonstrate a good surface area (BET = 108 m^2/g), illustrating the importance of the four methyl groups per repeat unit of PIM-1 presumably due to great flexibility of the spiro-fused ring structure which may allow the polymer chains to pack more efficiently in the solid state. This polymer also demonstrated reduced solubility in organic solvents and was only fully soluble in hot quinoline (Scheme 3.16).

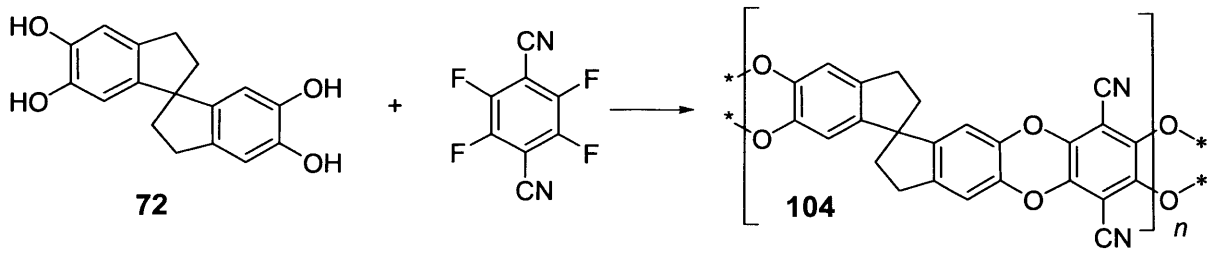

Scheme 3.16. Synthesis of spiro-indane polymer **104**

3.3.4 *Phthalocyanine-based network polymers 108 and 109*

The last experiment based on the thioketals as "sacrificial" groups, was based upon the synthesis of phthalocyanine-based network polymers, using a similar method to that described in previous work[69]. In order to create a term of comparison, we started from the nucleophilic aromatic substitution of the bis-catechol of the spiro-ketone **44** on the commercial 4,5-dichlorophthalonitrile (Scheme 3.17), obtaining the diphthalonitrile **105**. The same reaction was carried out with the thioketal bis-catechols to obtain the thioketal-containing diphthalonitriles **106** and **107** (Scheme 3.17 shows the 1,3-dithiolane-based diphthalonitrile **106**).

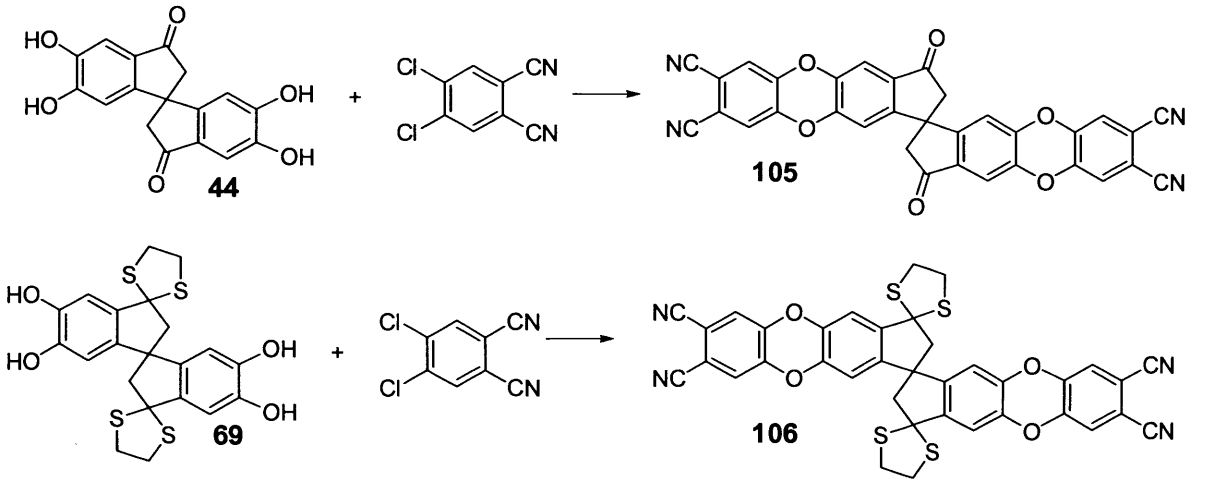

Scheme 3.17. Precursor formation. *Reagents and conditions*, K_2CO_3, DMF, 70 °C.

Both reactions were accomplished easily and in high yield. The only trouble was represented by the solubility of the thioketal-phthalonitriles (especially the 1,3-dithiane precursor **107**) that proved completely soluble only in DMSO. The subsequent

polymerization of the spiro-ketone and for the 1,3-dithiolane containing precursors in presence of Co(II)-acetate (Scheme 3.18), supplied the network polymers as green insoluble powders. However, the reaction failed for the 1,3-dithiane precursor, probably because of its poor solubility and a green solid was not obtained, despite the large excess of Co(II)-acetate and an increase in the temperature of the reaction. The two network polymers were purified using well-established methods[145].

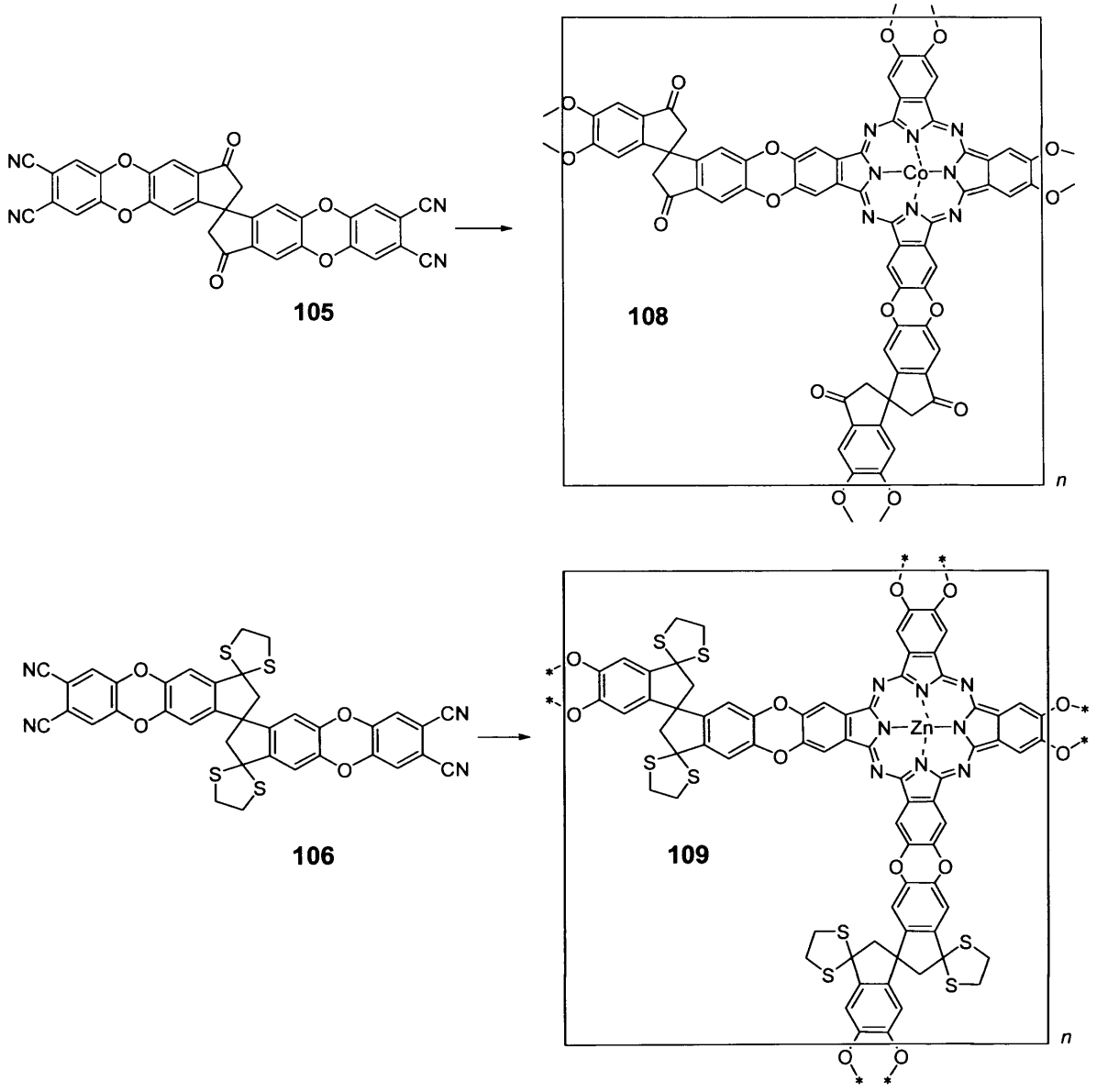

Scheme 3.18. Synthesis of phthalocyanine network polymers. *Reagents and conditions*, Co(II)-acetate, Quinoline, 70 °C.

The nitrogen adsorption measurement of the ketone-based network polymer, gave a BET surface area 284 m^2/g, whereas the one containing the 1,3-dithiolane-units did not

show any apparent surface area, which suggest that the thioketal groups block the micropores. Improvement of both synthesis and purification is required to confirm this conclusion and before any attempt at removal of the thioketal groups which is likely to be even more problematic than for the related ladder polymers **102** and **103**.

3.4 Summary of the physical properties

3.4.1 Nitrogen adsorption

In Fig 3.7 is shown the complete comparison of the nitrogen adsorption isotherms curves obtained for all the spiroindane-based polymers. Is possible to notice that the shape of the curve is always of type I^2, showing very significant adsorption at $P/P_0 < 0.01$ indicating the microporosity of the material.

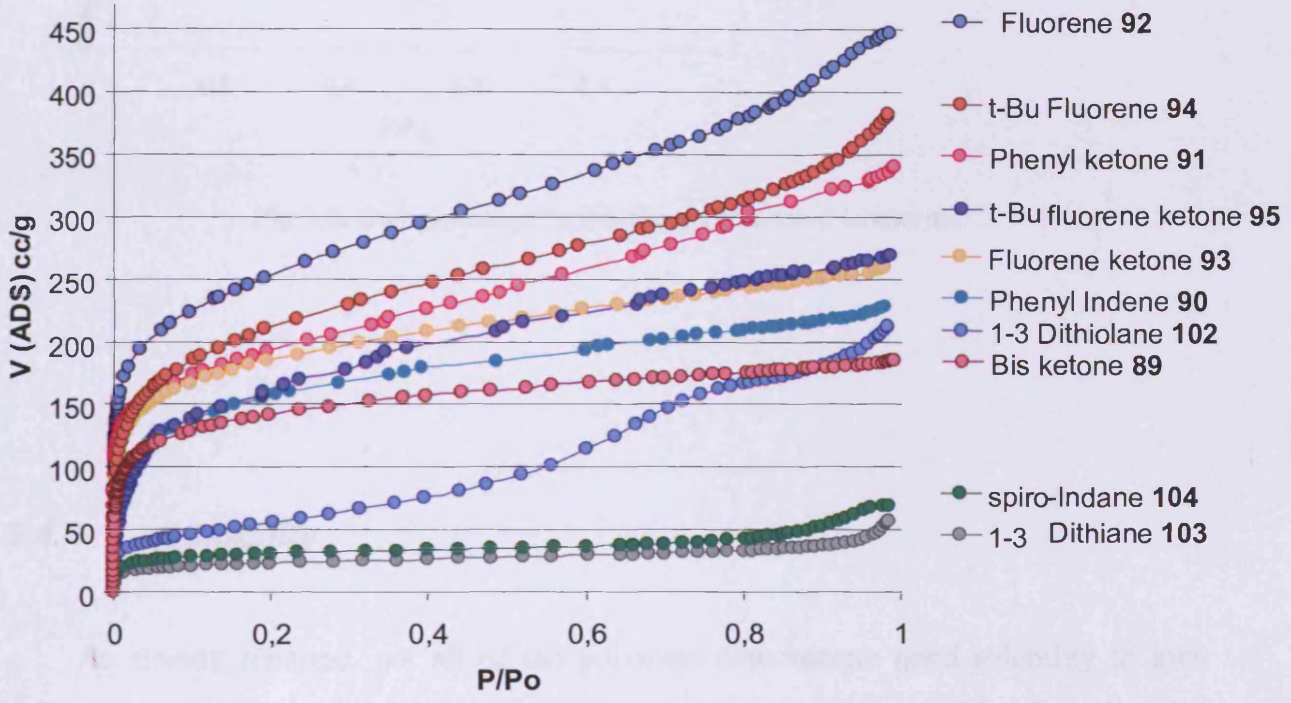

Fig 3.7. Comparison of the nitrogen adsorption isotherms for the spiro-indane polymers.

Comparing these isotherms with the one obtained for the "spiro-bisnaphthalene" (Fig 3.8) the significant difference in the amount of nitrogen (and hence BET surface areas) of the two families is readily noticed. Most evident is that the deviation of the curve from the

Y-axes, occurs earlier than in the spiro-indane polymers. The higher is this point, then the larger is the BET surface area. For instance, is worth noting that in the "spiro-bisnaphthalenes" isotherms, both fluorene and tetra-phenyl polymers reached a maximum adsorption of N_2 that is higher than for the bis-ketone polymer **98**, but the deviation from the Y-axis occurs later so that it records the highest surface area of the whole set.

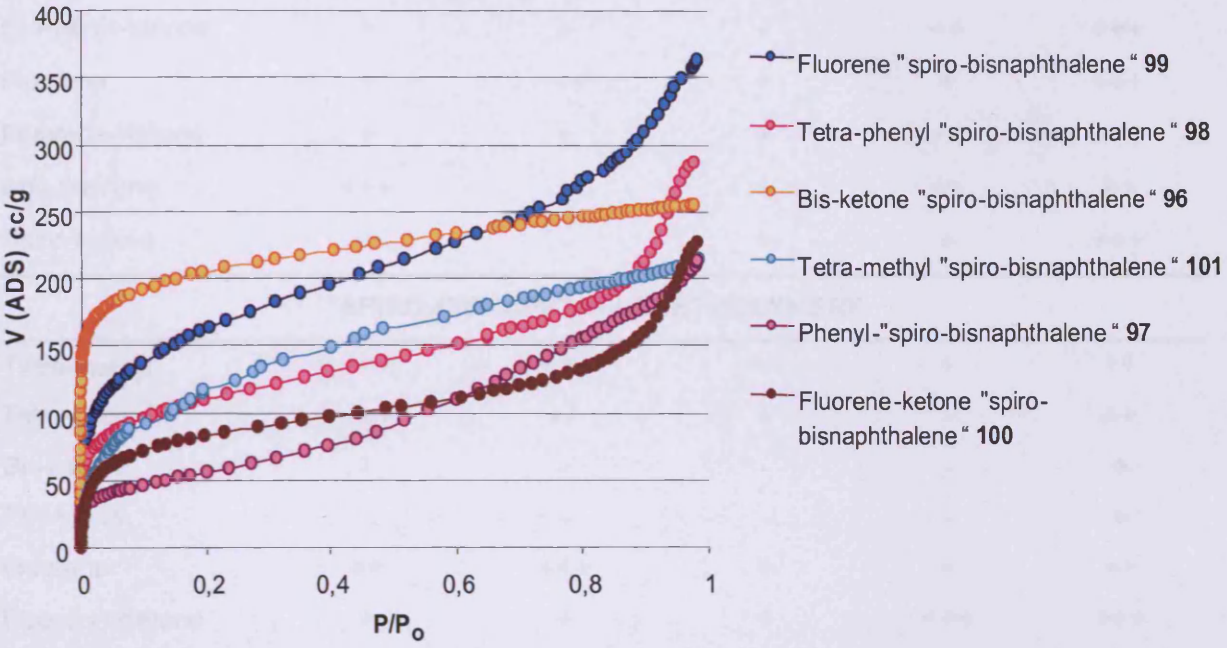

Fig 3.8. Comparison of "spiro-bisnaphthalenes" isotherms

3.4.2 *Solubility*

As already reported, not all of the polymers demonstrate good solubility in low-boiling organic solvents. The reasons for this can be complex and varied but it is clear that the methyl groups of PIM-1 play a crucial role in enhancing solubility and that replacing them with ketone groups drastically reduces solubility. Nevertheless, the fluorene-containing polymers proved significantly more soluble in organic solvents than PIM-1 and it appears that there is a rough correlation between good solubility and high microporosity. The results are outlined in Table 3.1.

POLYMER	SOLUBILITY				
	THF	$CHCl_3$	NMP	DMAc	Quinoline
SPIRO-BISINDANE POLYMERS					
Tetra-methyl	+++	++	+	+	+
Bis-ketone	+	-	-	-	+
Ph-indene	-	-	-	+	+++
Di-Phenyl-ketone	+	+	+	++	+++
Fluorene	+	+++	+	+	+++
Fluorene-Ketone	+	+	+	++	+++
t-Bu-fluorene	+++	+	+	++	++
Spiro-indane	+	-	+	+	+++
"SPIRO-BISNAPHTHALENE" POLYMERS					
Tetra-methyl	+++	+++	++	+	++
Tetra-phenyl	+++	++	+	-	++
Bis-ketone	-	-	-	-	+
Ph-indene	-	-	-	-	+
Fluorene	++	+++	+	+	++
Fluorene-Ketone	+	+	+	+++	+++
t-Bu-fluorene-ketone	++	+	+++	++	++
"THIOKETALS" POLYMERS					
1,3-dithiolane	+	-	++	+	++
1,3-dithiane	+	-	+	+	+++

Table 3.1. Summary of the solubility of PIMs

(+++ = completely soluble, ++ = mostly soluble, + = partially soluble, - = insoluble)

3.4.3 TGA analysis

The thermogravimetric analysis (TGA) shows another typical characteristic of these polymers, their excellent thermal stability.

The rate of increase of the temperature was of 20 °C/min from 30 to 1000 °C for all polymers, since it has been shown that different rates might produce different results[146,147,148]. Every polymer showed a loss of ~ 3-5% in mass above 300 °C, which may

be due to the tightly bound solvents still present in the microporous material. The thermal degradation of these polymers (T_{onset}) usually started in the range 450-490 °C, with a maximum loss of 42% of the total mass. Fig 3.9 shows a typical TGA curve: the fluorene-ketone spiro-bisindane polymer **93**. Differential scanning calorimetry (DSC) shows neither glass transition temperature (T_g) nor melting temperature (T_m) for any of these polymers.

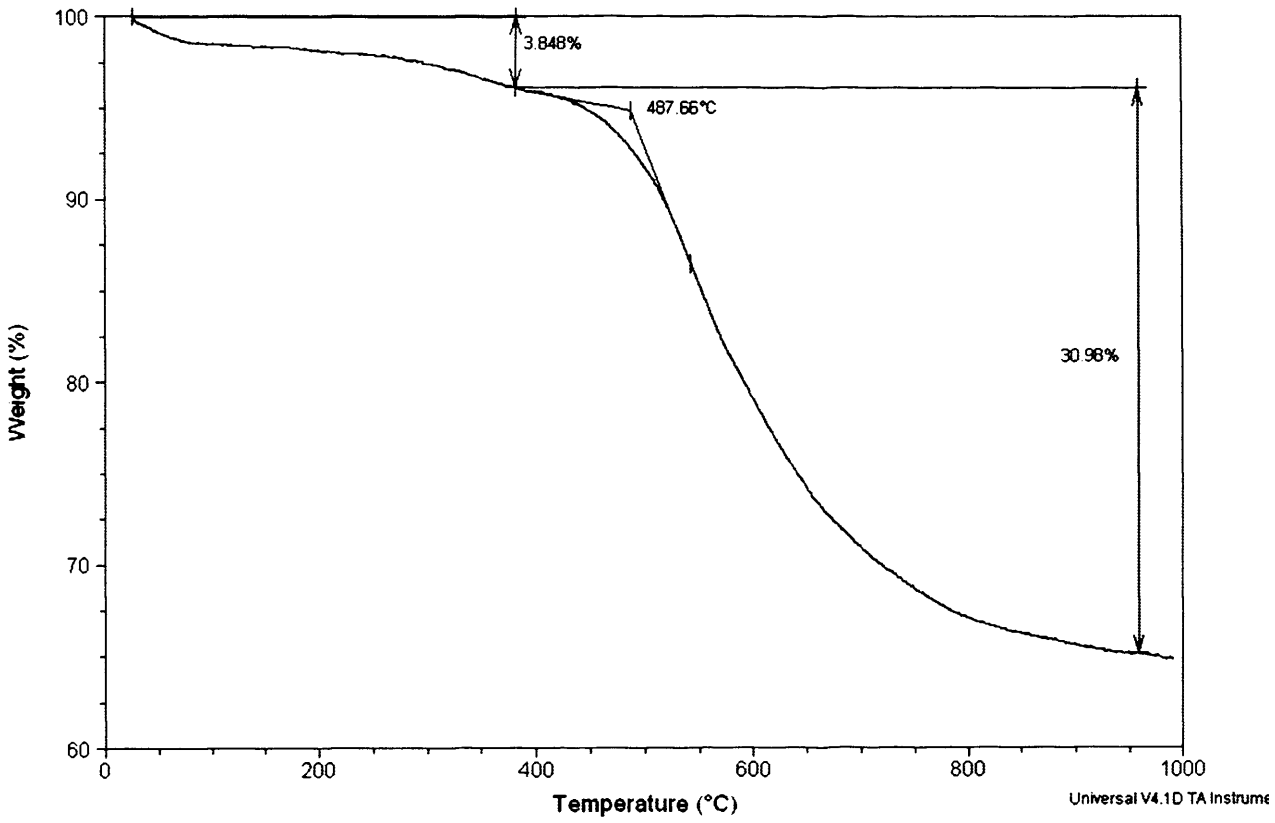

Fig 3.9. TGA result for the fluorene-ketone spiro-bisindane polymer

The TGA curve of the thioketal-containing polymers proved slightly different from the others. In addition to the usual loss of 3-5% due to included solvents, they showed two "steps" with greater loss of mass, the first corresponds to the complete removal of the thioketal groups, calculated from the repeat unit of the polymer, the second shows a typical T_{onset} as observed for the other polymers. These results suggest a thermal cleavage of the protecting groups. Fig 3.10 shows the TGA curve of a typical thioketal-containing polymer.

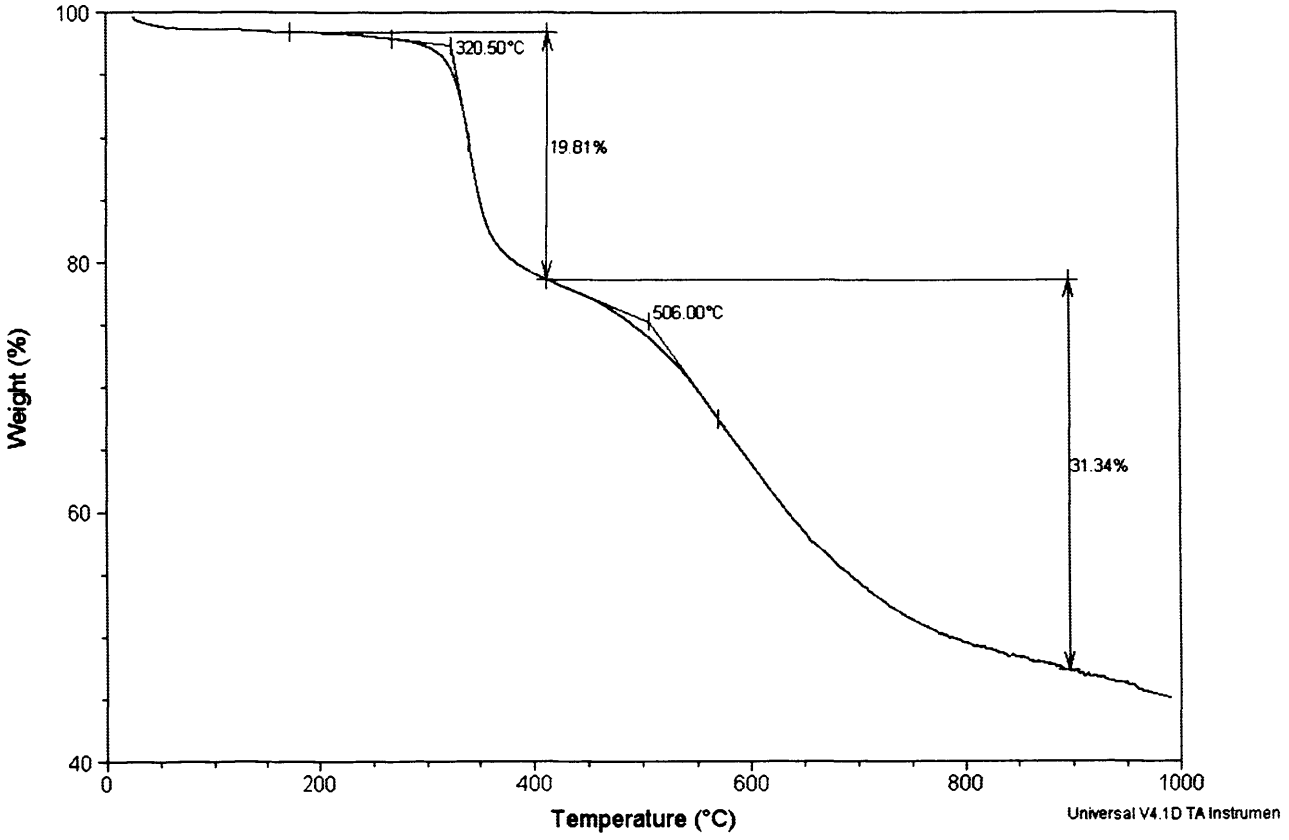

Fig 3.10. TGA result for the 1,3-dithiolane polymer

3.5 Conclusions

The work reported in this thesis described the successful synthesis of two new families of monomers and the polymers of intrinsic microporosity that can be prepared from them. The first one (the spiro-bisindanes, Scheme 3.19 a) is based on an extremely rigid monomer structure, due to the inclusion of the spiro-centre in two five-membered rings. In the other family (the "spiro-bisnaphthalenes"), the spiro-centre is included in a more flexible structure (Scheme 3.19 b).

Both families have been characterized by their physical properties, such as nitrogen adsorption and TGA. Some also proved soluble in organic solvents and were characterized by NMR and GPC.

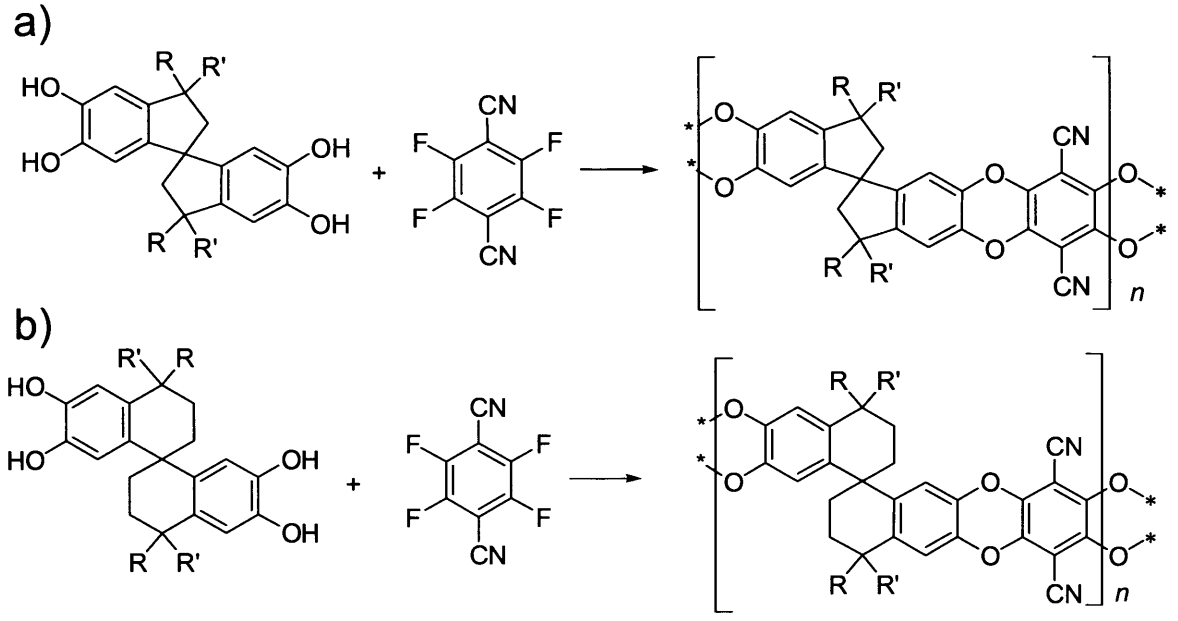

Scheme 3.19: Different families of PIMs

All polymers synthesized showed the typical properties of this class of materials. Every one, apart from the spiro-indane and the 1,3-dithiane, demonstrated very significant microporosity, with BET surface areas ranging from 895 m^2/g for the fluorene-containing spiro-bisindane **92**, to 203 m^2/g for the phenyl-substituted "spiro-bisnaphthalene" **96**.

Unfortunately, not all polymers proved soluble in low boiling solvents, preventing evaluation of their molecular weight and none formed high quality films for membrane studies, although optimisation of the molecular weight may improve this behaviour. From

the reported TGA results is noticeable that all polymers demonstrate a very high T_{onset} (> 350 °C) showing the good thermal stability of the materials, which is further confirmed by the relatively low loss of weight at 1000 °C (i.e. carbonisation).

All the most important results for both families of polymers are summarized in Table 3.2.

POLYMER	Surface area (m^2/g)	Mw /10^3 (g/mol)	3-5% weight loss (°C)	T_{onset} (°C)	Weight loss (%)
SPIRO- BISINDANE POLYMERS					
Bis-ketone	501	Insoluble	400	499	37
Bis-indene	560	Insoluble	390	513	32
Di-Phenyl-ketone	684	26	390	490	37
Bis-fluorene	895	75	390	550	27
Fluorene-Ketone	658	Insoluble	350	488	31
t-Bu-Fluorene	760	22	395	508	38
t-Bu-Fluorene-ketone	580	Insoluble	400	505	31
Spiro-indane	108	Insoluble	330	442	37
"SPIRO- BISNAPHTHALENE" POLYMERS					
Bis-ketone -"spiro-bisnaphthalene"	713	Insoluble	380	445	37
Phenyl-"spiro-bisnaphthalene"	203	Insoluble	390	466	27
Tetra-phenyl-"spiro-bisnaphthalene"	395	93	300	495	42
Bis-fluorene -"spiro-bisnaphthalene"	590	16	400	495	36
Fluorene-ketone-"spiro-bisnaphthalene"	300	Insoluble	380	486	35
Tetra-methyl-"spiro-bisnaphthalene"	432	22	390	490	37
"THIOKETALS" POLYMERS					
1,3-dithiolane	205	Insoluble	310	321, 507	19, 30
1,3-dithiane	82	Insoluble	320	332, 530	27, 27

Table 3.2. Summary of the physical properties of PIMs

3.6 Future work

The future development of this project will be based on the, functionalization of the fluorene monomer **56** (already started with the addition of *t*-Butyl groups) and further investigation of its properties as a polymer, in search of any possible improvement, especially regarding the formation of solvent-cast films. A possible synthetic approach might be represented by the bromination of the fluorene monomer, by well-established methods[117,116] , to be followed by substitution of the bromide with aromatic and alkyl substituents groups of interest [110](Scheme 3.20).

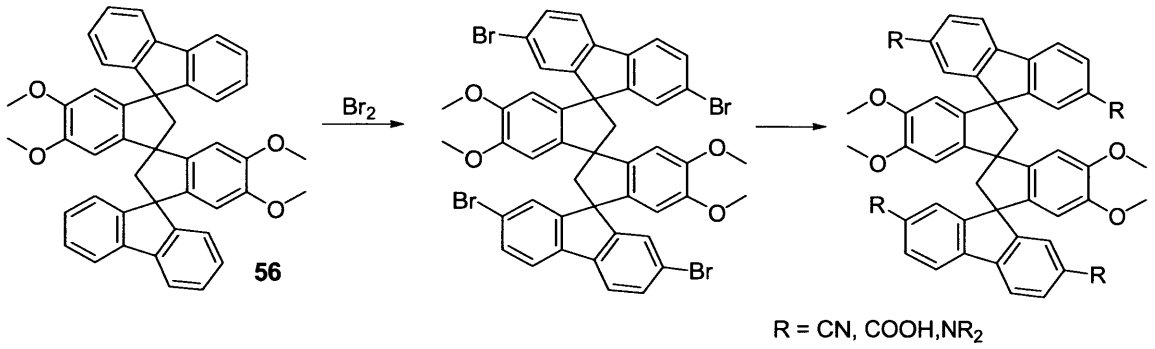

Scheme 3.20: Functionalization of the bisfluorene monomer **56**

More effort could be focused on the synthesis of the tetra-phenyl bisindane monomer **47** that, so far, has proved high problematic. A potential new approach towards this molecule is suggested by the synthesis of tetra-methyl catechol **A1** synthesised by Baker using phorone and catechol[88]. This route requires the synthesis of the known 1,1,5,5-tetraphenyl-1,4-pentadiene-3-one **110** that has been previously prepared by two different methods.[149,150]

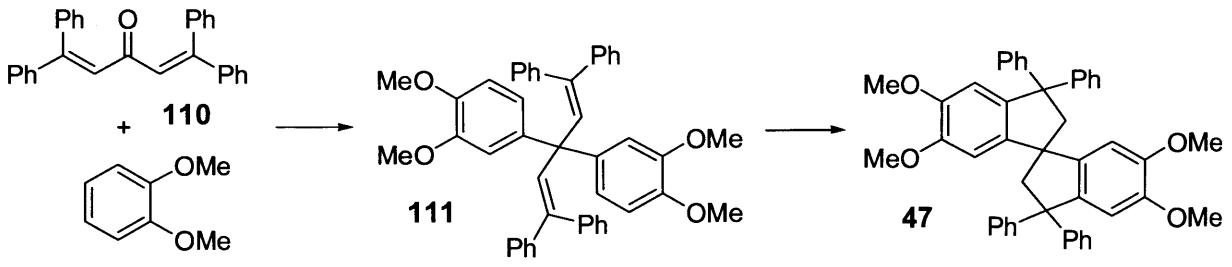

Scheme 3.21: Possible synthesis of tetra-phenyl bisindane monomer **47**

The first route is based on the coupling of 1-bromo-2,2-diphenylethene 112 and 2,2-diphenylacrylonitrile **113** by a Grignard type reaction (Scheme 3.22).

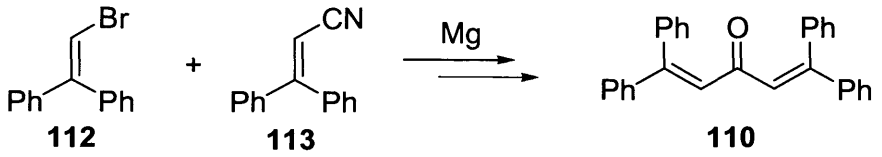

Scheme 3.22: First method for synthesis of ketone **110**

The second possibility (Scheme 3.23) involves the formation of 1,1,5,5-tetraphenyl-pent-2-yne-1,5-diol **117** in two steps of which the first one is the synthesis of 1,1-diphenyl-3-butyne-1-ol **116** by a Reformatsky type reaction, starting from propargyl bromide **114** and benzophenone **115** [151], whereas the second step is based on the reaction between 1,1-diphenyl-but-3-yne-1-ol **116** and benzophenone **115** mediated by potassium hydroxide and potassium tert-butoxide. The diol **117** can be converted into 1,1,5,5-tetraphenyl-1,4-pentadiene-3-one **110** by the Meyer-Schuster rearrangement[152].

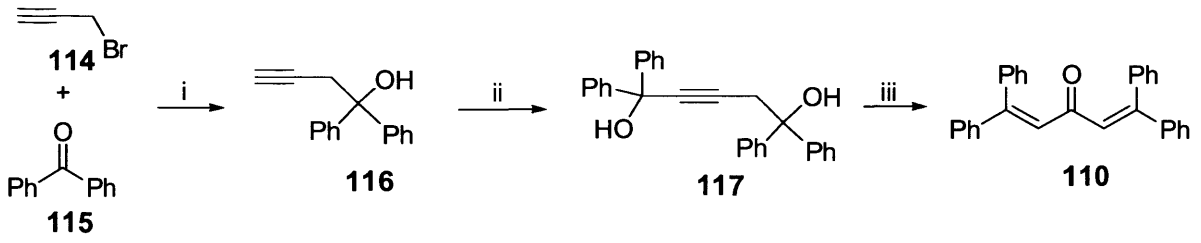

Scheme 3.23: Second method for synthesis of ketone **110**. *Reagent and conditions.* i . Mg, Al or Zn, THF, 0 °C. ii. benzophenone, KOH, KO-Bu, THF. iii. H_2SO_4, THF

To date, the synthesis of the tetra-phenyl intermediate **111** has been achieved[153], but the intramolecular cyclization to reach the monomer **47** following Baker's method has proved more difficult than expected, once again illustrating the stubborn inaccessibility of this simple target molecule.

Chapter 4

4.1 Experimental techniques

General remarks

Commercially available reagents were used without further purification. Anhydrous dichloromethane was obtained by distillation over calcium hydride under nitrogen atmosphere. Dry tetrahydrofurane was obtained by pre-drying commercially available tetrahydrofurane over sodium in presence of sodium benzophenone as indicator. Anhydrous *N,N*-Dimethylformamide was bought from Aldrich. All reactions using air/moisture sensitive reagents were performed in oven-dried or flame-dried apparatus, under a nitrogen atmosphere.

TLC analysis refers to analytical thin layer chromatography, using aluminum-backed plates coated with Merck Kieselgel 60 GF_{254}. Product spots were viewed either by the quenching of UV fluorescence, or by staining with a solution of Cerium Sulfate in aqueous H_2SO_4. Flash chromatography was performed on silica gel 60A (35-70 micron) chromatography grade (Fisher Scientific).

Under vacuum refers to evaporation at reduced pressure using a rotary evaporator and diaphragm pump, followed by the removal of trace volatiles using a vacuum oven.

Melting points were recorded using a Gallenkamp Melting Point Apparatus and are uncorrected.

InfraRed spectra (IR)

Infrared spectra were recorded in the range 4000-600 cm^{-1} using a Perkin-Elmer 1600 series FTIR instrument either as a thin film or as a nujol mull between sodium chloride plates. All absorptions are quoted in cm^{-1}.

Nuclear Magnetic Resonance (NMR)

^1H NMR spectra were recorded in $CDCl_3$ (unless otherwise stated) using an Avance Bruker DPX 400 instrument (400 MHz) or an Avance Bruker DPX 500 (500 MHz), with ^{13}C NMR spectra recorded at 100 MHz or 125 MHz respectively. Chemical shifts (δ_H and δ_C) were recorded in parts per million (ppm) from tetramethylsilane (or chloroform) and

are corrected to 0.00 (TMS) and 7.26 ($CHCl_3$) for ^1H NMR and 77.00 ($CHCl_3$), centre line, for ^{13}C NMR. The abbreviations s, d, t, q, m and br. denote singlet, doublet, triplet, quartet, multiplet and broadened resonances; all coupling constants were recorded in hertz (Hz).

Mass spectrometry

Low-resolution mass spectrometric data were determined using a Fisons VG Platform II quadrupole instrument using electrospray ionisation (ES) unless otherwise stated.
High-resolution mass spectrometric data were obtained in electrospray (ES) mode unless otherwise reported, on a Waters Q-TOF micromass spectrometer.

Nitrogen adsorption/desorption

Low-temperature (77 K) N_2 adsorption/desorption measurements of PIM powders were made using a Coulter SA3100.Samples were degassed for 800 min at 120 °C under high vacuum prior to analysis.

Thermo Gravimetric Analysis (TGA)

The TGA was performed using the device Thermal Analysis SDT Q600 at a heating rate of 20 °C/min from room temperature to 1000 °C.

Elemental analysis

Elemental analyses were obtained using a Carlo Erba Instruments CHNS-O EA 108 elemental analyzer.

X-Ray crystal structure determination

X-ray crystal structures data were recorded at Manchester University X-Ray Crystallography Facility, at 100 K or 150 K, on a Bruker APEX CCD diffractometer (graphite monochromated MoK_α radiation λ = 0.71073 Å) or using synchrotron radiation at Daresbury SRS, UK (Station 9.8), on a Bruker APEXII CCD diffractometer (λ = 0.6710

Å) and the structures were solved by direct methods. All calculations were carried out by using the SHELX-97 package.

Gel permeation chromatography

Gel permeation chromatography (GPC) analysis was carried out at Manchester University, using a set of Polymer Laboratories PLgel columns (two mixed-Band one 500 Å 10 μm), in $CHCl_3$ with Gilson 132 DR and Gilson 307 detectors, using a Knauer 64 pump operating at a flow rate of 1 cm^3/min. Calibration was achieved using a series of polystyrene standards up to Mw = 1.1 * 10^6 g mol^{-1}.

4.2 Experimental procedures

3,3-bis(3,4-Dimethoxyphenyl) pentanedioic acid (42).

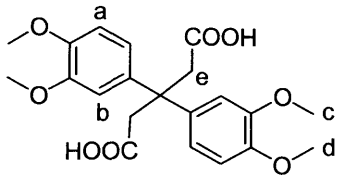

To a stirred solution of diethyl 3,3-bis(3,4-dimethoxyphenyl) pentanedioate (2.00 g, 4.34 mmol) and ethanol (25 ml) was added dropwise 40% aqueous NaOH (25 ml) and the solution stirred for a further 2 days at 40 °C, until complete consumption of the starting material was confirmed by TLC. To the reaction mixture was added water (25 ml) and the aqueous layer extracted with diethyl ether (3 x 50 ml). To the aqueous phase, cooled at 0 °C, was added dropwise concentrated HCl until acid pH, to precipitate the desired product as a pale yellow solid that was filtered off and washed with water. Recrystallization from diethyl ether/hexane (4/1) gave the desired product as a white solid (1.66 g, 95%). Mp 110-112 °C; IR (nujol): 2945, 1704, 1513, 1458, 1413, 1252, 1147, 1021, 810 cm^{-1}; ^1H NMR (400 MHz; $CDCl_3$) δ 6.58 (m, 4H, H_a), 6.41 (s, 2H, H_b), 3.69 (s, 6H, H_c), 3.57 (s, 6H, H_d), 3.39 (s, 4H, H_e); ^{13}C NMR (100 MHz; $CDCl_3$) δ 177.6, 148.7, 147.9, 138.9, 119.6, 111.3, 110.7, 56.2, 56.1, 45.9, 42.2; LRMS, *m/z*, ($APCI^+$): 403 (MH^+, 100%), 404 (20%)

Diethyl 3,3-bis(3,4-dimethoxyphenyl) pentanedioate (43).

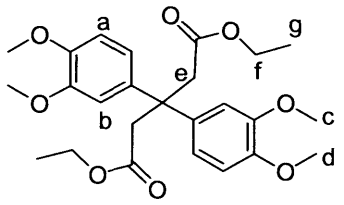

To a stirred mixture of veratrole (22.2 ml, 176 mmol) and diethyl 1,3-acetone dicarboxylate (4.00 ml, 22 mmol) cooled on an ice bath, was added dropwise concentrated sulphuric acid (10 ml). The solution was stirred at room temperature for further 20 h. The mixture was poured into an ice bath (50 ml) and extracted with diethyl ether (3 x 100 ml). The organic layer was dried with $MgSO_4$, filtered and evaporated under vacuum. The crude product was purified by column chromatography eluting with petroleum ether/ethyl

acetate (7/3) to give a white solid (5.97 g, 59%). Mp 84-86 °C; IR (nujol): 2922, 1729, 1605, 1510, 1396, 1249, 1017, 815 cm^{-1}; ^1H NMR (400 MHz; $CDCl_3$) δ 6.68 (m, 4H, H_a), 6.53 (s, 2H, H_b), 3.80 (q, 4H, J = 7.2 Hz, H_f), 3.76 (s, 6H, H_c), 3.67 (s, 6H, H_d), 3.41 (s, 4H, H_e), 0.92 (t, 6H, J = 7.2 Hz, H_g); ^{13}C NMR (100 MHz; $CDCl_3$) δ 171.8, 148.6, 147.7, 139.2, 120.1, 119.8, 111.6, 110.5, 60.3, 56.2, 56.1, 46.8, 43.0, 14.3; LRMS, *m/z*, ($APCI^+$): 461 (MH^+, 100%), 462 (20%)

5,6,5',6'-Tetramethoxy-1,1'-spirobisindane-3,3'-dione (41).

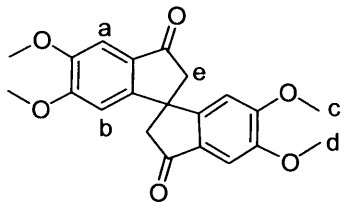

Finely powdered 3,3-bis(3,4-dimethoxyphenyl) pentanedioic acid **42** (2.00 g, 4.94 mmol) was added to Eaton's reagent at room temperature and the mixture was stirred for 15 h. The dark red solution was poured into an ice/water bath and stirred for an hour until the formation of a pale yellow precipitate. The solid was filtered off, washed with water and dried. Recrystallization from acetic acid/methanol (4/1), gave the desired compound as white solid (1.54 g, 84%). Mp 245-250 °C; IR (nujol): 2923, 1695, 1592, 1499, 1360, 1296 cm^{-1}; ^1H NMR (400 MHz; $CDCl_3$) δ 7.15 (s, 2H, H_a), 6.33 (s, 2H, H_b), 3.88 (s, 6H, H_c), 3.76 (s, 6H, H_d), 3.04 (d, 2H, J = 19.1 Hz, H_e), 2.98 (d, 2H, J = 19.1 Hz, H_e); ^{13}C NMR (100 MHz; $CDCl_3$) δ 202.8, 156.6, 155.0, 150.4, 128.8, 104.7, 103.7, 56.4, 56.2, 53.0, 47.5; LRMS, *m/z*, ($APCI^+$): 369 (MH^+, 100%) HRMS Calc. for $C_{21}H_{21}O_6$ 369.1338, found 369.1331;

5,6,5',6'-Tetrahydroxy-1,1'-spirobisindane-3,3'-dione (44).

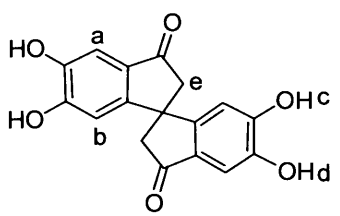

In a two-necked round bottom flask was added 5,6,5',6'-tetramethoxy-1,1'-spirobisindane-3,3'-dione **41** (2.00 g, 5.43 mmol) and dry dichloromethane (80 ml) under a dry nitrogen atmosphere that was maintained throughout the reaction. This mixture was cooled to 0 °C

then boron tribromide (3.08 ml, 32.6 mmol) was added dropwise and the reaction stirred at room temperature for a further 6 h. The reaction was poured into ice and left under vigorous stirring allowing the evaporation of the excess dichloromethane. The precipitate was filtered off, washed with water and dried. Recrystallization from methanol/acetic acid (1/1) gave the desired compound as pale brown solid (1.62 g, 96%). Mp over 300 °C; IR (nujol): 3210, 1660, 1589, 1510, 1315, 1053 cm^{-1}; ^1H NMR (400 MHz; Acetone-d_6) δ 8.94 (s, 2H, H_c), 8.72 (s, 2H, H_d), 7.10 (s, 2H, H_a), 6.54 (s, 2H, H_b), 3.03 (d, 2H, J = 18.4 Hz, H_e), 2.81 (d, 2H, J = 18.6 Hz, H_e); ^{13}C NMR (100 MHz; Acetone-d_6) δ 202.1, 154.1, 153.8, 146.4, 127.1, 109.0, 107.0, 52.1, 46.3; HRMS Calc. for $C_{17}H_{12}O_6$ 312.0634, found 312.0632;

5,6,5',6'-Tetramethoxy-3,3'-diphenyl-1,1'-spirobisindene (45).

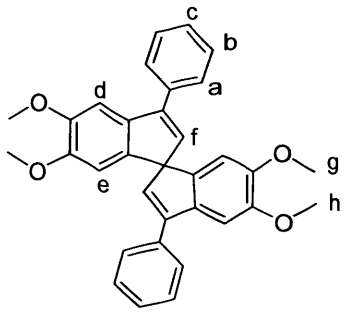

In a two-necked round bottom flask was added dry THF (30 ml) and 5,6,5',6'-tetramethoxy-1,1'-spirobisindane-3,3'-dione **41** (4.00 g, 10.84 mmol). Phenyl magnesium bromide (4.9 g, 27.1 mmol) was added dropwise, under nitrogen atmosphere, at 0 °C and under vigorous stirring. The mixture was kept under stirring for a further 24 h at room temperature. The solution was quenched with hydrochloric acid (1N, 100 ml), the organic layer was separated and the aqueous layer extracted with diethyl ether (3 x 100 ml). The combined organic layers were washed with saturated aqueous sodium hydrogen carbonate (2 x 100 ml) and the solvent evaporated under reduced pressure. To the crude product was added a solution of 20% aqueous sulphuric acid (50 ml) and stirred at 90 °C for 20 h. The solution was quenched with water (100 ml) and extracted with dichloromethane (3x 100 ml). Purification by chromatographic column, eluting with petroleum ether/ethyl acetate (7/3), gave the desired compound as white solid (3.91 g, 74%). Mp 105-110 °C; IR (nujol): 2918, 1605, 1565, 1490, 1341, 1264, 1206, 1088, 816, 702 cm^{-1}; ^1H NMR (400 MHz; $CDCl_3$) δ 7.72 (d, 4H, J = 7.6 Hz, H_a), 7.53 (dd, 4H, J = 7.6, 7.6 Hz, H_b), 7.44 (dd, 2H, J = 7.6, 7.6 Hz, H_c), 7.20 (s, 2H, H_d), 6.52 (s,2H, H_e), 6.14 (s, 2H, H_f), 3.96 (s, 6H, H_g), 3.78

(s, 6H, H_h); ^{13}C NMR (100 MHz; $CDCl_3$) δ 148.9, 148.5, 138.1, 137.1, 136.1, 133.5, 129.2, 128.3, 127.9, 107.0, 104.9, 68.6, 56.7, 56.6; HRMS Calc. for $C_{33}H_{29}O_4$ 489.2066, found 489.2052.

5,6,5',6'-Tetrahydroxy-3,3'-diphenyl-1,1'-spiro-bisindene (46).

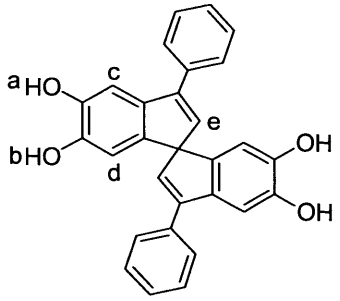

In a two-necked round bottom flask was added 5,6,5',6'-tetramethoxy-3,3'-diphenyl-1,1'-spirobisindene **45** (0.65 g, 1.53 mmol) and dry dichloromethane (40 ml) under a dry nitrogen atmosphere that was maintained throughout the reaction. This mixture was cooled to 0 °C then boron tribromide (0.43 ml, 4.58 mmol) was added dropwise and the reaction stirred at room temperature for a further 6 h. The reaction was poured into ice and left under vigorous stirring allowing the evaporation of the excess dichloromethane. The precipitate was filtered off, washed with water and dried. Recrystallization from dichloromethane/hexane (1/1) gave the desired compound as pale yellow solid (0.51 g, 78%). Mp 195-200 °C; IR (nujol): 3357, 2920, 1700, 1624, 1305, 1223, 879 cm^{-1}; ^1H NMR (400 MHz; Acetone-d_6) δ 7.75 (s,2H, H_a), 7.70 (s, 2H, H_b), 7.49 (m, 10H, H_{Ar}), 7.07 (s, 2H, H_c), 6.37 (s, 2H, H_d), 6.03 (s, 2H, H_e); ^{13}C NMR (100 MHz; Acetone-d_6) δ 145.2, 144.1, 143.7, 137.8, 135.9, 128.6, 127.7, 127.3, 110.0, 107.9; HRMS Calc. for $C_{29}H_{20}O_4$ 432,1362, found 432,1365.

4,4'-Dimethoxyphenyl-6,6-diphenyl-tetrahydro-2H-pyran-2-one (48).

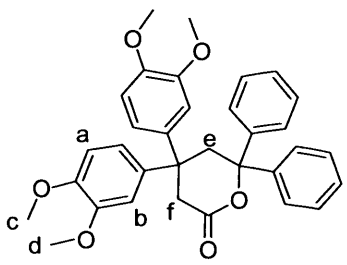

In a two-necked round bottom flask was added dry THF (30 ml) and diethyl 3,3-bis(3,4-dimethoxyphenyl) pentanedioate **43** (2.00 g, 4.34 mmol). Phenyl magnesium bromide

(2.36 g, 13.1 mmol) was added dropwise, under nitrogen atmosphere and under vigorous stirring. The mixture was kept under reflux for 3 h. The solution was quenched with saturated aqueous NH_4Cl (100 ml), the organic layer was separated and the aqueous layer extracted with ethyl acetate (3 x 100 ml). The combined organic layers were washed with saturated aqueous sodium hydrogen carbonate (2 x 100 ml) and the solvent evaporated under reduced pressure. Recrystallization from diethyl ether/hexane (4/1) gave the product as a white solid (1.93 g, 85%). Mp 70-73 °C; IR (dichloromethane): 2935, 1732, 1591, 1517, 1450, 1254, 1150, 1026, 734 cm^{-1}; ^1H NMR (400 MHz; $CDCl_3$) δ 7.16 (m, 10H, H_{Ar}), 6.66 (s, 4H, H_a), 6.41 (s, 2H, H_b), 3.79 (s, 6H, H_c), 3.62 (s, 6H, H_d), 3.51 (s, 2H, H_e), 2.96 (s, 2H, H_f); ^{13}C NMR (100 MHz; $CDCl_3$) δ 170.9, 148.7, 147.7, 145.1, 139.4, 128.3, 127.2, 125.3, 118.6, 110.8, 110.7, 55.8, 55.7, 46.1, 45.3, 43.7, 39.8; LRMS, *m/z*, ($APCI^+$): 547.5 M + Na^+, 100%), 563.5 (M + K^+ 70%)

Methyl (1-(3-4 dimethoxyphenyl)-5,6-dimethoxy-3,3-diphenhyl-2,3-dihydro-1H-inden-1-yl)acetate (49).

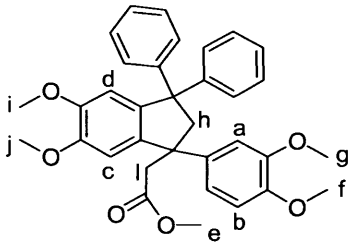

To a stirred mixture of 4,4'-dimethoxyphenyl-6,6-diphenyl-tetrahydro-2*H*-pyran-2-one **48** (2.00 g, 3.81 mmol) and methanol (50 ml) cooled on an ice bath, was added dropwise concentrated sulphuric acid (10 ml). The solution was stirred at room temperature for further 5 h until the formation of a white precipitate. The crude product was filtrated and washed many times with water and dried. Recrystallization from methanol gave a white solid of (5.97 g, 59%). Mp 125-127 °C; IR (nujol): 2922, 1724, 1602, 1503, 1252, 1209, 1025, 866 cm^{-1}; ^1H NMR (400 MHz; $CDCl_3$) δ 6.94 (m, 10H, H_{Ar}), 6.84 (s, 1H, H_a), 6.56 (m, 2H, H_b), 6.49 (s, 1H, H_c), 6.41 (s, 1H, H_d), 3.81 (s, 3H, H_e), 3.72 (s, 3H, H_f), 3.69 (s, 3H, H_g), 3.56 (s, 3H, H_i), 3.44 (s, 3H, H_j), 3.43 (d, 1H, J = 13.6 Hz, H_h), 3.32 (d, 1H, J = 13.6 Hz, H_h), 2.88 (s, 2H, H_l); ^{13}C NMR (100 MHz; $CDCl_3$) δ 171.8, 148.7, 148.6, 148.4, 148.1, 146.9, 146.8, 141.1, 139.3, 138.9, 128.7, 128.6, 128.0, 127.5, 126.1, 125.8, 118.8, 110.5, 109.5, 108.2, 60.5, 59.3, 56.1, 56.0, 55.8, 55.7, 53.0, 51.5, 45.1; LRMS, *m/z*, ($APCI^+$): 561.1 (M + Na^+, 100%).

1,1-Diphenyl-2-[3,3-diphenyl-1-(3,4-dimethoxyphenyl)-5,6-dimethoxy-2,3-dihydro-1H-inden-1-yl]ethanol (50).

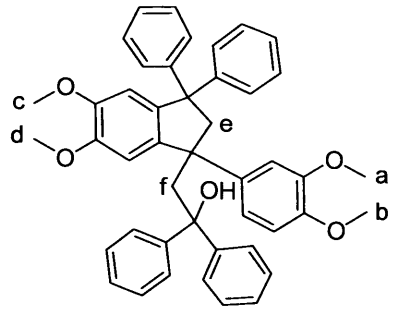

In a two-necked round bottom flask was added dry THF (30 ml) and methyl (1-(3-4 dimethoxyphenyl)-5,6-dimethoxy-3,3-diphenhyl-2,3-dihydro-1*H*-inden-1-yl)acetate **49** (2.00 g, 3.71 mmol). Phenyl magnesium bromide (2.02 g, 11.2 mmol) was added dropwise under nitrogen atmosphere and under vigorous stirring,. The mixture was kept under reflux for 3 h. The solution was quenched with saturated aqueous NH_4Cl (100 ml). The precipitate formed was filtered off, washed with water and dried. Recrystallization from methanol gave the desired product as a white solid (2.09 g, 85%). Mp 168-170 °C, IR (nujol): 3394, 2923, 1602, 1586, 1336, 1288, 1233, 1085, 1001, 871 cm^{-1} ^1H NMR (400 MHz; $CDCl_3$) δ 6.85 (m, 25H, H_{Ar}), 3.71 (s, 3H, H_a), 3.66 (s, 3H, H_b), 3.61 (s, 3H, H_c), 3.50 (s, 3H, H_d), 3.04 (d, 1H, J = 15.2 Hz, H_e), 2.80 (d, 1H, J = 15.2 Hz, H_e), 2.32 (s, 2H, H_f); ^{13}C NMR (100 MHz; $CDCl_3$) δ 149.9, 148.8, 148.4, 148.3, 147.8, 147.7, 147.1, 147.0, 140.1, 139.6, 138.9, 128.8, 128.1, 127.9, 127.3, 126.4, 126.2, 125.6, 125.4, 119.3, 111.0, 110.9, 110.2, 109.9, 60.3, 57.9, 56.2, 56.1, 55.9, 55.7, 54.2, 51.5; LRMS, *m/z*, ($APCI^+$): 465 [M - 1,1-diphenylethanol (fragmentation), 100%].

5,6,5',6'-Tetrahydroxy-1,1'-spirobisindane-3-diphenyl-3'-one (54).

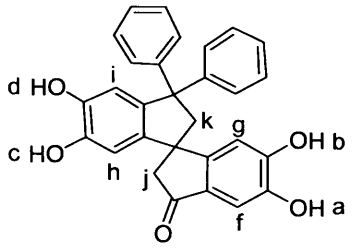

In a two-necked round bottom flask was added 4,4'-dimethoxyphenyl-6,6-diphenyl-tetrahydro-2*H*-pyran-2-one **48** (2.00 g, 3.81 mmol) and dry dichloromethane (60 ml) under a dry nitrogen atmosphere that was maintained throughout the reaction. This mixture was

cooled to 0 °C then boron tribromide (2.17 ml, 22.87 mmol) was added dropwise and the reaction stirred at room temperature for a further 6 h. The reaction was poured into ice and left under vigorous stirring allowing the evaporation of the excess dichloromethane. The precipitate was filtered off, washed with water and dried. Recrystallization from ethanol/water gave the desired compound as pale purple solid (1.37 g, 80%). Mp over 300 °C; IR (nujol): 3160, 1644, 1589, 1293, 1162, 872 cm^{-1}; ^1H NMR (400 MHz; Acetone-d_6) δ 8.89 (s, 1H, H_a), 8.75 (s, 1H, H_b), 7.87 (s, 1H, H_c), 7.84 (s, 1H, H_d), 7.29 (m, 10H, H_{Ar}), 7.07 (s, 1H, H_f), 6.88 (s, 1H, H_g), 6.43 (s, 1H, H_h), 6.22 (s, 1H, H_i), 3.49 (d, 1H, J = 13.2 Hz, H_j), 3.10 (d, 1H, J = 13.2 Hz, H_j), 2.19 (d, 1H, J = 18.8 Hz, H_k), 2.13 (d, 1H, J = 18.8 Hz, H_k); ^{13}C NMR (100 MHz; Acetone-d_6) δ 205.6, 156.7, 154.3, 147.9, 147.4, 146.5, 145.5, 144.7, 140.2, 139.8, 128.8, 128.5, 128.1, 127.7, 127.6, 126.0, 125.7, 112.6, 109.7, 108.8, 106.6, 60.5, 60.1, 52.4, 52.0; LRMS, *m/z*, (APCI-): 449 (M^-, 100%)

5,6,5',6'-Tetramethoxy-3,3'-di(biphenyl-2-yl)-1,1'-spirobisindene (55).

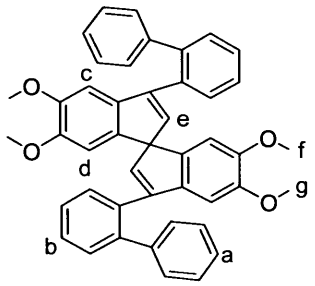

In a two-necked round bottom flask was added dry THF (30 ml) and 5,6,5',6'-tetramethoxy-1,1'-spirobisindane-3,3'-dione **41** (1.00 g, 2.71 mmol). 2-Biphenyl magnesium bromide (2.09 g, 8.14 mmol) was added dropwise under nitrogen atmosphere, at 0 °C and under vigorous stirring,. The mixture was kept under reflux for 3 days and then the reaction was quenched with water. The precipitate formed was filtered off, washed with water and dried. To the crude product was added a solution of 10% hydrochloric acid in methanol (50 ml) and stirred at room temperature for 5 h. The solution was quenched with water (100 ml). The precipitate formed was filtered off, washed with methanol and dried. Recrystallization from methanol gave the product as a white solid (0.65 g, 40%). Mp 195-198 °C; IR (nujol): 2923, 1599, 1572, 1336, 1268, 1210, 1085, 1009, 847 cm^{-1}; ^1H NMR (400 MHz; $CDCl_3$) δ 7.40 (m, 10H, H_b), 7.16 (m, 8H, H_a), 6.35 (s, 2H, H_c), 6.22 (s, 2H, H_d), 5.64 (s,2H, H_e), 3.66 (s, 6H, H_f), 3.62 (s, 6H, H_g); ^{13}C NMR (100 MHz; $CDCl_3$) δ

150.4, 149.4, 145.7, 142.4, 141.7, 141.4, 132.4, 129.8, 128.3, 128.2, 128.0, 106.7, 105.9, 58.9, 56.5, 56.2, 56.1; LRMS, *m/z*, (APCI$^+$): 641 (MH^+, 100%).

3,3'-bis-(spiro-9-fluorenyidene)-5,6,5',6'-tetramethoxy-1,1'-spirobisindane (56) and 3-(spiro-9-fluorenyidene)-5,6,5',6'-tetramethoxy-1,1'-spirobisindane-3'-one (58).

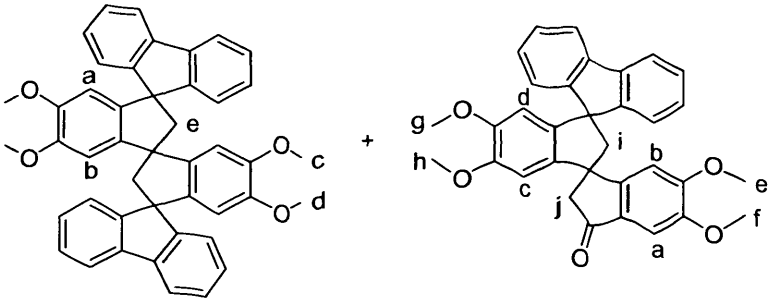

In a two-necked round bottom flask was added dry THF (30 ml) and 5,6,5',6'-tetramethoxy-1,1'-spirobisindane-3,3'-dione **41** (1.00 g, 2.71 mmol). 2-Biphenyl magnesium bromide (2.09 g, 8.14 mmol) was added dropwise under nitrogen atmosphere, at 0 °C and under vigorous stirring in THF (50 ml). The mixture was kept under reflux for 2 days. The reaction was quenched with water and the precipitate was filtered off, washed with water and dried. To the crude product was added a solution of 10% hydrochloric acid in methanol (50 ml) and the mixture was stirred at room temperature for 5 h. The precipitate resulting was filtered off, washed with cold methanol and dried. The solid was added to Eaton's reagent (10 ml) and the mixture was stirred at room temperature for 3 h. The dark red solution was poured into an ice/water bath and stirred for an hour until the formation of a white precipitate. The product was filtered off, washed with water and dried. Purification by chromatographic column, eluting with petroleum ether/ethyl acetate (7/3), gave **56** ($\mathbf{R_f}$ **=0.6)** as white solid (0.65 g, 40%) and **58** ($\mathbf{R_f}$ **= 0.3)** as white solid (0.68 g, 50%).

(56) Mp 300 °C; IR (nujol): 2923, 1705, 1600, 1496, 1284, 1214, 1100, 1016, 850 cm^{-1}; ^1H NMR (400 MHz; $CDCl_3$) δ 7.34 (m, 16H, H_{Ar}), 6.64 (s, 2H, H_a), 5.82 (s, 2H, H_b), 3.84 (s, 6H, H_c), 3.50 (s, 6H, H_d), 3.31 (d, 2H, J = 13.6 Hz, H_e), 3.04 (d, 2H, J = 13.6 Hz, H_e); ^{13}C NMR (100 MHz; $CDCl_3$) δ 153.8, 153.2, 150.1, 149.6, 144.4, 140.7, 139.2, 138.2, 128.0, 127.8, 127.6, 127.1, 124.4, 124.0, 119.8, 119.7, 106.3, 105.3, 63.0, 59.9, 58.5, 56.2, 55.9 ; LRMS, *m/z*, (APCI$^+$): 641 (MH^+, 100%). HRMS Calc. for $C_{45}H_{36}O_4$ 640.2614, found 640.2589

(58) Mp 275-278 °C; IR (nujol): 2928, 1680, 1602, 1510, 1448, 1403, 1251, 1205, 1045, 762 cm^{-1}; ^1H NMR (400 MHz; $CDCl_3$) δ 7.43 (m, 8H, H_{Ar}), 7.19 (s, 1H, H_a), 6.67 (s, 1H, H_b), 6.22 (s, 1H, H_c), 5.85 (s, 1H, H_d), 4.05 (s, 3H, H_e), 4.03 (s, 3H, H_f), 3.67 (s, 3H, H_g), 3.49 (s, 3H, H_h), 3.26 (d, 1H, J = 18.4 Hz, H_i), 3.15 (d, 1H, J = 18.4 Hz, Hi), 3.17 (d, 1H, J = 14 Hz, H_j), 2.58 (d, 1H, J = 14 Hz, H_j) ; ^{13}C NMR (100 MHz; $CDCl_3$) δ 204.5, 157.9, 156.8, 153.4, 153.0, 150.6, 150.5, 150.2, 141.8, 141.2, 139.6, 138.4, 130.0, 128.4, 128.2, 127.8, 124.5, 124.1, 120.4, 120.3, 106.1, 106.0, 105.5, 103.6, 63.0, 56.8, 56.6, 56.5, 56.4, 56.2, 54.1; HRMS Calc. for $C_{33}H_{28}O_5$ 504.1937, found 504.1933.

3,3'-bis-(spiro-9-fluorenyidene)-5,6,5',6'-tetrahydroxy-1,1'-spirobisindane (57).

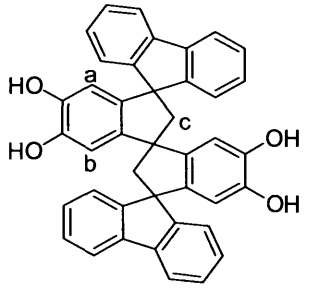

In a two-necked round bottom flask was added 3,3'-bis-(spiro-9-fluorenyidene)-5,6,5',6'-tetramethoxy-1,1'-spirobisindane **56** (0.60 g, 0.93 mmol) and dry dichloromethane (40 ml) under a dry nitrogen atmosphere that was maintained throughout the reaction. This mixture was cooled to 0 °C then boron tribromide (0.35 ml, 3.74 mmol) was added dropwise and the reaction stirred at room temperature for a further 30 min. The reaction was poured into ice and left under vigorous stirring allowing the evaporation of the excess dichloromethane. The precipitate was filtered off, washed with water and dried. Recrystallization from dichloromethane/hexane (1/1) gave the desired compound as a white solid (0.49 g, 90%). Mp over 300 °C; IR (nujol): 3388, 2922, 1700, 1603, 1496, 1274, 1217, 1096, 850 cm^{-1}, ^1H NMR (400 MHz; Acetone-d_6) δ 7.51 (m, 16H, H_{Ar}), 6.81 (s, 2H, H_a), 5.82 (s, 2H, H_b), 3.96 (d, 2H, J = 18.8 Hz, H_c), 3.10 (d, 2H, J = 18.8 Hz, H_c); ^{13}C NMR (100 MHz; Acetone-d_6) δ 155.3, 146.9, 146.2, 145.6, 141.5, 140.0, 138.6, 128.9, 128.6, 128.4, 127.9, 125.2, 125.0, 120.6, 111.1, 109.7, 63.6, 60.4, 59.6; HRMS Calc. for $C_{41}H_{29}O_4$ 585.2066, found 585.2057.

3-(spiro-9-fluorenyidene)-5,6,5',6'-tetrahydroxy-1,1'-spirobisindane-3'-one (59).

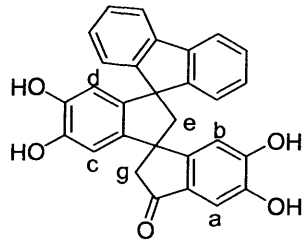

In a two-necked round bottom flask was added 3-(spiro-9-fluorenyidene)-5,6,5',6'-tetramethoxy-1,1'-spirobisindane-3'-one **58** (0.67 g, 1.32 mmol) and dry dichloromethane (30 ml) under a dry nitrogen atmosphere that was maintained throughout the reaction. This mixture was cooled to 0 °C then boron tribromide (0.50 ml, 5.30 mmol) was added dropwise and the reaction stirred at room temperature for a further 3 h. The reaction was poured into ice and left under vigorous stirring allowing the evaporation of the excess dichloromethane. The precipitate was filtered off, washed with water and dried. Recrystallization from dichloromethane/hexane (1/1) gave the desired compound as a white solid (0.53 g, 90%). Mp over 300 °C; IR (nujol): 3494, 2935, 1683, 1650, 1578, 1295, 1163, 870, 816 cm^{-1}; ^1H NMR (400 MHz; MeOD) δ 7.57 (m, 8H, H_{Ar}), 7.20 (s, 1H, H_a), 6.91 (s, 1H, H_b), 6.23 (s, 1H, H_c), 5.74 (s, 1H, H_d), 3.25 (d, 1H, J = 20.4 Hz, H_e), 3.22 (d, 1H, J = 13.6 Hz, H_g), 3.18 (d, 1H, J = 20.4 Hz, H_e), 2.61 (d, 1H, J = 13.6 Hz, H_g); ^{13}C NMR (100 MHz; MeOD) δ 205.5, 145.8, 127.6, 127.3, 127.2, 126.9, 123.6, 119.4, 119.3, 108.9, 108.6, 106.4, 62.0, 56.3, 53.1; HRMS Calc. for $C_{29}H_{20}O_5$ 448.1311, found 448.1297.

2-Bromo-4,4'-di-tert-butylbiphenyl (60)

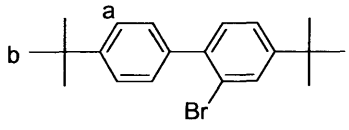

To a solution of 4,4'-di-*tert*-butylbiphenyl (5.00 g, 18.76 mmol) in CCl_4 (25 ml) was added under ice bath a solution of Br_2 (1.06 ml, 20.64 mmol) in CCl_4 (5 ml) in presence of a catalytic amount of Fe powder. The reaction mixture was stirred at room temperature for 5 h and than poured into a large beaker of water. The organic layer was extracted with diethyl ether, washed with 10% NaOH, water, dried with $MgSO_4$ and evaporated under

vacuum to give a white solid (5.18 g, 80%). Mp 75-77 °C[120]; ^{1}H NMR (400 MHz; $CDCl_3$) δ 7.09 (m, 7H, H_a), 1.29 (s, 18H, H_b). HRMS Calc. for $C_{20}H_{25}{}^{79}Br$ 344.1140, found 344.1153.

3,3'-bis(4,4'-di-tert-butyl- spiro-9-fluorenyidene)-5,6,5',6'-tetramethoxy-1,1'-spirobisindane (62) and 3-(4,4'-di-tert-butyl- spiro-9-fluorenyidene)-5,6,5',6'-tetramethoxy-1,1'-spirobisindane-3'-one (63).

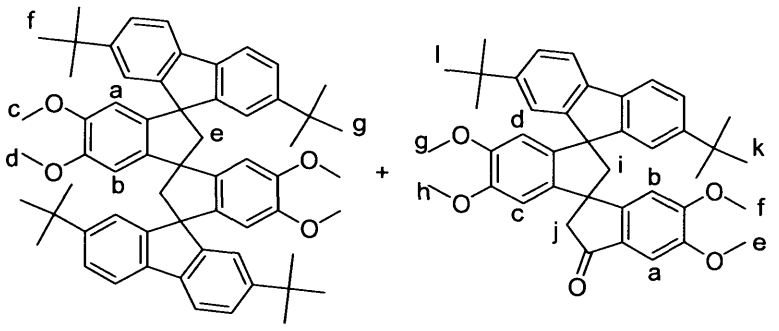

In a two-necked round bottom flask was added dry THF (30 ml) and 5,6,5',6'-tetramethoxy-1,1'-spirobisindane-3,3'-dione **41** (1.30 g, 3.57 mmol). 4,4'-Di-*tert*-butylbiphenyl-2-magnesium bromide (6.17 g, 17.86 mmol) was added dropwise under nitrogen atmosphere, at 0 °C and under vigorous stirring,. The mixture was kept under reflux for 2 days. The reaction was quenched with water. The precipitate formed was filtered off, washed with water and dried. To the crude product was added a solution of 10% hydrochloric acid in methanol (50 ml) and stirred at room temperature for 5 h. The solution was quenched with water (100 ml). The precipitate formed was filtered off, washed with methanol and dried. The solid was added to Eaton's reagent (10 ml) and the mixture was stirred at room temperature for 3 h. The dark red solution was poured into an ice/water bath and stirred for an hour until the formation of a white precipitate. The product was filtered off, washed with water and dried. Purification by chromatographic column, eluting with petroleum ether/ethyl acetate (8/2), gave **62** ($\mathbf{R_f = 0.6}$) as white solid (0.65 g, 20%) and **63** ($\mathbf{R_f = 0.3}$) as white solid (0.88 g, 41%).

(62) Mp 153-155 °C; IR (nujol): 2923, 1600, 1496, 1284, 1214, 1100, 1016, 850 cm^{-1}; ^{1}H NMR (400 MHz; $CDCl_3$) δ 7.15 (m, 12H, H_{Ar}), 6.71 (s, 2H, H_a), 5.85 (s, 2H, H_b), 3.91 (s, 6H, H_c), 3.56 (s, 6H, H_d), 3.40 (d, 2H, J = 14 Hz, H_e), 3.10 (d, 2H, J = 14 Hz, H_e), 1.36 (s, 18H, H_f), 1.09 (s, 18H, H_g); ^{13}C NMR (100 MHz; $CDCl_3$) δ 154.4, 154.0, 150.7, 149.8, 149.3, 146.3, 144.7, 138.9, 138.1, 136.5, 124.6, 124.0, 121.0, 120.8, 118.9, 105.6, 63.1, 59.3, 56.0, 55.7, 35.0, 34.8, 31.6, 31.4; LRMS, *m/z*, (EI$^+$): 865 (M^+, 100%).

(63) Mp 138-140 °C; IR (nujol): 2925, 2754, 1701, 1594, 1079, 1006, 889, 773 cm^{-1}; ^1H NMR (400 MHz; $CDCl_3$) δ 7.38 (m, 6H, H_{Ar}), 7.08 (s, 1H, H_a), 6.77 (s, 1H, H_b), 6.22 (s, 1H, H_c), 5.88 (s, 1H, H_d), 3.91 (s, 3H, H_e), 3.90 (s, 3H, H_f), 3.69 (s, 3H, H_g), 3.51 (s, 3H, H_h), 3.20 (d, 1H, J = 19.1 Hz, H_i), 3.19 (d, 1H, J = 19.1 Hz, H_i), 3.17 (d, 1H, J = 14.4 Hz, H_j), 2.60 (d, 2H, J = 14.4 Hz, H_j), 1.26 (s, 9H, H_l), 1.21 (s, 9H, H_k); ^{13}C NMR (100 MHz; $CDCl_3$) δ 158.2, 156.4, 153.4, 152.9, 150.8, 150.0, 141.4, 138.5, 138.2, 136.6, 129.5, 124.9, 124.6, 120.6, 120.1, 119.6, 106.0, 105.4, 104.9, 103.2, 62.7, 57.6, 56.3, 56.1, 56.0, 55.9, 35.0, 34.9, 31.6, 31.5.; HRMS Calc. for $C_{41}H_{44}O_5$ 616.3189, found 616.3176.

3,3'-bis(4,4'-di-tert-butyl-9-fluorenyidene)-5,6,5',6'-tetrahydroxy-1,1'-spirobisindane (64)

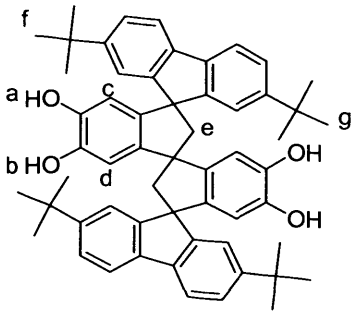

In a two-necked round bottom flask was added 3,3'-bis(4,4'-di-tert-butyl- spiro-9-fluorenyidene)-5,6,5',6'-tetramethoxy-1,1'-spirobisindane **62** (0.87 g, 1.01 mmol) and dry dichloromethane (30 ml) under a dry nitrogen atmosphere that was maintained throughout the reaction. This mixture was cooled to 0 °C then boron tribromide (0.47 ml, 5.05 mmol) was added dropwise and the reaction stirred at room temperature for a further 1 h. The reaction was poured into ice and left under vigorous stirring allowing the evaporation of the excess dichloromethane. The precipitate was filtered off, washed with water and dried. Recrystallization from dichloromethane/hexane (1/1) gave the desired compound as a white solid (0.72 g, 89%). Mp over 300 °C; IR (nujol): 3498, 2923, 1595, 1502, 1466, 1298, 1187, 1065, 866 cm^{-1}; ^1H NMR (400 MHz; MeOD) δ 7.51 (m, 12H, H_{Ar}), 7.30 (s, 2H, H_a), 7.12 (s, 2H, H_b), 6.71 (s, 2H, H_c), 5.77 (s, 2H, H_d), 3.27 (d, 2H, J = 16.4 Hz, H_e), 3.06 (d, 2H, J = 16.4 Hz, H_e), 1.39 (s, 18H, H_f), 1.08 (s, 18H, H_g); ^{13}C NMR (100 MHz; MeOD) δ 154.5, 153.8, 150.7, 150.1, 145.9, 145.2, 144.5, 138.0, 137.8, 136.4, 124.1, 123.6, 120.5, 118.5, 109.7, 108.8, 62.6, 59.2, 34.5, 34.2, 30.7, 30.4; HRMS Calc. for $C_{57}H_{60}O_4$ 808.4492, found 808.5021.

3-(4,4'-di-tert-butyl-9-fluorenyidene)-5,6,5',6'-tetrahydroxy-1,1'-spirobisindane-3'-one (65)

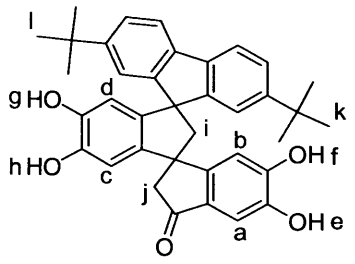

In a two-necked round bottom flask was added 3-(4,4'-di-tert-butyl- spiro-9-fluorenyidene)-5,6,5',6'-tetramethoxy-1,1'-spirobisindane-3'-one **63** (0.82 g, 1.33 mmol) and dry dichloromethane (40 ml) under a dry nitrogen atmosphere that was maintained throughout the reaction. This mixture was cooled to 0 °C then boron tribromide (0.63 ml, 6.64 mmol) was added dropwise and the reaction stirred at room temperature for further 5 h. The reaction was poured into ice and left under vigorous stirring allowing the evaporation of the excess dichloromethane. The precipitate was filtered off, washed with water and dried. Recrystallization from dichloromethane gave the desired compound as a white solid (0.65 g, 88%). Mp over 300 °C; IR (nujol): 3494, 2928, 1683, 1653, 1588, 1300, 1163, 1070, 872, 824 cm^{-1}; ^1H NMR (400 MHz; Acetone-d_6) δ 8.98 (s, 2H, H_e), 8.67 (s, 2H, H_f), 7.54 (m, 6H, H_{Ar}), 7.15 (s, 1H, H_a), 7.00 (s, 1H, H_b), 6.34 (s, 1H, H_c), 5.84 (s, 1H, H_d), 3.25 (d, 1H, J = 13.8 Hz, H_j), 3.25 (d, 1H, J = 18.1 Hz, H_i), 3.16 (d, 1H, J = 18.1 Hz, H_j), 2.67 (d, 2H, J = 13.8 Hz, H_j), 1.37 (s, 9H, H_l), 1.31 (s, 9H, H_k); ^{13}C NMR (100 MHz; Acetone-d_6) δ 205.2, 146.8, 143.2, 139.1, 133.0, 130.2, 125.5, 125.1, 121.6, 121.3, 120.0, 111.0, 110.1, 107.8, 63.4, 57.8, 57.2, 41.8, 35.5, 32.0, 31.9; HRMS Calc. for $C_{37}H_{36}O_5$ 560.2563, found 560.2568.

Bis-1,3-dithiolane of 5,6,5',6'-tetramethoxy-1,1'-spirobisindane-3,3'-dione (67)

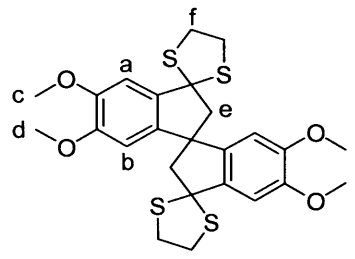

To a solution of 5,6,5',6'-tetramethoxy-1,1'-spirobisindane-3,3'-dione **41** (2.00 g, 5.42 mmol) in dichloromethane (60 ml) and trifluoroacetic acid (10 ml) was added 1,2-

ethanedithiol (2.04 g, 21.68 mmol) followed by boron trifluoride diethyl etherate (3.07 g, 21.68 mmol) under nitrogen atmosphere. After 18 hours the mixture was quenched with water (200 ml) and washed with a solution of NaOH 1 N (3 x 100 ml) and brine (2 x 100 ml). The organic layer was dried with $MgSO_4$, filtered and evaporated under vacuum to obtain a white solid (2.34 g, 83%). Mp 215-217 °C; IR (nujol): 2930, 1600, 1488, 1278, 1002, 877cm^{-1}, ^{1}H NMR (400 MHz; $CDCl_3$) δ 7.09 (s, 2H, H_a), 6.37 (s, 2H, H_b), 3.96 (s, 6H, H_c), 3.77 (s, 6H, H_d), 3.51 (m, 8H, H_f), 3.37 (d, 2H, J = 13.2 Hz, H_e), 2.88 (d, 2H, J = 13.2 Hz, H_e); ^{13}C NMR (100 MHz; $CDCl_3$) δ 150.5, 149.6, 140.0, 136.3, 106.6, 105.5, 71.6, 62.4, 57.7, 56.2, 56.1, 41.3, 41.1; HRMS Calc. for $C_{25}H_{28}O_4S_4$ 520.0870, found 520.0872.

Bis-1,3-dithiolane of 5,6,5',6'-tetrahydroxy-1,1'-spirobisindane-3,3'-dione (69)

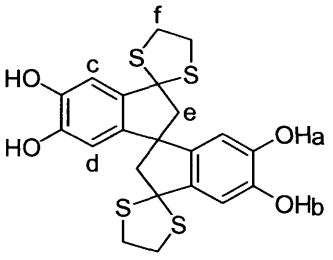

To a solution of 5,6,5',6'-tetrahydroxy-1,1'-spirobisindane-3,3'-dione **44** (1.00 g, 3.20 mmol) in tetrahydrofuran (60 ml) and trifluoroacetic acid (7 ml) was added 1,2-ethanedithiol (3.01 g, 32 mmol) followed by boron trifluoride diethyl etherate (2.72 g, 19.2 mmol) under nitrogen atmosphere. After 96 hours the mixture was quenched with water (200 ml). The tetrahydrofuran was evaporated under vacuum and the solid product collected under vacuum filtration. The crude product was washed repeatedly with dichloromethane to give a pale yellow solid (1.33 g, 89%). Mp 240-241 °C; IR (nujol): 3290, 2923, 1603, 1289, 1009, 796 cm^{-1}, ^{1}H NMR (400 MHz; Acetone-d_6) δ 8.00 (s, 2H, H_a), 7.93 (s, 2H, H_b), 7.03 (s, 2H, H_c), 6.32 (s, 2H, H_d), 3.48 (m, 8H, H_f), 3.34 (d, 2H, J = 15.0 Hz, H_e), 2.77 (d, 2H, J = 15.0 Hz, H_e); ^{13}C NMR (100 MHz; Acetone-d_6) δ 147.4, 146.4, 140.9, 137.4, 111.6, 110.1, 72.0, 63.61, 57.9, 54.9, 41.7, 41.6; HRMS Calc. for $C_{21}H_{21}O_4S_4$ 465.0323, found 465.0329.

Bis-1,3-dithiane of 5,6,5',6'-tetramethoxy-1,1'-spirobisindane-3,3'-dione (68)

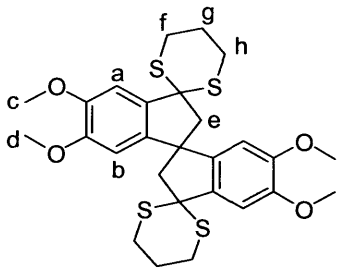

To a solution of 5,6,5',6'-tetramethoxy-1,1'-spirobisindane-3,3'-dione **41** (2.00 g, 5.42 mmol) in dichloromethane (60 ml) and trifluoroacetic acid (10 ml) was added 1,3-propanedithiol (2.34 g, 21.68 mmol) followed by boron trifluoride diethyl etherate (3.07 g, 21.68 mmol) under nitrogen atmosphere. After 24 hours the mixture was quenched with water (200 ml) and washed with a solution of NaOH 1 N (3 x 100 ml) and brine (2 x 100 ml). The organic layer was dried with $MgSO_4$, filtered and evaporated under vacuum to obtain a white solid (2.67 g, 90%). Mp 208-210 °C; IR (nujol): 2920, 1605, 1512, 1310, 1198, 865 cm^{-1}, ^1H NMR (400 MHz; $CDCl_3$) δ 7.06 (s, 2H, H_a), 6.48 (s, 2H, H_b), 3.96 (s, 6H, H_c), 3.84 (d, 2H, J = 13.6 Hz, H_e), 3.76 (s, 6H, H_d), 3.19 (m, 4H, H_f), 2.91 (m, 4H_h), 2.84 (d, 2H, J = 13.6 Hz, H_e), 2.08 (m, 4H, H_g); ^{13}C NMR (100 MHz; $CDCl_3$) δ 150.9, 149.5, 140.8, 136.4, 106.5, 59.0, 58.2, 57.6, 56.2, 56.1, 30.1, 28.7, 24.9; HRMS Calc. for $C_{27}H_{33}O_4S_4$ 549.1262, found 549.1257.

Bis-1,3-dithiane of 5,6,5',6'-tetrahydroxy-1,1'-spirobisindane-3,3'-dione (70)

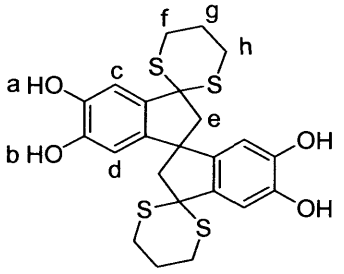

To a solution of 5,6,5',6'-tetrahydroxy-1,1'-spirobisindane-3,3'-dione **44** (1.00 g, 3.20 mmol) in tetrahydrofuran (60 ml) and trifluoroacetic acid (7 ml) was added 1,2-ethanedithiol (3.46 g, 32.0 mmol) followed by boron trifluoride diethyl etherate (2.72 g, 19.2 mmol) under nitrogen atmosphere. After 96 hours the mixture was quenched with water (200 ml). The tetrahydrofuran was evaporated under vacuum and the solid product collected under vacuum filtration. The crude product was washed repeatedly with dichloromethane to give a pale yellow solid (1.37 g, 87%). Mp 254-256 °C; IR (nujol):

3399, 2921, 1608, 1505, 1301, 1195, 1099, 994, 927, 802 cm^{-1}; ^1H NMR (400 MHz; Acetone-d_6) δ 8.03 (s, 4H, H_a), 6.99 (s, 2H, H_b), 6.41 (s, 2H, H_c), 3.83 (d, 2H, J = 13.6 Hz, H_e), 3.20 (m, 4H, H_f), 2.87 (m, 4H, H_h), 2.74 (d, 2H, J = 13.6 Hz, H_e), 2.21 (m, 4H, H_g); ^{13}C NMR (100 MHz; Acetone-d_6) δ 146.8, 145.2, 141.1, 136.3, 110.5, 110.2, 59.0, 58.3, 57.1, 29.6, 28.3, 24.9; HRMS Calc. for $C_{23}H_{25}O_4S_4$ 493.0636, found 493.0620.

5,5',6,6'-Tetramethoxy-2,2',3,3'-tetrahydro-1,1'-spirobisindene (71)

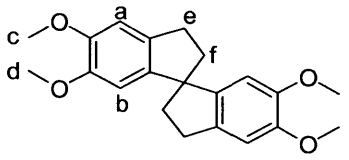

To a magnetically stirred solution of bis-1,3-dithiane of 5,6,5',6'-tetramethoxy-1,1'-spirobisindane-3,3'-dione **68** (1.40 g, 2.55 mmol) in EtOH (3 ml) was added Raney nickel (3.00 g, excess). The mixture was refluxed for 3 h then cooled and filtered through a short silica gel column using excess ethyl acetate. Evaporation of the solvent furnished the desired product as white solid (0.74 g, 86%). Mp 80-82 °C [89]; IR (nujol): 2920, 1599, 1520, 1456, 1326, 1265, 1201, 1139, 1044, 870 cm^{-1}; ^1H NMR (400 MHz; $CDCl_3$) δ 6.85 (s, 2H, H_a), 6.49 (s, 2H, H_b), 3.94 (s, 6H, H_c), 3.77 (s, 6H, H_d), 2.95 (m, 4H, H_e), 2.32 (m, 2H, H_f), 2.13 (m, 2H, H_f); ^{13}C NMR (100 MHz; $CDCl_3$) δ 148.4, 142.0, 135.3, 107.3, 106.4, 61.2, 56.2, 56.1, 40.9, 30.7; HRMS Calc. for $C_{21}H_{24}O_4S_4$ 340.1675, found 340.1672.

5,5',6,6'-Tetrahydroxy-2,2',3,3'-tetrahydro-1,1'-spirobisindene (72)

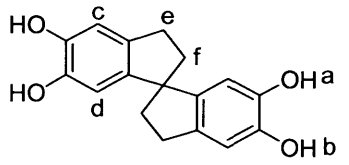

In a two-necked round bottom flask was added 5,5',6,6'-tetramethoxy-2,2',3,3'-tetrahydro-1,1'-spirobisindene **71** (0.60 g, 1.76 mmol) and dry dichloromethane (30 ml) under a dry nitrogen atmosphere that was maintained throughout the reaction. This mixture was cooled to 0 °C then boron tribromide (0.67 ml, 7.05 mmol) was added dropwise and the reaction stirred at room temperature for a further 1 h. The reaction was poured into ice and left under vigorous stirring allowing the evaporation of the excess dichloromethane. The precipitate was filtered off, washed with water and dried. Recrystallization from dichloromethane/hexane (1/1) gave the desired compound as a white solid (0.45 g, 90%). Mp over 240/242 °C [89]; IR (nujol): 3452, 1578, 1510, 1466, 1355, 1278, 1201, 1058, 872

cm^{-1}; ^1H NMR (400 MHz; Acetone-d_6) δ 7.45 (s, 2H, H_a), 7.37 (s, 2H, H_b), 6.65 (s, 2H, H_c), 6.21 (s,2H, H_d), 2.64 (m, 4H, H_e), 2.09 (m, 2H, H_f), 1.87 (m, 2H, H_f); ^{13}C NMR (100 MHz; Acetone-d_6) δ 143.8, 141.0, 134.2, 110.5, 109.6, 60.0, 40.8, 29.8; HRMS Calc. for $C_{17}H_{16}O_4$ 284.1049, found 284.1042.

4,4-bis(3,4-Dimethoxyphenyl) heptanedioic acid (74).

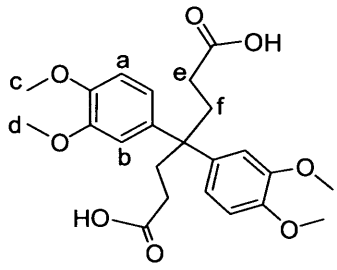

To 4-oxopimelate (4 ml, 17.4 mmol) was added, dropwise in an ice bath Eaton's reagent (10 ml) and this solution was kept under stirring for 1 hour. To the mixture was, then, added veratrole (19.1 ml, 137 mmol). The solution was kept at room temperature for further 7 days. The mixture was poured into an ice bath (50 ml) and extracted with diethyl ether (3 x 100 ml). The organic layer was dried with $MgSO_4$, filtered off and evaporated under vacuum. To the crude product was added methanol (50 ml) and 20% aqueous NaOH (50 ml) and the solution stirred for further 1 day at room temperature, until complete consumption of the starting material was confirmed by TLC. To the reaction mixture was added water (25 ml) and the aqueous layer extracted with diethyl ether (3 x 100 ml). To the aqueous phase, cooled at 0 °C, was added dropwise concentrated HCl until acid pH, to precipitate the desired product as a pale brown solid that was filtered off and washed with water. Recrystallization from ethyl acetate gave the desired product as a pale yellow solid (2.40 g, 32%). Mp 173-175 °C; IR (nujol): 2614, 1695, 1589, 1512, 1338, 1305, 1145, 765 cm^{-1}; ^1H NMR (400 MHz; $CDCl_3$) δ 6.78 (m, 4H, H_a), 6.53 (s, 2H, H_b), 3.85 (s, 6H, H_c), 3.72 (s, 6H, H_d), 2.34 (t, 4H, J = 7.2 Hz, H_e), 2.07 (t, 4H, J = 7.2 Hz, H_f); ^{13}C NMR (100 MHz; $CDCl_3$) δ 181.2, 149.0, 147.7, 140.1, 119.8, 111.5, 110.6, 56.3, 56.2, 48.7, 31.6, 30.0; LRMS, *m/z*, ($APCI^+$): 415 (M – H_2O, 100%).

Dimethyl 4,4-bis(3,4-dimethoxyphenyl) heptanedioate (73).

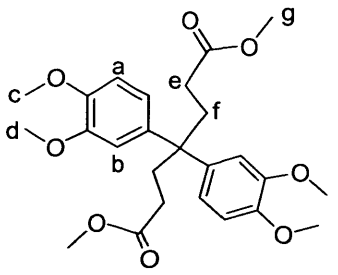

To a stirred mixture of 4,4-bis(3,4-dimethoxyphenyl) heptanedioic acid **74** (1 g, 2.31 mmol) and methanol (25 ml) cooled on an ice bath, was added dropwise concentrated sulphuric acid (5 ml). The solution was stirred at room temperature for further 2 h until the complete dissolution of the solid. The reaction was quenched with water (50 ml) and extracted with ethyl acetate (3 x 100), washed with $NaHCO_3$ (100 ml) and brine (2 x 100 ml). The organic layer was dried over $MgSO_4$, filtered and evaporated under vacuum to give the product as brown oil (1.01 g, 95%). ^{1}H NMR (400 MHz; $CDCl_3$) δ 6.73 (m, 4H, H_a), 6.54 (s, 2H, H_b), 3.78 (s, 6H, H_c), 3.67 (s, 6H, H_d), 3.52 (s, 6H, H_g), 2.28 (t, 4H, J = 10.2 Hz, H_e), 1.97 (t, 4H, J = 10.2 Hz, H_f); ^{13}C NMR (100 MHz; $CDCl_3$) δ 173.7, 149.0, 147.6, 139.4, 120.2, 111.8, 109.3, 56.5, 56.4, 51.6, 48.2, 35.0, 30.0; LRMS, *m/z*, ($APCI^+$): 483.1 ($M + Na^+$, 100%).

6,7,6',7'-Tetramethoxy-tetrahydro--2H,2H'-1,1'-spirobisnaphthalene-4,4'-dione (75).

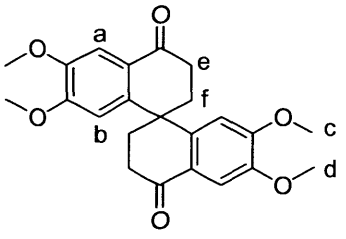

Finely powdered 4,4-bis(3,4-dimethoxyphenyl) heptanedioic acid **74** (1 g, 2.31 mmol) was added to polyphosphoric acid at 80 °C and the mixture was stirred at this temperature for 3 h. The dark red solution was poured into an ice/water bath and stirred for an hour until the formation of a dark brown precipitate. The solid was filtered off, washed with water and dried. Recrystallization from acetic acid/methanol (4/1), gave the desired compound as pale brown solid (0.62 g, 68%). Mp 210-213 °C; IR (nujol): 2938, 1670, 1598, 1509, 1276, 1208, 1052, 875 cm^{-1}; ^{1}H NMR (400 MHz; $CDCl_3$) δ 7.53 (s, 2H, H_a), 6.30 (s, 2H, H_b), 3.90 (s, 6H, H_c), 3.66 (s, 6H, H_d), 2.73 (m, 4H, H_e), 2.39 (m, 4H, H_f); ^{13}C NMR (100 MHz;

$CDCl_3$) δ 195.8, 153.7, 148.3, 144.8, 126.2, 110.2, 108.4, 56.2, 56.1, 42.5, 34.6, 34.5; HRMS Calc. for $C_{23}H_{25}O_6$ 397.1651, found 397.1640.

6,7,6',7'-Tetrahydroxy- tetrahydro-2H,2H'-1,1'-spirobisnaphthalene-4,4'-dione (76).

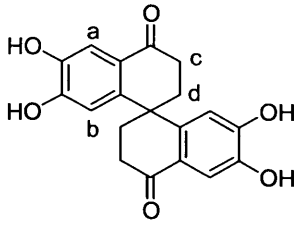

In a two-necked round bottom flask was added 6,7,6',7'-tetrahydroxy-2H,2H'-1,1'-spirobisnaphtalene-4,4'-dione **75** (0.50 g, 1.26 mmol) and dry dichloromethane (40 ml) under a dry nitrogen atmosphere that was maintained throughout the reaction. This mixture was cooled to 0 °C then boron tribromide (0.50 ml, 5.04 mmol) was added dropwise and the reaction stirred at room temperature for a further 2 h. The reaction was poured into degassed water and left under vigorous stirring for 1 h. The precipitate was filtered off under nitrogen atmosphere, washed with water and dried. Recrystallization from dichloromethane/hexane (1/1) gave the desired compound as a white solid (0.55 g, 73%). Mp 230-232 °C; ^{1}H NMR (400 MHz; MeOD) δ 7.47 (s, 2H, H_a), 6.43 (s, 2H, H_b), 2.62 (m, 4H, H_c), 2.39 (m, 4H, H_d); ^{13}C NMR (100 MHz; MeOD) δ 199.1, 153.1, 145.9, 115.9, 113.9, 35.8, 35.4; HRMS Calc. for $C_{19}H_{16}O_6$ 340.0947, found 340.0935.

6,7,6',7'-Tetramethoxy-4,4'-diphenyl-2H,2H'-1,1'-spirobisnaphthalene (77).

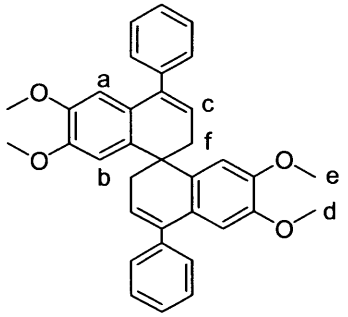

In a two-necked round bottom flask was added dry THF (30 ml) and 6,7,6',7'-tetramethoxy-2H,2H'-1,1'-spirobisnaphtalene-4,4'-dione **75** (1 g, 2.52 mmol). Phenyl magnesium bromide (1.83 g, 10.08 mmol) was added dropwise under nitrogen atmosphere, at 0 °C and under vigorous stirring. The mixture was kept under stirring for a further 24 h

under reflux. The solution was quenched with hydrochloric acid (1N, 100 ml). The organic layer was separated and the aqueous layer extracted with diethyl ether (3 x 100 ml). The combined organic layers were washed with saturated aqueous sodium hydrogen carbonate (2 x 100 ml) and the solvent evaporated under reduced pressure. To the crude product was added a solution of 20% aqueous sulphuric acid (50 ml) and the mixture was stirred at 90 °C for 20 h. The solution was quenched with water (100 ml) and extracted with dichloromethane (3x 100 ml). Purification by chromatographic column, eluting with petroleum ether/ethyl acetate (6/4), gave the desired compound as white solid (1.02 g, 78%). Mp 126-128 °C; IR (nujol): 2938, 1601, 1578, 1490, 1341, 1264, 1080, 816 cm^{-1}; ^1H NMR (400 MHz; $CDCl_3$) δ 7.30 (m, 10H, H_{Ar}), 6.82 (s, 2H, H_a), 6.63 (s, 2H, H_b), 5.80 (m, 2H, H_c), 3.71 (s, 6H, H_d), 3.62 (s, 6H, H_e), 2.71 (m, 4H, H_f); ^{13}C NMR (100 MHz; $CDCl_3$) δ 147.8, 146.9, 140.8, 139.0, 135.3, 128.7, 128.3, 128.0, 127.3, 123.7, 110.7, 110.0, 56.0, 55.9, 42.1, 35.0; HRMS Calc. for $C_{35}H_{32}O_4$ 516.2301 found 516.2310.

6,7,6',7'-Tetrahydroxy-4,4'-diphenyl-2H,2H'-1,1'-spirobisnaphthalene (78).

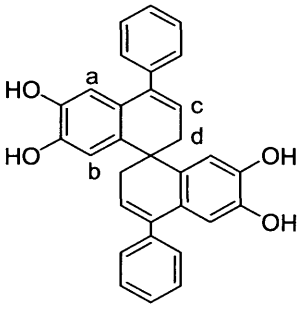

In a two-necked round bottom flask was added 6,7,6',7'-tetramethoxy-4,4'-diphenyl-2H,2H'-1,1'-spirobisnaphthalene **77** (0.61 g, 1.18 mmol) and dry dichloromethane (40 ml) under a dry nitrogen atmosphere that was maintained throughout the reaction. This mixture was cooled to 0 °C then boron tribromide (0.45 ml, 4.72 mmol) was added dropwise and the reaction stirred at room temperature for a further 6 h. The reaction was poured into ice and left under vigorous stirring allowing the evaporation of the excess dichloromethane. The precipitate was filtered off, washed with water and dried. Recrystallization from dichloromethane/hexane (1/1) gave the desired compound as pale yellow solid (0.54 g, 88%). Mp 147-149 °C; IR (nujol): 3380, 2918, 1694, 1633, 1305, 1223, 856 cm^{-1} ^1H NMR (400 MHz; MeOD) δ 7.36 (m ,10H, H_{Ar}), 6.84 (s, 2H, H_a), 6.33 (s, 2H, H_b), 5.75 (m, 2H, H_c), 2.83 (m, 2H, H_d), 2.61 (m, 2H, H_d); ^{13}C NMR (100 MHz; MeOD) δ 145.4, 144.0,

142.9, 141.0, 135.9, 129.9, 129.2, 128.9, 128.0, 123.5, 115.8, 115.1, 42.2, 36.6; HRMS Calc. for $C_{31}H_{24}O_4$ 460.1675, found 460.1661.

4,4'-bis-(3,4-dimethoxyphenyl)-1,1,7,7-tetraphenylhepta-1,6-diene (79).

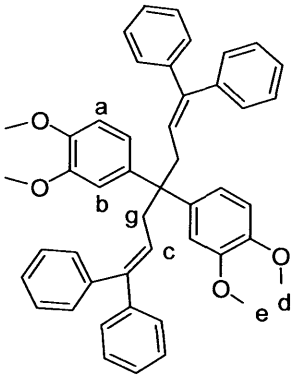

In a two-necked round bottom flask was added dry THF (40 ml) and dimethyl 4,4-bis(3,4-dimethoxyphenyl) heptanedioate **73** (1,00 g, 2.31 mmol). Phenyl magnesium bromide (2.50 g, 13.9 mmol) was added dropwise under nitrogen atmosphere, at 0 °C and under vigorous stirring. The mixture was kept under reflux for 1 h. The resulting precipitate was filtered off, washed with water and dried. To the crude product was added a solution of 10% hydrochloric acid in methanol (50 ml) and the mixture was stirred at room temperature for 5 h. The solution was quenched with water (100 ml). The precipitate formed was filtered off, washed with methanol and dried. Recrystallization from methanol gave the desired product as a white solid (1.16 g, 75%). Mp 135-140 °C; IR (nujol): 2923, 1597, 1568, 1341, 1258, 1085, 1003, 867 cm^{-1}; ^1H NMR (400 MHz; $CDCl_3$) δ 7.01 (m, 20H, H_{Ar}), 6.68 (m, 4H, H_a), 6.33 (s, 2H, H_b), 5.62 (t, 2H, J = 7.2 Hz, H_c), 3.78 (s, 6H, H_d), 3.51 (s, 6H, H_e), 2.85 (d, 4H, J = 7.2 Hz, H_g); ^{13}C NMR (100 MHz; $CDCl_3$) δ 148.2, 147.1, 143.3, 142.7, 140.0, 139.9, 129.9, 129.3, 128.3, 128.2, 128.0, 127.9, 127.8, 127.2, 126.9, 126.8, 126.1, 125.8, 119.8, 112.0, 109.9, 55.8, 55.5, 50.6, 38.7. ; LRMS, *m/z*, ($APCI^+$): 673 (MH^+, 100%).

6,7,6',7'-Tetramethoxy-4,4,4',4'-tetraphenyl-3,3',4,4'-tetrahydro-2H,2H'-1,1'-spirobisnaphthalene (80).

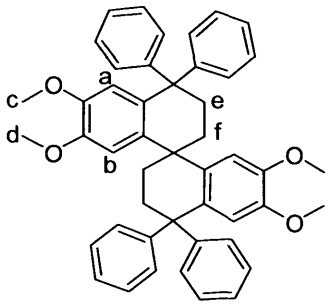

Finely powdered 4,4'-bis-(3,4-dimethoxyphenyl)-1,1,7,7-tetraphenylhepta-1,6-diene **79** (1.00 g, 1.48 mmol) was added to Eaton's reagent and the mixture was stirred at room temperature overnight. The dark red solution was poured into an ice/water bath and stirred for an hour until the formation of a white precipitate. The solid was filtered off, washed with water and dried. Recrystallization from acetic methanol, gave the desired compound as a white solid (0.84 g, 73%). Mp 175-178 °C; IR (nujol): 2923, 1605, 1517, 1245, 1212, 1038, 945, 867, 760 cm^{-1}; ^1H NMR (400 MHz; $CDCl_3$) δ 7.41 (m, 20H, H_{Ar}), 6.24 (s, 2H, H_a), 6.20 (s, 2H, H_b), 3.63 (s, 6H, H_c), 3.62 (s, 6H, H_d), 2.91 (m, 4H, H_e), 2.23 (m, 4H, H_f); ^{13}C NMR (100 MHz; $CDCl_3$) δ 149.9, 147.4, 146.8, 146.0, 139.9, 134.9, 129.7, 129.2, 128.0, 127.8, 126.2, 126.1, 113.4, 112.6, 55.7, 55.4, 53.8, 44.5, 35.8, 35.5; HRMS Calc. for $C_{47}H_{44}O_4$ 672,3240, found 672,3239.

6,7,6',7'-Tetrahydroxy-4,4,4',4'-tetraphenyll-3,3',4,4'-tetrahydro-2H,2H'-1,1'-spirobisnaphthalene (81).

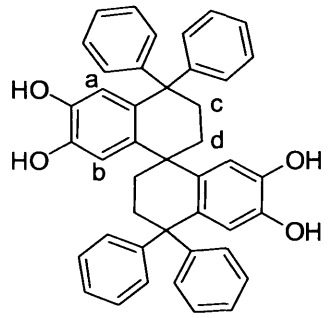

In a two-necked round bottom flask was added 6,7,6',7'-tetramethoxy-4,4,4',4'-tetraphenyl-3,3',4,4'-tetrahydro-2H,2H'-1,1'-spirobisnaphthalene **80** (0.83g, 1.23 mmol) and dry dichloromethane (40 ml) under a dry nitrogen atmosphere that was maintained throughout the reaction. This mixture was cooled to 0 °C then boron tribromide (0.47 ml, 4.93 mmol) was added dropwise and the reaction stirred at room temperature for a further

4 h. The reaction was poured into ice and left under vigorous stirring allowing the evaporation of the excess dichloromethane. The precipitate was filtered off, washed with water and dried. Recrystallization from dichloromethane/hexane (1/1) gave the desired compound as a white solid (0.55 g, 73%). Mp 228-230 °C; IR (nujol): 3395, 2923, 1703, 1601, 1476, 1282, 1220, 1103, 856 cm^{-1}, ^1H NMR (400 MHz; MeOD) δ 7.13 (m, 20H, H_{Ar}), 6.14 (s, 2H, H_a), 5.98 (s, 2H, H_b), 2.64 (m, 4H, H_c), 1.79 (m, 4H, H_d); ^{13}C NMR (100 MHz; MeOD) δ 129.8, 129.3, 128.2, 127.9, 127.8, 126.3, 125.9, 117.4, 116.8, 36.1, 35.6, 31.0; HRMS Calc. for $C_{43}H_{37}O_4$ 617.2692, found 617.2688.

4,4'-bis-(spiro-9-fluorenyidene)-6,7,6',7'-tetramethoxy-tetrahydro-2H,2H'-1,1'-spirobisnaphthalene (82) and 4-(spiro-9-fluorenyidene)-6,7,6',7'-tetramethoxy-tetrahydro-2H,2H'-1,1'-spirobisnaphthalene-4'-one (83).

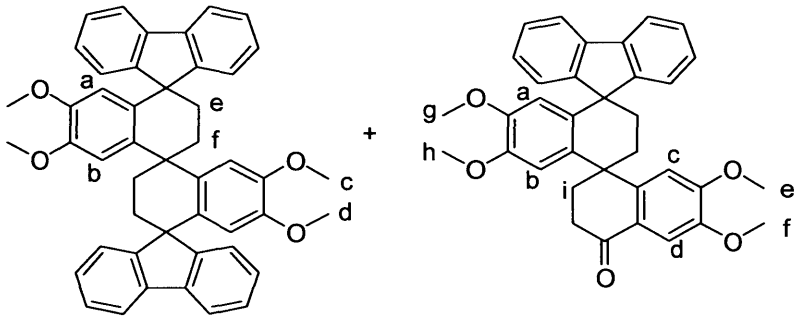

In a two-necked round bottom flask was added dry THF (30 ml) and 6,7,6',7'-tetramethroxy-2H,2H'-1,1'-spirobisnaphthalene-4,4'-dione **75** (1.27 g, 3.20 mmol). 2-Biphenyl magnesium bromide (3.92 g, 15.13 mmol) was added dropwise under nitrogen atmosphere, at 0 °C and under vigorous stirring. The mixture was kept under reflux for 3 days. The reaction was quenched with water. The precipitate formed was filtered off, washed with water and dried. To the crude product was added a solution of 10% hydrochloric acid in methanol (50 ml) and stirred at room temperature for 5 h. The solution was quenched with water (20 ml). The solid was filtered off and to the crude product was added to Eaton's reagent (10 ml) and the mixture stirred at room temperature for 3 h. The dark red solution was poured into an ice/water bath and stirred for an hour until the formation of a white precipitate. The product was filtered off, washed with water and dried. Purification by chromatographic column, eluting with petroleum ether/ethyl acetate (7/3), gave **82** ($\mathbf{R_f}$ **=0.6)** as white solid (0.40 g, 19%) and **83** ($\mathbf{R_f}$ **= 0.3)** (0.68 g, 50%).

(82) Mp 157-160 °C; IR (nujol): 2926, 1609, 1510, 1255, 1212, 1144, 1028, 938, 861, 760 cm^{-1}; ^1H NMR (400 MHz; $CDCl_3$) δ 7.57 (m, 16H, H_{Ar}), 6.80 (s, 2H, H_a), 5.77 (s, 2H, H_b), 3.82 (s, 6H, H_c), 3.44 (s, 6H, H_d), 2.80 (m, 4H, H_e), 2.60 (m, 4H, H_f); ^{13}C NMR (100 MHz; $CDCl_3$) δ 155.4, 148.2, 147.9, 140.5, 139.8, 131.9, 128.3, 127.7, 127.6, 124.8, 124.7, 120.8, 120.3, 112.2, 110.7, 56.2, 55.9, 55.2, 33.5; HRMS Calc. for $C_{47}H_{40}O_4$ 668.2927, found 668.2908.

(83) Mp 105-107 °C; IR (nujol): 2935, 1669, 1599, 1510, 1448, 1403, 1251, 1205, 1045, 863, 762 cm^{-1}; ^1H NMR (400 MHz; $CDCl_3$) δ 7.66 (s, 1H, H_a), 7.44 (m, 8H, H_{Ar}), 6.68 (s, 1H, H_b), 6.49 (s, 1H, H_c), 5.77 (s, 1H, H_d), 4.04 (s, 3H, H_e), 3.87 (s, 3H, H_f), 3.70 (s, 3H, H_g), 3.42 (s, 3H, H_h), 2.67 (m, 8H, H_i); ^{13}C NMR (100 MHz; $CDCl_3$) δ 197.8, 154.7, 149.0, 148.4, 148.2, 140.3, 132.3, 128.2, 127.9, 127.6, 124.9, 142.4, 120.8, 120.4, 111.6, 111.4, 110.6, 108.9, 56.5, 56.3, 55.8, 55.0, 42.0, 38.0, 34.8, 33.4; HRMS Calc. for $C_{35}H_{32}O_5$ 532.2250, found 532.2231.

4,4'-bis-(spiro-9-fluorenyidene)-6,7,6',7'-tetrahydroxy-tetrahydro-2H,2H'-1,1'-spirobisnaphthalene (84).

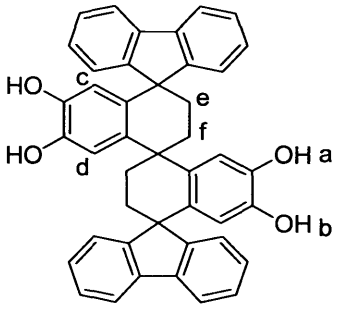

In a two-necked round bottom flask was added 4,4'-bis-(spiro-9-fluorenyidene)-6,7,6',7'-tetramethoxy-tetrahydro-2H,2H'-1,1'-spirobisnaphthalene **82** (0.35 g, 0.52 mmol) and dry dichloromethane (40 ml) under a dry nitrogen atmosphere that was maintained throughout the reaction. This mixture was cooled to 0 °C then boron tribromide (0.20 ml, 2.09 mmol) was added dropwise and the reaction stirred at room temperature for a further 1 h. The reaction was poured into ice and left under vigorous stirring allowing the evaporation of the excess dichloromethane. The precipitate was filtered off, washed with water and dried. Recrystallization from dichloromethane /hexane (1/1) gave the desired compound as a white solid (0.28 g, 90%). Mp 236-238 °C; IR (nujol): 3395, 2922, 1700, 1605, 1488, 1276, 1212, 1108, 867 cm^{-1}; ^1H NMR (400 MHz; Acetone-d_6) δ 7.93 (s, 2H, H_a)7.57 (m, 16H, H_{Ar}), 7.29 (s, 2H, H_b), 6.79 (s, 2H, H_c), 2.76 (m, 2H, H_d), 2.56 (m, 4H, H_e), 1.83 (m,

bromide (3M in Et_2O, 5.42 ml, 16.28 mmol) was added dropwise under nitrogen atmosphere, at 0 °C and under vigorous stirring. The mixture was kept under reflux for 1 h. The reaction was quenched with water and extracted with ethyl acetate (3 x 200 ml). The organic layer was dried by $MgSO_4$, filtrated and evaporated under vacuum. Recrystallization from methanol gave the product as yellow oil (1.14 g, 91%). ^1H NMR (400 MHz; $CDCl_3$) δ 6.77 (m, 4H, H_a), 6.68 (s, 2H, H_b), 6.52 (s, 2H, H_g), 3.77 (s, 6H, H_c), 3.65 (s, 6H, H_e), 2.02 (m, 8H, H_f), 1.06 (s, 12H, H_g); ^{13}C NMR (100 MHz; $CDCl_3$) δ 148.6, 147.4, 141.6, 119.9, 112.0, 110.0, 71.3, 56.2, 56.0, 48.2, 37.9, 31.9, 30.0 ; LRMS, *m/z*, (APCI$^+$): 461 (MH^+, 100%).

6,7,6',7'-Tetramethoxy-4,4,4',4'-tetramethyl-3,3',4,4'-tetrahydro-2H,2H'-1,1'-spirobisnaphthalene (87).

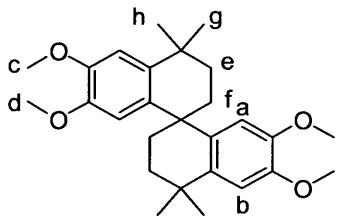

5,5-bis(3,4-dimethoxyphenyl)-2,8-dimethylnonane-2,8-diol **86** (1.00 g, 2.17 mmol) was added to methanesulfonic acid and the mixture was stirred overnight at 50 °C. The dark red solution was poured into an ice/water bath and stirred for an hour until the formation of a white precipitate. The solid was filtered off, washed with water and dried. Purification by chromatographic column, eluting with petroleum ether/ethyl acetate (7/3) followed by recrystallization from methanol, gave the desired compound as a white solid (0.18 g, 20%). Mp 220/222°C, IR (nujol): 2930, 1655, 1506, 1482, 1255, 1067, 868, cm^{-1}; ^1H NMR (400 MHz; $CDCl_3$) δ 6.87 (s, 2H, H_a), 6.22 (s, 2H, H_b), 3.89 (s, 6H, H_c), 3.59 (s, 6H, H_d), 2.01 (m, 4H, H_e), 1.90 (m, 2H, H_f), 1.55 (m, 2H, H_f), 1.39 (s, 6H, H_h), 1.36 (s, 6H, H_g); ^{13}C NMR (100 MHz; $CDCl_3$) δ 147.2, 146.9, 144.2, 138.5, 137.7, 120.8, 112.7, 111.7, 56.4, 45.4, 35.4, 34.5, 32.0, 31.5. HRMS Calc. for $C_{27}H_{36}O_4$ 424.2614, found 424.2610.

6,7,6',7'-Tetrahydroxy-4,4,4',4'-tetramethyl-3,3',4,4'-tetrahydro-2H,2H'-1,1'-spirobisnaphthalene (88).

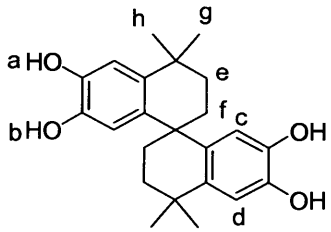

In a two-necked round bottom flask was added 6,7,6',7'-Tetramethoxy-4,4,4',4'-tetramethyl-3,3',4,4'-tetrahydro-2H,2H'-1,1'-spirobisnaphthalene **87** (0.22 g, 0.52 mmol) and dry dichloromethane (20 ml) under a dry nitrogen atmosphere that was maintained throughout the reaction. This mixture was cooled to 0 °C then boron tribromide (0.15 ml, 1.55 mmol) was added dropwise and the reaction stirred at room temperature for a further 1 h. The reaction was poured into ice and left under vigorous stirring allowing the evaporation of the excess dichloromethane. The precipitate was filtered off, washed with water and dried. Recrystallization from dichloromethane/hexane (1/1) gave the desired compound as a white solid (0.18 g, 94%). Mp over 300 °C; IR (nujol): 3445, 2920, 1653, 1520, 1456, 1269, 1201, 1047, 868, 790 cm^{-1}; ^1H NMR (400 MHz; Acetone-d_6) δ 7.63 (s, 2H, H_a), 7.35 (s, 2H, H_b), 6.78 (s, 2H, H_c), 6.15 (s, 2H, H_d), 1.95 (m, 4H, H_e), 1.83 (m, 2H, H_f), 1.54 (m, 2H, H_f), 1.30 (s, 6H, H_g), 1.29 (s, 6H, H_h); ^{13}C NMR (100 MHz; Acetone-d_6) δ 147.8, 143.0, 135.3, 127.4, 127.0, 124.6, 115.6, 114.0, 54.4, 47.8, 35.7, 34.1, 32.7; HRMS Calc. for $C_{23}H_{28}O_4$ 368.1988, found 368.1989.

Bis phthalonitrile derived from 5,6,5',6'-tetrahydroxy-1,1'-spirobisindane-3,3'-dione (105).

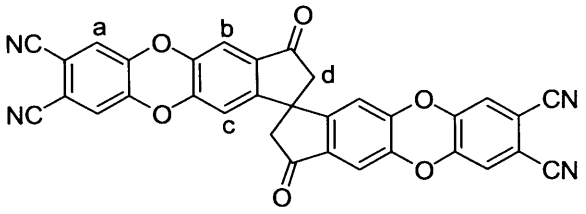

To a solution of 5,6,5',6'-tetrahydroxy-1,1'-spirobisindane-3,3'-dione **44** (0.23 mg, 0.73 mmol) in dry dimethylformamide (15 ml), under nitrogen and with stirring, was added dry potassium carbonate (1.00 g, 7.35 mmol). The mixture was heated to 60 °C, then dichlorophthalonitrile (0.29 mg, 1.47 mmol) was added and the temperature increased to

80 °C. After 24 h the reaction was cooled, poured into water (100 ml) and neutralized with hydrochloric acid 2N. The aqueous solution was filtrated, washed with water and dried under vacuum. Recrystallization by methanol gave a pale grey solid (0.30 mg, 80%). Mp over 300 °C, IR (nujol): 2724, 2233, 1633, 1569, 1326, 891 cm^{-1}; ^1H NMR (400 MHz; DMSO-d6) δ 7.89 (s, 4H, H_a), 7.24 (s, 2H, H_b), 6.97 (s, 2H, H_c), 3.18 (d, 2H, J = 19.2 Hz, H_d), 3.02 (d, 2H, J = 19.2 Hz, H_d); ^{13}C NMR (100 MHz; DMSO-d6) δ 201.7, 174.2, 146.5, 145.1, 144.7, 141.4, 133.0, 122.4, 115.5, 113.1, 111.9, 111.5, 110.1, 52.1, 48.9, 47.6, 30.6, 29.5, 17.7; HRMS Calc. for $C_{33}H_{12}N_4O_6$ 560.0757, found 560.0768.

Bis phthalonitrile derived from bis-1,3-dithiolane of 5,6,5',6'-tetrahydroxy-1,1'-spirobisindane-3,3'-dione (106)

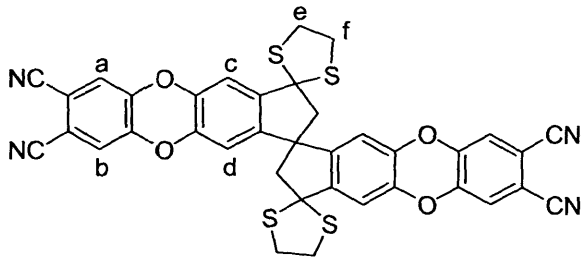

To a solution of bis-1,3-dithiolane of 5,6,5',6'-tetrahydroxy-1,1'-spirobisindane-3,3'-dione **69** (1.00 g, 2.15 mmol) in dry dimethylformamide (40 ml), under nitrogen and with stirring, was added dry potassium carbonate (1.48 g, 10.75 mmol). The mixture was heated to 60 °C, then dichlorophthalonitrile (0.85 mg, 4.30 mmol) was added and the temperature increased to 80 °C. After 24 h the reaction was cooled, poured into water (100 ml) and neutralized with hydrochloric acid 2N. The aqueous solution was filtrated, washed with water and dried under vacuum. Recrystallization by methanol gave a pale grey solid (1.24 g, 81%).Mp over 300°C, IR (nujol): 2935, 2237, 1567, 1503, 1333, 904, 880 cm^{-1}; ^1H NMR (400 MHz; DMSO-d6) δ 7.82 (s, 2H), 7.77 (s, 2H), 7.13 (s, 2H), 6.57 (s, 2H), 3.61 (m, 4H), 3.47 (m, 4H), 3.13 (d, 2H, J = 13.8 Hz), 2.80 (d, 2H, J = 13.8 Hz); ^{13}C NMR (100 MHz; DMSO-d6) δ 146.2, 144.6, 143.8, 141.8, 141.6, 122.3, 116.0, 113.0, 112.4, 111.3, 69.9, 60.7, 57.2, 41.5; HRMS Calc. for $C_{37}H_{20}N_4O_4S_4$ 712.0367, found 712.0373.

Bis phthalonitrile derived from bis-1,3-dithiane of 5,6,5',6'-tetrahydroxy-1,1'-spirobisindane-3,3'-dione (107)

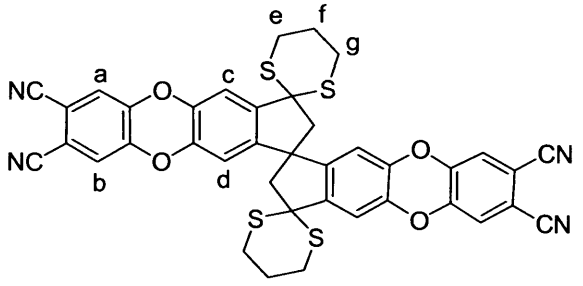

To a solution of Bis-1,3-dithiane of 5,6,5',6'-tetrahydroxy-1,1'-spirobisindane-3,3'-dione **70** (1.00 g, 2.03 mmol) in dry dimethylformamide (40 ml), under nitrogen and with stirring, was added dry potassium carbonate (1.68 g, 12.18 mmol). The mixture was heated to 60 °C, then dichlorophthalonitrile (800 mg, 4.06 mmol) was added and the temperature increased to 80 °C. After 24 h the reaction was cooled, poured into water (100 ml) and neutralized with hydrochloric acid 2N. The aqueous solution was filtrated, washed with water and dried under vacuum. Recrystallization by methanol gave a pale grey solid (1.33 g, 88%).Mp over 300°C, IR (nujol): 2933, 2236, 1591, 1505, 1376, 905, 878 cm^{-1}; ^1H NMR (400 MHz; DMSO-d6) δ 7.88 (s, 2H), 7.79 (s, 2H), 6.99 (s, 2H), 6.64 (s, 2H), 3.37 (d, 2H, J = 13.8 Hz), 3.14 (m, 4H), 2.96 (m, 2H), 2.89 (m, 4H), 2.40 (d, 2H, J = 13.8 Hz); ^{13}C NMR (100 MHz; DMSO-d6) δ 156.1, 146.1, 145.5, 141.3, 133.2, 128.8, 116.5, 114.6, 111.8, 104.0, 69.2, 53.4, 45.6, 24.5, 22.9; HRMS Calc. for $C_{39}H_{24}N_4O_4S_4$ 740.0680, found 740.0694.

Polymer from 1,1'-spirobisindane-3,3'-dione (89)

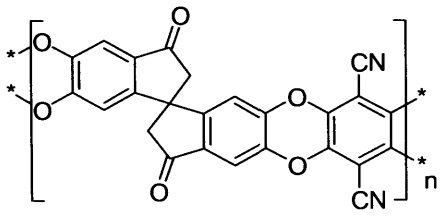

Under a nitrogen atmosphere **44** (1.500 g, 4.80 mmol), and 2,3,5,6-tetrafluoroterephthalonitrile **28** (961 mg, 4.80 mmol) were added to anhydrous dimethylformamide (75 ml). This mixture was heated to 65 °C until complete dissolution of the two starting material was observed, then dry potassium carbonate (5.30 g, 38.4 mmol) was added and the mixture stirred for 72 h at 65 °C. The solution was quenched with water (100 ml), the yellow precipitate filtrated and washed repeatedly with water and

acetone. The product was washed in boiling methanol (24 h), collected by vacuum filtration and dried under vacuum overnight to give a yellow solid (1.60 g, 80%); IR (nujol): 2852, 2230, 1710, 1607, 1267, 998, 735 cm^{-1}; BET surface area = 501 m^2/g; total pore volume = 0.29 cm^3/g at (P/P_0) 0.98, adsorption; TGA analysis (nitrogen): 5% loss of weight occurred at ~ 400 °C. Initial weight loss due to thermal degradation commences at ~ 499 °C.

Polymer from 3,3'-diphenyl-1,1'-spirobisindene (90)

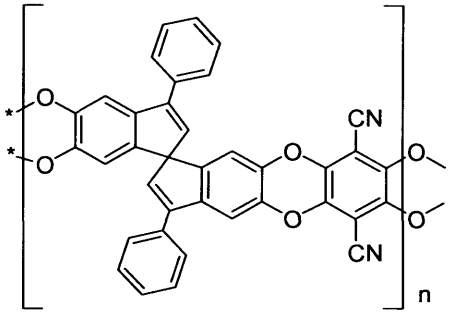

In a two-necked round bottom flask was added under a dry nitrogen atmosphere 5,6,5',6'-tetrahydroxy-3,3'-diphenyl-1,1'-spiro-bisindene **46** (509 mg, 1.18 mmol), and 2,3,5,6-tetrafluoroterephthalonitrile **28** (235 mg, 1.18 mmol), and dry dimethylformamide (20 ml). This mixture was heated to 65 °C, until complete dissolution of the two starting material was observed, then dry potassium carbonate (1.30 g, 9.41 mmol) was added and the mixture kept to stirring for 96 h. The solution was quenched with water (100 ml), filtrated and washed repeatedly with water and acetone. The product was refluxed with methanol (24 h). The purified product was dried under high vacuum overnight to give a yellow solid (551 mg, 80% based on the molecular weight of the repeated unit). IR (nujol): 2897, 2243, 1627, 1267, 1139, 1011 cm^{-1}; BET surface area = 560 m^2/g; total pore volume) 0.35 cm^3/g at (P/P_0) 0.98, adsorption); TGA analysis (nitrogen): 5% loss of weight occurred at ~ 390 °C. Initial weight loss due to thermal degradation commences at ~ 513 °C.

Polymer from 1,1'-spirobisindane-3-diphenyl-3'-one (91)

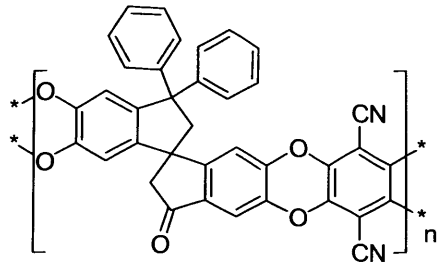

In a two-necked round bottom flask was added under a dry nitrogen atmosphere 5,6,5',6'-tetrahydroxy-1,1'-spirobisindane-3-diphenyl-3'-one **54** (600 mg, 1.33 mmol), 2,3,5,6-tetrafluoroterephthalonitrile **28** (266 mg, 1.33 mmol) and dry dimethylformamide (15 ml). This mixture was heated to 65 °C, until complete dissolution of the two starting material was observed, then dry potassium carbonate (1.46 g, 10.64 mmol) was added and the mixture kept to stirring for 72 h. The solution was quenched with water (100 ml), filtrated and washed repeatedly with water and acetone. The solid was dissolved in THF (20 ml) and, throughout filtration by cotton wool, poured in a flask containing a mixture of acetone/methanol (2/1, 80 ml). The product was dried under high vacuum overnight to give the final product as yellow solid (591 mg, 77% based on the molecular weight of the repeated unit). IR (nujol): 2868, 2233, 1700, 1598, 1267, 1120, 879 cm-^{1}; ^{1}H NMR (400 MHz; $CDCl_3$) δ 7.34 (br m,10H), 6.60 (br s, 4H), 1.68 (br s, 4H); Analysis by GPC ($CHCl_3$): *M*n) 19 000, *M*w) 26 000 g/mol relative to polystyrene. BET surface area = 685 m^2/g; total pore volume = 0.52 cm^3/g at (P/P_0) 0.98, adsorption; TGA analysis (nitrogen): 5% loss of weight occurred at ~ 390 °C. Initial weight loss due to thermal degradation commences at ~ 490 °C.

Polymer from 3,3'-bis-(spiro-9-fluorenyidene)-5,6,5',6'-tetrahydroxy-1,1'-spirobisindane (92)

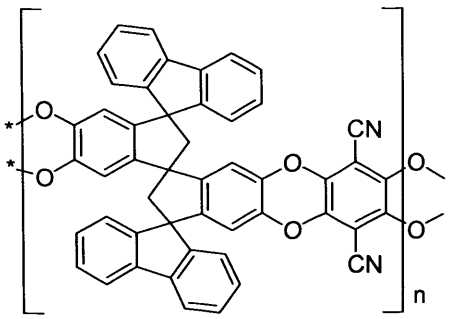

In a two-necked round bottom flask was added under a dry nitrogen atmosphere 3,3'-bis-(spiro-9-fluorenyidene)-5,6,5',6'-tetrahydroxy-1,1'-spirobisindane **57** (579 mg, 0.99 mmol),

2,3,5,6-tetrafluoroterephthalonitrile **28** (198 mg, 0.99 mmol) and dry dimethylformamide (15 ml). This mixture was heated to 65 °C, until complete dissolution of the two starting material was observed, then dry potassium carbonate (1.09 mg, 7.92 mmol) was added and the mixture kept to stirring for 96 h. The solution was quenched with water (100 ml), filtrated and washed repeatedly with water and acetone. The solid was dissolved in $CHCl_3$ (20 ml) and, throughout filtration by cotton wool, poured in a flask containing a mixture of acetone/methanol (2/1, 80 ml). The product was dried under high vacuum overnight to give the final product as yellow solid (568 mg, 78% based on the molecular weight of the repeated unit). IR (nujol): 2935, 2235, 1601, 1293, 1261, 1146, 883 cm^{-1}; ^1H NMR (400 MHz; $CDCl_3$) δ 7.34 (br m, 16H), 6.76 (br m, 2H), 6.09 (br m, 2H), 3.35 (br m, 2H), 3.16 (br m, 2H); ^{13}C NMR (100 MHz; $CDCl_3$) δ 152.3, 152.2, 151.3, 151.3, 140.5, 140.5, 138.9, 128.3, 127.8, 124.1, 123.9, 120.1, 112.4, 100.7, 62.4, 59.4, 30.3, 29.6, Analysis by GPC ($CHCl_3$): *M*n) 16 000, *M*w) 75 000 g/mol relative to polystyrene. BET surface area = 895 m^2/g; total pore volume = 0.69 cm^3/g at (P/P_0) 0.98, adsorption); TGA analysis (nitrogen): 5% loss of weight occurred at ~ 390 °C. Initial weight loss due to thermal degradation commences at ~ 550 °C.

Polymer from 3-(spiro-9-fluorenyidene)-5,6,5',6'-tetrahydroxy-1,1'-spirobisindane-3'-one (93)

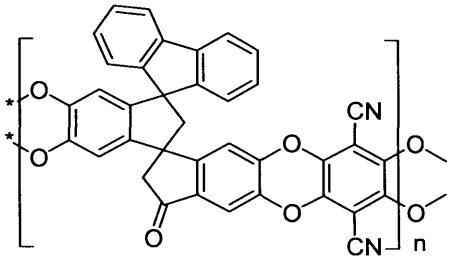

In a two-necked round bottom flask was added under a dry nitrogen atmosphere 3-(spiro-9-fluorenyidene)-5,6,5',6'-tetrahydroxy-1,1'-spirobisindane-3'-one **59** (460 mg, 1.02 mmol), and 2,3,5,6-tetrafluoroterephthalonitrile **28** (205 mg, 1.02 mmol), and dry dimethylformamide (10 ml). This mixture was heated to 65 °C, until complete dissolution of the two starting material was observed, then dry potassium carbonate (1.13 g, 8.16 mmol) was added and the mixture kept to stirring for 96 h. The solution was quenched with water (100 ml), filtrated and washed repeatedly with water and acetone. The product was refluxed with methanol (24 h). The purified product was dried under high vacuum

overnight to give a yellow solid (521 mg, 85% based on the molecular weight of the repeated unit). IR (nujol): 2858, 2236, 1697, 1595, 1267, 1139, 883, 709 cm^{-1}; BET surface area = 658 m^2/g; total pore volume = 0.40 cm^3/g at (P/P_0) 0.98, adsorption; TGA analysis (nitrogen): 5% loss of weight occurred at ~ 350 °C. Initial weight loss due to thermal degradation commences at ~ 490 °C.

Polymer from 3,3'-bis(4,4'-di-tert-butyl-9-fluorenyidene)-5,6,5',6'-tetrahydroxy-1,1'-spirobisindane (94)

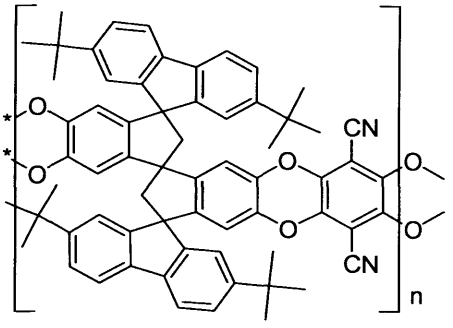

In a two-necked round bottom flask was added under a dry nitrogen atmosphere 3,3'-bis(4,4'-di-tert-butyl-9-fluorenyidene)-5,6,5',6'-tetrahydroxy-1,1'-spirobisindane **64** (716 mg, 0.88 mmol), 2,3,5,6-tetrafluoroterephthalonitrile **28** (177 mg, 0.88 mmol) and dry dimethylformamide (15). This mixture was heated to 65 °C, until complete dissolution of the two starting material was observed, then dry potassium carbonate (970 mg, 7.04 mmol) was added and the mixture kept to stirring for 96 h. The solution was quenched with water (100 ml), filtrated and washed repeatedly with water and acetone. The solid was dissolved in $CHCl_3$ (20 ml) and, throughout filtration by cotton wool, poured in a flask containing a mixture of acetone/methanol (2/1, 80 ml). The product was dried under high vacuum overnight to give the final product as yellow solid (665 mg, 81% based on the molecular weight of the repeated unit). IR (nujol): 2930, 1606, 1501, 1278, 1214, 1102, 1011, 844 cm^{-1}; ^1H NMR (400 MHz; $CDCl_3$) δ 7.47 (br m, 12H), 6.89 (br s, 2H), 6.08 (br s, 2H), 3.44 (br m, 2H), 3.17 (br m, 2H), 1.40 (br s, 18H), 1.14 (br s, 18H); Analysis by GPC ($CHCl_3$): *M*n) 7 000, *M*w) 22 000 g/mol relative to polystyrene. BET surface area = 760 m^2/g; total pore volume = 0.59 cm^3/g at (P/P_0) 0.98, adsorption; TGA analysis (nitrogen): 5% loss of weight occurred at ~ 395 °C. Initial weight loss due to thermal degradation commences at ~ 508 °C.

Polymer from 3-(4,4'-di-tert-butyl-9-fluorenyidene)-5,6,5',6'-tetrahydroxy-1,1'-spirobisindane-3'-one (95)

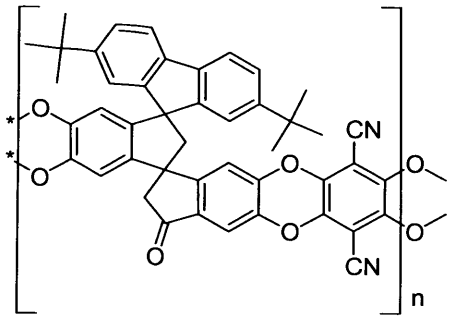

In a two-necked round bottom flask was added under a dry nitrogen atmosphere 3-(4,4'-di-tert-butyl-9-fluorenyidene)-5,6,5',6'-tetrahydroxy-1,1'-spirobisindane-3'-one **65** (560 mg, 1.00 mmol), 2,3,5,6-tetrafluoroterephthalonitrile **28** (200 mg, 1.00 mmol) and dry dimethylformamide (15 ml). This mixture was heated to 65 °C, until complete dissolution of the two starting material was observed, then dry potassium carbonate (1.10 mg, 8.00 mmol) was added and the mixture kept to stirring for 96 h. The solution was quenched with water (100 ml), filtrated and washed repeatedly with water and acetone. The solid was dissolved in $CHCl_3$ (20 ml) and, throughout filtration by cotton wool, poured in a flask containing a mixture of acetone/methanol (2/1, 80 ml). The product was dried under high vacuum overnight to give the final product as yellow solid (545 mg, 81% based on the molecular weight of the repeated unit). IR (nujol): 2958, 1699, 1669, 1602, 1295, 1163, 1088, 872 cm^{-1}; BET surface area = 580 m^2/g; total pore volume = 0.41 cm^3/g at (P/P_0) 0.98, adsorption; TGA analysis (nitrogen): 5% loss of weight occurred at ~ 400 °C. Initial weight loss due to thermal degradation commences at ~ 505 °C.

Polymer from 1,1'-spirobisnaphtalene-4,4'-dione (96)

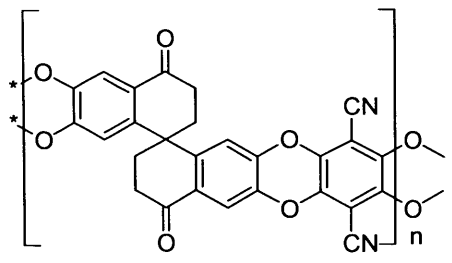

In a two-necked round bottom flask was added under a dry nitrogen atmosphere 6,7,6',7'-tetrahydroxy-tetrahydro-*2H,2H'*-1,1'-spirobisnaphtalene-4,4'-dione **76** (323 mg, 0.95

mmol), and 2,3,5,6-tetrafluoroterephthalonitrile **28** (173 mg, 0.86 mmol), and dry dimethylformamide (15 ml). This mixture was heated to 65 °C, until complete dissolution of the two starting material was observed, then dry potassium carbonate (1.05 g, 7.60 mmol) was added and the mixture kept to stirring for 96 h. The solution was quenched with water (100 ml), filtrated and washed repeatedly with water and acetone. The product was refluxed with methanol (24 h). The purified product was dried under high vacuum overnight to give a yellow solid (326 mg, 74% based on the molecular weight of the repeated unit). IR (nujol): 2855, 2231, 1707, 1600, 1256, 998, 882, 726 cm^{-1}; BET surface area = 713 m^2/g; total pore volume = 0.39 cm^3/g at (P/P_0) 0.98, adsorption; TGA analysis (nitrogen): 5% loss of weight occurred at ~ 380 °C. Initial weight loss due to thermal degradation commences at ~ 445 °C.

Polymer from Tetrahydroxy-4,4'-diphenyl-2H,2H'-1,1'-spirobisnaphthalene (97)

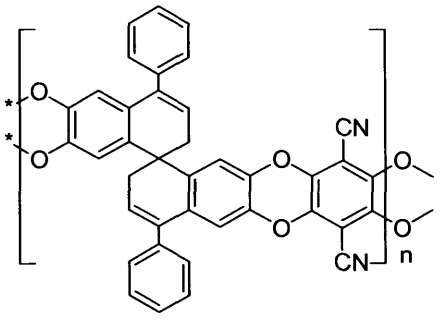

In a two-necked round bottom flask was added under a dry nitrogen atmosphere 6,7,6',7'-tetrahydroxy-4,4'-diphenyl-*2H,2H'*-1,1'-spirobisnaphthalene **78** (425 mg, 0.92 mmol), and 2,3,5,6-tetrafluoroterephthalonitrile **28** (185 mg, 0.92 mmol), and dry dimethylformamide (15 ml). This mixture was heated to 65 °C, until complete dissolution of the two starting material was observed, then dry potassium carbonate (1.01 g, 7.36 mmol) was added and the mixture kept to stirring for 96 h. The solution was quenched with water (100 ml), filtrated and washed repeatedly with water and acetone. The product was refluxed with methanol (24 h). The purified product was dried under high vacuum overnight to give a yellow solid (462 mg, 86% based on the molecular weight of the repeated unit). IR (nujol): 2932, 1596, 1569, 1355, 1256, 1077, 826 cm^{-1}; BET surface area = 203 m^2/g; total pore volume = 0.33 cm^3/g at (P/P_0) 0.98, adsorption; TGA analysis (nitrogen): 5% loss of weight occurred at ~ 390 °C. Initial weight loss due to thermal degradation commences at ~ 466 °C.

Polymer from 6,7,6',7'-tetrahydroxy-4,4,4',4'-tetraphenyll-3,3',4,4'-tetrahydro-2H,2H'-1,1'-spirobisnaphthalene (98)

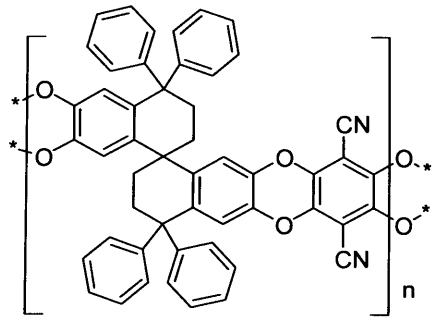

In a two-necked round bottom flask was added under a dry nitrogen atmosphere 6,7,6',7'-tetrahydroxy-4,4,4',4'-tetraphenyll-3,3',4,4'-tetrahydro-2H,2H'-1,1'-spirobisnaphthalene **81** (510 mg, 0.83 mmol), 2,3,5,6-tetrafluoroterephthalonitrile **28** (158 mg, 0.83 mmol) and dry dimethylformamide (15). This mixture was heated to 65 °C, until complete dissolution of the two starting material was observed, then dry potassium carbonate (870 mg, 6.30 mmol) was added and the mixture kept to stirring for 72 h. The solution was quenched with water (100 ml), filtrated and washed repeatedly with water and acetone. The solid was dissolved in THF (20 ml) and, throughout filtration by cotton wool, poured in a flask containing a mixture of acetone/methanol (2/1, 80 ml). The product was dried under high vacuum overnight to give the final product as yellow solid (530 mg, 86% based on the molecular weight of the repeated unit). IR (nujol): 2955, 1607, 1528, 1257, 1029, 945, 883cm^{-1}; ^{1}H NMR (400 MHz; $CDCl_3$) δ 7.34 (br m, 20H), 7.04 (br s, 2H), 6.22 (br s, 2H), 2.63 (br m, 4H), 1.90 (br m, 4H); ^{13}C NMR (100 MHz; $CDCl_3$) δ 148.1, 145.3, 144.9, 129.4, 129.0, 128.9, 128.7, 128.6, 128.3, 128.3, 118.7, 109.0, 94.2, 53.6, 44.5, 44.5, 35.6; Analysis by GPC ($CHCl_3$): *M*n) 18 000, *M*w) 93 000 g/mol relative to polystyrene. BET surface area = 395 m^2/g; total pore volume = 0.44 cm^3/g at (P/P_0) 0.98, adsorption; TGA analysis (nitrogen): 5% loss of weight occurred at ~ 300 °C. Initial weight loss due to thermal degradation commences at ~ 495 °C.

Polymer from 4,4'-bis-(spiro-9-fluorenyidene)-6,7,6',7'-tetramethoxy-tetrahydro-2H,2H'-1,1'-spirobisnaphthalene (99)

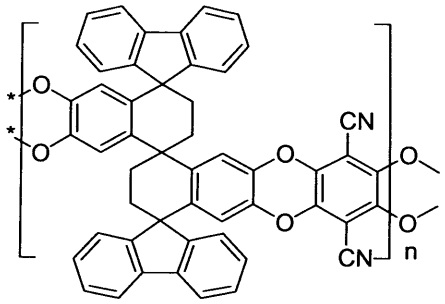

In a two-necked round bottom flask was added under a dry nitrogen atmosphere 4,4'-bis-(spiro-9-fluorenyidene)-6,7,6',7'-tetramethoxy-tetrahydro-2H,2H'-1,1'-spirobisnaphthalene **82** (400 mg, 0.65 mmol), 2,3,5,6-tetrafluoroterephthalonitrile **28** (130 mg, 0.65 mmol) and dry dimethylformamide (10). This mixture was heated to 65 °C, until complete dissolution of the two starting material was observed, then dry potassium carbonate (720 mg, 7.92 mmol) was added and the mixture kept to stirring for 96 h. The solution was quenched with water (100 ml), filtrated and washed repeatedly with water and acetone. The solid was dissolved in $CHCl_3$ (20 ml) and, throughout filtration by cotton wool, poured in a flask containing a mixture of acetone/methanol (2/1, 80 ml). The product was dried under high vacuum overnight to give the final product as yellow solid (390 mg, 82% based on the molecular weight of the repeated unit). IR (nujol): 2930, 2236, 1605, 1293, 1261, 1102, 1158, 879 cm^{-1}; ^{1}H NMR (400 MHz; $CDCl_3$) δ ^{13}C NMR (100 MHz; $CDCl_3$) δ 153.9, 153.8, 153.8, 138.9, 138.5, 138.5, 138.4, 128.0, 127.9, 124.0, 120.4, 117.1, 116.6, 110.3, 109.4, 94.1, 94.1, 54.1, 40.3, 35.0, 34.8, 31.8, 31.8; Analysis by GPC ($CHCl_3$): *M*n) 5 000, *M*w) 26 000 g/mol relative to polystyrene. BET surface area = 590 m^2/g; total pore volume = 0.56 cm^3/g at (P/P_0) 0.98, adsorption; TGA analysis (nitrogen): 5% loss of weight occurred at ~ 400 °C. Initial weight loss due to thermal degradation commences at ~ 495 °C.

Polymer from 4-(spiro-9-fluorenyidene)-6,7,6',7'-tetramethoxy-tetrahydro-2H,2H'-1,1'-spirobisnaphthalene-4'-one(100)

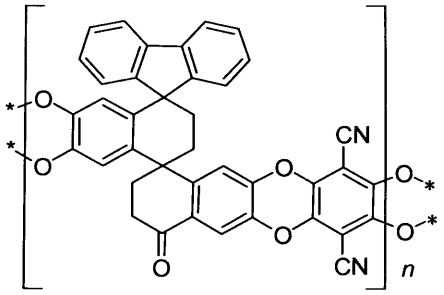

In a two-necked round bottom flask was added under a dry nitrogen atmosphere 4-(spiro-9-fluorenyidene)-6,7,6',7'-tetramethoxy-tetrahydro-2H,2H'-1,1'-spirobisnaphthalene-4'-one **83** (400 mg, 0.83 mmol), 2,3,5,6-tetrafluoroterephthalonitrile **28** (168 mg, 0.83 mmol) and dry dimethylformamide (10). This mixture was heated to 65 °C, until complete dissolution of the two starting material was observed, then dry potassium carbonate (910 mg, 6.64 mmol) was added and the mixture kept to stirring for 96 h. The solution was quenched with water (100 ml), filtrated and washed repeatedly with water and acetone. The solid was put in THF (25 ml), left under stirring (24 h) and filtrated. The product was refluxed with methanol (24 h). The purified product was dried under high vacuum overnight to give a yellow solid (476 mg, 80% based on the molecular weight of the repeated unit). IR (nujol): 2938, 1690, 1656, 1580, 1293, 1163, 886 cm^{-1}; BET surface area = 300 m^2/g; total pore volume = 0.35 cm3/g at (P/P0) 0.98, adsorption; TGA analysis (nitrogen): 5% loss of weight occurred at ~ 380 °C. Initial weight loss due to thermal degradation commences at ~ 486 °C.

Polymer from 4,4,4',4'-tetrahydroxy-3,3',4,4'-tetrahydro-2H,2H'-1,1'-spirobisnaphthalene (101)

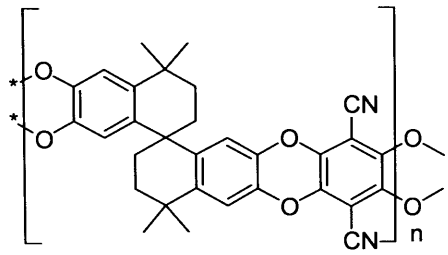

In a two-necked round bottom flask was added under a dry nitrogen atmosphere 5,5',6,6'-tetrahydroxy-2,2',3,3'-tetrahydro-1,1'-spirobisindene **88** (260 mg, 0.91 mmol), 2,3,5,6-tetrafluoroterephthalonitrile **28** (182 mg, 0.91 mmol) and dry dimethylformamide (15 ml).

This mixture was heated to 65 °C, until complete dissolution of the two starting material was observed, then dry potassium carbonate (1.00 g, 7.28 mmol) was added and the mixture kept to stirring for 96 h. The solution was quenched with water (100 ml), filtrated and washed repeatedly with water and acetone. The solid was dissolved in $CHCl_3$ (20 ml) and, throughout filtration by cotton wool, poured in a flask containing a mixture of acetone/methanol (2/1, 80 ml). The product was dried under high vacuum overnight to give the final product as yellow solid (334 mg, 90% based on the molecular weight of the repeated unit). IR (nujol): 2933, 1628, 1500, 1263, 1062, 879, cm^{-1}; ^1H NMR (400 MHz; $CDCl_3$) δ 7.19 (br m, 2H), 6.23 (br s, 2H), 1.92 (br m, 2H), 1.76 (br m, 4H), 1.48 (br m, 2H), 1.25 (br s, 12H; ^{13}C NMR (100 MHz; $CDCl_3$) δ 144.0, 142.6, 138.8, 137.7, 137.2, 117.0, 114.1, 109.6, 93.8, 82.9, 43.6, 33.6, 31.2; Analysis by GPC ($CHCl_3$): *M*n) 7 000, *M*w) 22 000 g/mol relative to polystyrene. BET surface area = 432 m^2/g; total pore volume = 0.33 cm^3/g at (P/P_0) 0.98, adsorption; TGA analysis (nitrogen): 5% loss of weight occurred at ~ 390 °C. Initial weight loss due to thermal degradation commences at ~ 490 °C.

Polymer from bis-1,3-dithiolane of 5,6,5',6'-tetrahydroxy-1,1'-spirobisindane-3,3'-dione (102)

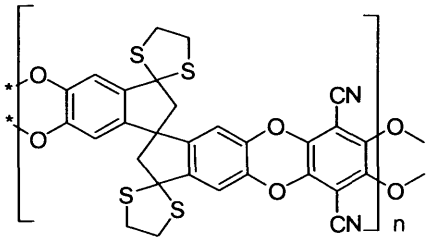

In a two-necked round bottom flask was added under a dry nitrogen atmosphere bis-1,3-dithiolane of 5,6,5',6'-tetrahydroxy-1,1'-spirobisindane-3,3'-dione **69** (900 mg, 1.94 mmol), and 2,3,5,6-tetrafluoroterephthalonitrile **28** (387 mg, 1.94 mmol), and dry dimethylformamide (25 ml). This mixture was heated to 65 °C, until complete dissolution of the two starting material was observed, then dry potassium carbonate (2.14 g, 15.50 mmol) was added and the mixture kept to stirring for 96 h. The solution was quenched with water (100 ml), filtrated and washed repeatedly with water and acetone. The solid was put in THF (25 ml), left under stirring (24 h) and filtrated. The product was refluxed with methanol (24 h). The purified product was dried under high vacuum overnight to give a yellow solid (600 mg, 52% based on the molecular weight of the repeated unit). IR (nujol):

2954, 2232, 1722, 1604, 1270, 1005, 866, 735 cm^{-1}; BET surface area = 205 m^2/g; total pore volume = 0.25 cm^3/g at (P/P_0) 0.98, adsorption; TGA analysis (nitrogen): 19% loss of weight occurred at ~ 321 °C. Initial weight loss due to thermal degradation commences at ~ 507 °C.

Polymer from bis-1,3-dithiane of 5,6,5',6'-tetrahydroxy-1,1'-spirobisindane-3,3'-dione (103)

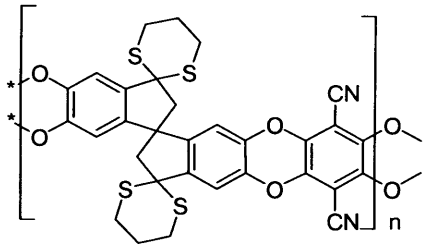

In a two-necked round bottom flask was added under a dry nitrogen atmosphere bis-1,3-dithiane of 5,6,5',6'-tetrahydroxy-1,1'-spirobisindane-3,3'-dione **70** (800 mg, 1.62 mmol), and 2,3,5,6-tetrafluoroterephthalonitrile **28** (320 mg, 1.62 mmol), and dry dimethylformamide (25 ml). This mixture was heated to 65 °C, until complete dissolution of the two starting material was observed, then dry potassium carbonate (1.79 g, 12.96 mmol) was added and the mixture kept to stirring for 96 h. The solution was quenched with water (100 ml), filtrated and washed repeatedly with water and acetone. The solid was put in THF (25 ml), left under stirring (24 h) and filtrated. The product was refluxed with methanol (24 h). The purified product was dried under high vacuum overnight to give a yellow solid (755 mg, 75% based on the molecular weight of the repeated unit). IR (nujol): 2936, 22362, 1728, 1601, 1256, 998, 872 cm^{-1}; BET surface area = 82 m^2/g; total pore volume = 0.08 cm^3/g at (P/P_0) 0.98, adsorption; TGA analysis (nitrogen): 30% loss of weight occurred at ~ 335 °C. Initial weight loss due to thermal degradation commences at ~ 519 °C.

Polymer from 2,2',3,3'-tetrahydroxy-1,1'-spirobisindane (104)

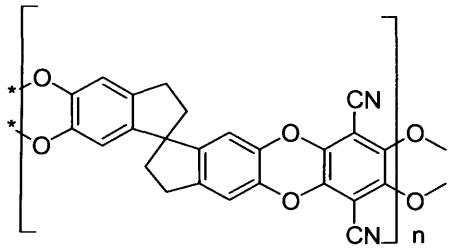

In a two-necked round bottom flask was added under a dry nitrogen atmosphere 5,5',6,6'-tetrahydroxy-2,2',3,3'-tetrahydro-1,1'-spirobisindene **72** (240 mg, 0.84 mmol), 2,3,5,6-tetrafluoroterephthalonitrile **28** (168 mg, 0.84 mmol) and dry dimethylformamide (15 ml). This mixture was heated to 65 °C, until complete dissolution of the two starting material was observed, then dry potassium carbonate (0.92 g, 6.72 mmol) was added and the mixture kept to stirring for 96 h. The solution was quenched with water (100 ml), filtrated and washed repeatedly with water and acetone. The solid was put in THF (25 ml), left under stirring (24 h) and filtrated. The product was refluxed with methanol (24 h). The purified product was dried under high vacuum overnight to give a yellow solid (293 mg, 80% based on the molecular weight of the repeated unit). IR (nujol): 2926, 1599, 1520, 1456, 1346, 1265, 1221, 1140, 1045, 882 cm^{-1}; ^1H NMR (400 MHz; $CDCl_3$) δ 6.60 (br s, 2H), 5.93 (br s, 2H), 2.91 (br m, 4H), 2.29 (br m, 2H), 2.15 (br m, 2H); BET surface area = 108 m^2/g; total pore volume = 0.11 cm^3/g at (P/P_0) 0.98, adsorption; TGA analysis (nitrogen): 5% loss of weight occurred at ~ 330 °C. Initial weight loss due to thermal degradation commences at ~ 442 °C.

Phthalocyanine network (Co) polymer from the bis phthalonitrile derived from 5,6,5',6'-tetrahydroxy-1,1'-spirobisindane-3,3'-dione (108).

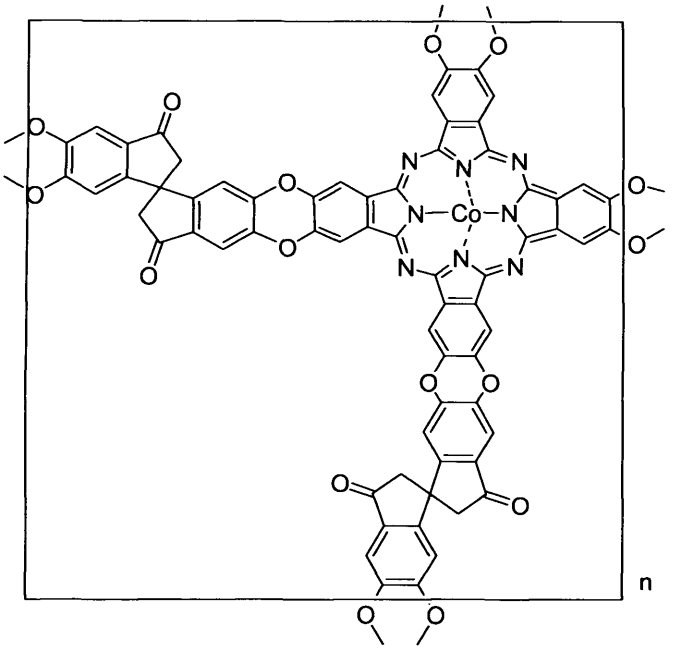

In a two-necked round bottom flask was added under a dry nitrogen atmosphere bis phthalonitrile derived from 5,6,5',6'-tetrahydroxy-1,1'-spirobisindane-3,3'-dione **105** (800 mg, 1.43 mmol), anhydrous Co(II)acetate (130 mg, 0.715) and heated to 100 °C for 15 min. Dry quinoline (4 ml) was added and the temperature increased first to 120 °C (30 min) and then to 165 °C. After 120 min a dark green precipitate began to form. The reaction mixture was left at 165 °C for 24 h, then cooled and the precipitate filtered off. The product was washed with ethanol (2 h), acetone (1 h), methanol (2 h), and acetone (1 h), refluxed with tetrahydrofuran (24 h), refluxed with dichloromethane (24 h), washed with acetone, refluxed with dimethylacetamide (24 h), washed with acetone, refluxed with dimethylformamide (24 h), washed with acetone, and then Soxhlet-extracted with tetrahydrofuran (6 days). The purified product was dried at 127 °C under vacuum (20 h). BET surface area = 284 m^2/g; total pore volume = 0.38 cm^3/g at (P/P_0) 0.98, adsorption; TGA analysis (nitrogen): 5% loss of weight occurred at ~ 390 °C. Initial weight loss due to thermal degradation commences at ~ 482 °C.

Phthalocyanine network (Co) polymer from the bis phthalonitrile derived from bis-1,3-dithiolane of 5,6,5',6'-tetrahydroxy-1,1'-spirobisindane-3,3'-dione (109)

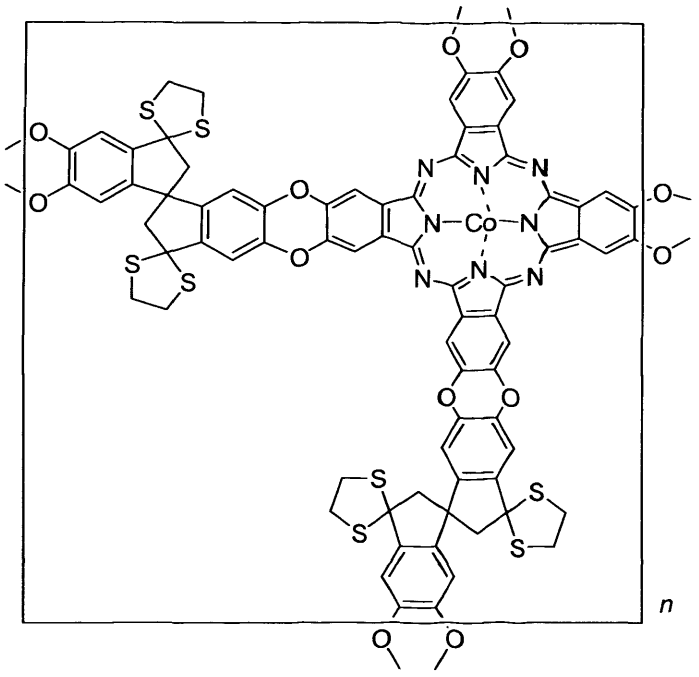

In a two-necked round bottom flask was added under a dry nitrogen atmosphere bis phthalonitrile derived from bis-1,3-dithiolane of 5,6,5',6'-tetrahydroxy-1,1'-spirobisindane-3,3'-dione **106** (900 mg, 1.26 mmol), anhydrous Co(II)acetate (232 mg, 1.26) and heated to 100 °C for 15 min. Dry quinoline (5 ml) was added and the temperature increased first to 120 °C (30 min) and then to 165 °C. After 120 min a dark green precipitate began to form. The reaction mixture was left at 165 °C for 24 h, then cooled and the precipitate filtered off. The product was washed with ethanol (2 h), acetone (1 h), methanol (2 h), and acetone (1 h), refluxed with tetrahydrofuran (24 h), refluxed with dichloromethane (24 h), washed with acetone, refluxed with dimethylacetamide (24 h), washed with acetone, refluxed with dimethylformamide (24 h), washed with acetone, and then Soxhlet-extracted with tetrahydrofuran (6 days). The purified product was dried at 127 °C under vacuum (20 h). TGA analysis (nitrogen): 14% loss of weight occurred at ~ 310 °C. Initial weight loss due to thermal degradation commences at ~ 535 °C.

Bibliography

(1) Zhao, X. S. *J. Mater. Chem.* **2006**, *16*, 623-25.
(2) Sing, K. S. W.; Everett, D. H.; Haul, R. A. W.; Moscou, L.; Pierotti, R. A.; Rouquerol, J.; Siemieniewska, T. *Pure Appl. Chem.* **1985**, *57*, 603-19.
(3) Kuznicki, S. M.; Bell, V. A.; Nair, S.; Hillhouse, H. W.; Jacubinas, R. M.; Braunbarth, C. M.; Toby, B. H.; Tsapatsis, M. *Nature* **2001**, *412*, 720-24.
(4) Wang, D.; Teo, W. K.; Li, K. *Sep. Purif. Technol.* **2004**, *35*, 125-31.
(5) Matson, S. L.; Lee, E. K. L.; Friesen, D. T.; Kelly, D. J.; (Bend Research, Inc., USA). Application: US 1989, p 11 pp Cont -in-part of U S 4,737,166.
(6) Barton, T. J.; Bull, L. M.; Klemperer, W. G.; Loy, D. A.; McEnaney, B.; Misono, M.; Monson, P. A.; Pez, G.; Scherer, G. W.; Vartuli, J. C.; Yaghi, O. M. *Chem. Mater.* **1999**, *11*, 2633-56.
(7) Braunbarth, C.; Hillhouse, H. W.; Nair, S.; Tsapatsis, M.; Burton, A.; Lobo, R. F.; Jacubinas, R. M.; Kuznicki, S. M. *Chem. Mater.* **2000**, *12*, 1857-65.
(8) Brunauer, S.; Emmett, P. H.; Teller, E. *J. Am. Chem. Soc.* **1938**, *60*, 309-19.
(9) Campos, V.; Buchler, P. M. *Environ. Geol.* **2007**, *52*, 1187-92.
(10) Alvarez-Ayuso, E.; Garcia-Sanchez, A.; Querol, X. *Water Res.* **2003**, *37*, 4855-62.
(11) Qiu, W.; Zheng, Y. *J. Hazard. Mater.* **2007**, *148*, 721-26.
(12) Sekhon, B. S.; Sangha, M. K. *Resonance* **2004**, *9*, 35-45.
(13) Usui, K.; Kidena, K.; Murata, S.; Nomura, M.; Trisunaryanti, W. *Fuel* **2004**, *83*, 1899-906.
(14) Velu, S.; Ma, X.; Song, C. *Ind. Eng. Chem. Res.* **2003**, *42*, 5293-304.
(15) Hernandez-Maldonado, A. J.; Yang, R. T. *Angew. Chem., Int. Ed.* **2004**, *43*, 2321.
(16) Tchernev, D. I. *Rev. Mineral. Geochem.* **2001**, *45*, 589-617.
(17) Hyun, S. H.; Song, J. K.; Kwak, B. I.; Kim, J. H.; Hong, S. A. *J. Mater. Sci.* **1999**, *34*, 3095-103.
(18) Jayaraman, A.; Hernandez-Maldonado, A. J.; Yang, R. T.; Chinn, D.; Munson, C. L.; Mohr, D. H. *Chem. Eng. Sci.* **2004**, *59*, 2407-17.
(19) Tomita, T.; Nakayama, K.; Sakai, H. *Micropor. Mesopor. Mater.* **2004**, *68*, 71-75.
(20) Qi, G.; Yang, R. T.; Chang, R.; Cardoso, S.; Smith, R. A. *Appl. Catal., A* **2004**, *275*, 207-12.
(21) Zhan, B.-Z.; Iglesia, E. *Angew. Chem. Int. Ed.* **2007**, *46*, 3697-700.
(22) Bansal, R. C.; Donnet, J. B.; Stoeckli, F. *Active Carbon*, 1988.
(23) Nyazi, K.; Yaacoubi, A.; Bacaoui, A.; Bennouna, C.; Dahbi, A.; Rivera-Utrilla, J.; Moreno-Castilla, C. *J. Phys. IV* **2005**, *123*, 121-24.
(24) Osmond, N. M. *Adsorpt. Sci. Technol.* **2000**, *18*, 529-39.
(25) Su, C.-I.; Yeh, R.-S.; Wang, C.-L. *Text. Res. J.* **2004**, *74*, 966-69.
(26) Cheremisinoff, P. N.; Morresi, A. C. *Carbon Adsorption Handb.* **1978**, 1-53.
(27) Kalpakli, Y. K.; Koyuncu, I. *Ann. Chim.* **2007**, *97*, 1291-302.
(28) Areerachakul, N.; Vigneswaran, S.; Ngo, H. H.; Kandasamy, J. *Sep. Purif. Technol.* **2007**, *55*, 206-11.
(29) Oterhals, A.; Solvang, M.; Nortvedt, R.; Berntssen, M. H. G. *Eur. J. Lipid Sci. Technol.* **2007**, *109*, 691-705.

(30) Lopez, F.; Medina, F.; Prodanov, M.; Guell, C. *J. Colloid Interface Sci.* **2003**, *257*, 173-78.
(31) Tanaka, K.; Yamaguchi, M. *Adv. Compos. Mater.* **1995**, *4*, 309-26.
(32) Patrick, J. W.; Walker, A. *Porosity Carbons* **1995**, 195-208.
(33) Lennon, D.; Lundie, D. T.; Jackson, S. D.; Kelly, G. J.; Parker, S. F. *Langmuir* **2002**, *18*, 4667-73.
(34) Mangun, C. L.; Yue, Z.; Economy, J.; Maloney, S.; Kemme, P.; Cropek, D. *Chem. Mater.* **2001**, *13*, 2356-60.
(35) Germain, J.; Hradil, J.; Frechet, J. M. J.; Svec, F. *Chem. Mater.* **2006**, *18*, 4430-35.
(36) Lee, J.-Y.; Wood, C. D.; Bradshaw, D.; Rosseinsky, M. J.; Cooper, A. I. *Chem. Commun.* **2006**, 2670-72.
(37) Beth, M.; Unger, K. K.; Tsyurupa, M. P.; Davankov, V. A. *Chromatographia* **1993**, *36*, 351-5.
(38) Tsyurupa, M. P.; Davankov, V. A. *React. Funct. Polym.* **2006**, *66*, 768-79.
(39) Ahn, J.-H.; Jang, J.-E.; Oh, C.-G.; Ihm, S.-K.; Cortez, J.; Sherrington, D. C. *Macromolecules* **2006**, *39*, 627-32.
(40) Urban, C.; McCord, E. F.; Webster, O. W.; Abrams, L.; Long, H. W.; Gaede, H.; Tang, P.; Pines, A. *Chem. Mater.* **1995**, *7*, 1325-32.
(41) Webster, O. W.; Gentry, F. P.; Farlee, R. D.; Smart, B. E. *Polym. Prepr. (Am. Chem. Soc., Div. Polym. Chem.)* **1991**, *32*, 412-13.
(42) Webster, O. W.; Gentry, F. P.; Farlee, R. D.; Smart, B. E. *Makromol. Chem., Macromol. Symp.* **1992**, *54/55*, 477-82.
(43) Sawaki, T.; Aoyama, Y. *J. Am. Chem. Soc.* **1999**, *121*, 4793-98.
(44) Husing, N.; Schubert, U. *Angew. Chem., Int. Ed.* **1998**, *37*, 22-45.
(45) Sawaki, T.; Dewa, T.; Aoyama, Y. *J. Am. Chem. Soc.* **1998**, *120*, 8539-40.
(46) Endo, K.; Sawaki, T.; Koyanagi, M.; Kobayashi, K.; Masuda, H.; Aoyama, Y. *J. Am. Chem. Soc.* **1995**, *117*, 8341-52.
(47) Kobayashi, S.; Komiyama, S.; Ishitani, H. *Angew. Chem., Int. Ed.* **1998**, *37*, 979-81.
(48) Shea, K. J.; Loy, D. A.; Webster, O. *J. Am. Chem. Soc.* **1992**, *114*, 6700-10.
(49) Lindner, E.; Kemmler, M.; Mayer, H. A.; Wegner, P. *J. Am. Chem. Soc.* **1994**, *116*, 348-61.
(50) Schubert, U.; Huesing, N.; Lorenz, A. *Chem. Mater.* **1995**, *7*, 2010-27.
(51) Battioni, P.; Cardin, E.; Louloudi, M.; Schollhorn, B.; Spyroulias, G. A.; Mansuy, D.; Traylor, T. G. *Chem. Commun.* **1996**, 2037-38.
(52) Kadish, K. M.; Han, B. C.; Franzen, M. M.; Araullo-McAdams, C. *J. Am. Chem. Soc.* **1990**, *112*, 8364-8.
(53) Traylor, T. G.; Byun, Y. S.; Traylor, P. S.; Battioni, P.; Mansuy, D. *J. Am. Chem. Soc.* **1991**, *113*, 7821-3.
(54) Wilkes, G. L.; Huang, H. H.; Glaser, R. H. *Adv. Chem. Ser.* **1990**, *224*, 207-26.
(55) Ziegler, J. M.; Fearon, F. W. G. *Adv. Chem. Ser.,American Chemical Society, Washington, D.C.* **1990**, *224*, 207.
(56) Yaghi, O. M.; Li, H.; Davis, C.; Richardson, D.; Groy, T. L. *Acc. Chem. Res.* **1998**, *31*, 474-84.
(57) Kepert, C. J.; Rosseinsky, M. J. *Chem. Commun.* **1999**, 375-76.
(58) O'Keeffe, M.; Stuart, J. A. *Inorg. Chem.* **1983**, *22*, 177-9.
(59) Li, H.; Eddaoudi, M.; Groy, T. L.; Yaghi, O. M. *J. Am. Chem. Soc.* **1998**, *120*, 8571-72.
(60) Yaghi, O. M.; O'Keeffe, M.; Ockwig, N. W.; Chae, H. K.; Eddaoudi, M.;

Kim, J. *Nature* **2003**, *423*, 705-14.
(61) Gregg, S. J.; Sing, K. S. W. *Adsorption, Surface Area and Porosity. 2nd Ed*, 1982.
(62) Kitaura, R.; Fujimoto, K.; Noro, S.-i.; Kondo, M.; Kitagawa, S. *Angew. Chem., Int. Ed.* **2002**, *41*, 133-35.
(63) Millange, F.; Serre, C.; Ferey, G. *Chem. Commun.* **2002**, 822-23.
(64) Davis, M. E. *Nature* **2002**, *417*, 813-21.
(65) Cote, A. P.; Benin, A. I.; Ockwig, N. W.; O'Keeffe, M.; Matzger, A. J.; Yaghi, O. M. *Science* **2005**, *310*, 1166-70.
(66) Brock, C. P.; Minton, R. P.; Niedenzu, K. *Acta Crystallogr., Sect. C: Cryst. Struct. Commun.* **1987**, *C43*, 1775-9.
(67) Zettler, F.; Hausen, H. D.; Hess, H. *Acta Crystallogr., Sect. B* **1974**, *30, Pt. 7*, 1876-8.
(68) Denoyel, R.; Rouquerol, F. *Handb. Porous Solids* **2002**, *1*, 276-308.
(69) McKeown, N. B.; Makhseed, S.; Budd, P. M. *Chem. Commun.* **2002**, 2780-81.
(70) McKeown, N. B.; Budd, P. M.; Msayib, K. J.; Ghanem, B. S.; Kingston, H. J.; Tattershall, C. E.; Makhseed, S.; Reynolds, K. J.; Fritsch, D. *Chem.-Eur. J.* **2005**, *11*, 2610-20.
(71) McKeown, N. B. *Phthalocyanine Materials: Structure, Synthesis and Function*, 1998.
(72) McKeown, N. B. *J. Mater. Chem.* **2000**, *10*, 1979-95.
(73) McKeown, N. B.; Hanif, S.; Msayib, K.; Tattershall, C. E.; Budd, P. M. *Chem. Commun.* **2002**, 2782-83.
(74) Meunier, B. *Chem. Rev.* **1992**, *92*, 1411-56.
(75) McKeown, N. B.; Gahnem, B.; Msayib, K. J.; Budd, P. M.; Tattershall, C. E.; Mahmood, K.; Tan, S.; Book, D.; Langmi, H. W.; Walton, A. *Angew. Chem., Int. Ed.* **2006**, *45*, 1804-07.
(76) Budd, P. M.; Elabas, E. S.; Ghanem, B. S.; Makhseed, S.; McKeown, N. B.; Msayib, K. J.; Tattershall, C. E.; Wang, D. *Adv. Mater.* **2004**, *16*, 456-59.
(77) Skujins, S.; Webb, G. A. *Tetrahedron* **1969**, *25*, 3935-45.
(78) Kestemont, G.; de Halleux, V.; Lehmann, M.; Ivanov, D. A.; Watson, M.; Geerts, Y. H. *Chem. Commun.* **2001**, 2074-75.
(79) Budd, P. M.; Ghanem, B.; Msayib, K.; McKeown, N. B.; Tattershall, C. *J. Mater. Chem.* **2003**, *13*, 2721-26.
(80) Lindsey, A. S. *J. Chem. Soc.* **1965**, 1685-92.
(81) Budd, P. M.; Ghanem, B. S.; Makhseed, S.; McKeown, N. B.; Msayib, K. J.; Tattershall, C. E. *Chem. Commun.* **2004**, 230-31.
(82) Wolf, R.; Marvel, C. S. *J. Polym. Sci., Part A-1: Polym. Chem.* **1969**, *7*, 2481- 91.
(83) Cordes, A. W.; Fair, C. K. *Acta Crystallogr., Sect. B* **1974**, *30, Pt. 6*, 1621-3.
(84) Horvath, G.; Kawazoe, K. *J. Chem. Eng. Jpn.* **1983**, *16*, 470-5.
(85) Ghanem, B. S.; McKeown, N. B.; Budd, P. M.; Fritsch, D. *Macromolecules* **2008**, *41*, 1640-46.
(86) Baker, W.; McGowan, J. C. *J. Chem. Soc.* **1943**, 486-7.
(87) Jacob, P., III; Callery, P. S.; Shulgin, A. T.; Castagnoli, N., Jr. *J. Org. Chem.* **1976**, *41*, 3627-9.
(88) Baker, W. *J. Chem. Soc.* **1934**, 1678.
(89) Baker, W.; Williams, H. L. *J. Chem. Soc.* **1959**, 1295.
(90) Korgaonkar, U. V.; Samant, S. D.; Deodhar, K. D.; Kulkarni, R. A. *Indian J. Chem., Sect. B* **1981**, *20B*, 572-4.

(91) Schneider, M. R.; Ball, H. *J. Med. Chem.* **1986**, *29*, 75-9.
(92) Koo, J. *J. Am. Chem. Soc.* **1953**, *75*, 1891-5.
(93) Gilmore, R. C., Jr. *J. Am. Chem. Soc.* **1951**, *73*, 5879-80.
(94) Maslak, P.; Varadarajan, S.; Burkey, J. D. *J. Org. Chem.* **1999**, *64*, 8201-09.
(95) Eaton, P. E.; Mueller, R. H.; Carlson, G. R.; Cullison, D. A.; Cooper, G. F.; Chou, T.-C.; Krebs, E. P. *J. Am. Chem. Soc.* **1977**, *99*, 2751-67.
(96) Eaton, P. E.; Carlson, G. R.; Lee, J. T. *J. Org. Chem.* **1973**, *38*, 4071-3.
(97) Davis, B. R.; Hinds, M. G.; Johnson, S. J. *Aust. J. Chem.* **1985**, *38*, 1815-25.
(98) Hao, X.-j.; Node, M.; Fuji, K. *J. Chem. Soc., Perkin Trans. 1* **1992**, 1505-9.
(99) McOmie, J. F. W.; Watts, M. L.; West, D. E. *Tetrahedron* **1968**, *24*, 2289-92.
(100) Vickery, E. H.; Pahler, L. F.; Eisenbraun, E. J. *J. Org. Chem.* **1979**, *44*, 4444-6.
(101) Katritzky, A. R.; Zhang, G.; Xie, L. *Synth. Commun.* **1997**, *27*, 2467-78.
(102) Lantano, B.; Aguirre, J. M.; Finkielsztein, L.; Alesso, E. N.; Brunet, E.; Moltrasio, G. Y. *Synth. Commun.* **2004**, *34*, 625-41.
(103) Bachmann, W. E.; Horton, W. J. *J. Am. Chem. Soc.* **1947**, *69*, 58-61.
(104) Grove, D. D.; Corte, J. R.; Spencer, R. P.; Pauly, M. E.; Rath, N. P. *J. Chem. Soc., Chem. Commun.* **1994**, 49-50.
(105) Gilmore, R. C., Jr.; Horton, W. J. *J. Am. Chem. Soc.* **1951**, *73*, 1411.
(106) Snyder, H. R.; Werber, F. X. *J. Am. Chem. Soc.* **1950**, *72*, 2965-7.
(107) Yu, H.; Kim, I. J.; Folk, J. E.; Tian, X.; Rothman, R. B.; Baumann, M. H.; Dersch, C. M.; Flippen-Anderson, J. L.; Parrish, D.; Jacobson, A. E.; Rice, K. C. *J. Med. Chem.* **2004**, *47*, 2624.
(108) McDonald, E.; Smith, P. *J. Chem. Soc., Perkin Trans. 1* **1980**, 837-42.
(109) Angle, S. R.; Arnaiz, D. O. *J. Org. Chem.* **1992**, *57*, 5937-47.
(110) Wong, K.-T.; Wang, Z.-J.; Chien, Y.-Y.; Wang, C.-L. *Org. Lett.* **2001**, *3*, 2285-88.
(111) McEwen, W. E.; Hernandez, M. A.; Ling, C.; Marmu, E.; Padronaggio, R. M.; Zepp, C. M.; Lubinkowski, J. J. *J. Org. Chem.* **1981**, *46*, 1656.
(112) Ego, C.; Grimsdale, A. C.; Uckert, F.; Yu, G.; Srdanov, G.; Müllen, C. *Adv. Mater* **2002**, *14*, 509.
(113) Lambert, J. B.; Larson, E. G.; Bosch, R. J.; TeVrucht, M. L. E. *J. Am. Chem. Soc.* **1985**, *107*, 5443.
(114) Mandeville, W. H.; Whitesides, G. M. *J. Org. Chem.* **1986**, *51*, 3257.
(115) Langer, P.; Schroeder, R. *Eur. J. Org. Chem.* **2004**, 1025.
(116) Pei, J.; Ni, J.; Zhou, X.-H.; Cao, X.-Y.; Lai, Y.-H. *J. Org. Chem.* **2002**, *67*, 4924-36.
(117) Debroy, P.; Shukla, R.; Lindeman, S. V.; Rathore, R. *J. Org. Chem.* **2007**, *72*, 1765-69.
(118) Krasovskiy, A.; Knochel, P. *Angew. Chem., Int. Ed.* **2004**, *43*, 3333-36.
(119) Kimura, M.; Kuwano, S.; Sawaki, Y.; Fujikawa, H.; Noda, K.; Taga, Y.; Takagi, K. *J. Mater. Chem.* **2005**, *15*, 2393-98.
(120) Tashiro, M.; Yamato, T. *J. Org. Chem.* **1979**, *44*, 3037-41.
(121) Leinweber, D.; Weidner, I.; Wilhelm, R.; Wartchow, R.; Butenschoen, H. *Eur. J. Org. Chem.* **2005**, 5224-35.
(122) Dunn, J. P.; Green, D. M.; Nelson, P. H.; Rooks, W. H., II; Tomolonis, A.; Untch, K. G. *J. Med. Chem.* **1977**, *20*, 1557-62.
(123) Barbasiewicz, M.; Makosza, M. *Org. Lett.* **2006**, *8*, 3745-48.
(124) Kelsey, D. R.; Robeson, L. M.; Clendinning, R. A.; Blackwell, C. S. *Macromolecules* **1987**, *20*, 1204-12.
(125) Li, T.-S.; Li, L.-J.; Lu, B.; Yang, F. *J. Chem. Soc., Perkin Trans. 1* **1998**,

3561-64.
(126) Colquhoun, H. M.; Paoloni, F. P. V.; Drew, M. G. B.; Hodge, P. *Chem. Commun.* **2007**, 3365-67.
(127) Oishi, T.; Takechi, H.; Kamemoto, K.; Ban, Y. *Tetrahedron Lett.* **1974**, 11-14.
(128) Corey, E. J.; Chaykovsky, M. *J. Am. Chem. Soc.* **1965**, *87*, 1353-64.
(129) Srikrishna, A.; Rao, M. S. *Eur. J. Org. Chem.* **2004**, 499-503.
(130) Srikrishna, A.; Ravikumar, P. C. *Tetrahedron* **2006**, *62*, 9393-402.
(131) Yonezawa, N.; Hino, T.; Matsuda, K.; Matsuki, T.; Narushima, D.; Kobayashi, M.; Ikeda, T. *J. Org. Chem.* **2000**, *65*, 941-44.
(132) Kelly, T. R.; Ghoshal, M. *J. Am. Chem. Soc.* **1985**, *107*, 3879-84.
(133) McGarry, L. W.; Detty, M. R. *J. Org. Chem.* **1990**, *55*, 4349-56.
(134) Cushman, M.; Mohan, P. *J. Med. Chem.* **1985**, *28*, 1031-6.
(135) Edstrom, E.; Livinghouse, T. *J. Am. Chem. Soc.* **1986**, *108*, 1334-6.
(136) Marson, C. M.; Harper, S.; Walker, A. J.; Pickering, J.; Campbell, J.; Wrigglesworth, R.; Edge, S. J. *Tetrahedron* **1993**, *49*, 10339-54.
(137) Kuehne, M. E.; Bornmann, W. G.; Parsons, W. H.; Spitzer, T. D.; Blount, J. F.; Zubieta, J. *J. Org. Chem.* **1988**, *53*, 3439-50.
(138) Su, J.; Wulff, W. D.; Ball, R. G. *J. Org. Chem.* **1998**, *63*, 8440-47.
(139) Bjork, J. A.; Brostrom, M. L.; Whitcomb, D. R. *J. Chem. Crystallogr.* **1997**, *27*, 223-30.
(140) Olah, G. A.; Narang, S. C.; Salem, G. F. *Synthesis* **1980**, 657.
(141) Cossy, J. *Synthesis* **1987**, 1113-15.
(142) Olah, G. A.; Mehrotra, A. K.; Narang, S. C. *Synthesis* **1982**, 151-2.
(143) Krishnaveni, N. S.; Surendra, K.; Nageswar, Y. V. D.; Rao, K. R. *Synthesis* **2003**, 2295-97.
(144) Bandgar, B. P.; Kasture, S. P. *Green Chem.* **2000**, *2*, 154-56.
(145) Maffei, A. V.; Budd, P. M.; McKeown, N. B. *Langmuir* **2006**, *22*, 4225-29.
(146) Reyes-Labarta, J. A.; Olaya, M. M.; Marcilla, A. *Polymer* **2006**, *47*, 8194-202.
(147) Duann, Y.-F.; Liu, T.-M.; Cheng, K.-C.; Su, W. F. *Polym. Degrad. Stab.* **2004**, *84*, 305-10.
(148) McCoy, B. J. *Chem. Eng. Sci.* **2001**, *56*, 1525-29.
(149) Chodkiewicz, W.; Cadiot, P.; Willemart, A. *Bull. Soc. Chim. Fr.* **1958**, 1591-3.
(150) Marin, G.; Chodkiewicz, W.; Cadiot, P.; Willemart, A. *Bull. Soc. Chim. Fr.* **1958**, 1594-7.
(151) Friedrich, L. E.; De Vera, N.; Hamilton, M. *Synth. Commun.* **1980**, *10*, 637-43.
(152) Meyer, K. H.; Schuster, K. *Ber. Dtsch. Chem. Ges. B* **1922**, *55B*, 819-23.
(153) Lincke, J.; Carta, M.; McKeown, N. B. *unpublished result* **2008**.

Appendix A

ORGANIC LETTERS

2008
Vol. 10, No. 13
2641–2643

Novel Spirobisindanes for Use as Precursors to Polymers of Intrinsic Microporosity

Mariolino Carta,[†] Kadhum J. Msayib,[†] Peter M. Budd,[‡] and Neil B. McKeown*[,†]

School of Chemistry, Cardiff University, Cardiff CF10 3AT, U.K., and School of Chemistry, University of Manchester, Manchester M13 9PL, U.K.

mckeownnb@cardiff.ac.uk

Received March 15, 2008

ABSTRACT

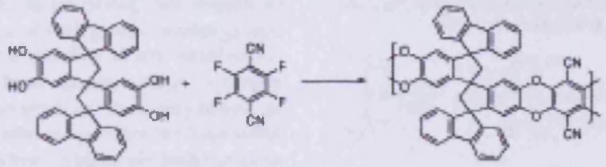

The synthesis of novel spirobisindane-based monomers for the preparation of polymers of intrinsic microporosity (PIMs) with bulky, rigid substituents is described. Polymers derived from monomers containing spiro-linked fluorene substituents display enhanced solubility and microporosity due to additional frustration of packing in the solid state.

Microporous materials derived from organic precursors are of increasing interest and several distinct aproaches have been adopted to achieve their preparation.[1−5] Over the past few years, we have developed a class of organic microporous material termed Polymers of Intrinsic Microporosity (PIMs). PIMs are materials which combine the high internal surface area of conventional microporous materials, such as zeolites or activated carbons, with the processability of polymers.[6−9] They have potential applications as heterogeneous catalysts,[10,11] hydrogen storage materials[12−15] and as polymer membranes,[16] especially for the separation of gases.[17] The microporosity of PIMs is due to their rigid and contorted macromolecular structures which cannot fill space efficiently, leaving molecular-sized interconnected voids. The rigidity is enforced by the polymer being composed of fused rings

[†] Cardiff University.
[‡] University of Manchester.

(1) Nagai, K.; Masuda, T.; Nakagawa, T.; Freeman, B. D.; Pinnau, I. *Prog. Polym. Sci.* **2001**, *26*, 721.
(2) Webster, O. W.; Century, F. P.; Farlee, R. D.; Smart, B. E. *Makromol. Chem., Macromol. Symp.* **1992**, *54/55*, 477.
(3) Tsyurupa, M. P.; Davankov, V. A. *React. Funct. Polym.* **2002**, *53*, 193.
(4) Cote, A. P.; Benin, A. I.; Ockwig, N. W.; O'Keeffe, M.; Matzger, A. J.; Yaghi, O. M. *Science* **2005**, *310*, 1166.
(5) Jiang, J. X.; Su, F.; Trewin, A.; Wood, C. D.; Campbell, N. L.; Niu, H.; Dickinson, C.; Ganin, A. Y.; Rosseinsky, M. J.; Khimyak, Y. Z.; Cooper, A. I. *Angew. Chem., Int. Ed.* **2007**, *46*, 8574.
(6) Budd, P. M.; Ghanem, B. S.; Makhseed, S.; McKeown, N. B.; Msayib, K. J.; Tattershall, C. E. *Chem. Commun.* **2004**, 230.
(7) Budd, P. M.; McKeown, N. B.; Fritsch, D. *J. Mater. Chem.* **2005**, *15*, 1977.
(8) McKeown, N. B.; Budd, P. M.; Msayib, K. J.; Ghanem, B. S.; Kingston, H. J.; Tattershall, C. E.; Makhseed, S.; Reynolds, K. J.; Fritsch, D. *Chem. Eur. J.* **2005**, *11*, 2610.
(9) McKeown, N. B.; Budd, P. M. *Chem. Soc. Rev.* **2006**, *35*, 675.
(10) MacKenzie, H.; Budd, P. M.; McKeown, N. B. *J. Mater. Chem.* **2008**, *18*, 573.
(11) Budd, P. M.; Ghanem, B.; Msayib, K.; McKeown, N. B.; Tattershall, C. *J. Mater. Chem.* **2003**, *13*, 2721.
(12) McKeown, N. B.; Ghanem, B.; Msayib, K. J.; Budd, P. M.; Tattershall, C. E.; Mahmood, K.; Tan, S.; Book, D.; Langmi, H. W.; Walton, A. *Angew. Chem., Int. Ed.* **2006**, *45*, 1804.
(13) Budd, P. M.; Butler, A.; Selbie, J.; Mahmood, K.; McKeown, N. B.; Ghanem, B.; Msayib, K.; Book, D.; Walton, A. *PCCP* **2007**, *9*, 1802.
(14) Ghanem, B.; McKeown, N. B.; Hardy, K. D. M.; Pan, Z.; Budd, P. M.; Butler, A.; Selbie, J.; Book, D.; Walton, A. *Chem. Commun.* **2007**, 67.
(15) McKeown, N. B.; Budd, P. M.; Book, D. *Macromol. Rapid Commun.* **2007**, *28*, 995.
(16) Budd, P. M.; Elabas, E. S.; Ghanem, B. S.; Makhseed, S.; McKeown, N. B.; Msayib, K. J.; Tattershall, C. E.; Wang, D. *Adv. Mater.* **2004**, *16*, 456.
(17) Budd, P. M.; Msayib, K. J.; Tattershall, C. E.; Ghanem, B. S.; Reynolds, K. J.; McKeown, N. B.; Fritsch, D. *J. Membr. Sci.* **2005**, *251*, 263.

10.1021/ol800673m CCC: $40.75
Published on Web 06/03/2008

and the nonlinear structure arises from the incorporation of 'sites of contortion' such as spiro-centers. One of the most useful spiro-containing monomers, 5,5′,6,6′-tetrahydroxy-3,3,3′,3′-tetramethyl-1,1′-spiro-bisindane 1, is readily prepared by the acid-mediated reaction between catechol and acetone and is commercially available.[18–20] For example, 1 reacts with 2,3,5,6-tetrafluoroterephthalonitrile 2 to give PIM-1 (Scheme 1), which is the archetypal and most studied PIM.[6] This polymerization reaction produces fused dioxan rings as linking groups via highly efficient aromatic nucleophilic substitution.

Scheme 1. Synthesis of PIM-1

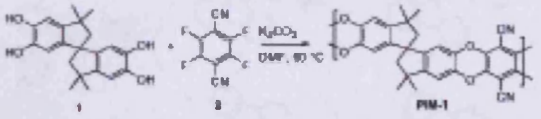

In order to gain insight into the effect of the macromolecular structure on the degree of microporosity, we desired a range of PIM-1 analogues in which bulky, rigid groups are attached to the polymer. In particular, we wished to determine whether the addition of such groups creates greater microporosity due to further frustration of macromolecular packing or, alternatively, reduces microporosity by simply filling space. In order that the steric or electronic effects of the new substituents do not adversely effect the successful polymerization reaction, it is best to place the bulky groups (e.g., phenyl or spirofluorenes) at the 3,3′-positions of the 1,1′-spiro-bisindane units in place of the methyl groups of PIM-1. Hence, novel monomers based on 5,5′,6,6′-tetrahydroxy-1,1′-spirobisindane are required. These monomers may also be of interest for the other established applications of spirobisindane 1, such as being precursors to self-assembled cyclic structures,[21–23] as chiral ligands,[24–27] as model systems to investigate spiro-conjugation[28,29] and as HIV-1 integrase inhibitors.[30]

The remarkably simple synthesis of monomer 1, in which two catechol and three acetone molecules are assembled in a straightforward, one-pot reaction, was first reported by Baker in 1934.[19] Simple adaptations of this procedure (e.g., using a mixture of catechol, acetone and a ketone containing bulky aryl groups) are unlikely to succeed due to the preference for acetone toward acid-mediated self-condensation to give phorone, which is a suspected intermediate in the formation of 1.[19,20] Instead, we decided to explore the potential of using the addition of an aryl Grignard reagent to the known 5,5′,6,6′-tetramethoxy-spiro(bisindane)-3,3′-dione 3 for the introduction of bulky groups. Baker prepared 3 in five steps with the last step being an inefficient oxidation of 5,5′,6,6′-tetramethoxy-spiro(bisindane) using chromium trioxide.[21] As a more satisfactory alternative, we found that the dione 3 is prepared from diethyl 1,3-acetonedicarboxylate in three steps (Scheme 2), with 35% overall yield, by acid-mediated reaction with veratrole,[32] followed by simple hydrolysis and a double intramolecular Friedel-Craft acylation mediated by PPA. Phenyl magnesium bromide added smoothly to 3 to give the dehydrated bisindene 4 after acidic workup. Monomers 5 and 6 are readily prepared from 3 and 4, respectively by treatment with BBr_3.

Scheme 2. Improved Synthesis of the Pivotal Intermediate 5,5′,6,6′-Tetramethoxytetraphenyl-1,1-spiro-bisindane-3,3-dione 3 and Tetrahydroxy Monomers 5 and 6

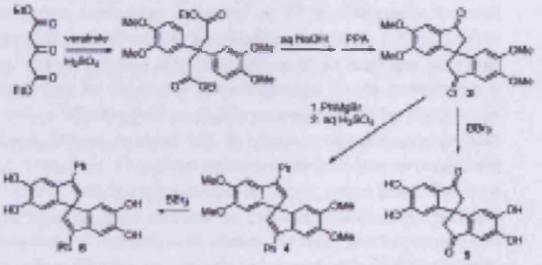

Monomer 7 which contains two spiro-fused bisfluorenes is an attractive target to demonstrate any potential benefits of large, rigid substituents on polymer microporosity. Its synthesis was achieved by adaptation of the established method of preparing spiro-bis(fluorene)s by the addition of 2-biphenyl Grignard reagent to fluorenones and subsequent formation of the spiro-center by an intermolecular Friedel-Craft alkylation.[33,34] Addition of excess 2-biphenyl magnesium bromide to 3 proceeds slowly even under rigorous conditions and a complex mixture of products is obtained following conventional aqueous workup. However, treatment of the crude mixture with Eaton's reagent gave a reasonable yield of the desired precursor 8 (40%) together with the monoadduct 9 (50%), which could be recycled to provide

(18) Björk, J. A.; Broström, M. L.; Whitcomb, D. R. *J. Chem. Crystallogr.* **1997**, *27*, 223.
(19) Baker, W. *J. Chem. Soc.* **1934**, 1678.
(20) Baker, W.; McOmie, J. C. *J. Chem. Soc.* **1938**, 347.
(21) Abrahams, B. F.; Price, D. J.; Robson, R. *Angew. Chem., Int. Ed.* **2006**, *45*, 806.
(22) McCord, D. J.; Small, J. H.; Greaves, J.; Van, Q. N.; Shukla, A. J.; Fleischer, E. B.; Shea, K. J. *J. Am. Chem. Soc.* **1998**, *120*, 9763.
(23) Pak, J. J.; Greaves, J.; McCord, D. J.; Shea, K. J. *Organometallics* **2002**, *21*, 3552.
(24) Brewster, J. H.; Prudence, R. T. *J. Am. Chem. Soc.* **1973**, *95*, 1217.
(25) Hill, R. K.; Cullison, D. A. *J. Am. Chem. Soc.* **1973**, *95*, 1229.
(26) Zhang, W. C.; Wu, S. L.; Zhang, Z. G.; Yeamwar, H. M.; Zhang, X. M. *Org. Biomol. Chem.* **2006**, *4*, 4474.
(27) Bilman, V. B.; Rheingold, A. L.; Lam, K. C. *Tetrahedron: Asymmetry.* **1999**, *10*, 125.
(28) Shiga, K.; Kurkani, H.; Kato, A.; Imajo, S. *Tetrahedron Lett.* **1980**, *21*, 3997.
(29) Mastak, P. *Adv. Mater.* **1994**, *6*, 405.
(30) Molteni, V.; Rhodes, D.; Rubins, K.; Hansen, M.; Bushman, F. D.; Siegel, J. S. *J. Med. Chem.* **2000**, *43*, 2031.

(31) Baker, W.; Williams, H. L. *J. Chem. Soc.* **1959**, 1295.
(32) Korgaonkar, U. V.; Sumat, S. D.; Deodhar, K. D.; Kulami, R. A. *Indian J. Chem., Sect B* **1981**, *20*, 572.
(33) Clarkson, R. G.; Gomberg, M. *J. Am. Chem. Soc.* **1930**, *52*, 2881.
(34) Kimura, M.; Kuwano, S.; Sawaki, Y.; Fujikawa, H.; Noda, K.; Taga, Y.; Takagi, K. *J. Mater. Chem.* **2005**, *15*, 2393.

further batches of 8. The complex mixture obtained from initial Grignard addition clearly contained a significant amount of the desired carbinol intermediate. On demethylation with BBr_3, 8 and 9 provide the desired monomer 7 and the unsymmetrical monomer 10, respectively (Scheme 3).

Scheme 3. Synthesis of Spiro-Fused Fluorene-Based Monomers

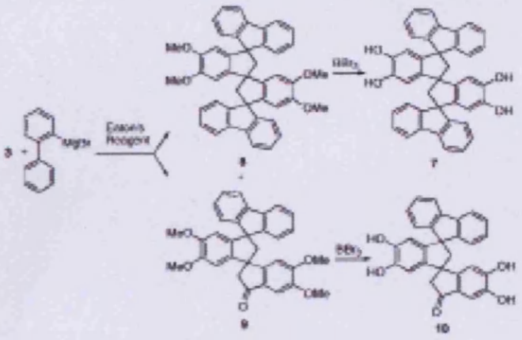

Polymers derived from the novel monomers 5, 6, 7 and 10 were prepared by copolymerization with monomer 2 using the condition previously optimized for the synthesis of PIM-1. The properties of these polymers are given in Table 1.

Table 1. Properties of the Novel PIMs

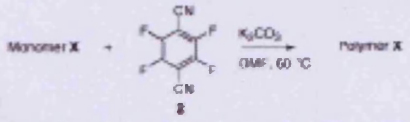

polymer X (monomer X)	$M_w \times 10^3$ (g mol^{-1})	solubility	surface area (m^2 g^{-1})
PIM-1 (1)	180[a]	THF, $CHCl_3$	780
polymer 5(5)	*b*	cH_2SO_4	501
polymer 6(6)	*b*	quinoline	560
polymer 7(7)	75[a]	THF, $CHCl_3$	895
polymer 10(10)	*b*	NMP, quinoline	656

[a] Relative to polystyrene standards. [b] Not soluble in a solvent compatible with gel permeation chromatography (GPC).

Figure 1. Two views of the molecular structure of 8 from a single-crystal X-ray diffraction study (oxygen atoms in black) showing the triple spiro-containing hydrocarbon framework.

The polymers derived from 5 and 6 are both insoluble in all common solvents with the exception of hot quinoline and conc. H_2SO_4, whereas the polymer derived from 7, like PIM-1, is freely soluble in $CHCl_3$ and THF. The polymer derived from 10 is soluble in high-boiling solvents (e.g., NMP and quinoline) at room temperature. In powder form all polymers show significant microporosity as demonstrated by nitrogen adsorption isotherms collected at 77 K. Polymers derived from 5, 6 and 10 exhibit less surface area than PIM-1, which may reflect greater cohesive interactions between polymer chains due to the polar ketone groups (from monomers 5 and 6) or blocking of available microporosity by the phenyl groups (from monomer 10). In contrast, the polymer derived from monomer 7 displays enhanced surface area as compared to PIM-1, which suggests that the rigid, spiro-fused fluorene units increase free volume by reducing further the packing efficiency of the polymer chains. Studies are in progress to determine whether the greater microporosity of this polymer offers advantages for applications such as hydrogen storage or gas separation. In addition, further PIMs designed using this useful paradigm are being prepared.

Acknowledgment. We thank EPSRC for funding.

Supporting Information Available: Experimental details and characterization data for all monomers and polymers. This material is available free of charge via the Internet at http://pubs.acs.org.

OL800573M

Appendix B

Crystallographic data (CIF files)on CD at the back of the thesis